DISSERTATION

Methods in groundwater monitoring: strategies based on statistical, geostatistical, and hydrogeological modelling and visualization

Submitted to the faculty of Natural Sciences III

of the

Martin Luther University, Halle-Wittenberg, Germany

In partial fulfilment of the requirements for the award of the

degree of Doctor of Natural Sciences (Dr. rer. nat.)

By

Jay Krishna Thakur

M.Sc. (Environmental Sciences), M.Sc. (WREM)

Born on: 03-02-1983 in Janakpur, Nepal

Committee: 1. Prof. Dr. Peter Wycisk

2. Prof. Dr. Holger Weiß

3. Prof. Dr. Carsten Lorz

Submitted: Halle (Saale), 06-05-2013

Date of Defence: 28.10.2013

Abstract

Information about the properties and behaviour of groundwater systems is required for strategic planning and operations in groundwater management. In order to improve groundwater monitoring strategies, improving groundwater monitoring networks is necessary as they are an important component of the groundwater monitoring framework. The objective of this work is to investigate new methods and improve existing methods based on statistical, geostatistical, and hydrogeological methods for groundwater monitoring network optimization. New approaches were formulated, and improvements were made to the existing methodology, and they were integrated for the spatiotemporal optimization of a groundwater monitoring network. The formulated and integrated methods were tested with the groundwater quality data set of Bitterfeld/Wolfen. Bitterfeld/Wolfen is a contaminated mega-site, comprising a Quaternary aquifer and a Tertiary aquifer.

Univariate and multivariate statistics were applied to the spatial optimization of the monitoring network; the temporal optimization of the monitoring network was carried out using Sen's method (1968). In terms of geostatistical methods, a geostatistical spatio-temporal algorithm was used to identify redundant wells on the basis of nearby wells offering the same information about the underlying plume in 2- and 2.5- dimensional Quaternary and Tertiary aquifers. When conducting this spatiotemporal optimization of the monitoring network, the factors influencing the monitoring network optimization were analysed. In another approach, a hydrogeological modelling based method with steady state flow and a transient transport model was used to determine the particle track of contaminant flow, flow velocity and concentration of mass at reference monitoring locations. The particle track was laid over the locations of reference monitoring wells. The monitoring wells were then tagged as essential or redundant based on model conditions such as, 'wells on the same path line from same aquifer are redundant'. The recommended relative sampling frequency for each monitoring well was also estimated using simulated groundwater flow velocity. Based on the strengths and weaknesses of the statistical, geostatistical, and hydrogeological methods, the results were compared and these methods were integrated in order to meet the objectives of the optimization.

The spatial optimization of the monitoring network shows higher redundancy when using statistical methods than when using geostatistical methods. The statistical methods were found to be better for monitoring networks with a high density of wells, while geostatistical methods can be recommended for monitoring networks with both high and low densities of monitoring wells. The

temporal optimization based on statistical methods recommends an optimal sampling frequency for each monitoring well considering each individual contaminant and all contaminants for each aquifer. In the case study of Bitterfeld/Wolfen, an overall optimized sampling interval was recommended in terms of lower quartile (238 days), median quartile (317 days), and upper quartile (401 days). However, the temporal optimization of the monitoring network based on hydrogeological modelling methods recommends different a sampling interval for each monitoring well. The spatial optimization using a hydrogeological model shows 30 (6.49%) of the 462 wells in the Quaternary aquifer and 14 (3.92%) of the 357 wells in the Tertiary aquifer to be redundant. The number of redundant wells identified based on this hydrogeological modelling method was lower than that identified using the statistical and geostatistical methods. The monitoring network optimization using geostatistical methods recommends monitoring of 292 of the 462 wells in the Quaternary aquifer and 256 of the 357 wells in Tertiary aquifer. The geostatistical method also recommends 41 and 22 new monitoring wells be installed in the Quaternary and Tertiary aquifers, respectively. In this study, it has been observed that the predicted redundancy in the monitoring network using these methods varies with several different factors.

In this work, it is demonstrated that the existing monitoring network could be optimized using the presented statistical, geostatistical, and hydrogeological methods, without losing any essential information from the monitoring network. As improvements to groundwater monitoring strategies are the key to groundwater resource management, the efforts presented to optimize and evaluate the monitoring network will enhance the performance of the water management system. The presented methods are useful for monitoring networks that are both too dense and not dense enough. In developing countries, where inadequate financial resources are the reason for insufficiently dense monitoring networks, the presented methods could be used to find redundancy in the existing monitoring network along with identifying recommended locations for new monitoring wells. In contrast, in developed countries, the presented methods can be applied to reduce the density of monitoring wells without losing valuable information from the monitoring network.

Acknowledgement

First of all, I express my gratitude to Helmholtz Interdisciplinary GRADuate School for Environmental Research (HIGRADE) program at the Helmholtz Centre for Environmental Research—UFZ, Leipzig, Germany, and the Department of Hydrogeology and Environmental Geology, Martin Luther University, Halle-Wittenberg, Germany, for the Helmholtz PhD scholarship and the opportunity to pursue doctoral research.

I express my heartiest appreciation to my supervisors Prof. Dr. Peter Wycisk, Martin Luther University, Halle-Wittenberg, Germany, and Prof. Dr. Holger Weiß, Helmholtz Centre for Environmental Research – UFZ, Leipzing, Germany, for the guidance, discussions, comments, and support extended to me during this whole research period. The encouragement and the critical reviews helped me immensely in shaping the thesis to meet the expectations.

My deepest gratitude goes to my advisor Dr. habil. Wolfgang Gossel, Martin Luther University Halle-Wittenberg. The valuable discussions, comments, and field visits and his kind support and encouragement gave me strength right from the inception of the topic to very final stage of the doctoral research.

I extend my special thanks to Dr. rer. nat. habil. Birgit Daus, Ralf Trabitzsch, Dr. Vera Bissinger, and Barbara Timmel who helped me at all times in organizing all formal matters and clarifying questions.

I am especially grateful to Dr. rer. nat. Reiner Stollberg and Ronny Lähne for providing a pleasant and creative working environment as well as for the valuable discussions and technical support.

I also thank to the LAF (Landesamt für Altlastenfreistellung Sachsen-Anhalt) for providing groundwater monitoring data for Bitterfeld/Wolfen under the data exchange embedded in the SAFIRA I and II projects (funding number 02WT0023 & 02WT00412).

I express my deepest gratitude to my parents, my wife, and family members for their support, prayers, and good wishes that made it possible for me able to complete this study.

Lastly, I offer my regards and blessings to all of those I have not mentioned here.

Table of Contents

List of Figures

List of Tables

List of Abbreviations

- ACO: Ant colony optimization
- AHC: Agglomerative hierarchical cluster
- ANOVA: Analysis of variance
- BC: Boundary conditions
- BGR: Federal Institute for Geosciences and Natural Resources
- BTEX: Benzene, ethylbenzene and xylene
- COC: Chemical of concern
- DL: Detection limit
- EC: Electric conductivity
- Eh: Reduction potential
- EMO: Evolutionary multi-objective optimization
- EU: European Union
- FDM: Finite difference method
- FEM: Finite element method
- GAs: Genetic algorithms
- GTS: Geostatistical temporal-spatial algorithm
- HCH: Hexachlorocyclohexane
- LTM: Long-term monitoring
- IMOGA: Interactive multi-objective genetic algorithm
- LAF: Landesamt für Altlastenfreistellung
- MAROS: Monitoring and remediation optimization system
- MCB: Monochlorobenzene
- MCL: Maximum contamination limit
- MCSGA: Monte Carlo simple genetic algorithm
- MODFLOW: Modular finite difference flow model
- MP: Multiple population
- MS: Master slave
- NGA: Noisy genetic algorithm

- NSGA: Nondominated sorted genetic algorithm
- PCA: Principal component analysis
- PSVM: Probabilistic support vector machine
- QLR: Quadratic logistic regression
- QWD: Quaternary well in dry hydrological period
- QWW: Quaternary well in wet hydrological period
- REV: Representative elemental volume
- SPEA: Strength pareto evolutionary algorithm
- SQD: Sample from quaternary well in dry hydrological period
- SQW: Sample from quaternary well in wet hydrological period
- SSE: Sum of the squared errors
- STD: Sample from tertiary well in dry hydrological period
- STW: Sample from tertiary well in wet hydrological period
- SVMs: Support vector machines
- TWD: Tertiary well in dry hydrological period
- TWW: Tertiary well in wet hydrological period
- UFZ: Helmholtz Centre for Environmental Research
- WHO: World Health Organization

List of Symbols

- A: cross-sectional area [L^2]
- c: concentration in the water [M/L^3]
- cref: reference concentration [M/L^3]
- d: thickness of the clogging layer [L]
- iC(t): indictor value [-]
- K: hydraulic conductivity [L/T]
- kvG: global kriging variance [M^2]
- h: hydraulic head in groundwater [L]
- M1: upper confidence interval [-]
- M2: lower confidence interval [-]
- Q: volume discharge rate [L^3/T]
- q = Q/A: volume rate of flow per unit area [$L^3/T\ M^2$]
- qmass: mass transport BC flux [M]
- qflow: flow BC flux [M]
- Qf: inflow or outflow to/from the model [L^3/T]
- Qmass: inflow or outflow to/from the model [L^3/T]
- Q': median slope [-]
- Φ : transfer rate = K/d [1/T]
- σ: standard deviation [M]
- X: parameter concentration [M]
- λG: global interpolation weights [M]
- μ: parameter mean [M]
- z(t): concentration at time t [M/L^3]
- Z(x,y): concentration of contaminant at location (x,y) [M/L^3]
- x: Spatial coordinate [L]
- y: Spatial coordinate [L]
- z: Spatial coordinate [L]

1. Introduction

1.1 Background

“Water is life! It is a precondition for human, animal and plant life as well as an indispensable resource for the economy” (European Commission, 2011). Groundwater, a vital and essential resource, is in continuously increasing demand due to rapid population growth and extensive economic development in the whole world. Therefore, rising water use per capita is putting pressure on available resources (Arnell, 1999; Repetto and Holmes, 1983). Although groundwater is the predominant and safe source of water supply in many countries, growing water scarcity and alarming groundwater pollution indicate that water policies in most of the world are failing to protect life's most vital resource (Johnson *et al.*, 2001).

1.1.1 Groundwater systems

A groundwater system can be defined as a set of interconnected components, located beneath the earth's surface in soil pore spaces and in the fractures of rock formations, in which water is present (Srebotnjak *et al.*, 2011). Groundwater is an integral part of the hydrologic system. Its movement is largely dependent upon porosity and permeability of the rocks through which it flows. In groundwater systems, gravity plays an important role, as it pulls groundwater from the surface to the underground aquifer through pore spaces in the rocks.

In groundwater systems, the water table is the upper surface of the zone of saturation, the upper surface at which water pressure is equal to atmospheric pressure. Below this groundwater table, the water is under hydrostatic pressure, which is greater than atmospheric pressure. This hydrostatic pressure increases with depth. In general, groundwater is believed to be clean and free from pollution. However, in areas where pollutants are deposited on the ground surface, these pollutants can readily sink into the groundwater, depending upon the permeability of the aquifer. Groundwater can thus be easily polluted by landfills, leaky underground gas tanks, and from overuse of fertilizers and pesticides. Groundwater systems are also easily disturbed by anthropogenic activities such as mining (Heidrich *et al.*, 2004b).

1.1.2 Data, information, models, and methods

Data refer to raw unorganized factual information derived from measurements. In groundwater studies, data refer to qualitative and quantitative information obtained from measurements of various parameters related to groundwater. If data are interpreted correctly, meaningful information can be abstracted from it. When groundwater data are processed, organized, and structurally presented in a given context, they can provide valuable information for groundwater monitoring decision makers. In groundwater studies, models are developed to represent natural groundwater flow in the environment. These groundwater models are used to predict the fate and movement of physical and chemical aspects of groundwater in natural and hypothetical scenarios. Groundwater models are discussed further in chapter 4. In this thesis, "methods" are the procedure or systematic way of investigating, experimenting with, and presenting groundwater processes.

1.1.3 Groundwater monitoring strategies

In almost all major water resource management programs, such as the European Union Water Framework Directive (EU, 2006), groundwater monitoring is required (van Geer *et al.*, 2006). A typical groundwater monitoring program aims to prevent potential threats to human health, assess the impact of anthropogenic substances that have been transported via groundwater on aquatic ecosystems, document the state of groundwater pollution, and show the efficiency of water protection measures. Groundwater monitoring consists of long-term standardized measurement, observation, evaluation of status and trends, and reporting of groundwater conditions to meet monitoring programme objectives (Erechtchoukova *et al.*, 2009; Thakur *et al.*, 2011a). In Germany, approximately 75% of all water for public water supply is obtained from groundwater (BGR, 2011). Accurate quantification and quality evaluation of the available groundwater resources is therefore a basic requirement for effective public water management, and consequently, groundwater monitoring is required. As a result, a large number of ground water monitoring networks exist.

A groundwater monitoring network is a set of strategically located groundwater monitoring well with measurement devices that collect data of interest from a groundwater system at a given temporal scale. These monitoring networks are important because they collect data that, after being interpreted, may provide insights for strategic planning and decision making (Thakur *et al.*, 2012). This requires a complex infrastructure to support the entire sampling, laboratory, and field based analysis and data processing activities. Consequently, long-term groundwater quality monitoring constitutes a significant economic burden at many industrial and urban groundwater contamination sites.

1.2 *Motivation* of this thesis

There are a number of challenges in planning and formulating strategies for groundwater monitoring. To do this, in depth knowledge of components and variables need to be acquired and considered. In groundwater monitoring strategies, one of the major challenges is optimizing the groundwater monitoring network. Another challenge to overcome is inadequate or excess data availability, in terms of both quality and quantity.

Although there are several groundwater monitoring network optimization methods available, the majority of methods do not consider hydrology and hydrogeological characteristics of the aquifer. Even if the groundwater monitoring network is optimized with a standard method, other factors that influence the method may not be considered. For this reason, available and new methods must be integrated, such that they consider the quality and quantity of data, the hydrology and hydrogeological characteristics of the aquifer, and the objective and influencing factors of the chosen applied methods. In optimizing the groundwater monitoring network, the spatial and temporal dimension of study plays major role. In some of previous studies, spatial and temporal optimizations have been treated as two separate processes. However, as these two optimizations correlate with each other, a combined method is required.

1.3 Research objectives and questions

The objective of this piece of research is to investigate new methods and improve existing statistical, geostatistical, and hydrogeological methods for groundwater monitoring network optimization, in order to improve groundwater monitoring strategies.

The specific objectives of the study are:

- To explore different approaches using statistical, geostatistical, and hydrogeological methods for optimization of monitoring networks.
- To formulate new approaches and improve existing methodology for the spatiotemporal optimization of a groundwater monitoring network.
- To incorporate unmonitored concentrations at different potential monitoring locations into the groundwater monitoring optimization method.
- To analyse factors that influence groundwater monitoring optimization methods.

- To compare new and improved approaches of statistical, geostatistical, and hydrogeological methods by testing those with groundwater monitoring network optimization at contaminated megasite.

In the context of the motivation and objective presented, the main questions that arise are as follows: how can groundwater monitoring optimization methods be improved using statistical, geostatistical, and hydrogeological methods, and how can these methods be compared to incorporate the factors that influence a study area.

These main questions can be clarified by re-phrasing them in the form of the following separate questions:

- What, where, and when should groundwater be monitored, based on statistical, geostatistical, and hydrogeological methods?
- How are groundwater monitoring network optimization methods dependent upon site specific and methods specific parameters?
- How can inter connecting statistical, geostatistical, and hydrogeological methods be integrated for better optimization of the monitoring network?
- How can unmonitored concentrations be incorporated at different potential monitoring locations during the monitoring network optimization?
- What would be the best spatiotemporal optimized monitoring network in a test study area, using new and improved methods?

1.4 Scope of this thesis

The research presented in this thesis has following scope:

1.4.1. Investigating and improving approaches

Several studies have documented the spatial optimization of groundwater quality monitoring networks (Datta *et al.*, 2009; Loaiciga *et al.*, 1988), whereas few have focused on multiobjective aspects of optimal spatiotemporal designs of groundwater monitoring networks that explicitly involve both space and time (Herrera and Pinder, 2005; Nabi *et al.*, 2011). This thesis explores possible new approaches and improves existing approaches using statistical, geostatistical, and hydrogeological methods as well as interactive visualization for monitoring network optimization.

1.4.2. Integrating available and possible methods

In previous studies, the monitoring network was optimized using different individual methods, such as statistical methods and physically-based mathematical models (Meyer *et al.*, 1994; Prakash and Datta, 2012). However, these methods were not applied on the same datasets in order to investigate their functionality (Wang *et al.*, 2012). In this study, an effort has been made to apply new and existing approaches to the data set from the existing monitoring network. Statistical, geostatistical, and hydrogeological methods have also been integrated in order to understand the underlying facts and optimize the existing network.

1.4.3. Demonstrating the investigated approaches in real and ideal world scenarios

According to the objective of this thesis, new and improved approaches of statistical, geostatistical, and hydrogeological methods have been tested in a contaminated mega-site, Bitterfeld/Wolfen, located in the Federal State Saxony-Anhalt, Germany, to optimize the groundwater monitoring network there. These methods of network optimization have been used to improve the existing monitoring network of this former chemical industrial site, which has significant groundwater contamination (Wycisk *et al.*, 2003), in both real and ideal world scenarios.

In this study, although these new and improved methods have been applied only to this contaminated mega-site, they should be valid for the optimization of other monitoring networks around the world. The results obtained from the application of these methods in this contaminated mega-site scenario may or may not be representative to the other monitoring network optimization. These three different methods, which each have unique underlying assumptions, were applied to the same dataset. The optimization results revealed a different number of essential and redundant monitoring wells for the different methods. Moreover, the study also demonstrates that these numbers of essential and redundant monitoring wells are largely dependent upon the underlying assumptions and influencing factors.

In this thesis, a distinction is made between local and regional scale monitoring networks. The local scale has a typical contributing area of about 50–100 km^2, whilst the regional scale corresponds has a typical contributing area of about 100–10,000 km^2. Similarly, monitoring programs lasting longer than five years are considered to be long-term monitoring programs.

1.5 Structure of this thesis

The research questions posed in the previous section, in the context of the motivation and objective of this thesis, are answered through the development of seven interconnected chapters as follows:

Chapter 1: Introduction

This chapter introduces the background of the study. It presents the motivation, research objective and questions, scope and structure of the thesis.

Chapter 2: Literature review

This chapter presents the state of the art through a detailed review of the literature and the theories used in the course of the present thesis.

Chapter 3: Research location and data set

This chapter introduces the study area by describing the research location, aquifer characteristics, and nature and availability of data set.

Chapter 4: Method

This chapter gives the step-wise application of improved and new methods. This chapter has been divided into four sections. The first section, presents existing statistical methods for data analysis and data reduction. This section is followed by proposed methods for optimization of monitoring networks. This second section on geostatistical methods integrates existing and proposed methods for the monitoring network optimization, whilst also considering the dependency of the methods. The third section presents an application of a hydrogeological model for optimizing the monitoring network. Finally, the last section correlates and compares these methods.

Chapter 5: Results

This chapter contains new findings from the application of existing, improved and proposed methods for the optimization of the existing monitoring network of the former industrial and mining site.

Chapter 6: Discussion

This chapter discusses new and improved approaches based on statistical, geostatistical, and hydrogeological methods for monitoring network optimization. It also discusses factors and their influence on the application of these methods with the reference of tested research area. This chapter also summarizes the implications and limitations of the presented methods.

Chapter 7: Conclusion and recommendation

Chapter 7 concludes with an evaluation of the presented methods and work flow. Finally, this chapter presents a recommendation about the investigated new and improved methods along with outlining their limitations. The chapter also contains recommendations for future work.

2. Literature review

During the last three decades, many advances have been made in the design and optimization of groundwater monitoring networks; these advances have led to improvements in groundwater monitoring strategies. Most advances have concentrated on contamination problems caused by point sources and focused strongly on the statistical approach for monitoring locations and sample size (Ben-Jemaa *et al.*, 1994; MacKenzie *et al.*, 1987; Nabi *et al.*, 2011). Relatively little work has been published on considerations of groundwater monitoring network optimization using multiple contaminants in multiple aquifers. The main approaches in these design and optimization advances can be classified into the groups of hydrogeological (Polemio *et al.*, 2009), statistical (Khan *et al.*, 2008; Nabi *et al.*, 2011) and a combination of hydrogeological and statistical approaches (Chadalavada and Datta, 2008; Reed *et al.*, 2000).

Groundwater quality assessment programs are usually based on existing observation points, such as domestic wells, public water supply wells or existing observation wells for groundwater heads (Broers, 2002; Hudak, 2006).

Everett (1984) provides an overview of groundwater quality monitoring guidelines and methodology for cost-effective, generic groundwater pollution monitoring methodology that can be applied on a local or regional scale.

Lauterbach and Luckner (1999) distinguished monitoring programs into information oriented and decision oriented monitoring. Information oriented monitoring is used to evaluate quality and quantity of groundwater resources while decision oriented monitoring is used for strategic planning and design of groundwater management programs (Knödel *et al.*, 2007). For strategic planning and design of management measures, the overall groundwater status is characterized. For programs with objectives to improve the state of the art, a comprehensive evaluation of the groundwater monitoring program is carried out, whilst at operational level real time action is taken in order to prevent potential disasters.

In order to design a groundwater monitoring strategy for management objectives, it is necessary to ascertain what information is needed and how this can be abstracted from the measured variables (van Geer *et al.*, 2006). Once the monitoring objective is defined, the monitoring strategy can be derived based on optimization of the groundwater monitoring network and considerations of the uncertainty associated with spatial and temporal variability (Chadalavada *et al.*, 2011; Datta *et al.*, 2009).

Design of a groundwater quality monitoring network includes selecting the best sampling location and sampling frequency to determine physical, chemical, and biological properties of ground water (Loaiciga *et al.*, 1992b). Loaiciga, Charbeneau et al. (1992b). This is defined in the monitoring network optimization as a process of improving sampling location and sampling frequency in the existing groundwater monitoring network.

In the last three decades, genetic algorithms (GAs) have been widely used, in combination with other approaches, for optimizing groundwater monitoring networks with a limited number of monitoring stations. Meyer and Brill (1988) coupled a model that simulates contaminant transport with a facility location model for locating wells in a monitoring network under conditions of high uncertainty. Following this work, Cieniawski and Eheart (1995) used GAs for groundwater monitoring network optimization, managing to maximize reliability and minimize the contaminated area at the time of first detection, separately yet simultaneously. Harrouni and Ouazar (1996) then applied GAs to optimizing monitoring networks using the dual reciprocity boundary element method with global interpolation functions. Reed and Minsker (2000) later combined a fate-and-transport model, plume interpolation, and a genetic algorithm to identify cost-effective sampling plans that accurately quantify the total mass of dissolved contaminant.

Reed, Minsker et al (2001) combined nonlinear spatial interpolation with a nondominated sorted genetic algorithm (NSGA) to identify the tradeoff curve (or Pareto frontier) between sampling costs and local concentration estimation errors.

Zhang, Pinder et al. (2005) combined GAs with a static Kalman filter and a stochastic groundwater flow and contaminant transport model to determine when and where to take samples in the study area, with their associated uncertainties.

Taking a different approach, Kollat and Reed (2006) compared the performances of several evolutionary multi-objective optimization (EMO) algorithms: the Non-Dominated Sorted Genetic Algorithm II (NSGAII), the Epsilon-Dominance Non-Dominated Sorted Genetic Algorithm II ([epsilon]-NSGAII), the Epsilon-Dominance Multi-Objective Evolutionary Algorithm ([epsilon]MOEA), and the Strength Pareto Evolutionary Algorithm 2 (SPEA2). They were compared on the basis of minimizing sampling cost and error in estimating contaminant concentration in the monitoring network. Meanwhile, Wu, Zheng et al. (2006) evaluated and compared a Monte Carlo simple genetic algorithm (MCSGA) and a noisy genetic algorithm (NGA), for design of a cost-effective sampling network when there are uncertainties in the hydraulic conductivity (K) field.

Kollat and Reed (2007a) assessed how decision variables impact the computational complexity of using multiple objective evolutionary algorithms (MOEAs) to solve long-term groundwater monitoring problems. In their study, the epsilon-dominance non-dominated sorted genetic algorithm II ([epsilon]-NSGAII) was used for computational scaling. Meanwhile, Tang, Reed et al. (2007) used a formal metrics-based framework to demonstrate Master-Slave (MS) and the Multiple-Population (MP) parallelization schemes for the Epsilon-Nondominated Sorted Genetic Algorithm-II ([epsilon]-NSGAII). The MS and MP versions of the [epsilon]-NSGAII generalize the algorithm's auto-adaptive population sizing, [epsilon]-dominance archiving, and time continuation to a distributed processor environment using the Message Passing Interface.

Babbar-Sebens and Minsker (2010) proposed a new interactive optimization algorithm—Case-Based Micro Interactive Genetic Algorithm—that uses a case-based memory and case-based reasoning to manage the effects of nonstationarity in decision maker's preferences within the search process without impairing the performance of the search algorithm. They also compared this with a non-interactive genetic algorithm and a previous version of the interactive genetic algorithm.

Masoumi and Kerachian (2010) used discrete entropy theory and transinformation–distance (T–D) curves to quantify the efficiency of sampling locations and sampling frequencies in an existing monitoring network. In most of the above-mentioned studies, GAs in combination with other methods have been used for single contaminants and for monitoring networks with a limited number of monitoring stations (less than 25 stations). In these studies, authors considered a single groundwater aquifer during the monitoring network optimization, without considering hydrogeological heterogeneity of the aquifer.

To address hydrogeological heterogeneity, Storck, Eheart et al. (1997) presented an optimization method for the design of monitoring well networks in three-dimensional (3-D) heterogenous aquifers. A Monte Carlo based approach was used to generate a random hydraulic conductivity field and contaminant leak location. A finite difference groundwater flow model and a particle-tracking model were used to generate a contaminant plume for each realization. Simulated annealing was then used to determine optimal trade-off curves for optimization of groundwater monitoring networks.

Nunes, Cunha et al. (2004b) used a simulated annealing optimization algorithm to minimize the variance of the estimation error obtained by kriging in combinatorial problems, optimized monitoring network by selecting an optimal subset of monitoring well locations from the original groundwater monitoring network. They presented this method for optimization of a groundwater nitrate monitoring network with 89 stations within a larger monitoring network in the south of Portugal.

Asefa, Kemblowski et al. (2005) presented a hydrologic application of support vector machines (SVMs) to reproduce the behaviour of Monte Carlo based flow and transport models, and in turn used them in the design of a ground water contamination detection monitoring system.

Bashi-Azghadi and Kerachian (2009) presented two different single and multi-objective optimization models, a Monte Carlo analysis, MODFLOW, MT3D groundwater quantity and quality simulation models and a Probabilistic Support Vector Machine (PSVM). The single-objective optimization model based on the Monte Carlo analysis and the reliability of contamination detection was used to select the initial location of monitoring wells. The multi-objective optimization models were used to minimize the number of monitoring wells, maximize the reliability of contamination detection and maximize the probability of detecting an unknown pollution source in Tehran Refinery, Iran.

In addition to these approaches, geostatistical methods have been widely used in groundwater monitoring network design and optimization. Cameron and Hunter (2002) presented a geostatistical temporal-spatial algorithm for optimizing long-term monitoring (LTM) networks. In the spatial optimization, a plume map is generated and redundant wells are removed based on kriging variances. Meanwhile, variogram and San’s method have been used to find temporally redundant wells in the temporal optimization. The method has been tested in the Massachusetts Military Reserve, United States of America.

Aziz, Ling et al. (2003) developed the Monitoring and Remediation Optimization System (MAROS), a decision-support software to assist in formulating long-term cost-effective groundwater monitoring plans. In this software, plume stability was characterized using Mann-Kendall analysis and linear regression analysis for concentration trends, modelling results and empirical data. The spatial optimization was performed in a two-dimensional (2-D) plain, and a temporal optimization provided detailed sampling location and frequency results.

Li and Chan Hilton (2007) developed the ant colony optimization (ACO) paradigm. The ACO algorithm is inspired by the ability of an ant colony to identify the shortest route between their nest and a food source.

Singh, Minsker et al. (2008) presented the Interactive Multi-Objective Genetic Algorithm' (IMOGA) to solve the groundwater inverse problem, considering different sources of quantitative data as well as qualitative expert knowledge about the site. In this method, the IMOGA considers groundwater model calibration as a multi-objective problem consisting of quantitative objectives—calibration error and regularization—and a ‘qualitative’ objective based on the preference of the geological expert for different spatial characteristics of the conductivity field.

The methods documented in the previous studies were analyzed in order to propose, formulate and test new approaches based on the new and existing statistical, geoststistical and hydrogeological methods.

3. Research location and data set

3.1 Research location

In order to test improved and developed methods, Bitterfeld/Wolfen, located in the Federal State Saxony-Anhalt, Germany, was selected as a research location (figure 3.1). To study the overall groundwater scenario, an area of 320 km^2, latitude 51°30′12.6″–51°41′44″ and longitude 12°5′26″–12°26′0.5″, was used for the three-dimensional (3-D) hydrogeological flow and transport modelling (Gossel *et al.*, 2009). This area constitutes 436 wells in the Tertiary and 510 wells in the Quaternary aquifer in the existing groundwater long-term monitoring (LTM) network. However, to apply improved and developed methods more precisely, in this study area, an area of about 100 km^2 in urbanized zone of Bitterfeld/Wolfen, latitude 51°35′30″–51°41′30″ and longitude 12°14′10″–12°20′0.5″, which has a LTM network of 357 wells in the Tertiary and 462 wells in the Quaternary aquifer, was selected (figure 3.1).

Geographically, the western part of the research location is covered by glacial outwash sediments, whilst the flood plain of the Mulde river constitutes the eastern part of research area. Geologically, the southern area consists of Cenozoic sediments that overly Pre-Tertiary rocks, hydrogeologically separated from one another by an undisturbed clay layer at a depth of 50–70 m (Heidrich *et al.*, 2004b). The geological setting of Bitterfeld/Wolfen has evolved through several geological periods, experiencing transgression and regression of the sea, orogenesis, solidification under snow and ice, fluvial erosion etc. A typical geological cross section of the subsurface obtained with the Bitterfeld/Wolfen model (Stollberg *et al.*, 2009) shows an upper Quaternary aquifer system, lower Tertiary aquifer system and Pre-Tertiary as basement, as depicted in figure 3.2. A detailed geological overview of the Quaternary, Tertiary and Pre-Tertiary aquifers in this area is summarized by Eissmann and Müller (1978); Wansa and Wimmer (1990); Eissmann (1994); and Knoth (1995).

3.1.1 Quaternary aquifer

The upper aquifer consists of Quaternary sands, silt, clay and gravels, which are formed by mechanical degradation of the Tertiary sediments (Wycisk *et al.*, 2003). Additionally, the upper Quaternary aquifer system can be divided into upper sediments composed of braided river deposits of stream tributaries, and lower terrace sediments of the Weichselian Mulde. Both units are partially separated by Saalian and Elsterian varved clay layer acting as a hydraulic barrier for groundwater flow (Wycisk *et al.*, 2005).

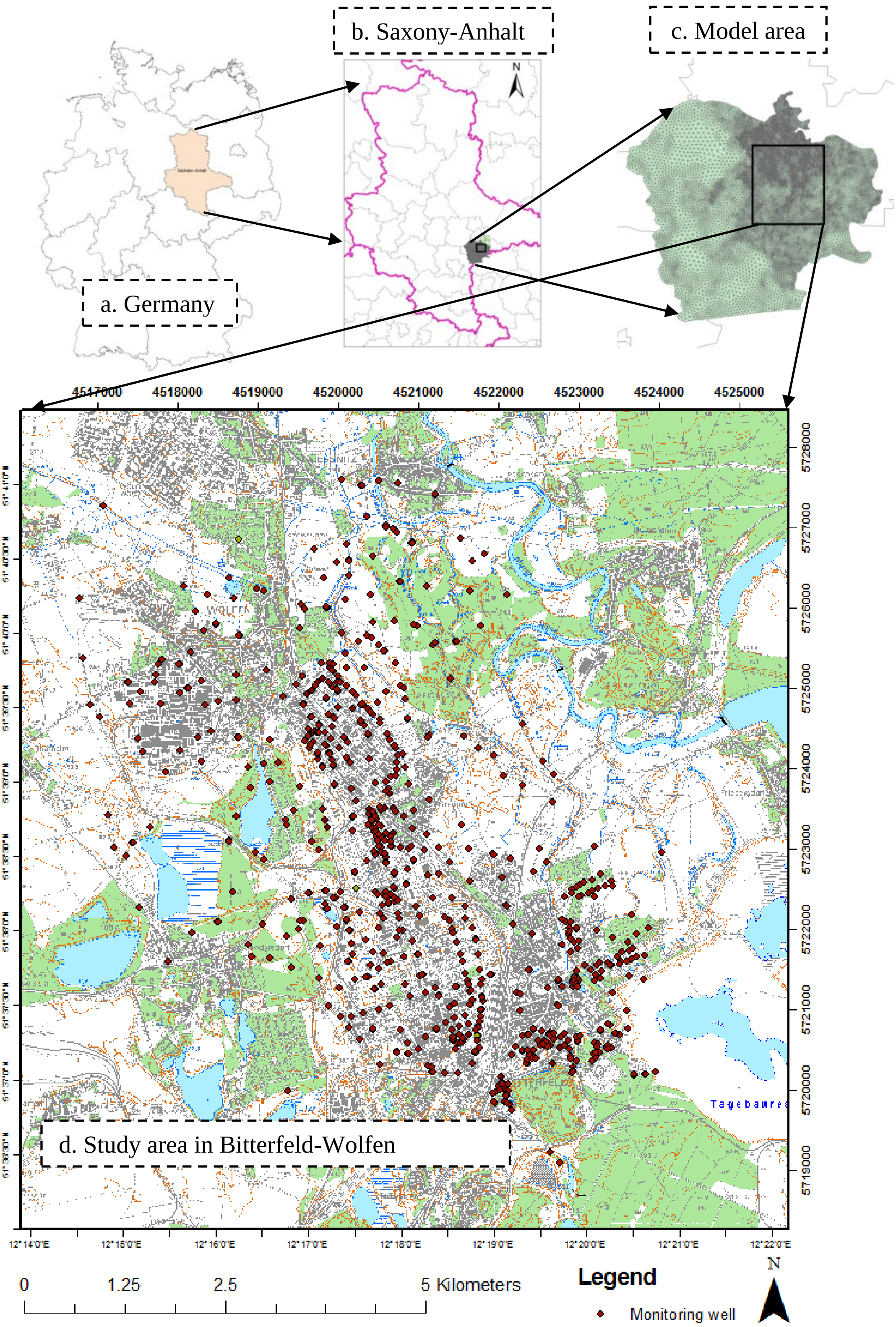

Figure 3.1: A location map of the study area in Bitterfeld, Federal State of Saxony-Anhalt, Germany (a. Saxony-Anhalt in eastern Germany, b. Federal State of Saxony-Anhalt, c. the hydrogeological model domain of 320 km² used to simulate groundwater flow and run a transport model, and d. research locations of 100 km² used for monitoring network optimization in Bitterfeld/Wolfen showing location of groundwater monitoring wells).

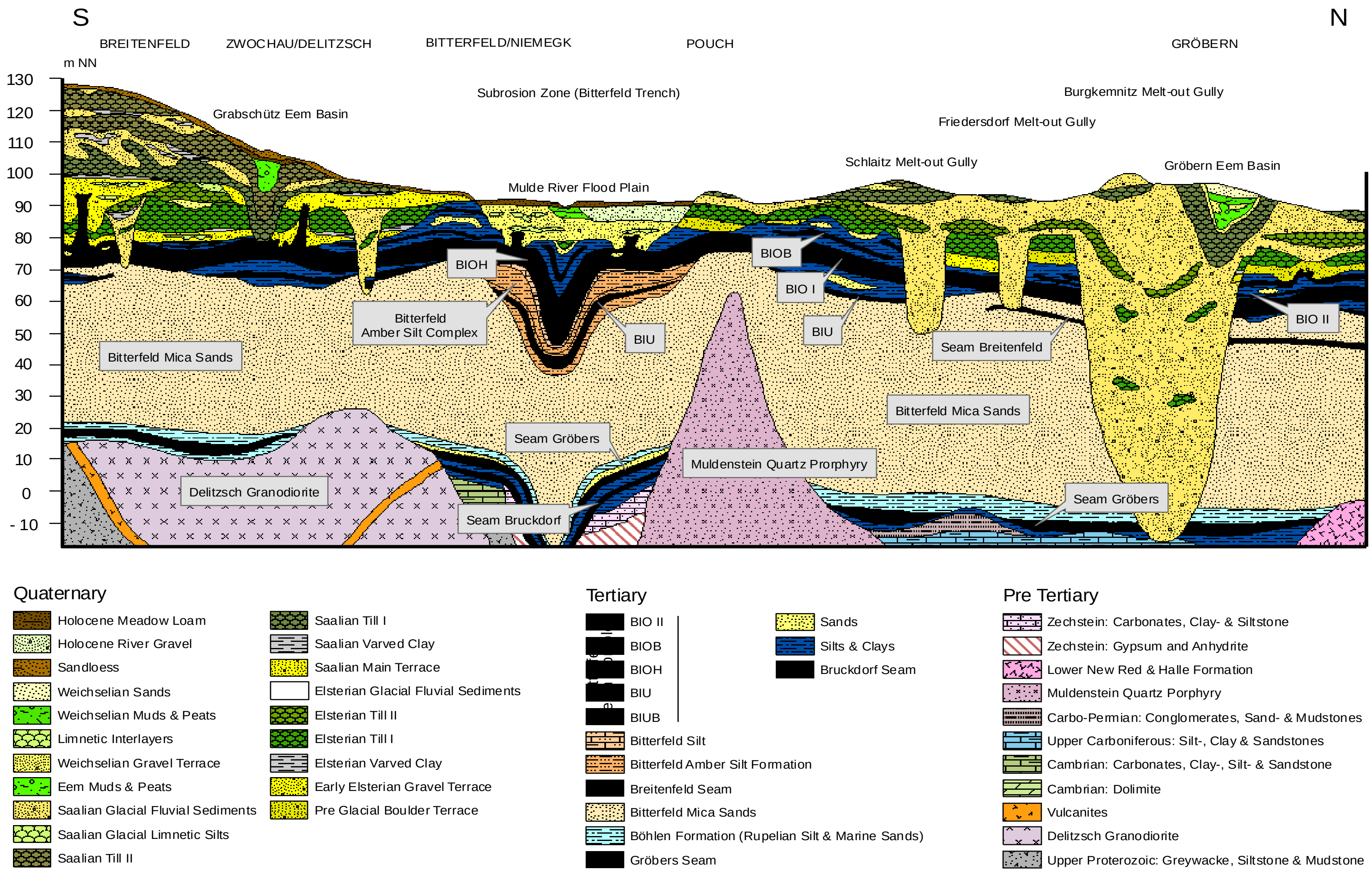

Figure 3.2: A typical geological cross section of Bitterfeld/Wolfen, showing an upper Quaternary aquifer system, a lower Tertiary aquifer system, and a Pre-Tertiary basement (Eissmann, 2002; Stollberg, 2013).

This aquifer mainly constitutes Holocene meadow loam, which is characterized by an accretion of river gravel and flood plain loam, Bruckdorf glacial varved clay, Saalian ground moraine, recessional sediments, Breitenfeld glacial clay, Saalian till and recessional outwash sediments (Eissmann, 1994). The hydraulic conductivities of the Quaternary aquifers are between 2×10^{-5} and 1×10^{-2} m/s (Ruske *et al.*, 1997).

According to Gossel *et al.* (2009), the hydraulic conductivities of the Quaternary layers widely vary with type of hydrogeological unit between 2×10^{-8} and 1×10^{-4} m/s. Units such as anthropogenically altered hydrogeological units, Pleistocene, and glacial cover sand have higher hydraulic conductivities. However, the bottom layers that reach down into the Tertiary have lower hydraulic conductivities.

3.1.2 Tertiary aquifer

The Tertiary aquifer consists of sand, silt, clay and lignite layers deposited by meandering river systems and transgression and regression of the ocean. The thickness of the Tertiary aquifer ranges from 70 to 120 m (Standke, 2004). The base of the Tertiary aquifer is a Rupelian clay barrier. The oldest Tertiary units are the Eocene seams: Bruckdorf and Gröbers. The next unit is classified as the Oligocene Rupelian formation. The Lower Tertiary complex is completed by Upper Oligocene Rupelian Silt, which is missing in areas of the pre Tertiary outliers (Stollberg *et al.*, 2009). The groundwater flow direction is directed to the receiving river Mulde, although it has been distracted towards to the Goitsche Lake because of lignite mining. The Tertiary aquifer has a hydraulic conductivity of about 10^{-5} to 10^{-4} m/s (Ruske *et al.*, 1997). However, the aquitard present between the Tertiary aquifers and younger Quaternary units shows a relatively higher hydraulic conductivity: $5{\cdot}10^{-5}$–$1{\cdot}10^{-7}$, compared to the lower end of the aquifer (Weiß *et al.*, 2002a).

3.1.3 Pre-Tertiary

The basement of the Tertiary aquifer consists of several tectonic blocks of Pre-Variscan and Variscan folded rocks in a complex fault system. This unit contains sandstones and conglomerates of different stratigraphic ages. The upper 10 to 30 m of the lower Permian basement are intensively kaolinitic decomposed and act as a massive aquitard (Eissmann *et al.*, 2008; Stollberg *et al.*, 2009). The upper Permian consists of Zechstein carbonates, claystone, and siltstone; the upper Carboniferous silt consists of clay and sandstone, and minor parts also consist of Cambrian dolomite, vulcanites, Delizsch Granodiorite, etc., as shown in figure 3.2.

3.2 Groundwater contamination

The overall study area is a former chemical industrial site, which has significant groundwater contamination and a volume of 200 million m^3 (Wycisk *et al.*, 2003). This area is used for monitoring activities of the Agency for Environmental Protection (“Landesamt für Umweltschutz Sachsen-Anhalt") and state-offices for environmental protection (“Staatliche Ämter für Umweltschutz"). Former intensive open cast mining activities (1830–1992) and industrial waste deposits (from 1890) in contact with the groundwater has changed the hydrogeological situation of the area (Chemie AG, 1983; Wycisk *et al.*, 2009). Groundwater flow and contaminants transport patterns have changed over time. In addition, a big flooding event of the river Mulde in August 2002 led to quick filling of open pit lignite mining lake, resulting in a water level rise of over 8 m (Wycisk *et al.*, 2005). The groundwater contaminants are heterogeneously distributed and have temporal variation in the flow direction. The main organic contaminants are benzene, ethylbenzene and xylene (BTEX), chlorobenzene, dichloroethene, trichloroethene, hexachlorocyclohexane (HCH); while the main inorganic contaminants are sulphate, chlorides, and heavy metals (Heidrich *et al.*, 2004a; Popp *et al.*, 2000). In a depth-oriented sampling of the study area under the SAFIRA pilot project, chlorobenzene concentration was higher from a depth of 16-20 m below the surface.

3.3 Nature and availability of data

The groundwater quality monitoring data of the former industrial and mining region from the Federal State Agency for Abandoned Polluted Areas – LAF (Landesamt für Altlastenfreistellung Sachsen-Anhalt) has been used under a data exchange contract between LAF, the Department for Groundwater Remediation at Helmholtz Centre for Environmental Research (UFZ), and the Department for Hydrogeology and Environmental Geology at Martin Luther University Halle-Wittenberg. In Bitterfeld/Wolfen, 436 wells in the Tertiary and 510 wells in the Quaternary aquifer constitute the existing groundwater long-term monitoring (LTM) network for the monitoring, remediation and management of groundwater contamination.

Although groundwater monitoring data from the existing LTM network is available from the year 1991 to 2009, a data set of physicochemical parameters and associated information from 30th Sept. 2003 to 15th Dec. 2009 has been used for LTM network optimization, hydrogeological numerical modelling and strategies. This date range was chosen due to considerations of prior flooding events (Wycisk *et al.*, 2005) and data quality based on statistical analysis. Physicochemical properties and contaminants concentration data including α-Hexachlorocyclohexane (α-HCH), Monochlorobenzene (MCB) and other inorganic parameters such as temperature, pH-value, and electric conductivity (EC), concentrations of sulphate (SO_4^{2-}), sulphite (SO_3^{2-}), nitrate (NO_3^-), ammonium (NH_4^+), and iron (Fe^{3+}) from the period 2003 to 2009 were used in this methodological study. The groundwater monitoring database also includes the name of the groundwater observation well, coordinates, elevation data of the monitoring well, and the screen depth, stratigraphic geological layer, stratigraphic horizon [Quaternary (Q), Tertiary (T) and Quaternary-Tertiary (Q-T)], the date and time of sampling and the name of the analysing laboratory (Table 3.1). In table 3.1, columns 2-8 summarize the total number of wells and samples for each contaminant. The 9th column gives the total number of wells and samples during the overall period 2003-09. The majority of wells were frequently sampled.

Table 3.1: Number of wells and samples from 30th Sept. 2003 to 15th Dec. 2009, showing number of wells monitored each year for physicochemical parameters.

Year	2003	2004	2005	2006	2007	2008	2009	2003-09*
No of well	477	579	496	663	682	521	38	827
No of sample	796	749	729	847	711	519	38	4389
Temperature	787	719	703	841	501	519	38	4108
pH	786	719	720	865	501	519	38	4148
Eh	787	701	703	841	501	519	38	4090
NO_3^-	787	709	719	866	414	519	31	4045
SO_3^{2-}	796	703	700	864	424	519	31	4037
SO_4^{2-}	795	729	720	866	424	519	31	4084
NH_4^+	717	729	720	866	420	519	31	4002
Fe^{2+}	0	8	102	18	0	0	0	128
Fe^{3+}	772	709	694	841	475	519	38	4048
α-HCH	772	682	698	823	500	519	38	4032
MCB	735	678	739	2156	1954	2307	2097	10666
Screen above sea level	765	728	708	853	484	519	38	4095
Elevation AMSL	796	729	720	866	501	519	38	4169

Note: The numbers listed under the column 2003-09* indicate the total number of samples from 2003 to 2009. Some of the wells were found to be sampled more than once in a year.

A 3-D geological model of 64 km^2 and a 3-D hydrogeological model of 320 km^2, developed at the Department of Hydrogeology and Environmental Geology, Martin Luther University, Halle (Saale), Germany, were used to understand the spatial and temporal hydrogeological heterogeneity of the area (Gossel *et al.*, 2009; Wollmann:, 2008). The groundwater contaminants are heterogeneously distributed and vary temporally in the flow direction.

4. Method

4.1 Long-term groundwater monitoring strategies

Information about properties and behaviour of groundwater systems are required for strategic planning and operational actions in groundwater management. In order to design and improve monitoring strategies, it is necessary to describe the components of monitoring strategies. The components of a groundwater monitoring strategy were analysed as a case study of a groundwater monitoring scenario in the study area of Bitterfeld/Wolfen in the Federal State Saxony-Anhalt, Germany, as shown in the logic diagram (figure 4.1). In this component analysis, the monitoring site characteristics and long-term monitoring data were obtained from various sources including cooperation of the SAFIRA I and II projects and the LAF Sachsen-Anhalt (section 3.2).

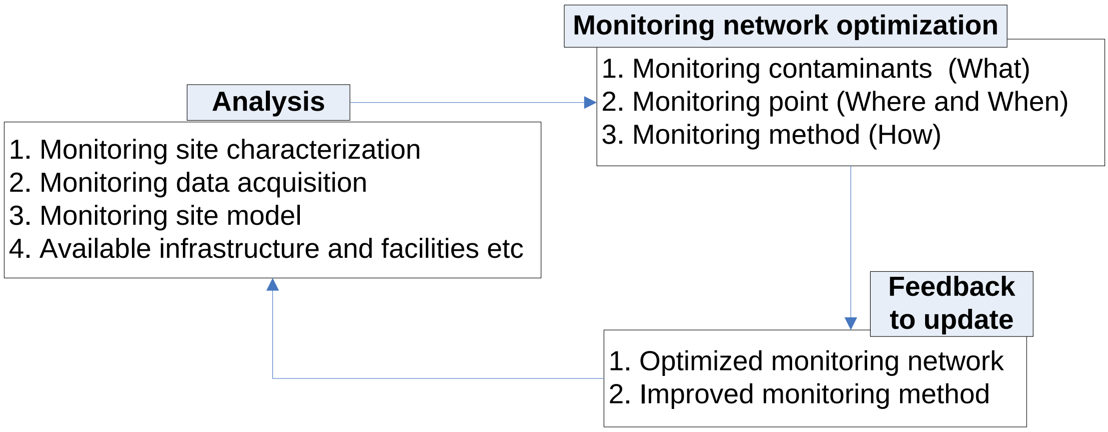

Figure 4.1: Logic diagram showing components of groundwater monitoring strategies as a circular continuous process.

Among the groundwater physicochemical properties and contaminants concentration data, representative contaminants were identified for the monitoring strategy. In this analysis, priority was given to the representative contaminants in the groundwater system alone with associated uncertainties with their spatial and temporal variabilities. The representative contaminants were identified using descriptive statistics and statistical modelling of all available water quality and contaminant concentration data. While identifying representative contaminants, World Health Organization (WHO) standards for drinking water and maximum contamination limit (MCL) of pollutants and contaminant concentration were considered along with the associated human health risk and the performance of groundwater remediation plans in the study area (EPA, 2012; WHO, 2011).

4.2 Statistical methods

The available data set (in Excel file format (*.xls)), as presented in section 3.2, consists of physicochemical properties and contaminant concentration values recorded from 1991 to 2009. The recoded physicochemical properties and contaminant concentrations had both negative and positive values. Parameter values with a negative sign indicate a measurement below the detection limit. These negative values were replaced by a value of one tenth of the detection limit for that parameter at their respective laboratory. Statistical methods were used to analyse and evaluate the distribution of data quality from groundwater monitoring. Univariate statistical analysis was undertaken to distinguish the spatial distribution of one variable from that of others. Similarly, multivariate analysis was applied to calculate the effects of variables and their statistical correlation other variables at a given time. Moreover, multivariate statistics were used to optimize the existing groundwater monitoring network.

4.2.1 Univariate statistics

Univariate analysis of physicochemical parameters (summarized in table 3.1) was carried out for quantitative analysis of characteristics of variables in terms of the central tendency, distribution, and dispersion (defined in appendix 1). In this analysis, it was assumed that the response variable was influenced by only one other factor.

Homogeneity of variance

Homogeneous variance means that variances should be the same throughout the data (Tabachnick *et al.*, 2001). If separate groups of data within one data set are collected from the study area, then the variance of outcome variables should be the same in each of these groups if the variance in homogeneous. If monitoring data is continuously collected, then this assumption means that the variance of one variable should be stable at all levels of the other variable. This analysis was carried out to find whether to use parametric or nonparametric statistical tests for the groundwater monitoring study. In order to use parametric statistical tests, the data set should be normally distributed (McCluskey and Lalkhen, 2007). In order to test homogeneity of variance of the data set, a mean vs variance test and Levene's test were carried out.

To test homogeneity of variance of the data set in terms of mean vs variance, the overall data set was divided into five data sets based on the geographical distribution of the monitoring wells. A plot of the computed variance versus the mean of each physicochemical parameter in the five data sets was used to study homogeneity of variance in the dataset. The plot of the variance versus the mean gives an insight into the homogeneity of variance. However, since this could be subjective, Levene's test (Levene, 1960) was conducted to overcome this problem of subjectivity.

Levene's test tests the null hypothesis that the variances in different groups are equal. The test is based on a one-way analysis of variance (ANOVA) conducted on the deviation scores; i.e., the absolute difference between each score and the mean of the group from which it came. If Levene's test is significant at $p \leq .05$ then the null hypothesis is incorrect and hence the variances are significantly different, meaning that the assumption of homogeneity of variances has been violated. However, if the Levene's test is non-significant (i.e. $p > .05$) then the variances are roughly equal and the assumption is tenable.

Data normalization

Based on homogeneity tests such as the mean vs variance test and Levene's test, the data set of each physicochemical parameter was subjected to normalization. In the data normalization process the data attributes within each data set were organised so as to increase the cohesion of entity types and reduce the data redundancy. In this process, the data set was filtered and legitimate outliers were removed. The data set, with parameter concentration x, parameter mean μ and standard deviation σ, was then normalized using following mathematical relation:

$$\mathrm{NORMDIST} = \frac{-\frac{1}{2}\left(\frac{x-\mu}{\sigma}\right)^2}{\sqrt{2\pi\sigma}}$$ Eqn. 4.1

If mode is 0, NORMDIST calculates the probability density function of the normal distribution.

$$\mathrm{NORMDIST} = \int_{-\infty}^{x} \frac{e^{-\frac{1}{2}\left(\frac{x-\mu}{\sigma}\right)^2}}{\sqrt{2\pi\sigma}}\,dt$$ Eqn. 4.2

If mode is 1, NORMDIST calculates the cumulative distribution function of the normal distribution.

4.2.2 Multivariate statistics

As the univariate analysis assumes that the response variable is influenced only by one other factor, multivariate analysis of physicochemical parameters (summarized in table 3.1) was also carried out to test this assumption. Multivariate analysis involves analysis of more than one statistical outcome variable at a time. The multivariate analysis was carried in terms of principal component analysis and cluster analysis.

Principal component analysis

Principal Component Analysis (PCA) was applied on experimental data standardized through a z-scale transformation in order to avoid misclassification due to wide differences in data dimensionality (Simeonov *et al.*, 2003). PCA transforms the original variable into uncorrelated variables called principal components, which are linear combinations of the original variables. The new axes lie along the direction of the maximum variance. PCA provides an objective means of data reduction with minimum loss of original information, so that the variation in the data can be accounted for as concisely as possible (Singh *et al.*, 2009). PCA provides information about the variables responsible for spatial variation in groundwater quality (Wold *et al.*, 1987). PCA of the normalized variables was performed to extract significant PCs.

Cluster analysis

Based on similarities within a class and dissimilarities between classes, cluster analysis (CA) groups the objects into classes or clusters (Johnson and Wichern, 2002; Singh *et al.*, 2009). The monitoring wells that have similar characteristics to each other are grouped together. The greater the similarity (or homogeneity) within a group and the greater the difference between groups, the better or more distinct the clusters that are formed. CA helps in data interpretation and reveals patterns within the data. Among clustering approaches such as K-means, agglomerative hierarchical clustering, and DBSCAN (for density-based spatial clustering of applications with noise) etc., the agglomerative hierarchical clustering (AHC) technique was chosen because the algorithm combines or divides existing groups, creating a hierarchical structure that reflects the order in which groups are merged or divided (Morey *et al.*, 1983). Hierarchical agglomerative cluster analysis was performed on the normalized data set by means of Ward's method, using squared Euclidean distances as a measure of similarity (Day and Edelsbrunner, 1984). Ward's algorithm (Ward Jr, 1963) assumes that a cluster is represented by its centroid. The algorithm measures the proximity between two clusters in terms of the increase in the sum of the squared errors (SSE) that results from merging the two clusters, which is given by:

$$SSE = \sum_{i=1}^{n} x_i^2 - \frac{1}{n}\left(\sum_{i=1}^{n} x_i\right)^2 \qquad \text{Eqn. 4.3}$$

where n is total number of contaminants concentration observation.

This method attempts to minimize the sum of the squared distances of points from their cluster centroids (Tan *et al.*, 2005). AHC techniques produce an ordering of the monitoring wells. This is informative for displaying monitoring well locations in the monitoring network. When smaller clusters are generated, identification of typical monitoring wells in the cluster becomes easier. However, there is no provision for relocation of monitoring wells that may have been 'incorrectly' grouped at an early stage of clustering. CA was applied to the water quality data set with a view to grouping similar sampling monitoring locations, which resulted in agglomerative hierarchical clustering (dendrogram). It was applied to detect similarities between different sampling sites, separately for Quaternary and Tertiary aquifers and for different hydrological seasons from 2003 to 2009. The clustering convincingly reveals groups of similar sampling sites.

4.2.3 Pre-processing of LTM network data

The data set of physicochemical parameters (table 3.1) and associated information from the monitoring wells of Bitterfeld/Wolfen from 30th September 2003 to 15th December 2009 was used for optimization of the monitoring network. The data set was divided into seven annual groups (2003-2009). The annual groups were further divided into subgroups based on dry and wet hydrological seasons, and quaternary and tertiary aquifers. As a result, the overall data set was divided into 26 subgroups based on annual hydrological seasons and aquifer types. It should be noted that some of the wells were sampled twice in the same hydrological seasons, as shown in figure 4.2.

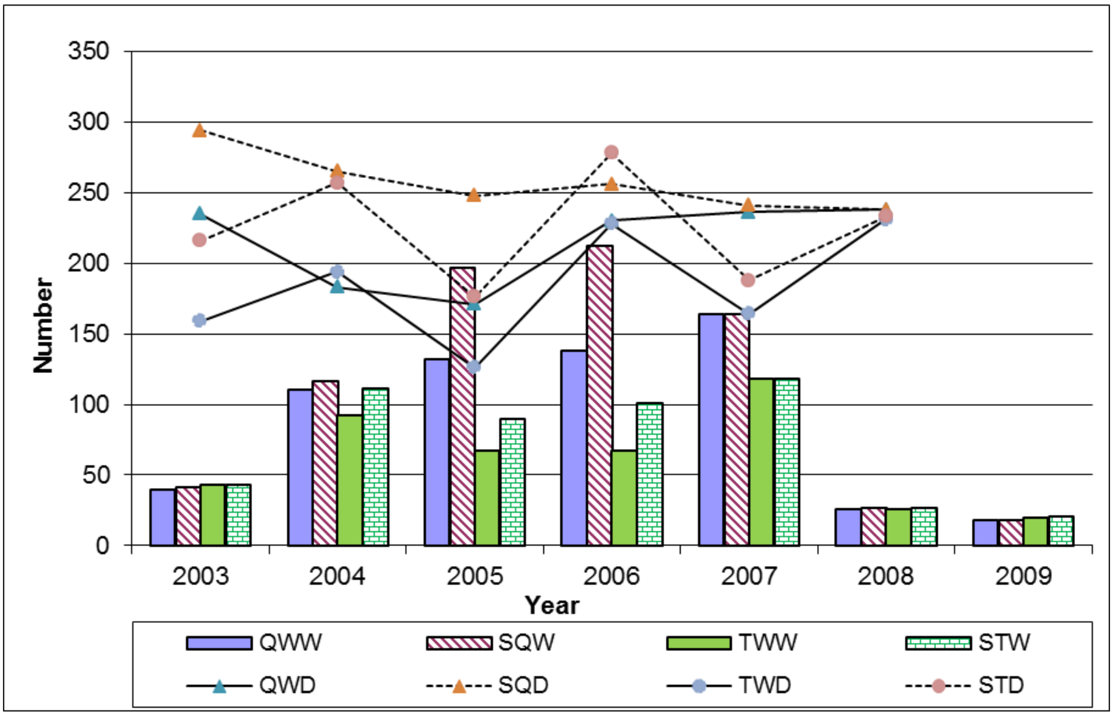

Figure 4.2: Number of wells and samples from the monitoring network. (QWW: Quaternary well in wet hydrological period, QWD: Quaternary well in dry hydrological period, SQW: sample from quaternary well in wet hydrological period, SQD: sample from quaternary well in dry hydrological period, TWW: Tertiary well in wet hydrological period, TWD: Tertiary well in dry hydrological period, STW: sample from tertiary well in wet hydrological period, STD: sample from tertiary well in dry hydrological period).

4.2.4 Spatial optimization of the LTM network

Taking into account the multiple variables in the data set (table 3.1) from the monitoring network, the AHC method was used to classify monitoring wells based on observed contaminant concentrations from individual samples in each subgroup, so that monitoring wells of the resulting cluster are similar to each other but distinct from other clusters. Dendrogram was used to illustrate the arrangement of the clusters of monitoring wells. In the cluster, when a group constitutes three or more monitoring wells, the middle monitoring well was considered to be an essential well, whilst the remaining wells of the group were labelled as redundant wells. In this way, the AHC method was used to classify monitoring wells into essential and redundant wells for each of the twenty-six subgroups. Among these 26 subgroups of monitoring wells, the wells that were labelled as essential wells and those that have a low degree of redundancy were recommended for continuous monitoring in the groundwater monitoring network. Meanwhile, many of the monitoring wells that were labelled as redundant were recommended to be eliminated from the monitoring network. Figure 4.3 depicts a flowchart of the applied methods.

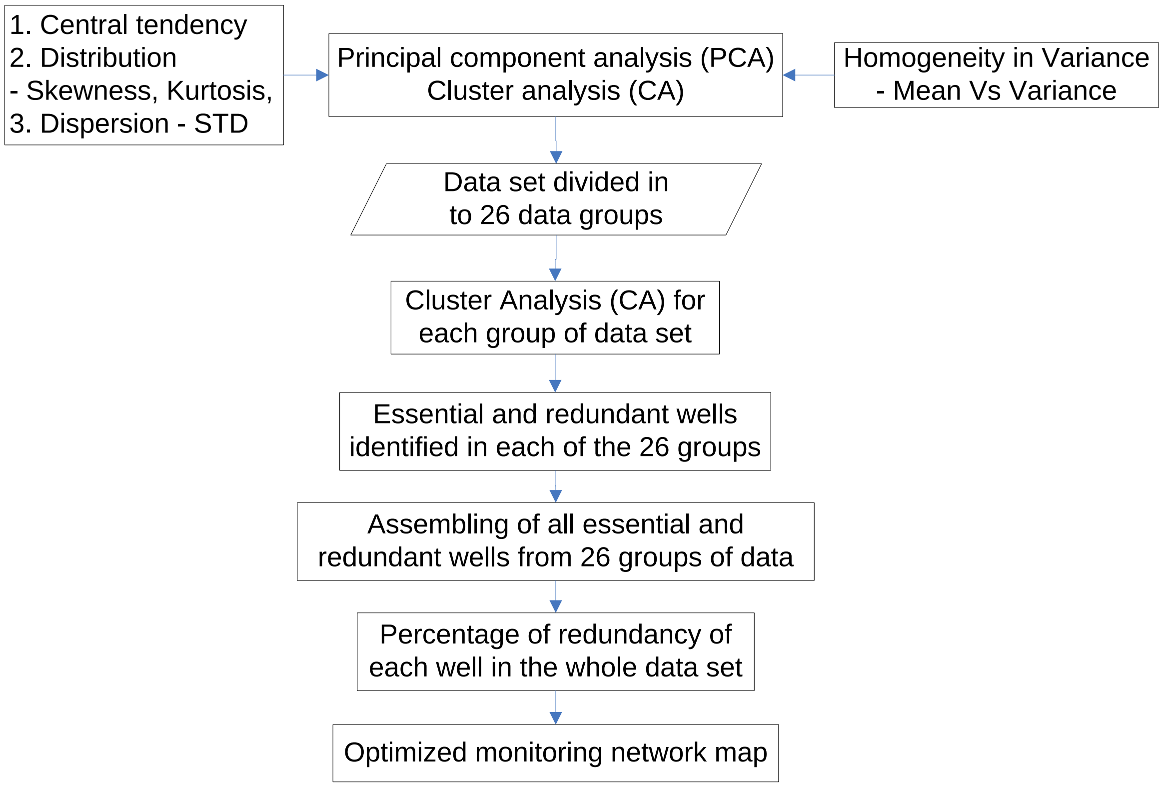

Figure 4.3: A flow chart of the applied methods for optimization of the existing long-term monitoring network showing use of various statistical method in order locate redundant monitoring wells in the network.

The monitoring wells labelled as essential and redundant wells, along with their percentage of redundancy, were used to prepare an optimized monitoring network map.

Dependency on the limit of the percentage of redundancy

In the statistical monitoring network optimization method, the AHC method was used to classify monitoring wells into essential and redundant wells based on the clustering result from several subgroups of the data set. In this case, the wells that were labelled as redundant in several subgroups were tagged as redundant wells. The question arose about what would be the limit for deciding whether the well is essential or redundant. In order to solve this issue, the limit of the redundancy was analysed in terms of percentage of redundancy in the subgroup of the data set. As described above, the data set from the tested research area, Bitterfeld/Wolfen, was divided in to 26 subgroups based on the hydrological season and year of sampling. The AHC method was used to classify monitoring wells into essential and redundant wells for each subgroup of data. If a monitoring well was tagged as redundant well in more than 13 subgroups of data, then it was assigned to be redundant in more than 50% of the 26 data sets. For the data set from the tested research area, Bitterfeld/Wolfen, this 50% of redundancy was considered as a possible redundancy limit.

In this methodological study, as the classification of monitoring wells into essential and redundant depends upon percentage of redundancy in the data sets, dependency of the redundancy limit was analysed. The monitoring wells were categorised into essential and redundant wells with at percentage of redundancy limits varying from 10% to 100%. Dependency of this statistical method for the monitoring network optimization was graphically visualized.

4.2.5 Temporal optimization of the LTM network using a statistical method

Groundwater monitoring network optimization has previously been carried out by iterative thinning using Sen's method (Gilbert, 1987). The Iterative thinning refers to temporary removal of randomly selected data points from a time series of measurements of a given well. The algorithm consists of (i) estimating a trend using the entire time series; (ii) thinning the time series by a randomly selected fraction of the measurements, and then (iii) re-estimating the trend to determine if the slope estimate is still close to the original slope. The randomly removed fractions of the data is only allowed remain removed from the time series if the slope estimated on the reduced data set is within the bounds of the confidence interval on the slope using the full dataset (Cameron and Hunter, 2002). To avoid statistical assumptions inherent in standard linear regression methods, trend estimation was carried out using Sen's method (Gilbert, 1987; Sen, 1968). Sen's procedure is non-parametric, and is readily adapted to non-detect measurements and to irregular sampling frequencies (Brauner, 2006). The method does not calculate the slope for missing data points and can be used to predict a median slope if the number of non-detected (ND) measurements is less than (n-1)/2.

Sen's estimate (Q') is simply the median value of the resulting list of slopes and is given by:

$$Q = \frac{x_j - x_i}{j - i} \qquad \text{Eqn. 4.4}$$

Q is the slope between data points. x_i and x_j are concentrations measured at times i and j. Time j is after time i (j > i).

$$Q' = \text{median slope} = Q_{[(N+1)/2]} \qquad \text{if N is odd,} \qquad \text{Eqn. 4.5}$$

$= (Q_{[N/2]} + Q_{[(N+2)/2]})/2$ if N is even

where N is the number of calculated slopes.

A two side (M_1, upper and M_2, lower) confidence interval for the median slope is estimated using $Z_{statistic}$ and Mann-Kendall statistic (VAR(S)). If there is a two-sided confidence interval of 95%, the $Z_{(1-0.05/2)} = Z_{0.975} = 1.96$. Mann-Kendall statistic (VAR(S)) (Kendall and Stuart, 1976; Mann, 1945) is given by:

$$VAR(S) = \frac{1}{18}\left[n(n-1)(2n+5) - \sum_{p-1}^{q} t_p(t_p-1)(2t_p+5)\right]$$

Eqn. 4.6

where n is number of sampling data points, t_p is the number of ties for the p^{th} value and q is the number of tied values. Eqn. 4.6 may be used for values of n between 10 and 40. The range of ranks for the specified confidence interval (C_i) (Gilbert, 1987) is given as shown below:

$$C_i = Z_{1-i/2} * \sqrt{VAR(S)}$$

Eqn. 4.7

Taking the value of Eqn. 4.7, the ranks of the lower (M1) and upper (M2 + 1) confidence limits can be found using the following relation:

$$M_1 = \frac{N - C_i}{2}$$

and Eqn. 4.8

$$M_2 = \frac{N + C_i}{2}$$

The values of lower (M1) and upper (M2 + 1) confidence limits were used to define lower and upper boundaries along the median slope. The temporal optimization of the existing groundwater monitoring network was carried out using α-HCH, MCB and SO_4^{2-} concentration data set from 2003 – 2009 for each contaminant separately and together.

4.3 Geostatistical methods in groundwater monitoring

4.3.1 LTM network optimization using geostatistical methods

Optimizing an LTM network for multiple objectives requires the consideration of contaminant information, their physicochemical and toxicological properties, hydrogeochemical properties of the aquifer, and other associated information. In a polluted site, groundwater may contain various types of organic and inorganic contaminants. Based on the statistical analysis, the three representative contaminants selected from the groundwater physicochemical properties and contaminants concentration data for monitoring network optimization were viz MCB, SO_4^{2-} and α-HCH. MCB and SO_4^{2-} represent organic and inorganic contamination, respectively, in the research area. α-HCH, which is an organochloride, one of the isomers of hexachlorocyclohexane (HCH), represents pesticides. The contaminant concentration data of these three chemical parameters was used for monitoring network optimization separately, as shown in figure 4.4.

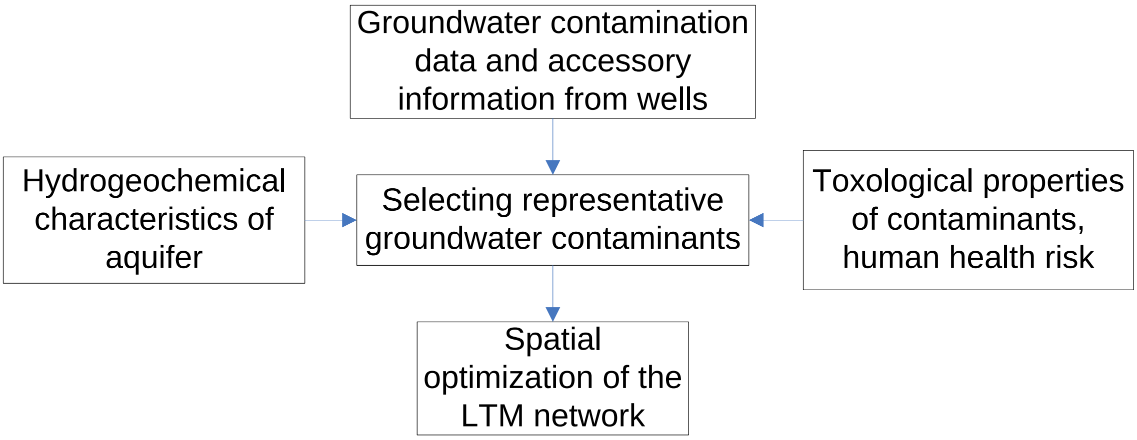

Figure 4.4 Conceptual flowchart of groundwater monitoring network optimization showing use of information in selecting representative contaminates in the monitoring network optimization.

A geostatistical spatial optimization algorithm, Geostatistical Temporal-Spatial algorithm (GTS), was used to predict redundant wells when the nearby wells offered the same information about the underlying plume (Cameron and Hunter, 2002; Cameron and Philip M. Hunter, 2010). In the GTS concept, a well is considered redundant if its removal does not significantly change the interpolated map of the contaminant plume. Location-based contaminant concentration data at a particular depth in the groundwater well on the monitoring date is prerequisite information for LTM network optimization. The investigation steps involved in locating redundant wells are shown in figure 4.5.

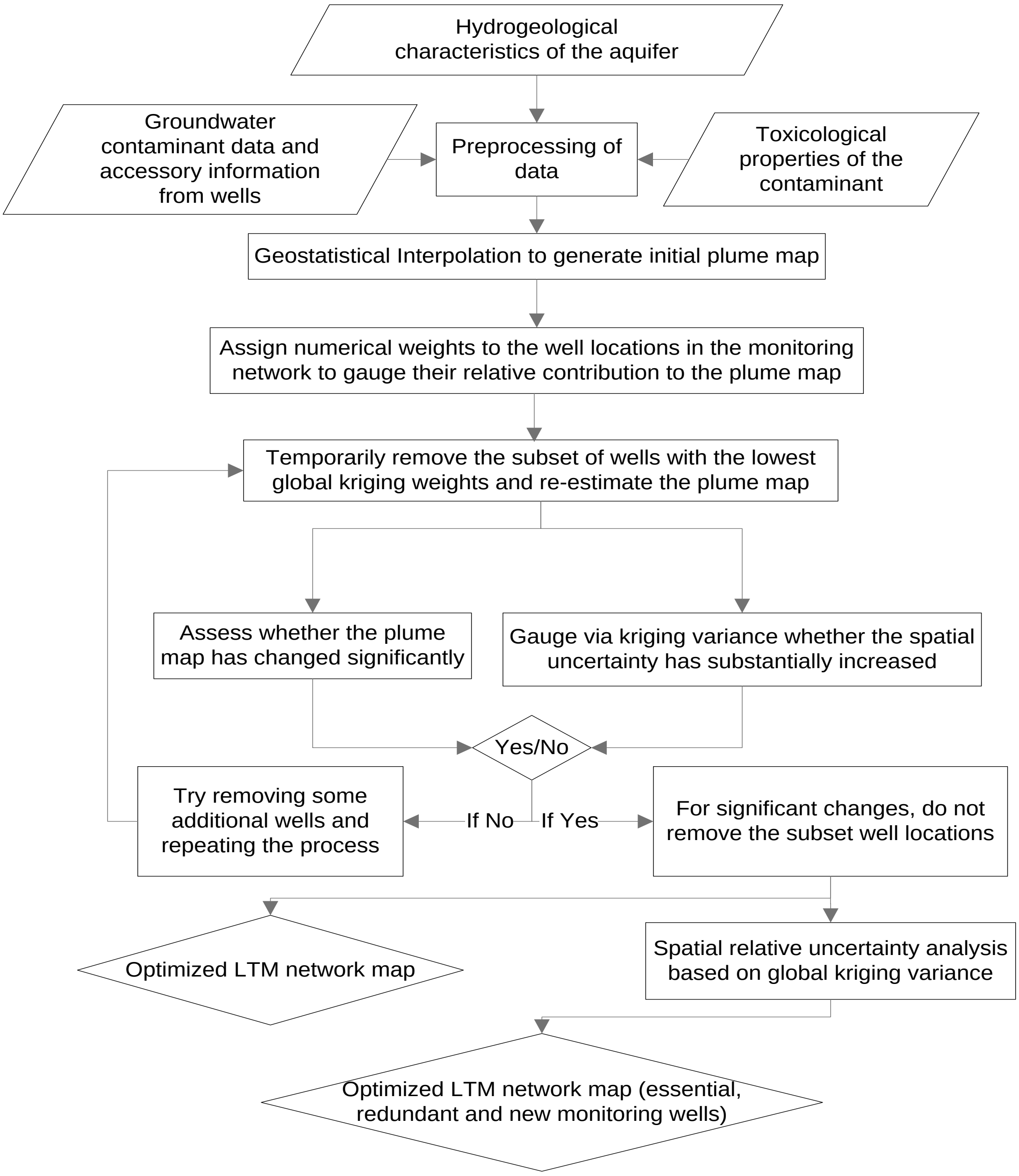

Figure 4.5 Research steps to locate essential and redundant wells and to propose new wells in the existing monitoring network (Modified from Cameron and Philip M. Hunter, 2010).

A contaminant concentration plume was generated, based on the input data of the concentration of MCB at a particular location of the well. The maximum contamination limit (MCL) of 100 µg/L, 0.2 µg/L, and 0.25 g/L for MCB, α-HCH and SO_4^{2-} respectively, as per US EPA, was given as the indicator limit for the statistical algorithm (EPA, 2001). The contaminate concentration was converted into an indicator value as:

$i_C(t) = 1$ if $z(t) > C$ and 0 if $z(t) \le C$ Eqn. 4.9

where, *i*C(t) is the indictor value, z(t) is the concentration at time t, and C is the maximum contamination limit (MCL).

In areas with more uncertain groundwater contaminant concentrations, some wells were sampled more often than others in the neighbourhood. To avoid assuming more statistical weight to often-sampled wells, each dataset was divided arbitrarily into a series of quarterly time slices (Cameron and Hunter, 2010). That is to say, for a three-month time span, each well's relative weight will be considered as one sample, even if it is sampled more frequently.

To measure the correlation based on the distance and direction between pairs of sampling locations for each contaminant, an empirical variogram was modelled by fitting a positive definite covariance model. The empirical spatial variogram, γ, can be expressed as:

$$\gamma(\Delta h) = \frac{1}{2N(\Delta h)} \sum_{i.j \left\| x_j - x_i \right| - \Delta h \ \| \le \varepsilon} \left[i_C(x_j) - i_C(x_i) \right]^2 \quad \text{Eqn. 4.10}$$

where Δh is the targeted lag distance and may depend on direction; x_i and x_j are the i^{th} and j^{th} monitoring well locations; and N(Δh) is the number of indicator pairs contributing to the summation for lag Δh.

A plume map was created for the monitoring network from the numerical weights of the wells based on global kriging. In this process, two intermediate computations are used: (i) the local kriging weights assigned to sampled locations are accumulated and averaged to generate a ‘global’ interpolation weight for each well (Isaaks and Srivastava, 1989) and (ii) the local kriging estimation variance is used to indicate the relative uncertainty of the local block estimate, as compared to estimates at other blocks (Cameron and Hunter, 2002).

The ordinary kriging algorithm divides the monitoring area into a series of non-overlapping blocks. At each block, a simple search algorithm locates the set of sampled locations closest to the block. Then, using the modelled spatial covariance function, local kriging weights (λ^B) were computed based on the spatial configuration of the known indicator values within and surrounding the block, and the spatial correlation between the average block location and each known indicator. These local weights are then combined with the known indicator values to generate a block indicator estimate, consisting of a weighted average of the $n(x_B)$ indicators located within the search radius of the block (x_B), which is estimated as (Cameron and Hunter, 2002):

$$i_C(x_B) = \sum_{i=1}^{n(x_B)} \lambda_i^B i_C(x_i) \quad \text{for } x_i \in \text{ search radius of block } x_B \qquad \text{Eqn. 4.11}$$

Averaging of the local kriging weights assigned to a given well generates global interpolation weights (λ^G) that can be used to estimate the well's overall contribution to the interpolated map (Cameron and Hunter, 2002), and are given by:

$$\lambda^G(x_i) = \frac{1}{N_B}\sum_{B=1}^{N_B} \lambda_i^B(x_i) \qquad \text{Eqn. 4.12}$$

where N_B is the total estimated number of blocks and x_i is the location of the i^{th} sampled well.

The global kriging weights give relative rankings of well locations in terms of independent spatial information that is provided. The wells with the lowest global kriging weights, owing to smaller local kriging weights, are potentially spatially redundant wells. The subsets of wells with the lowest global kriging weights were then temporarily removed from the network and the plume map was re-estimated. In the cases when the removal of the subset of wells did not significantly change the plume map, the subset of wells was permanently removed. This process was repeated until the removal of a subset of wells changed the plume map. In the cases when the removal of a subset of wells significantly changed the plume, that subset of wells was not removed from the monitoring network. To limit changes to the plume map, a two-sided (lower and upper) confidence interval of 95% was assigned when considering the lower and upper limit of median plume concentration. The relative spatial uncertainty for the installation of new monitoring wells in the existing LTM network is based on the local kriging variance and is given by the global kriging variance (kv^G), defined as:

$$\mathrm{kv}^{\mathrm{G}} = \frac{1}{N_B}\sum_{B=1}^{N_B} kv^B(x_B) \qquad \text{Eqn. 4.13}$$

where x_B denotes the location of the B^{th} block and $kv^B(x_B)$ is the local kriging variance of the B^{th} block (Cameron and Hunter, 2002).

The groundwater LTM network has been spatially optimized for MCB, α-HCH and SO_4^{2-} both individually and together, and in 2-D and 2.5-D of the groundwater aquifer. The 2-D analysis treats all well locations as if they exist on a flat 2-D plane regardless of potentially different depths of the well screens. This, of course, is most applicable when there is just a single, fairly uniform and well-connected aquifer. However, the 2.5-D analysis assumes that there are multiple aquifers, or hydrostratigraphic layers in the aquifer that have no hydraulic interconnection. In 2.5-D analysis, the LTM network is optimized separately for each hydrostratigraphic layer in the aquifer or aquifers. This also means that the maps for 2.5-D analysis are constructed on each layer separately using data from that layer only. The data used is segregated into subsets, each subset representing one Chemical of Concern (COC) for each vertical zone and time slice triplet. The Quadratic Logistic Regression (QLR) mapping algorithm then uses the data from a given subset to map the layer and time frame represented by that given triplet.

4.3.2 Grid width and dimension dependency

In recent decades, several studies have addressed methods for monitoring network optimization (Dhar and Datta, 2009; Nunes *et al.*, 2004a). However, these studies do not attempt to find which factors influence the monitoring optimization methods. In this study, an attempt has been made to thoroughly analyse the influence of various factors on the optimization method, which can remarkably change the decision about redundancy and necessity of new wells in the monitoring network.

In the monitoring network optimization using geostatistical methods, a plume map was created for the well locations in the monitoring network from the numerical weights of the wells obtained from global kriging. In this process, an average kriging weight is computed using an interpolation method. This interpolation of contaminant concentration depends upon width and number of grids. Hence, in the optimization process, a grid width from 1 m to 1000 m was defined in order to discover ambiguities in the method (figure 4.6). Visualizing the results obtained in terms of number of essential, redundant and new monitoring wells should help decision makers.

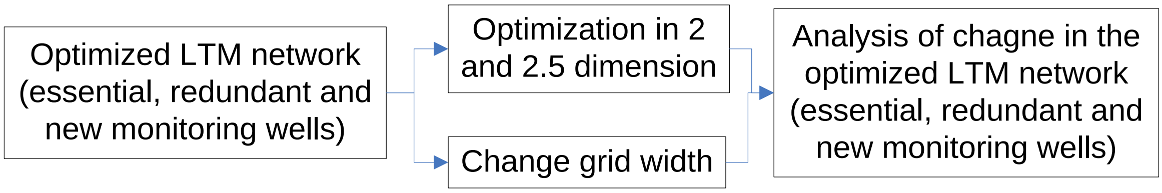

Figure 4.6: Research steps to study grid width dependency of geostatistical methods in groundwater monitoring network optimization.

Similarly, as aquifer characteristics remarkably influence the movement of groundwater, the monitoring network optimization was carried out separately for Quaternary and Tertiary aquifers. Moreover, in the interpolation method to compute plume maps, these aquifers were also defined as 2-D and 2.5-D aquifers. In the 2-D treatment of aquifers, the sampling depth of the monitoring wells was not taken in account. In this case, all of the wells were assumed to be in the same 2-D plain. Meanwhile, in the 2.5-D case, the aquifer is considered to have a number of hydrogeological layers. In this case, the sampling depth of the monitoring wells was taken in account.

In order to study the influence of dimension and grid width on monitoring network optimization methods, the optimization process was carried out considering grid widths from 1 m to 1000 m in both 2 and 2.5 dimensions.

4.3.3 Contaminants association

Based on principal component analysis of hydro-geochemical data, the three representative variables, concentration of α-HCH, MCB, SO_4^{2-}, were used individually to monitor network optimization. In the selected dataset (section 3.3), these representative variables have a low Pearson correlation. However, in order to study the influence of multiple variables on the optimization process, the monitoring network was optimized using the data sets of two and three variables together. In this case, co-kriging was used to compute co-kriging numerical weights from contaminant concentrations for each monitoring well. These numerical weights were used to create a plume map of the monitoring network. Temporary removal of the subset of wells with the lowest co-kriging weights and re-estimation of the plume map was conducted to assess whether the plume map had changed significantly, to decide whether to permanently remove these wells, as explained in section 4.3.1.

4.3.4 Groundwater flow direction and aquifer homogeneity

The directional dependency of groundwater monitoring has been studied using directional variograms. Mathematically, the experimental spatial variogram, γ(Δx, Δy), can be written as follows:

$$\gamma(\Delta x, \Delta y) = \frac{1}{2} E[\{Z(x + \Delta x, y + \Delta y) - Z(x, y)\}^2] \qquad \text{Eqn. 4.14}$$

where Z(x,y) is the concentration of contaminant at location (x,y), and E[] is the statistical expectation operator. In a set of observed data denoted as $\{(x_1, y_1, z_1), (x_2, y_2, z_2), \ldots (x_n, y_n, z_n)$, (x_1, y_1, z_1) is the first sampling location. i and z_i are the associated observed concentrations. Therefore, $(\Delta x_{i,j}, \Delta y_{i,j}) = (x_i - x_j, y_i - y_j) \approx (\Delta x, \Delta y)$.

Let S(Δx, Δy) be the set of all such pairs in the data set.

Then, $S(\Delta x, \Delta y) = \{(i,j) \mid (\Delta x_{i,j}, \Delta y_{i,j}) \approx (\Delta x, \Delta y)\}$

Also, let N(Δx, Δy) equal the number of pairs in data set S(Δx, Δy). Then the experimental variogram can be written as:

$$\hat{\gamma}(\Delta x, \Delta y) = \frac{1}{2\, N(\Delta x, \Delta y)} \sum_{(i,j) \epsilon S(\Delta x, \Delta y)} (z_i - z_j)^2 \qquad \text{Eqn. 4.15}$$

The experimental variogram estimation was carried out using Golden Surfer software (2011). Although 3-D geostatistical analysis was a topic of interest, it was not incorporated in this study. In this study more priority was given to the statistical approach to determine groundwater flow direction and aquifer heterogeneity.

A data set is said to be anisotropic if it has spatial correlation and depends on direction. The variograms constructed based on the contaminant concentration data set were anisotropic in nature. Therefore, valid variogram models that incorporate directional dependence were constructed. Standard models such as spherical, exponential, Gaussian, and power were used to model the data set. The best fitting model, considering range, sill, nugget effect and shape of the model, was selected. A variogram was constructed from α-HCH, MCB and SO_4^{2-} concentration data set for each year from 2003 – 2009, according to seasons (summer: May–October; winter: November–April), and to hydrologic seasons (March – May: high groundwater level, September – November: low groundwater level). The range and sill were estimated for various directional variogram models.

A homogeneity index (RV index) was defined based on range, sill and variance of the variogram (Hubert, 2011) and is given by:

$$\text{Homogeneity index} = \frac{\text{range}}{\frac{sill + variance}{2}}$$ Eqn. 4.16

The RV index numerically estimates homogeneity of the aquifer based on the variogram model.

4.4 Hydrogeological modelling and LTM Network Optimization

Groundwater models are designed to represent a simplified version of real groundwater scenarios in order to simulate and predict aquifer conditions (Prickett, 1975). Groundwater models can be broadly classified as sand tank models, analog models, and mathematical models. In this study, a mathematical model was used to simulate the groundwater scenario. Furthermore, mathematical models can be divided into two categories: (a) groundwater flow models, which solve for the distribution of head in a domain and (b) transport models, which solve for the concentration of solute as affected by advection, dispersion, and chemical reactions.

In this methodological study of monitoring network optimization for the verification of groundwater monitoring strategies using a 3-D groundwater hydrogeological model, the overall steps were divided into the following steps (Poeter and Hill, 1997):

a. Defining the problem

b. Defining the boundary conditions

c. Developing an initial model of the study area

d. Choosing the governing equations and describing the physical problem

e. Calibrating and validating the numerical model

g. Application of the hydrogeological model

The 3-D groundwater hydrogeological modelling approach has been used to simulate near to realistic situations of the study area when there is limited data availability.

4.4.1 3-D groundwater hydrogeological modelling

In general, mathematical models consists of a set of differential equations that are known to govern various functions, such as predictions of groundwater withdrawal (Gremmen *et al.*, 1990), design of groundwater protection zones (Thomsen *et al.*, 2004), and simulation of subsurface flow and solute transport (Gossel *et al.*, 2009; Meyer and Brill, 1988) at various scales (Ashraf and Ahmad, 2008; Singh and Woolhiser, 2002). The numerical method chosen to simulate subsurface flow and transport simulation can be a finite difference method (FDM) (Clement *et al.*, 1994; Hunt *et al.*, 1998) or a finite element method (FEM) (Simpson and Clement, 2003; Wang and Anderson, 1995; Yeh, 1981). Considering the spatial variation of material properties, flux boundaries and the possibility of fine discretization, FEM was chosen over FDM for the hydrogeological modelling. The Finite Element subsurface FLOW system (FEFLOW) (Diersch, 2009; Trefry and Muffels, 2007) was used to simulate groundwater flow and mass transfer in the model area.

FEM simulation is based on the principles of physical conservation of mass, linear momentum and energy in a transient numerical analysis. Darcy's Law and the continuity principle are basic principles involved. Henry Darcy formulated a relationship that states that volume discharge rate *(Q)* is directly proportional to the head drop $(h_2 – h_1)$ and to the cross-sectional area *(A),* but inversely proportional to the length difference $(l_2 – l_1)$ (Darcy, 1856). The equation can be written as follows:

$$Q = -K\,A\frac{(h2 - h1)}{(l2 - l1)} \qquad \text{Eqn. 4.17}$$

where K is the hydraulic conductivity. In three dimensions, the head, h = h(x, y, z), and the head drop is then given in three dimensions. Assuming a vertical directional of head h = h(z), an isotropic porous medium and a discharge rate Q that is independent of time, the volume rate of flow per unit area (q = Q/A) is called the specific discharge (Wang and Anderson, 1995). In the differential form, the specific discharge, also known as Darcy velocity, can be written as follows:

$$q = -K\,\frac{dh}{dl} \qquad \text{Eqn. 4.18}$$

In the 3-D scenario, q is the resultant vector of q_x, q_y and q_z corresponding to x, y and z components respectively.

4.4.2 3-D groundwater flow model

The differential 3-D groundwater flow equation is derived for a small representative elemental volume (REV), assuming effectively constant properties of the medium. The water that flows in and out of this small volume in terms of flux is used to balance mass, along with Darcy's law. The conservation of mass states that for a given increment of time (Δt) the difference between the mass flowing in across the boundaries, the mass flowing out across the boundaries, and the sources within the volume, is the change in storage. Darcy’s Law combined with a continuity equation for an inhomogeneous anisotropic confined aquifer is given by the following equation:

$$\frac{\partial}{\partial x}\left(K_x \frac{\partial h}{\partial x}\right) + \frac{\partial}{\partial y}\left(K_y \frac{\partial h}{\partial y}\right) + \frac{\partial}{\partial z}\left(K_z \frac{\partial h}{\partial z}\right) = S_s \frac{\partial h}{\partial t}$$ Eqn. 4.19

For a homogeneous anisotropic confined aquifer, equation 4.19 is reduced to the following:

$$K_x \frac{\partial^2 h}{\partial x^2} + K_y \frac{\partial^2 h}{\partial y^2} + K_z \frac{\partial^2 h}{\partial z^2} = S_s \frac{\partial h}{\partial t} \quad \text{or,} \quad K.\nabla^2 h = S_s \frac{\partial h}{\partial t}$$ Eqn. 4.20

In order to observe a range of scenarios, the groundwater flow model was simulated considering an anisotropic environment with initial and boundary conditions. At the test site, Bitterfeld/Wolfen megasite initial and boundary conditions were characterized in terms of global groundwater table elevation, water levels along river courses, model inflows and outflows (fluxes), groundwater recharge, and injection/extraction due to pumping wells. In groundwater flow modelling, initial and boundary conditions and material characteristics determine the flow.

Initial conditions

The initial condition is the head distribution in the model area at the beginning time (t = 0). The initial conditions may be represented by the following equation (Diersch, 1998):

$$h(x_i, 0) = h(x_i)$$ Eqn. 4.21

Considering the historical scenario of aquifer, appropriate initial conditions were assigned in the model.

Boundary conditions

Historically, the groundwater of Bitterfeld/Wolfen was relatively more dynamic because of lignite mining and associated spatial and temporal variations, shifting of Mulde river course, and seasonal variation in groundwater level. In order to incorporate these groundwater dynamics in the numerical code, four kinds of boundary condition (BC) must be applied. The first kind is a hydraulic head boundary condition (units is [L]), which is applied to define hydraulic head to node. The hydraulic head boundary is responsible for inflow into and outflow from the model. Inflow into the model area takes place when neighbouring nodes have a lower potential, whilst outflow occurs when there is a gradient from the neighbouring nodes towards the boundary condition.

The Neumann Boundary Condition, also known as second kind of boundary condition (unit is [L/T]), defines the inflow and outflow at a model element in the numerical model. In this case, inflows are considered as negative and outflows as positive when defining boundary conditions. Similarly, the Cauchy condition, also known as a third kind of boundary condition, defines transfer or leakage of a surface water body (Chen, 1987). In other words, this boundary condition is used to define a reference head combined with a conductance parameter. An example could be rivers or lakes with a limited connection to groundwater.

The inflow/outflow is calculated for an area perpendicular to flow (A), the transfer rate (Φ), and the difference between reference and groundwater head is given by:

$$Q = A*\Phi*(h_{ref}-h) \qquad \text{Eqn. 4.22}$$

where,Q is inflow or outflow to/from the model (units is [L]), h_{ref} is the reference water level, and h is the current hydraulic head in the groundwater. Again the transfer rate is given by:

$$\Phi : \text{transfer rate} = K/d \qquad \text{Eqn. 4.23}$$

where, K is hydraulic conductivity of the clogging layer, and d is thickness of the clogging layer. Additionally, the fourth kind of well boundary condition defines the specific extraction rate to a node or to a group of nodes along a well screen at well location. All of these four types of boundary condition were defined in the model.

4.4.3 3-D groundwater transport model (forward-in-time)

Although some modelling tools date back to the late 1960's, the development of hydrogeochemical models capable of describing multidimensional and multiple species solute transport is a relatively new pursuit (Elango *et al.*, 2004). In this study, the model in a 3-D environment, transport of single species, α-HCH, was simulated incorporating initial and boundary conditions and the nature of the transport material of the study area.

Initial conditions

Similar to the flow initial condition, the transport initial condition is the amount of mass distributed in the model area at the beginning (t = 0). An idealistic α-HCH concentration of 100 [mg/l] was induced in various hydrogeological layers of the model at a multi-source location as the initial condition. In inducing this idealistic concentration, it was kept in mind that an idealistic plume distribution would result. It would be easier to analyse and understand the plume scenario with this expected optimization result. The multi-source location of α-HCH was based on local HCH site investigation data and a literature review. These source locations of α-HCH include permanent and temporal mass production sites and α-HCH disposals sites (Heidrich *et al.*, 2004b; Paschke *et al.*, 2006; Petelet-Giraud *et al.*, 2007).

Boundary conditions

The Dirichlet boundary condition, also known as the 1st kind of BC (Cheng and Cheng, 2005), was used to define solute concentration [M/L^3] at the selected model nodes. This can result in mass inflow and outflow from the neighbouring nodes, depending upon concentration gradient of the neighbouring nodes in the model.

Similarly, a mass flux boundary condition, the 2nd kind of BC, is used to define mass flux [M/(L2*T)] to nodes enclosing faces of elements. The mass flux boundary condition (Diersch, 2009) is given by:

$$q_{mass} = q_{flow} * c \qquad \text{Eqn. 4.24}$$

where q_{mass} is mass transport BC flux, q_{flow} is flow BC flux and c is concentration of the inflowing water.

In addition, a mass transfer boundary condition, the 3rd kind of BC, is used to define a reference concentration linked to the concentration of groundwater with a separating medium. The transfer rate [M/L3] (Diersch, 2009) is given by:

$Q_{mass} = A*\Phi*(c_{ref}-c)$ Eqn. 4.25

where Q_{mass} is inflow or outflow to/from the model, A is relevant area, Φ is transfer rate, c_{ref} is reference concentration, and c is current concentration in groundwater.

An additional nodal sink or source boundary condition [M/T] for mass transport is used to define extraction or injection of a solute to a node. In addition to the existing boundary conditions in the model (Gossel *et al.*, 2009), the Dirichlet boundary condition was incorporated to define solute concentration at the selected nodes in the model area. This boundary condition was assigned in the model area with reference to α-HCH production sites, and α-HCH disposals sites of Bitterfeld/Wolfen.

Transport material

In addition to the model initial and boundary conditions, mass transport of material significantly determines the transport of contaminants in the model. In order to represent mass transport of material, transport related processes (advective, diffusive, dispersive transport, porosity sorption, decay, and reaction kinetics) are incorporated in the model. In order to improve the existing model (Gossel *et al.*, 2009), sorption and diffusion coefficients were incorporated considering α-HCH as a transport material.

4.4.4 Temporal control

As per objective of this study, the groundwater model developed was used for LTM network optimization. The prognostic groundwater flow and contaminant plume were required for the LTM network optimization. In the study area, long-term groundwater monitoring is planned for 20–25 years (Kollat and Reed, 2007b; Reed *et al.*, 2001). Considering this planning period, the groundwater flow and transport model was simulated for a period of 7665 days (21 years) with an initial time step length of 0.001 day.

4.4.5 Exporting head, mass and velocity

As for the existing LTM network optimization, in the modelled urbanized area of about 100 km^2, 462 reference wells in the Quaternary aquifer and 357 reference wells in the Tertiary aquifer were added to the transport model for tracing the spatio-temporal virtual contaminant scenario. The reference monitoring wells and their latitude, longitude and screen level elevations were assigned at 3-D nodes of the finite element mesh. The hydraulic head [m a.s.l.], the solute concentration [mg/l] and flow velocity (m/day) were recorded in the form of time series data at the reference monitoring wells. With these recorded hydraulic heads, the solute concentration and flow velocity were exported and used for the optimization of the existing LTM network.

Particle tracking

The evaluation of an imaginary solute location and velocity are of great importance for finite-element flow and transport modelling (Diersch, 2008). An advective particle tracking method was used to visualize an imaginary solute location (with respect to time) and groundwater velocity field by tracking movement of an imaginary particle with respect to the velocity distribution of the groundwater flow field. Particle tracking was computed using a previously simulated groundwater model. Particle tracking was performed in both forward (downstream) and backward (upstream) directions to the normal oriented flow velocity field, to assess past and future positions of the imaginary solute particles. Backward particle tracking, also called reverse particle tracking, was used to estimate probable source location and travel time in the modelled area.

4.4.6 LTM network optimization based on hydrogeological model

Although a substantial amount of work has been done on application of groundwater flow and transport models for several different purposes (Anderson and Cherry, 1979; Tripathi, 1991; Van Genuchten, 1978), groundwater quality monitoring network optimizations incorporating the transient state of the pollutant plumes are relatively rare (Datta *et al.*, 2009). A dynamic monitoring network optimization changes with time, reflecting the transient nature of the pollutant plume dynamics. Such an optimization can eliminate temporal redundancy and is, therefore, economically more efficient. A methodology was developed for groundwater quality monitoring network optimization that incorporates both steady state flow and transient transport processes in the aquifer (Figure 4.7). The advective particle tracking method and the reference observation point method were used to track solute concentration and its dynamics. The designed monitoring network is dynamic in nature, accounting for the transient state of plumes as it can be used for time varying network optimization. Therefore, the resulting optimization would be more accurate and economically efficient.

Spatial optimization of the LTM Network

A transient transport model was utilized for obtaining sets of pollutant concentration realisations at 462 reference wells in the Quaternary aquifer and 357 reference wells locations in the Tertiary aquifer. These mass (contaminant concentration) realisations are used as input to the spatial optimization model (figures 4.7 and 4.8). Even though contaminant concentration has been used for the monitoring optimization in this study, head and flow velocity were used for comparative analyses of random fluctuation of mass.

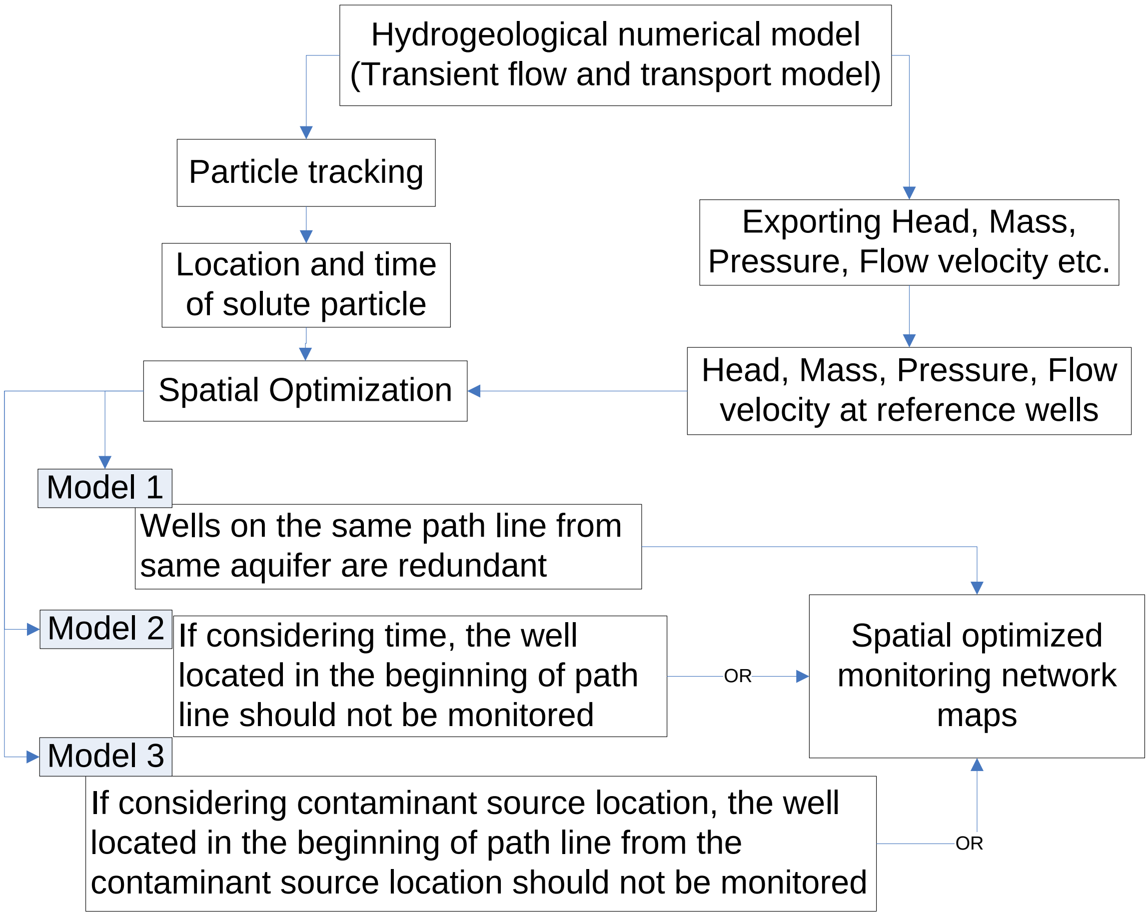

Figure 4.7: Steps involved in the spatial optimization of the monitoring network using 3-D groundwater hydrogeological modelling showing there conditional models for the monitoring network optimization.

Three optimization models were proposed to select the best subset of monitoring well locations from a large groundwater monitoring network:

Model 1: wells on the same path line from the same aquifer designated to be redundant. If there are more than two wells on the same particle track, the middle one is selected as essential;

Model 2: for prognostic optimization, when there are more than two monitoring wells on the same particle track, the well located at the beginning of particle track should not be monitored. Essential wells need to be selected from the remaining wells on the same particle track; and

Model 3: optimization towards contaminant source location, where the well located at the beginning of path line from the contaminant source location should have high priority for monitoring. However, if there are multiple wells located near the contaminant source location, the well located near contaminant sources on the same particle track will have less priority.

In addition to these conditions, in all of these models, wells in areas with high temporal fluctuation of contaminant concentration with high groundwater flow velocity are not assigned as redundant wells.

Model 1 was used for general optimization without special consideration to the contaminants source and time. However, model 2 was used for prognostic optimization in which spatial location of the well was considered. Model 2 should be considered when the optimization aims to ignore the contaminant source but track the present and future contaminant location. Similarly, model 3 was used when special consideration to specific contaminant sources was required.

Temporal optimization of the LTM Network

The temporal variation of concentration in the research area is related to groundwater flow velocity and contaminant transport. Therefore, understanding flow velocity is a key element in temporal optimization of the LTM Network. The steady state flow model was utilized for obtaining sets of flow velocity realizations at 462 reference wells in the Quaternary aquifer and 357 reference well locations in the Tertiary aquifer. These flow velocity realizations are used as inputs for temporal optimization of the monitoring network (figure 4.8).

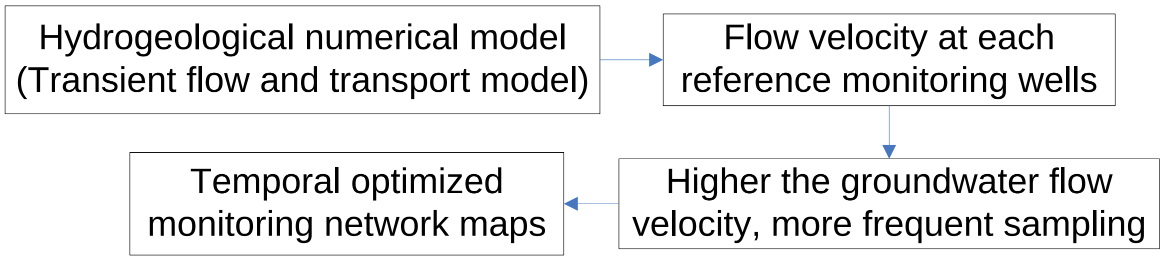

Figure 4.8 Steps involved in the temporal optimization of the monitoring network using 3-D groundwater hydrogeological modelling.

The simulated flow velocity in the model ranges from 2.1×10^{-6} to 1.1 m/day. This range of flow velocity was divided into five classes, which were assigned to have temporal sampling frequencies from three months to three years, as shown in table 4.1. The higher the groundwater flow velocity, the more frequent groundwater sampling is recommended.

Table 4.1: The range of groundwater flow velocity for each class and their assigned temporal sampling intervals.

S. No.	Lower velocity (m/day)	Higher velocity (m/day)	Sampling frequency
1	0.05	1.13	3 month
2	5.2×10^{-3}	4.4×10^{-2}	6 month
3	5.5×10^{-4}	5.0×10^{-3}	1 year
4	5.1×10^{-5}	5.0×10^{-4}	2 years
5	2.1×10^{-6}	5.0×10^{-5}	3 years

The monitoring wells from both aquifers and their different sampling frequencies were visualized on a map.

4.5. Comparison and correlation of methods

4.5.1 Spatial optimization of the LTM Network

The existing groundwater monitoring network was optimized using three separate methods viz. statistical, geostatistical, and hydrogeological methods. The statistical method classified wells into essential and redundant monitoring wells based on the AHC method (section 4.2.4). In the geostatistical method, kriging weights were used to compute plume maps and randomly remove the wells with the lowest kriging weights to identify the wells as essential or redundant (section 4.3.1). Similarly, in hydrological methods, particle tracking methods were used to tag a well as essential or redundant (section 4.4.6).

Using statistical methods, individual wells were classified based on percentage of redundancy (section 4.2.4). However, in geostatistical methods, the wells were classified according to their percentage of confidence level. In hydrogeological methods, this classification of wells was based on the model described in section 4.4.6. In addition to tagging the existing monitoring wells as essential and redundant, the geostatistical method (section 4.3.1) was applied to find new monitoring well locations based on an analysis of relative spatial uncertainties. In all of these three methods, the same individual well was tagged as essential or redundant. Therefore, comparison of results from these methods for individual wells was used to analyse the efficiency of the methods. The spatial optimization results based on applying the three methods were compared in term of the recommended total number of essential, redundant and new monitoring wells.

4.5.2 Temporal optimization of the LTM Network

In the statistical method, the monitoring network was temporally optimized using the iterative thinning of Sen's method. Alternatively, the hydrogeological method was based on flow velocity in an ideal environment. These two methods were compared in terms of sampling interval for each monitoring well, different contaminants and overall sampling frequency.

4.6 Improving groundwater monitoring strategies

As presented in section 4.1, in order to make recommendations for groundwater monitoring strategies, feedback from the monitoring network optimization was analysed. The feedback analysis was carried out to improve the existing monitoring network and the methods used. New and improved methods were developed based on integration of the statistical, geostatistical, and hydrogeological methods.

4.6.1 Integrating approaches for improving groundwater monitoring

New and improved methods were integrated with existing statistical, geostatistical, and hydrogeological methods to make several sets of methods. This integration of methods was carried out in the light of different optimization objectives. While integrating these methods, the basic framework and components of groundwater monitoring strategies were considered. The new integrated methods, although based on different approaches, could be used as a tool for groundwater monitoring network optimization and feedback for updating groundwater monitoring strategies. While integrating these methods, the advantages and disadvantages of the methods being used were also analysed.

4.6.2 Uncertainties in LTM network optimization

In addition to analysis of the monitoring network and methods, uncertainties associated with groundwater network optimization were highlighted. In the uncertainties analysis, the uncertainty associated with the observed data set and the amendment of optimization results in the real field scenario were analysed. Although the groundwater contamination scenario of the test research area, Bitterfeld/Wolfen, cannot represent all locations, an attempt was made to analyse abnormality in the magnitude of contaminant concentration and possible application of the methods.

5. Results

5.1 Long-term groundwater monitoring strategies

An understanding of the properties and behaviour of groundwater systems is required for strategic planning and operational actions in groundwater management. Strategic planning of the monitoring network optimization plays major role in groundwater monitoring, as it is a component of monitoring strategies (section 4.1). As per the research objectives (section1.3) new and improved methods for LTM network optimization were developed and analysed using statistical, geostatistical, and numerical modelling approaches. In order to improve monitoring strategies, the developed methods along with existing methods were applied to observed and model based data sets for the mega-contaminated site, Bitterfeld/Wolfen. The results based on statistical, geostatistical, and hydrogeological methods are presented in this chapter.

5.2 Statistical methods

5.2.1 Univariate statistics

The groundwater monitoring data set of Bitterfeld/Wolfen was quantitatively describing in terms of central tendency, distribution and dispersion. The analysis shows that the parameter values are widely distributed around the central tendency in both aquifers (table 5.1). In other words, the concentration of MCB, SO_4^{2-}, α-HCH, and Fe show a high standard deviation from the central mean concentration.

Table 5.1: Descriptive statistics of major parameters in the groundwater monitoring data of Quaternary and Tertiary horizons from 2003 to 2009.

Parameters	Range	Minimum	Maximum	Mean	Std. Dev.	Skewness	Kurtosis
Temperature	20.28	1.59	23.00	12.89	1.59	0.36	2.02
pH	11.96	0.79	12.75	6.24	1.30	1.42	6.37
Eh	10081.00	-541.00	9540.00	164.44	192.97	17.69	856.95
NO_3^-	2900.00	0.00	2900.00	10.84	84.13	24.99	731.20
SO_4^{2+}	76999.50	0.50	77000.00	1099.11	2545.11	17.68	416.21
SO_3^{2-}	401.99	0.01	402	2.96	12.89	12.31	255.45
NH_4^+	706	0	706	13.70	32.65	9.03	140.02
α-HCH	5600.00	0.00	5600.00	7.56	95.68	36.54	1920.02
Fe^{3+}	11000.00	0.00	11000.00	58.10	492.00	16.84	310.53
MCB	549999.98	0.02	550000.00	8488.26	25640.23	5.16	44.67

Based on descriptive statistics, the selected representative parameters (section 4.3.1), the data set of the concentration of MCB, α-HCH and SO_4^{2-}, were subjected to detailed analysis in terms of number of samples above and below the detection limit (DL) and WHO standard maximum contamination limit (MCL). α-HCH has a declining percentage of samples above MCL from

2003 to 2009 (Figure 5.1). α-HCH was not detected in the majority of samples, but a α-HCH concentration above MCL (0.2 μg/L) was detected in a relatively small number of samples. These groundwater samples with α-HCH concentration above MCL in the groundwater had extremely high concentrations.

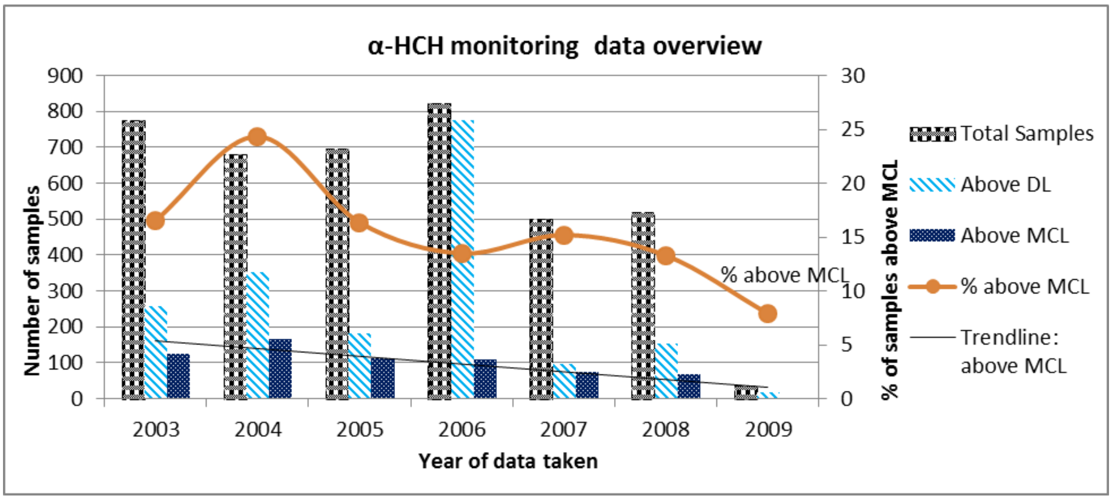

Figure 5.1: α-HCH monitoring results from 2003 to 2009. Number of samples on the left axis and % of samples above the MCL on the right axis.

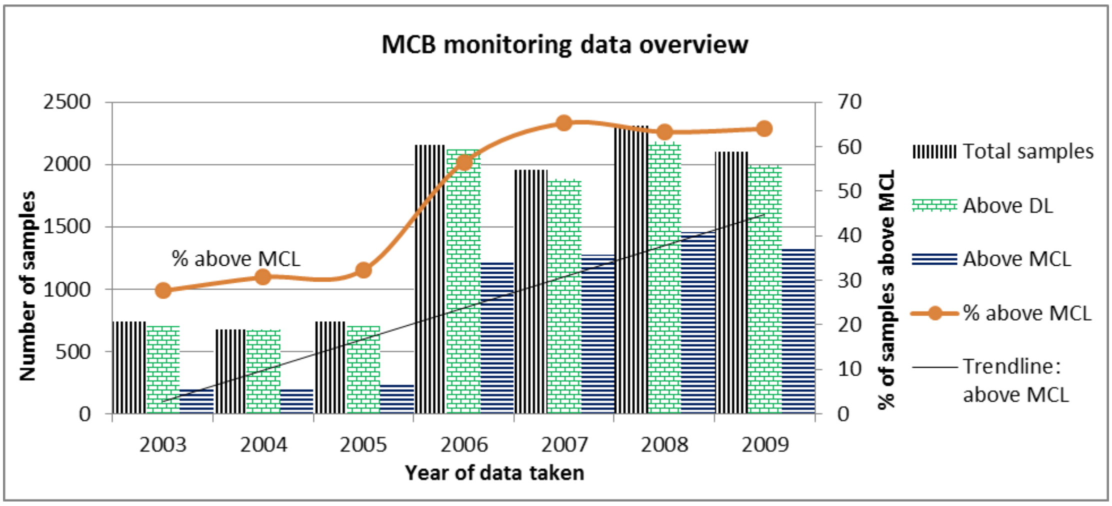

Figure 5.2: MCB monitoring results from 2003 to 2009. Number of samples on the left axis and % of samples above the MCL on the right axis.

The number of samples collected was higher in 2003, 2004, 2005, and 2006. In each of these years, most of the monitoring wells were sampled twice. During the years 2007 and 2008, the sampling frequency was lower. The percentage of samples above the MCL decreased with time. Meanwhile, MCB had an increasing percentage of samples above the MCL from 2003 to 2009 (figure 5.2). Contrary to α-HCH, the number of samples collected was lower in 2003, 2004, and 2005, and higher during the years 2006, 2007 and 2008. In these years, most of the monitoring wells were sampled twice in the year. The percentage of samples above MCL increased remarkably during the study period. MCB was above the DL in most of the samples from the study period.

SO_4^{2-} was detected in all samples. Over 60% of the samples had SO_4^{2-} concentration higher than 500 mg/l (WHO standard). Although the MCL value for SO_4^{2-} does not have WHO standard MCL, the concentrations of the SO_4^{2-} found in the study area were extremely high.

Homogeneity of variance

To study the homogeneity of variance, a mean vs variance test and Levene's test were used, as described in section 4.2.1. In the mean vs variance test, the first set of the five groups compiled from the entire data set showed drastic inconsistency in the homogeneity of variance. In the study area, analysis of the distibution pattern of the homogeneity of variance shows that the physicochemical parameters like temperature, pH, Eh, NO_3^-, SO_3^{2-}, SO_4^{2-}, and NH_4^+, were relatively homogeneously distributed. However, Fe^{3+}, MCB, and α-HCH had highly heterogeneous variance, as shown in figure 5.3. The source of this heterogeneity in the data set the monitoring wells located in the western part of the study area.

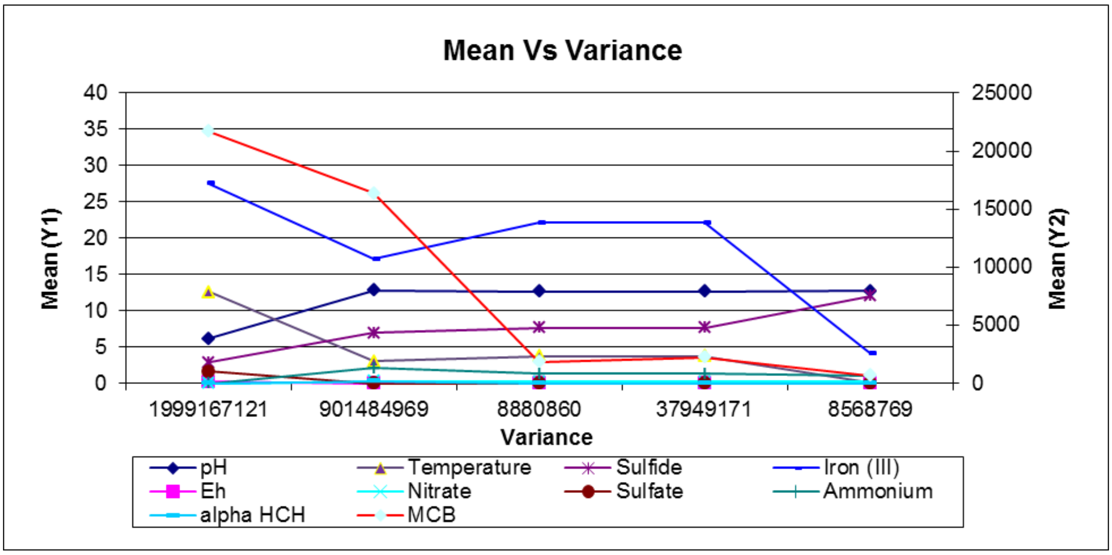

Figure 5.3: Mean vs variance, showing a higher variance of MCB and Fe^{3+} than other parameters in the reseach area (Y1 axis: ph, Eh, Temerature, Sulfide, Sulfate, Iron, NO_3^-, and NH_4^+ and Y2 axis: MCB and alpha HCH).

The significance values of p for the physicochemical parameters in Levene's test were from 0.001 to .01. More precisely, the Levene's test significance values of p for SO_4^{2-}, and MCB were < 0.005. The null hypothesis was thus incorrect as the variances were significantly different, meaning that the assumption of homogeneity of variances had been violated.

5.2.2 Multivariate statistics

Multivariate analysis performed on a matrix of hydro-geochemical data gives an in depth picture of groundwater quality in terms of major components and their inter-correlation.

Principal component analysis

PCA was applied to a matrix of hydro-geochemical data for dimension reduction, in order to observe and analyse major componet loading in the system and their variance. The scree plot, where the eigenvalues corresponding to each of the variables (Temperature, pH, Eh, NO_3^-, SO_4^{2-}, NH_4^+, Fe, α-HCH, and MCB) are plotted in decreasing order, shows the proportion of variance for each principal component (figure 5.4).

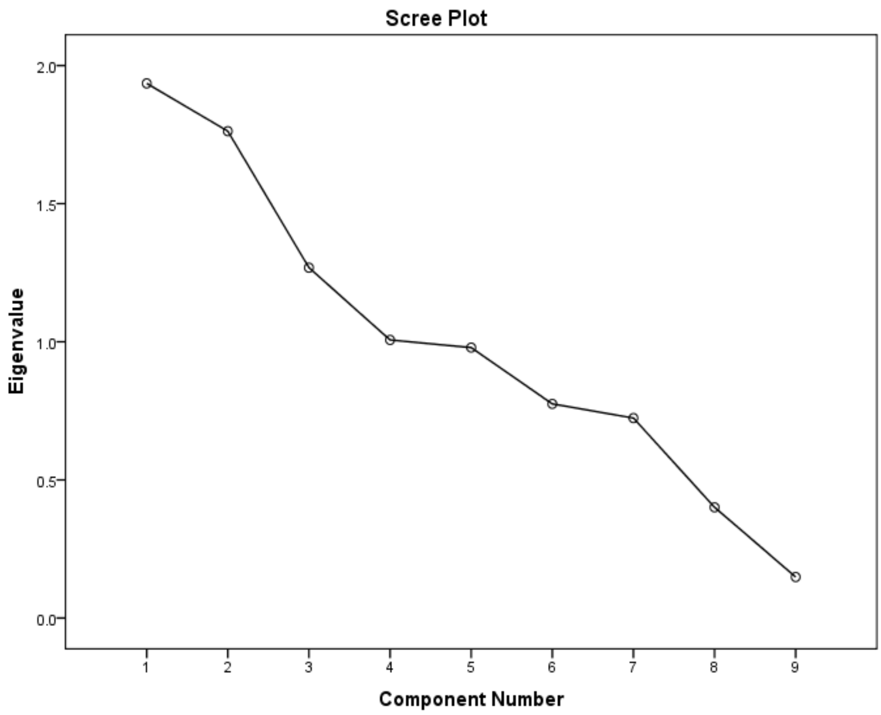

Figure 5.4: Scree plot showing the proportion of variance for each principal component.

Table 5.2: Initial eigenvalues and extraction sums of squared loadings in the system.

Component	Initial Eigenvalues			Extraction Sums of Squared Loadings		
	Total	% of Variance	Cumulative %	Total	% of Variance	Cumulative %
1	1.935	21.503	21.503	1.935	21.503	21.503
2	1.762	19.582	41.085	1.762	19.582	41.085
3	1.268	14.092	55.176	1.268	14.092	55.176
4	1.007	11.186	66.362	1.007	11.186	66.362
5	0.979	10.877	77.239			
6	0.775	8.612	85.851			
7	0.724	8.044	93.895			
8	0.401	4.454	98.349			
9	0.149	1.651	100.000			

In this dataset, the first four principal components, which all have eigenvalues greater than one, explain much more of the variance in the data than any of the subsequent principal components do (table 5.2). The first four components constitute 66% of the cumulative variance. The varaiances drop from the third to fourth component; and from the fifth to sixth component.

The component matrix extracted using principal component analysis and varimax with the Kaiser Normalization rotation method shows the significance of the parameters in the 4 components (table 5.3). With a 75% significance level, SO_4^{2-}, Fe, pH and Eh play a major role in the system. α-HCH and MCB are minor components. In the first component, SO_4^{2-} and Fe have positive loading. In second component, Eh has positive loading. However, pH is has negative loading because the acidic groundwater environment in the study area arises from a high SO_4^{2-} concentration.

Figure 5.5 depicts a loading plot in rotated 3-D space corresponding to the component matrix, using principal component analysis and varimax with the Kaiser Normalization rotation method. In Kaiser Normalization, the rows of x are re-scaled to unit length before rotation, and scaled back afterwards (Kaiser, 1958). In figure 5.5, the loading of various components in the system shows two clear patterns. SO_4^{2-} and Fe exhibit similar loading (figure 5.5 and table 5.3). Eh has positive loading and pH has negative loading, which are opposite directions to their performance in the system (figure 5.5 and table 5.3).

Table 5.3: Rotated Component Matrix showing 4 extracted components using PCA and varimax, with the Kaiser Normalization rotation method.

Rotated Component Matrix

	Component			
	1	2	3	4
Temperature	0.136	-0.208	0.464	0.437
pH	-0.067	-0.866	-0.028	0.004
Eh	-0.027	0.831	-0.236	0.095
NO_3^-	-0.043	0.096	-0.054	0.923
SO_4^{2-}	0.948	0.076	0.118	0.014
NH_4^+	0.093	-0.191	0.701	-0.005
Fe^{3+}	0.943	0.050	-0.050	-0.004
α-HCH	0.152	0.306	0.234	-0.084
MCB	-0.099	0.171	0.749	-0.010

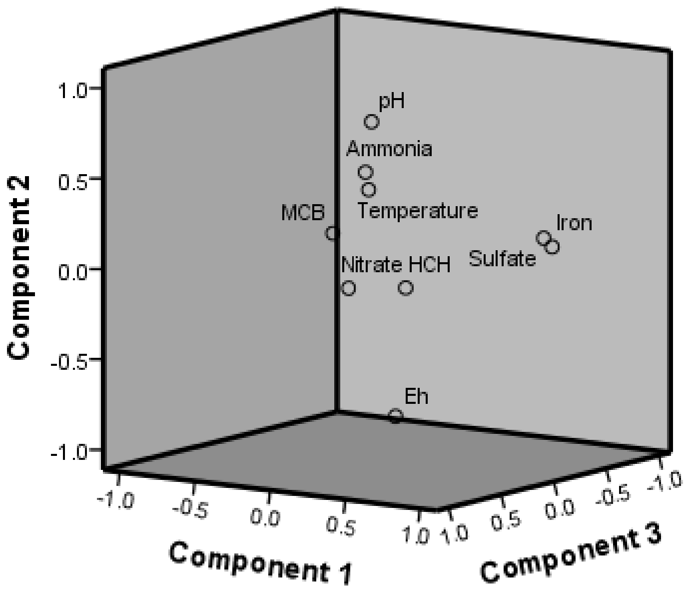

Figure 5.5: Component plot in rotated 3-D space using principal component analysis and varimax with the Kaiser Normalization rotation method.

Cluster analysis

The groundwater monitoring data set from Bitterfeld/Wolfen was statistically analysed and visualized using an agglomerative hierarchical cluster (AHC) of parameters and well locations as described in section 4.2.2 and shown in the dendrograms in appendixes 2 and 3. The dendrogram of well locations shows a number of clusters of different numbers of wells. In this case, a single monitoring well from each cluster represents all the wells belonging to that cluster. The single well, was tagged as essential, whilst the remaining wells of that cluster were tagged as redundant wells.

5.2.3 Spatial optimization of the network using the clustering method

Optimization of the LTM network according to the method described in section 4.2.4, using a redundancy limit of 50%, was carried out separately for both aquifers.

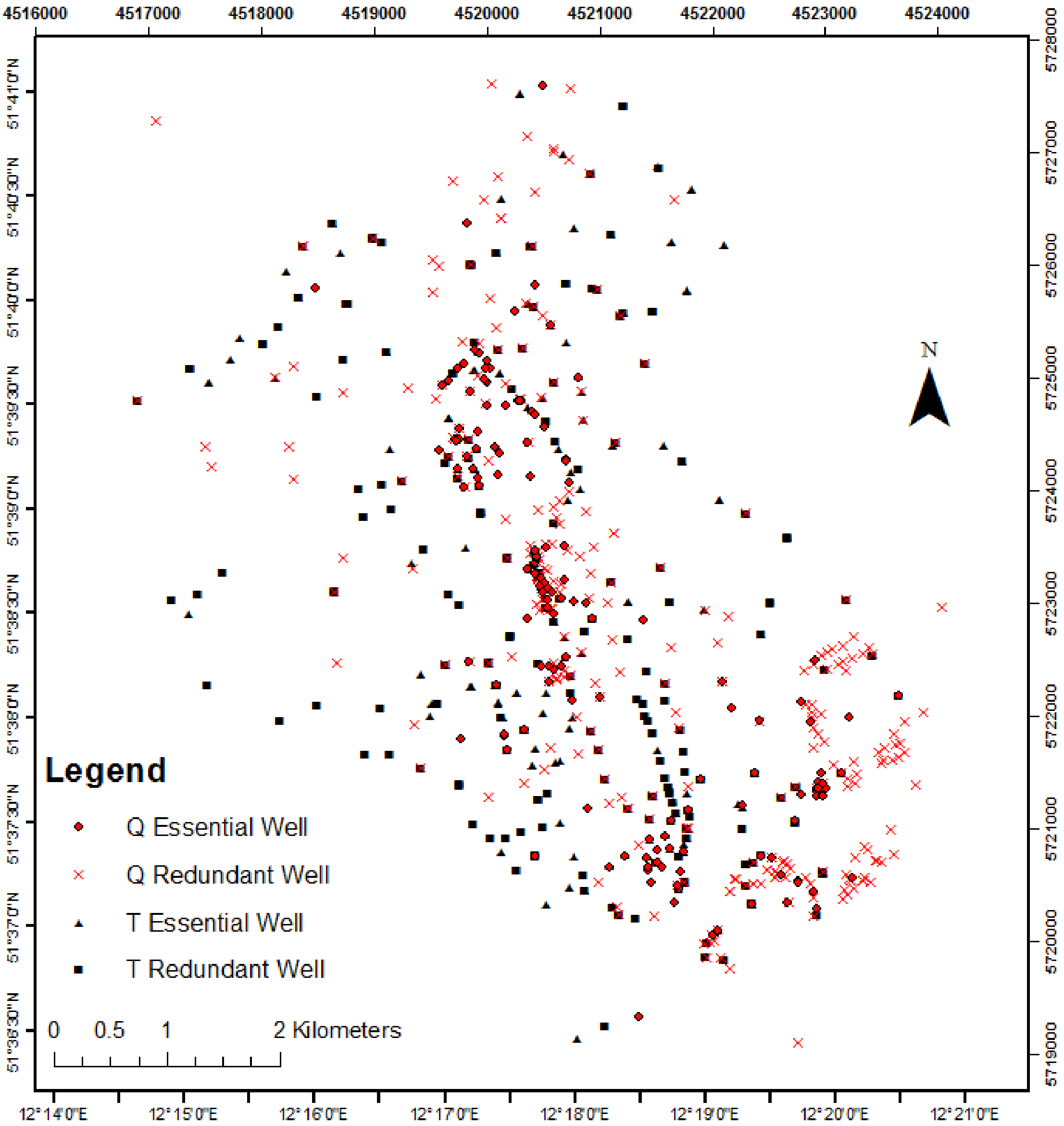

Figure 5.6: Statistically spatially optimized LTM network map showing essential and redundant wells in the Quaternary (Q) and Tertiary (T) aquifer in the monitoring network.

In the Quaternary aquifer, the optimized monitoring network suggests that 184 of the 462 wells should be monitored at the suggested temporal interval. In Tertiary aquifer, the optimization result based on the method described in section 4.2.4 suggests that monitoring of only 150 of the 357 wells currently being monitored is required. The spatial distribution of redundant and essential wells in the Quaternary and Tertiary aquifer is depicted in figure 5.6.

The remaining monitoring wells, i.e. 278 wells in the Quaternary aquifer and 207 wells in the Tertiary (T) aquifer, were tagged as redundant wells in the existing monitoring network.

Dependency on the limit of the percentage of redundancy

Figure 5.7 shows how the result of the monitoring network optimization, in terms of essential and redundant wells, changes with the limit of the percentage of redundancy. The percentage of redundancy of each monitoring well based on the statistical method is tabulated in appendix 5. The result of optimization shows high number of essential wells when the redundancy limit is 100% and vice versa.

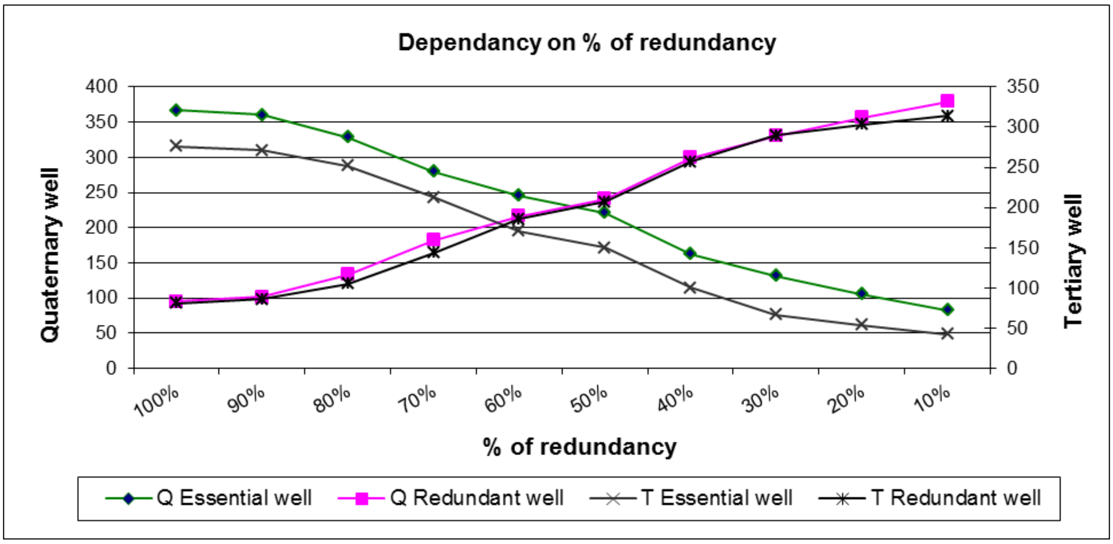

Figure 5.7: Changes in the optimization result in terms of essential and redundant wells with the limit for the percentage of redundancy.

5.2.4 Temporal optimization of the LTM network

The groundwater monitoring network was optimized using Sen's method, along with a calculation of 95% confidence intervals around the slope estimates, as described in section 4.2.5. The temporal optimization gives the sampling interval in terms of a lower quartile, median quartile, and upper quartile for each monitoring well and each monitoring parameter (tables 5.4-

5.7). The temporal optimization of the monitoring network shows that the optimization differs remarkably when considering pair and multiple contaminants.

Table 5.4: Temporal optimization of monitoring network in Quaternary and Tertiary aquifer for α-HCH and SO_4^{2-}.

Vertical Zone	COC	Present sampling interval (days)			Recommended sampling interval (days)		
		Lower Quartile	Median Quartile	Upper Quartile	Lower Quartile	Median Quartile	Upper Quartile
Q	α-HCH	138	181	224	309	335	429
Q	SO_4^{2-}	179	217	268	326	488	713
T	α-HCH	224	224	224	359	398	553
T	SO_4^{2-}	188	217	278	429	615	799
Q	all	158	199	246	317	411	571
T	all	206	220	251	394	506	676
Both	all	183	217	246	342	443	633

Table 5.5: Temporal optimization of monitoring network in Quaternary and Tertiary aquifer for MCB and α-HCH.

Vertical Zone	COC	Present sampling interval (days)			Recommended sampling interval (days)		
		Lower Quartile	Median Quartile	Upper Quartile	Lower Quartile	Median Quartile	Upper Quartile
Q	MCB	92	114	190	162	224	386
Q	α-HCH	138	181	224	194	289	376
T	MCB	143	221	280	180	330	640
T	α-HCH	224	224	224	372	392	573
Q	all	115	207	207	178	256	381
T	all	183	222	252	276	361	606
Both	all	149	214	230	187	309	479

Table 5.6: Temporal optimization of monitoring network in Quaternary and Tertiary aquifer for MCB and SO_4^{2-}.

Vertical Zone	COC	Present sampling interval (days)			Recommended sampling interval (days)		
		Lower Quartile	Median Quartile	Lower Quartile	Median Quartile	Lower Quartile	Median Quartile
Q	MCB	92	210	254	207	328	523
Q	SO_4^{2-}	179	217	268	335	504	701
T	MCB	143	221	280	275	436	815
T	SO_4^{2-}	188	217	278	425	605	829
Q	all	135	213	261	271	416	612
T	all	165	219	279	350	520	822
Both	all	161	217	273	305	470	758

Table 5.7: Temporal optimization of monitoring network in Quaternary and Tertiary aquifer for MCB, α-HCH and SO_4^{2-}.

V. Zone	COC	Present sampling interval (days)			Recommended sampling interval (days)		
		Lower Quartile	Median Quartile	Upper Quartile	Lower Quartile	Median Quartile	Upper Quartile
Q	MCB	92	210	254	205	328	503
Q	α-HCH	138	181	224	298	327	418
Q	SO_4^{2-}	179	217	268	325	506	704
T	MCB	143	221	280	282	443	810
T	α-HCH	224	224	224	342	398	553
T	SO_4^{2-}	188	217	278	435	589	836
Q	all	138	210	254	298	328	503
T	all	188	221	278	342	443	810
Both	all	161	217	261	311	420	628

In the results presented, it can be seen that when α-HCH was used for temporal optimization with SO_4^{2-} and MCB separately (tables 5.4 and 5.5, respectively) the recommended sampling interval differs (289 days with MCB and 335 with SO_4^{2+}). Similarly, when the monitoring network was optimized considering three contaminants, the recommended sampling interval was 327 days, which again differs from the optimization result considering two contaminants only. An average sampling interval for each of the monitoring wells, considering the three representative contaminants (α-HCH, MCB, and SO_4^{2-}) is tabulated in appendix 5. The overall sampling interval considering the three representative contaminants (α-HCH, MCB, and SO_4^{2-}) is given in table 5.7. Appendix 7 tabulates an average sampling interval for the monitoring wells considering each three representative contaminants i.e. α-HCH, MCB, and SO_4^{2-}.

In order to clearly visualize the temporal optimization results, the recommended median quartile sampling frequency for the monitoring wells (considering all three contaminants together) was divided into five classes; namely 3 months, 6 months, 1 year, 2 years, and 3 years. The number of monitoring wells for each temporal sampling interval is listed in table 5.8.

Table 5.8: Number of monitoring wells for each sampling interval.

Sampling Interval	3 months	6 months	1 year	2 years	3 years	Total
Quaternary	34	86	173	76	93	462
Tertiary	16	69	114	84	74	357
Total no. of wells	50	155	287	160	167	819

Figure 5.8 shows the distribution of monitoring wells and their recommended sampling intervals. The highest number of sampling wells is recommended at the yearly sampling interval.

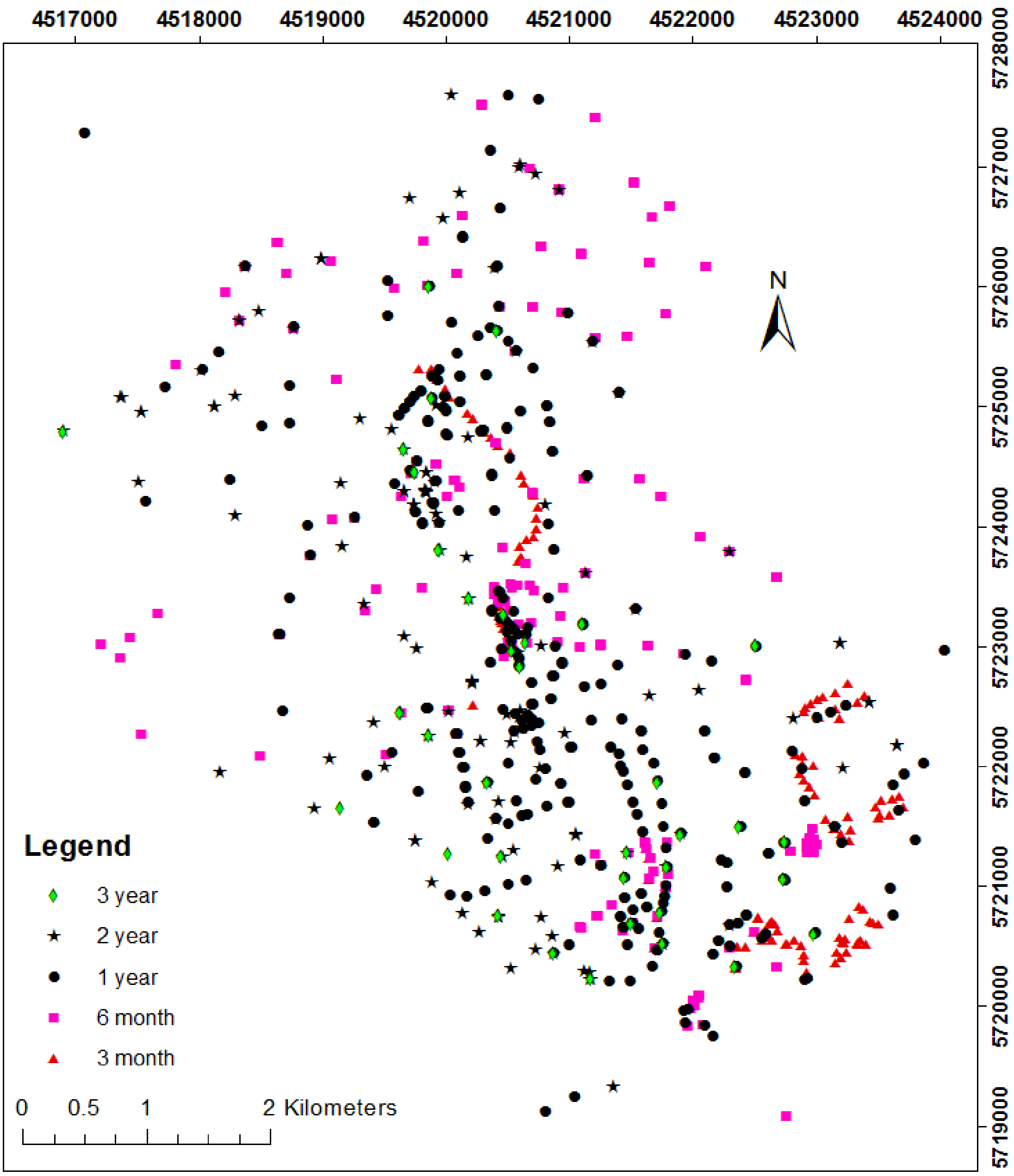

Figure 5.8: Statistically temporally optimized LTM network map showing recommended temporal frequency of the monitoring wells in the monitoring network.

In the study area, the overall optimized sampling interval was recommended in terms of the lower quartile (238 days), median quartile (317 days) and upper quartile (401 days).

5.3 Geostatistical methods in groundwater monitoring

5.3.1 LTM network optimization using geostatistical methods

The optimization of the LTM network was carried out for both aquifers separately, according to the method described in section 4.3.1. Among the 462 wells in the Quaternary aquifer, the optimized monitoring network suggests that 292 wells should be monitored at the suggested temporal interval. Similarly, in the Tertiary aquifer, 357 wells are monitored but the optimization result based on the method described in section 4.3.1 suggests that only 256 wells should be monitored.

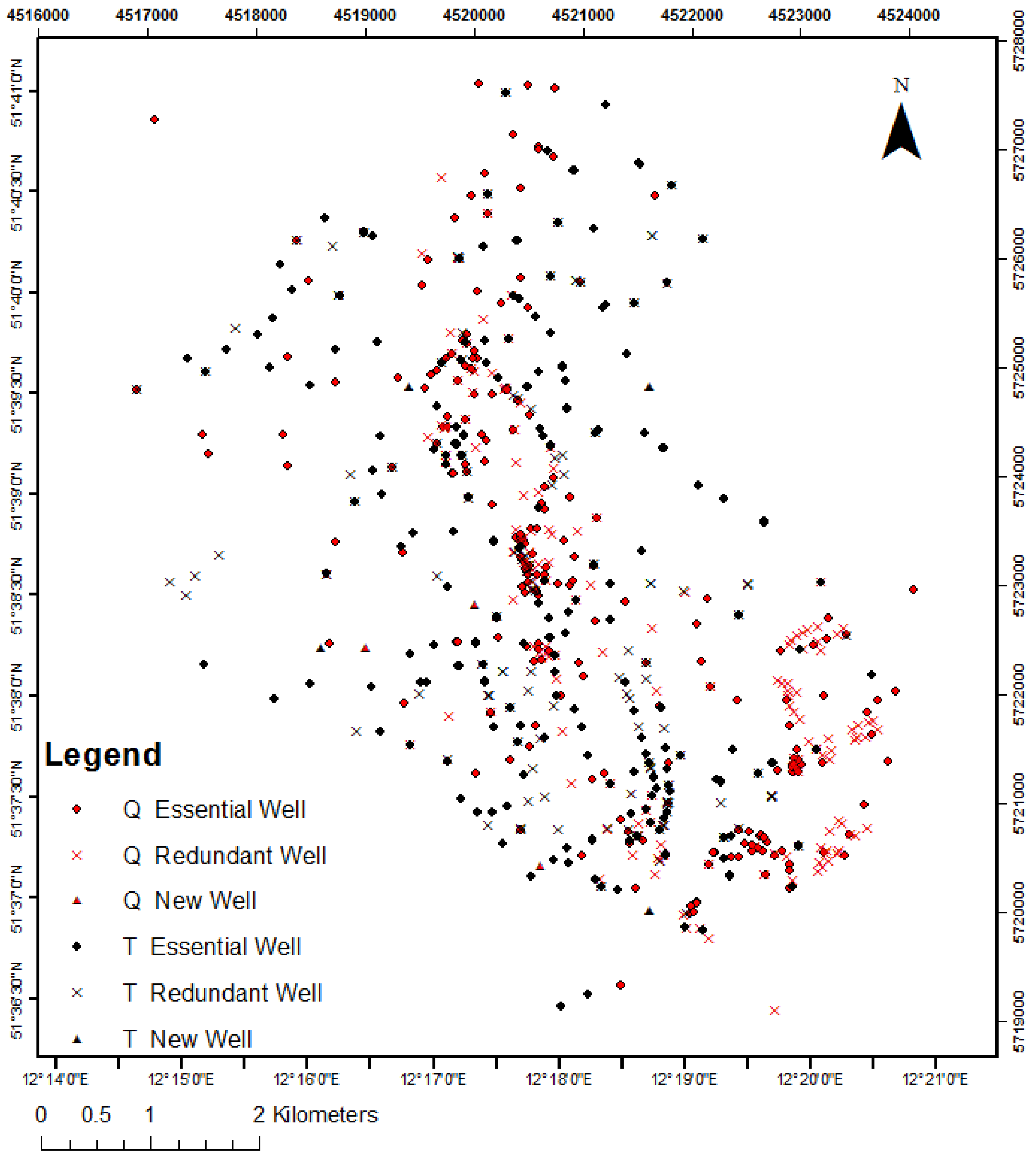

Figure 5.9: Optimized LTM network map showing location of essential, redundant, and proposed new wells in the monitoring network.

The spatial uncertainties analysis, in terms of the global kriging variance, also suggests that 22 and 41 new monitoring wells be installed in the Tertiary and Quaternary aquifers, respectively. The spatial distribution of redundant, essential, and proposed new wells in the Quaternary and Tertiary aquifer is depicted in figure 5.9. Appendix 4 shows the spatial distribution of location of essential, redundant, and proposed new wells along with existing uncertainties in the Quaternary and Tertiary aquifers in the monitoring network. Similarly, the essential and redundant monitoring wells based on statistical method are tabulated in appendix 5. The locations of the proposed new wells in the monitoring network are tabulated in appendix 6. The original and optimized LTM network datasets produced similar numerical kriging weights for the wells, which leads to the conclusion that a reduction in the number of observation points does not compromise the quality or resolution of the collected samples if the network distribution is properly designed.

5.3.2 Dimension and grid width dependency

The spatial optimization of the LTM network was carried out for different interpolation grid widths (from 1000 m to 1 m) for both aquifers separately in 2 and 2.5 dimension plains. The observed dependency of the monitoring network optimization is described in the following sections.

Optimization in a 2-D aquifer

The groundwater LTM network was spatially optimized for MCB, α-HCH and SO_4^{2-} by considering the groundwater aquifer as a 2-D plain. In this study, the number of suggested/ essential wells and redundant wells change significantly with the change in grid width for interpolation (from 1000 m to 1 m). As the grid width becomes smaller, the relative spatial uncertainty in the existing LTM network, which is based on the local kriging variance, gradually increases. When the relative spatial uncertainty in the existing LTM network increases the installation of new monitoring wells in the aquifer is recommended.

The optimization of the LTM network based on the concentration of MCB, α-HCH and SO_4^{2-}, considering the groundwater aquifer as a 2-D plain, shows a highly heterogeneous distribution of contaminants (figures 5.11 and 5.12). In the optimization, the relative spatial uncertainty increases with decreasing grid width from 200 m to 1 m in both aquifers. Consequently, the installation of 63 and 36 new monitoring wells are recommended in the Quaternary and Tertiary aquifers, respectively, at 1 m grid width.

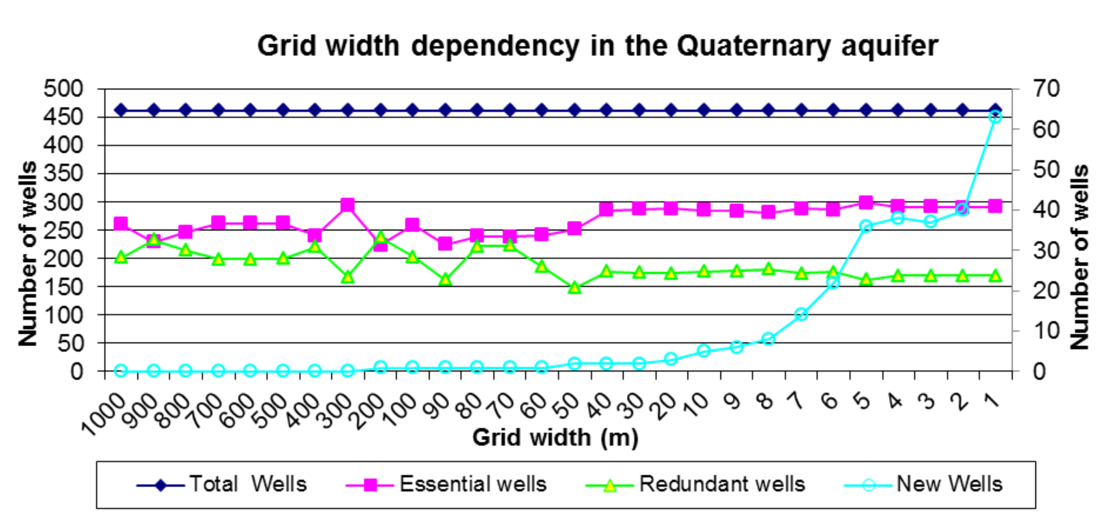

Figure 5.10: Grid width dependency in the LTM network optimization in the Quaternary aquifer for MCB, α-HCH and SO_4^{2-} in a 2-D plain. Essential, redundant and total number of wells on left Y-axis and number of new well on right Y-axis.

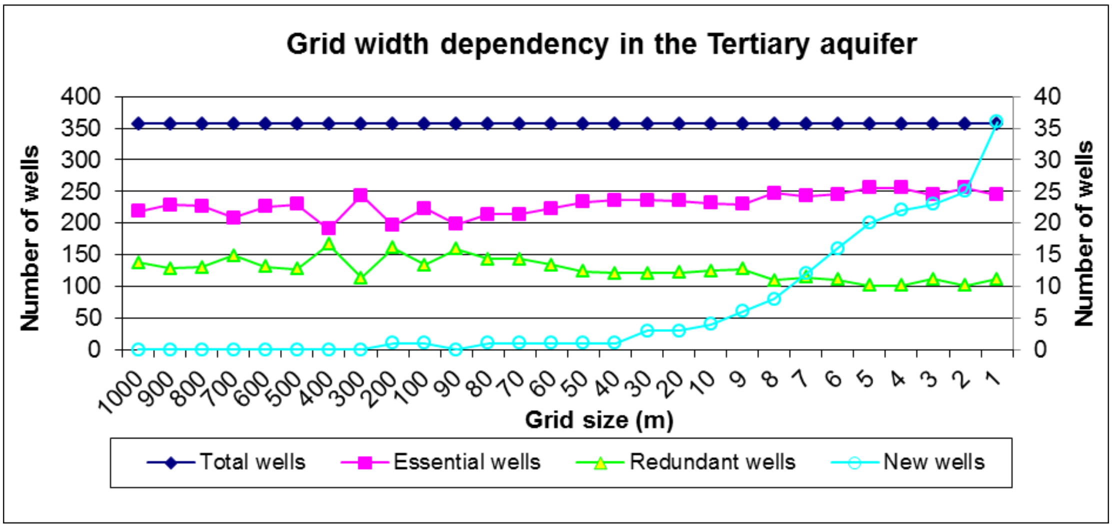

Figure 5.11: Grid width dependency in the LTM network optimization in the Tertiary aquifer for MCB, α-HCH and SO_4^{2-} in a 2-D plain. Essential, redundant and total number of wells on left Y-axis and number of new well on right Y-axis.

In the first round of grid width study, the LTM network was spatially optimized for α-HCH and SO_4^{2-}, considering the groundwater aquifer as a 2-D plain. Decreasing the grid width from 1000 m to 1 m, the numbers of recommended/ essential wells and redundant wells change significantly. Because of the homogeneity of the distribution of SO_4^{2-} concentration throughout the aquifer, the number of recommended/ essential wells is small and thus the number of redundant wells is high (Figure 5.12 and 5.14). This study shows smaller relative spatial uncertainty in both aquifers in the existing LTM network. In the

Quaternary aquifer, the relative spatial uncertainty increases with decreasing grid width from 200 m to 1 m. Consequently, the installation of 9 and 28 new monitoring wells is recommended in the Quaternary at the grid width of 10 m and 1 m, respectively. The relative spatial uncertainty is very low in the Tertiary aquifer, so no new wells are recommended.

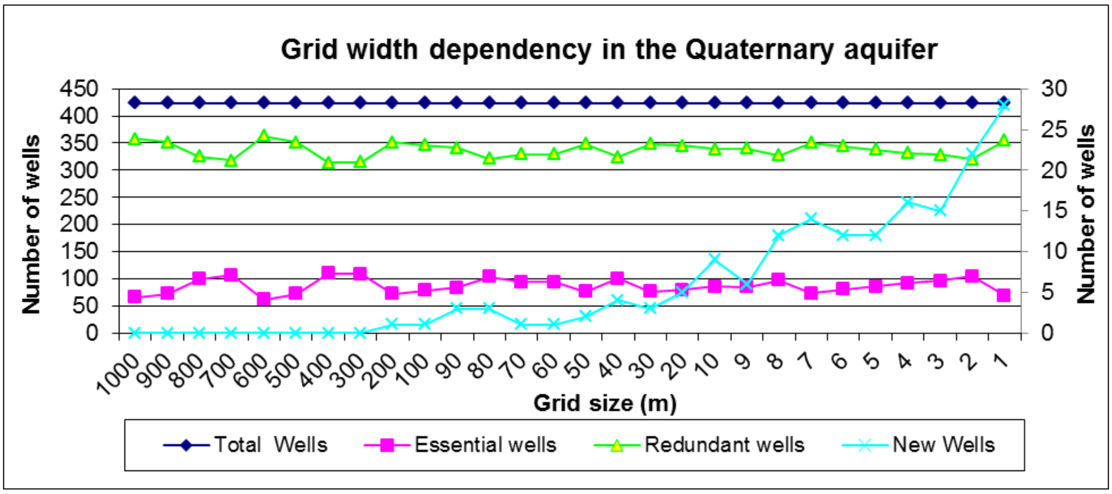

Figure 5.12: Grid width dependency in the LTM network optimization in the Quaternary aquifer for α-HCH and SO_4^{2-} in a 2-D plain. Essential, redundant and total number of wells on left Y-axis and number of new well on right Y-axis.

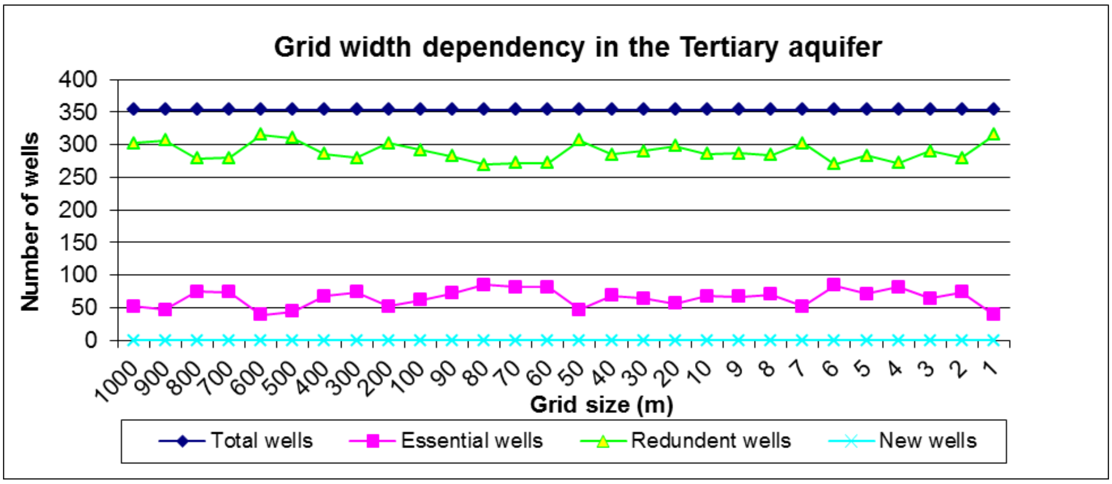

Figure 5.13: Grid width dependency in the LTM network optimization in the Tertiary aquifer for α-HCH and SO_4^{2-} in a 2-D plain.

In the second round of grid width analysis, the LTM network was spatially optimized for MCB and α-HCH, considering groundwater aquifer as a 2-D plain. In this study, the number of suggested/ essential wells and redundant wells also changes fairly with decreasing grid width (from 1000 m to 1 m). At the smaller grid size, the relative spatial uncertainty in the existing LTM network increases gradually. The spatial uncertainty started to increase from 500 m grid size, resulting in the recommendation of three new monitoring wells in the Quaternary aquifer (figures 5.15 and 5.16). Meanwhile, the spatial relative uncertainty is very low in the Tertiary aquifer and consequently no new wells are recommended.

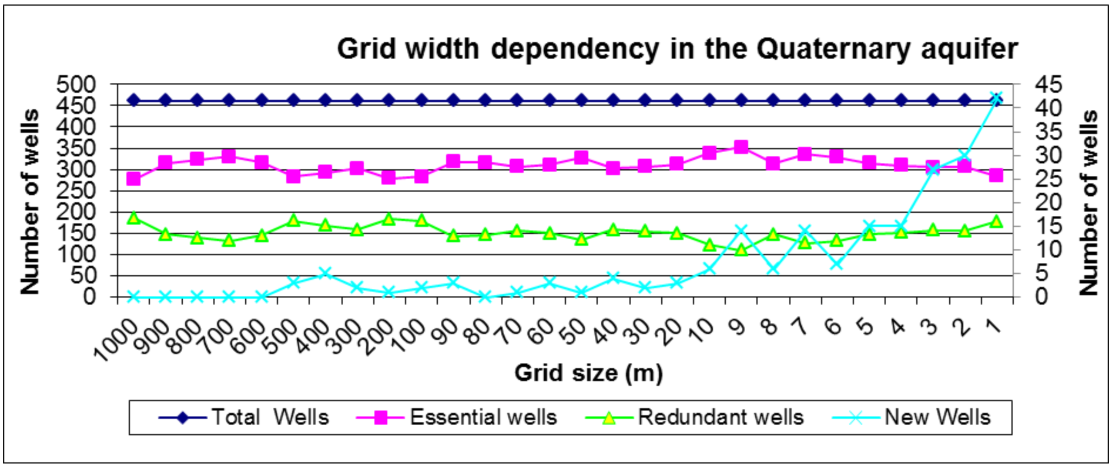

Figure 5.14: Grid width dependency in the LTM network optimization in the Quaternary aquifer for MCB and α-HCH in a 2-D plain. Essential, redundant and total number of wells on left Y-axis and number of new well on right Y-axis.

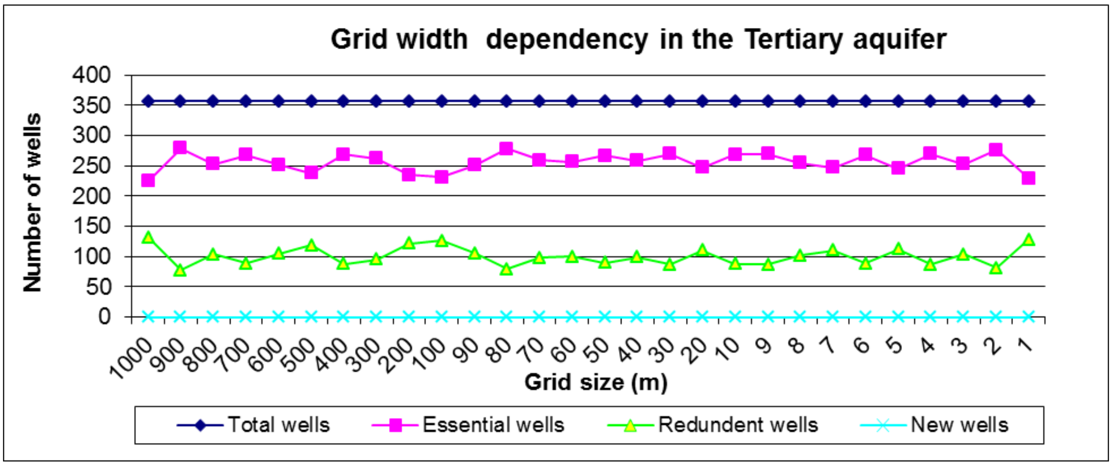

Figure 5.15: Grid width dependency in the LTM network optimization in the Tertiary aquifer for MCB and α-HCH in a 2-D plain.

In the third round of grid width analysis, the LTM network was spatially optimized for MCB, and SO_4^{2-}, considering the groundwater aquifer as a 2-D plain.

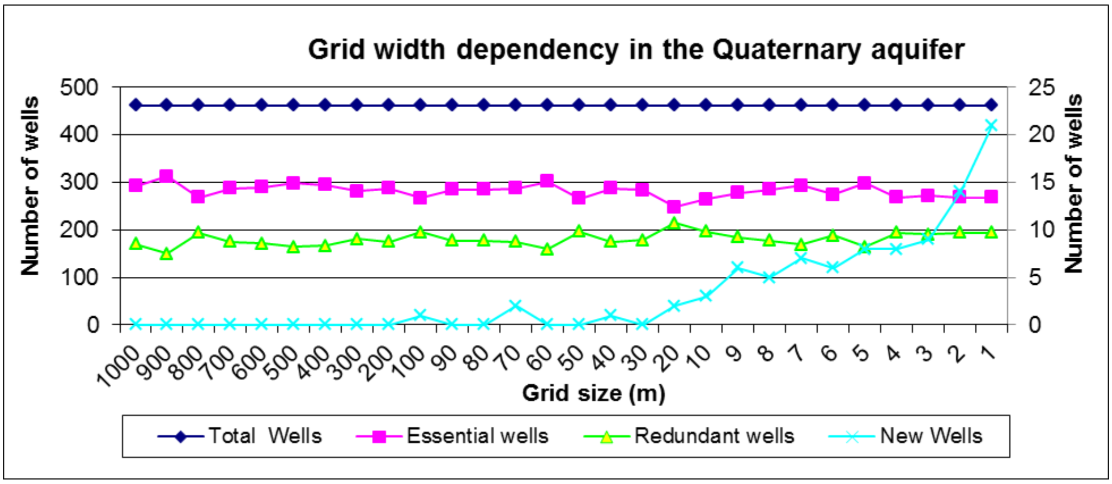

Figure 5.16: Grid width dependency in the LTM network optimization in the Quaternary aquifer for MCB and SO_4^{2-} in a 2-D plain. Essential, redundant and total number of wells on left Y-axis and number of new well on right Y-axis.

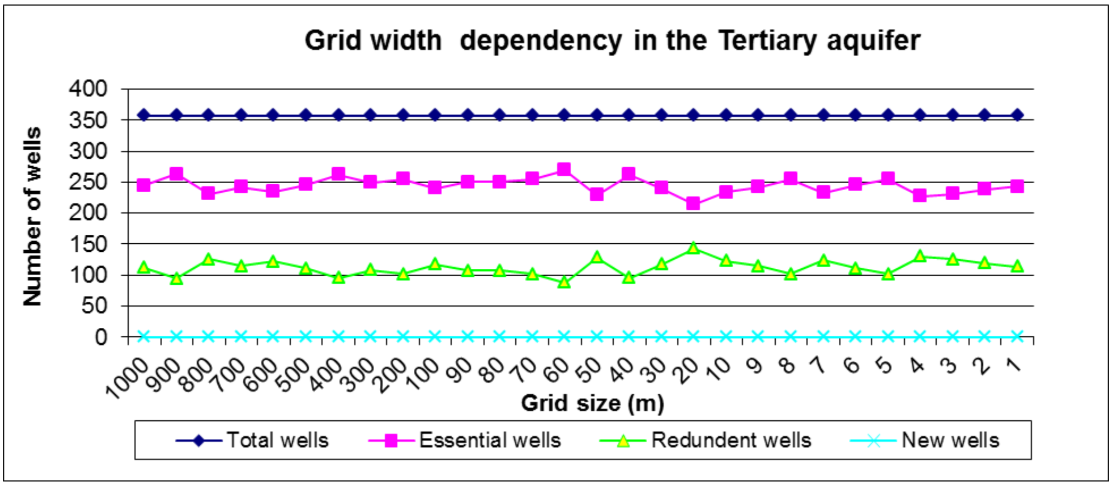

Figure 5.17: Grid width dependency in the LTM network optimization in the Tertiary aquifer for MCB and SO_4^{2-} in a 2-D plain.

In this study, the number of suggested/essential wells increases when the grid width for interpolation is reduced (1000 m to 1 m). At the smaller grid size, the relative spatial uncertainty gradually increases in the Quaternary aquifer for the existing LTM network (figures 5.17 and 5.18). The optimization recommends installation of a new well for grid width of 100m and increases to a recommendation for 21 new wells for grid width of 1m.

Optimization in a 2.5-D aquifer

The groundwater LTM network has been spatially optimized for MCB, α-HCH and SO_4^{2-} individually and in combination in a 2.5-D aquifer. The 2.5-dimension analysis assumes that there are multiple aquifers or hydrostratigraphic layers in the aquifer that do not have a hydraulic interconnection. In 2.5-dimension analysis, the LTM network is optimized separately for each hydrostratigraphic layer in the aquifer or aquifers. This also means that maps for a 2.5-D analysis are constructed for each layer separately using data from that layer only. The data used are segregated into subsets, each subset representing one Chemical of Concern (COC) for each vertical zone and time slice triplet, and the Quadratic Logistic Regression (QLR) mapping algorithm used the data from a given subset to map the layer and time frame represented by a given triplet.

With the change in grid width for interpolation (1 m to 1 km) the number of suggested i.e. essential wells and redundant wells does not change significantly (figures 5.19 and 5.20). However, the spatial relative uncertainty increases significantly with decreasing grid width for interpolation from 20 m to 1 m in both aquifers, and consequently the installation of 58 and 38 new monitoring wells in Quaternary and Tertiary aquifers are recommended, respectively.

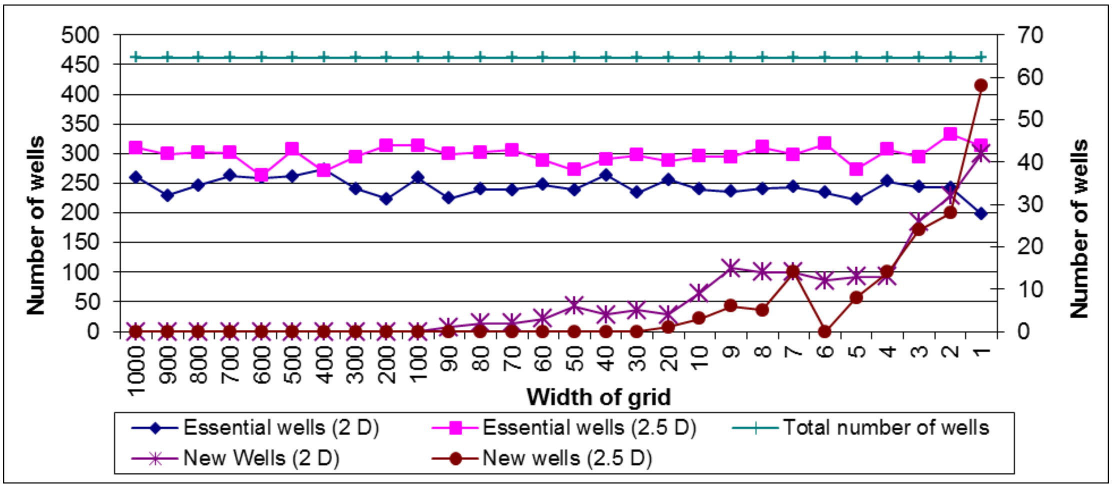

Figure 5.18: Grid width dependency in the LTM network optimization in the Quaternary aquifer for MCB, α-HCH and SO_4^{2-} considering 2-D and 2.5-D aquifers. Essential, redundant and total number of wells on left Y-axis and number of new well on right Y-axis.

The spatial optimization of the LTM network for α-HCH and $SO4^{2-}$ in a 2.5-D aquifer shows high redundancy because of the homogeneous distribution of SO_4^{2-} concentration.

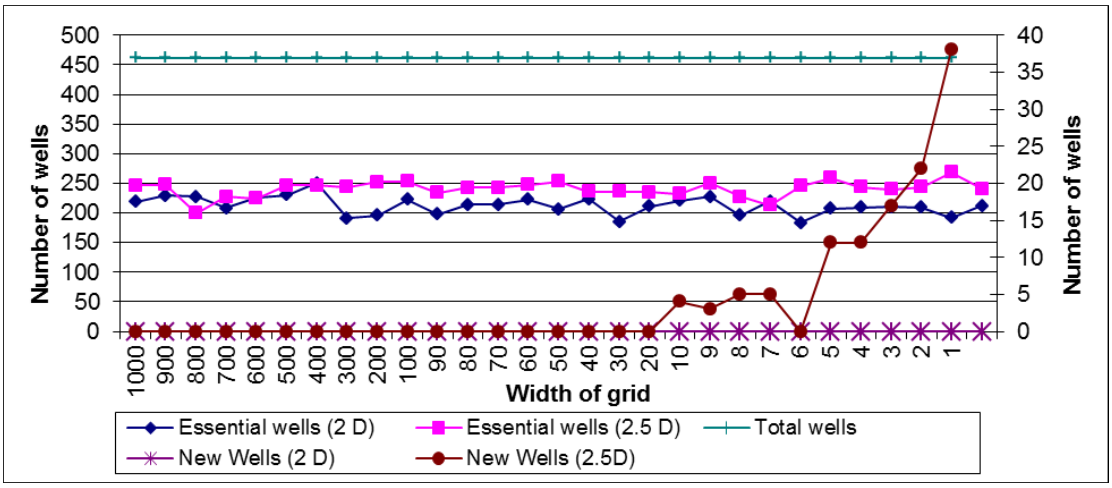

Figure 5.19: Grid width dependency in the LTM network optimization in the Tertiary aquifer for MCB, α-HCH and SO_4^{2-} in 2-D and 2.5-D aquifers. Essential, redundant and total number of wells on left Y-axis and number of new well on right Y-axis.

However, in both aquifers, the spatial uncertainty increases with decreasing grid width from 7 m to 1 m (figure 5.20 and 5.22). Consequently, the installation of 21 and 47 new monitoring wells is recommended in the Quaternary and Tertiary aquifers respectively at 1 m grid width. The relative spatial uncertainty, based on the local kriging variance, is very high at small grid widths in the Tertiary aquifer.

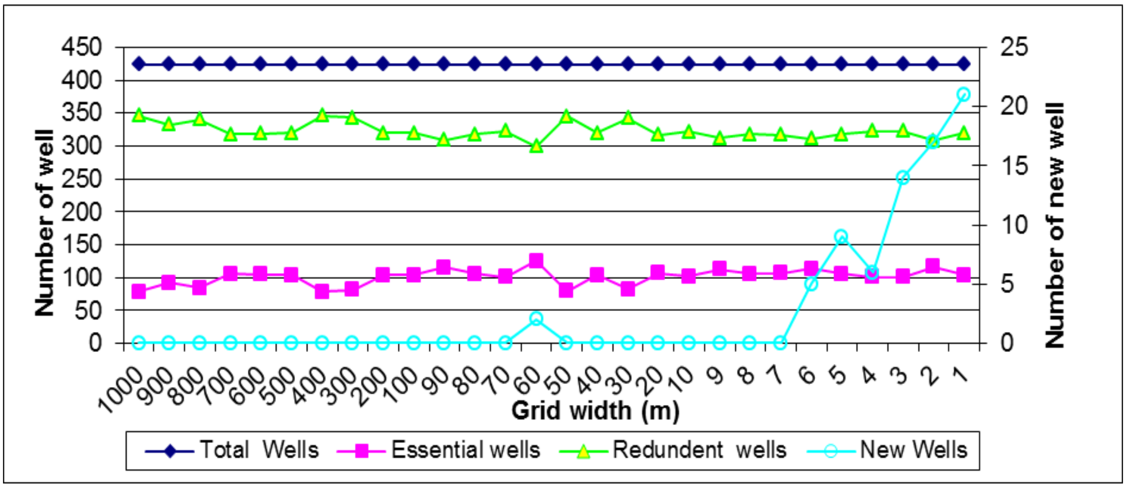

Figure 5.20: Grid width dependency in the LTM network optimization in the Quaternary aquifer for α-HCH and SO_4^{2-} in a 2.5-D aquifer. Essential, redundant and total number of wells on left Y-axis and number of new well on right Y-axis.

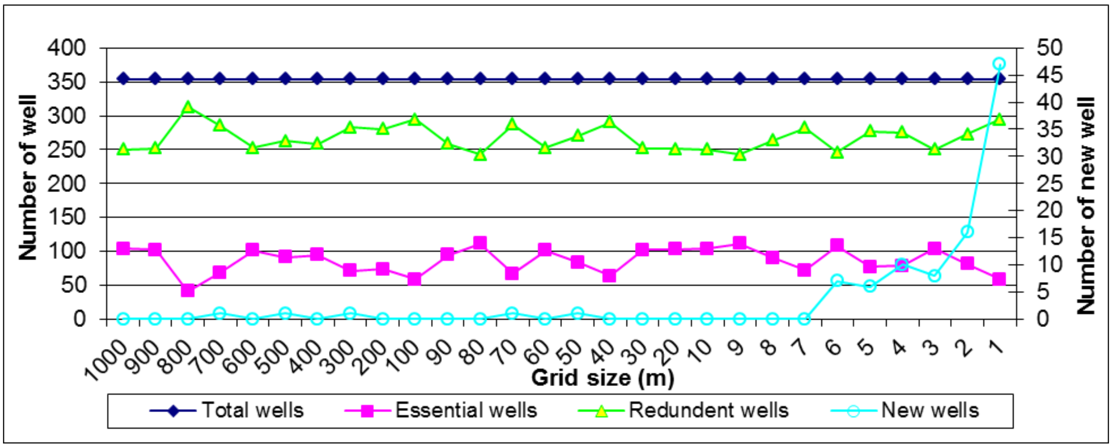

Figure 5.21: Grid width dependency in the LTM network optimization in the Tertiary aquifer for α-HCH and SO_4^{2-} in a 2.5-D aquifer. Essential, redundant and total number of wells on left Y-axis and number of new well on right Y-axis.

As both MCB and α-HCH have multiple contamination sources and are heterogeneously distributed, a higher number of monitoring wells is also required for a 2.5-D aquifer. In both aquifers, the relative spatial uncertainty increases with decreasing grid width from 8m to 1m (figure 5.22 and 5.24). Consequently, the installation of 51 and 70 new monitoring wells are recommended in the Quaternary and Tertiary aquifers, respectively, at 1 m grid width. This shows very high relative spatial uncertainty at small grid width for both aquifers.

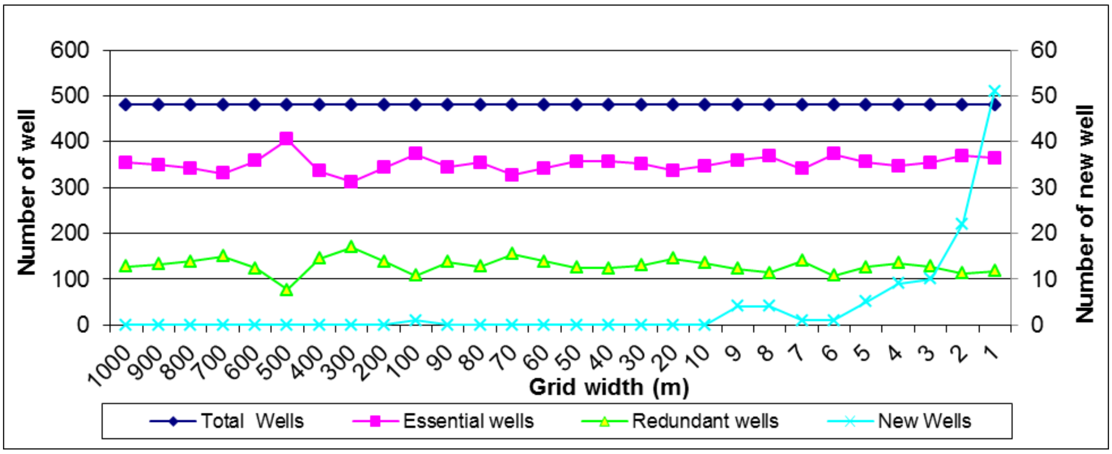

Figure 5.22: Grid width dependency in the LTM network optimization in the Quaternary aquifer for MCB and α-HCH in a 2.5-D aquifer. Essential, redundant and total number of wells on left Y-axis and number of new well on right Y-axis.

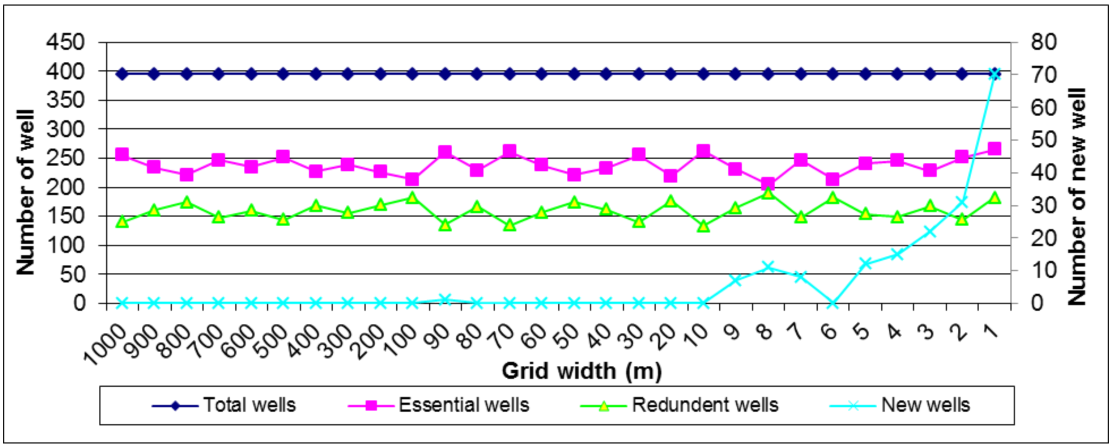

Figure 5.23: Grid width dependency in the LTM network optimization in the Tertiary aquifer for MCB and α-HCH in a 2.5-D aquifer. Essential, redundant and total number of wells on left Y-axis and number of new well on right Y-axis.

Although SO_4^{2-} is homogeneously distributed in both aquifers, the LTM network optimization for both MCB and SO_4^{2-} recommends a higher number of essential monitoring wells in the network in a 2.5-D aquifer. For both aquifers, the relative spatial uncertainty increases with decreasing grid width from 20 m to 1 m (figures 5.25 and 5.26). Consequently, the installation of 22 and 30 new monitoring wells are recommended in the Quaternary and Tertiary aquifers, respectively, at 1m grid width.

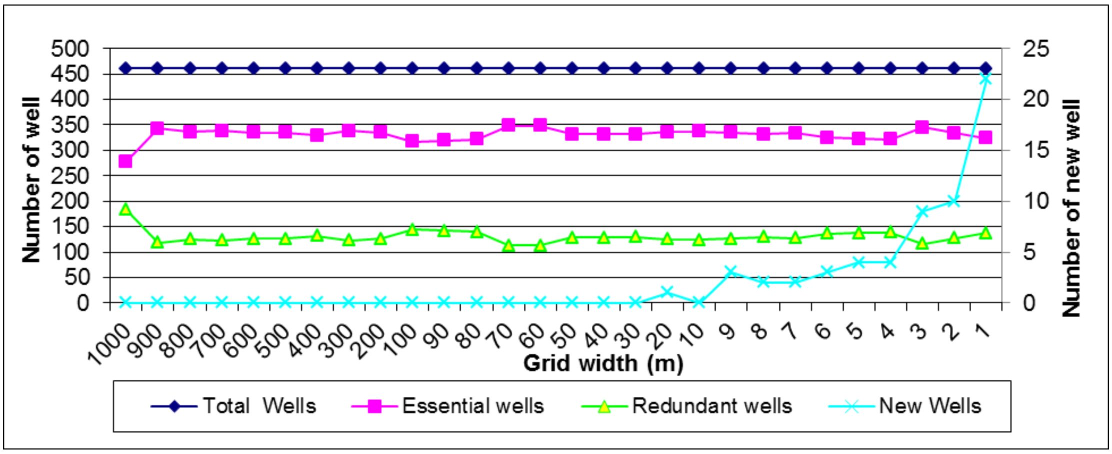

Figure 5.24: Grid width dependency in the LTM network optimization in the Quaternary aquifer for MCB and SO_4^{2-} in a 2.5-D aquifer. Essential, redundant and total number of wells on left Y-axis and number of new well on right Y-axis.

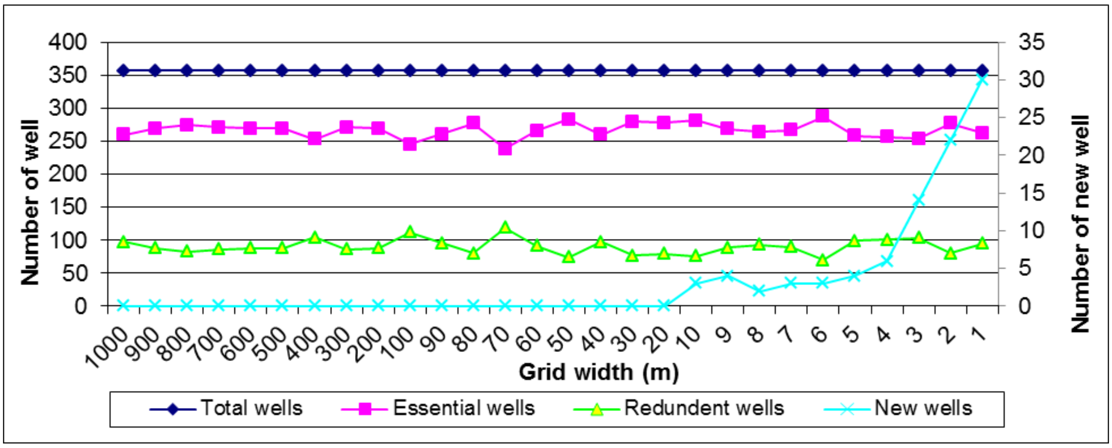

Figure 5.25: Grid width dependency in the LTM network optimization in the Tertiary aquifer for MCB and SO_4^{2-} in a 2.5-D aquifer. Essential, redundant and total number of wells on left Y-axis and number of new well on right Y-axis.

5.3.3 Contaminants association

The LTM network was spatially optimized for the contaminants MCB, α-HCH and SO_4^{2-} in pairs and all grouped together, considering the groundwater aquifer as a 2-D plain and as a 2.5-D aquifer. The spatial optimizations of the LTM network for MCB and α-HCH individually show less redundancy and recommendations for new monitoring wells. However, the optimization of the monitoring network for SO_4^{2-} recommends very high proportion of redundant wells (70%). The influence of incorporating a greater number of contaminants can be observed from figures 5.11 to 5.26. For example, in the Quaternary aquifer considered as a 2-D plain, for α-HCH and SO_4^{2-} 86 wells are recommended, for MCB and SO_4^{2-}: 282 wells, and for MCB and α-HCH: 310 wells. However 244 wells are recommended when considering all three contaminants, MCB, SO_4^{2-} and α-HCH, together.

When the LTM network was spatially optimized with these three contaminants in combination, the local kriging weights for each contaminant were averaged. Hence, the relative spatial uncertainty in the monitoring network depends upon the spatial distribution of the individual contaminants. The monitoring network optimization for both aquifers considering individual contaminants and the contaminants in combination gives recommendations for different numbers and locations of new wells (figures 5.11 to 5.26)

5.3.4 Groundwater flow direction and aquifer homogeneity

The groundwater flow direction needs to be analysed in order to optimize monitoring wells. When the groundwater flow direction is less constrained, more monitoring wells are needed. The groundwater flow direction and its dependency on the LTM network optimization was analysed using geostatistical and flow direction modelling methods. The spatial characterisation of the groundwater contamination scenario was observed using an experimental variogram displaying the contaminant concentration data of MCB, α-HCH and SO_4^{2-}. The experimental variogram characterises the degree of spatial correlation between contaminant concentration values as stochastic variables. The experimental variogram was estimated using Eqn. 4.14. The variogram was modelled using the Spherical-, Exponential-, Gaussian-, Linear-, and Nugget Effect models. However, the Spherical model is the best fit to the data set (figure 5.26).

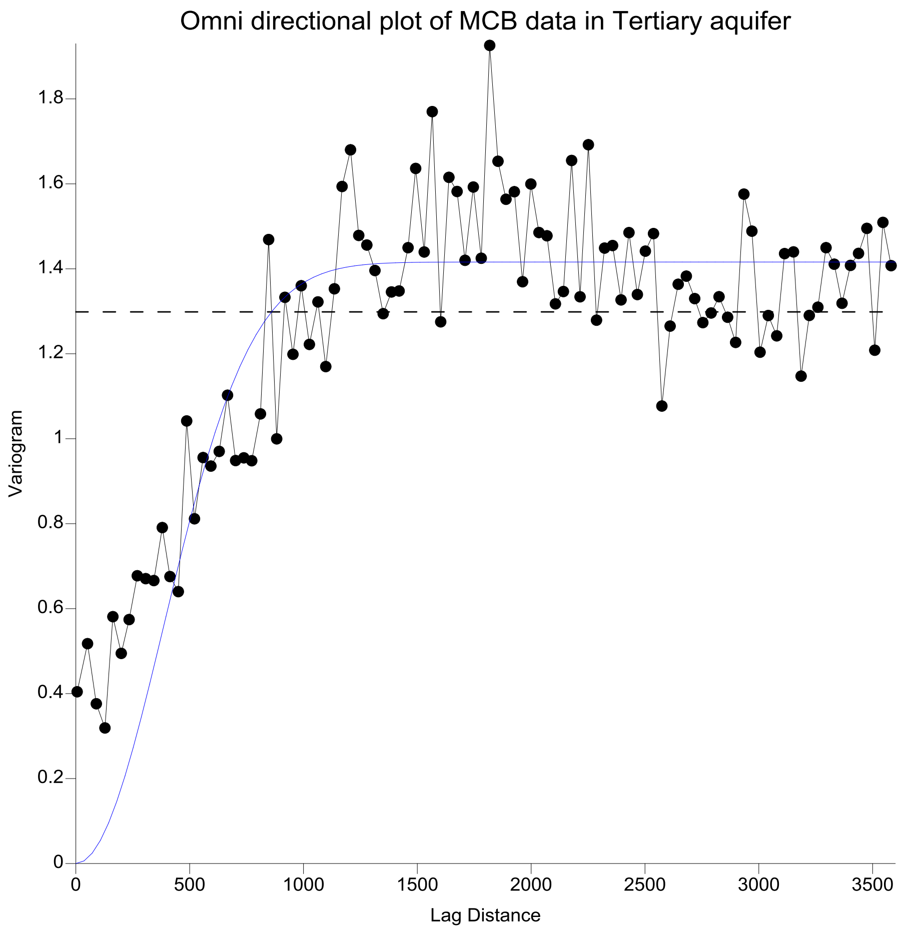

Figure 5.26: Experimental variogram (black) and model variogram (blue) based on MCB contaminant concentration data in the Tertiary aquifer (2003-2009). The variogram was calculated using 4576 data points of MCB contaminant concentration of the groundwater in the Tertiary aquifer (2003-2009). The Gaussian variogram model is defined by a range of 1448 m (x-axis) and a sill of 1.416 (y-axis).

The geometric anisotropy was found in the experimental variogram as range and sill differs in different directions. The anisotropy was observed for each

30° of lag direction with the reference of the North direction. The omnidirectional experimental variogram averages the behaviour over all directions. In this study, the heterogeneity of a geologic formation is quantified by using homogeneity index called RV Index (Eqn. 4.16) based on the spatial variability of contaminant concentration distribution.

Contaminant wise variogram modelling

Geometrical anisotropy was observed in the data set of MCB, α-HCH and SO_4^{2-} based on the experimental variogram, as the range differs in different directions.

In the Quaternary aquifer, the experimental variogram, which shows each 30° of lag direction, reveals that the range is highest in the Northern direction (0°), as shown in table 5.9. Similarly, the RV index, which corresponds to the estimated homogeneity, is highest in the Northern direction. However, for the Tertiary aquifer, the experimental variogram shows that the range is highest at 30° from the Northern direction. Similarly, in the Tertiary aquifer, the RV index is highest in the direction of 30° from the Northern direction, as shown in table 5.9. These results indicate that the overall prominent α-HCH concentration flows towards the North in both aquifers. In the Tertiary aquifer this flow is slightly diverted towards to east direction.

Table 5.9: Directional variogram modelling α-HCH concentration in the LTM network in Quaternary and Tertiary aquifers (January 2003 to February 2009)

α-HCH for Quaternary aquifer (2003-2009)				α-HCH for Tertiary aquifer (2003-2009)			
Model: Gaussian, Variance: 0.62				Model: Gaussian, Variance: 0.57			
Direction	Range	Sill	RV Index	Direction	Range	Sill	RV Index
Omni	404	0.64	641.27	Omni	1182	0.70	1862.88
0	666	0.62	1074.19	0	960	0.79	1416.97
30	464	0.64	736.51	30	1340	0.67	2161.29
60	385	0.66	601.56	60	999	0.69	1591.91
90	321	0.66	501.56	90	710	0.70	1118.11
120	360	0.65	566.93	120	722	0.70	1137.01
150	433	0.63	692.80	150	750	0.68	1200.00
180	590	0.62	951.61	180	960	0.69	1529.76

The RV index value in the Quaternary aquifer was lower than that in the Tertiary aquifer. This relatively lower RV index shows a high heterogeneity in the Quaternary aquifer.

For the data set of MCB, the experimental variogram, with 30° lag direction intervals, shows that the range is highest in the Northern direction. Similarly, the RV Index is also highest in the Northern direction in the Quaternary aquifer. However, in the Tertiary aquifer the RV index is highest in the direction of 60° from North, as shown in table 5.10. These results indicate that the overall prominent MCB concentration flows Northwards in the Quaternary aquifer, But i is slightly diverted towards the East in the Tertiary aquifer.

Although the concentration of SO_4^{2-} is more homogeneously distributed compared to the concentration of α-HCH and MCB concentration in the study area, the experimental variogram, with 30° lag direction intervals, clearly shows that the range is highest in the Northern direction with 30° deviation towards east in both aquifers (table 5.10).

Table 5.10: Directional variogram modelling MCB concentration in the LTM Network in Quaternary and Tertiary aquifers (January 2003 to February 2009).

MCB for Quaternary aquifer (2003-2009)				MCB for Tertiary aquifer (2003-2009)			
Model: Gaussian, Variance: 2.05				Model: Gaussian, Variance: 1.30			
Direction	Range	Sill	RV Index	Direction	Range	Sill	RV Index
Omni	1225	1.95	613	Omni	1285	1.41	948
0	2000	2.00	988	0	1290	1.42	949
30	1461	1.80	759	30	1811	1.40	956
60	1214	1.92	612	60	1958	1.42	1332
90	1286	1.95	643	90	1428	1.35	1078
120	1171	1.97	583	120	1428	1.32	1092
150	1571	1.99	778	150	1285	1.41	948
180	1931	2.00	954	180	1285	1.40	952

Similarly, the RV index, which corresponds to the estimated homogeneity, is highest in the direction of 30° from North in both aquifers (table 5.11). The RV index in the Quaternary aquifer is lower than that in the Tertiary aquifer. This lower value of the RV index reveals a higher heterogeneity in the Quaternary aquifer.

In general, the homogeneity index based on variogram modelling using α-HCH, MCB and SO_4^{2-} is lower in the Quaternary aquifer than the Tertiary aquifer. This high hydrogeological heterogeneity in the Quaternary aquifer shows a requirement for more groundwater monitoring wells in this aquifer.

Table 5.11: Directional variogram modelling SO_4^{2-} concentration in the LTM network in Quaternary and Tertiary aquifers (January 2003 to February 2009).

SO_4^{2-} for Quaternary aquifer (2003–2009)				SO_4^{2-} for Tertiary aquifer (2003–2009)			
Model: Gaussian, Variance: 0.128				Model: Gaussian, Variance: 0.158			
Direction	Range	Sill	RV Index	Direction	Range	Sill	RV Index
Omni	333	0.15	2404	Omni	728.5	0.15	4731
0	200	0.12	1613	0	833	0.135	5686
30	312	0.10	2694	30	866	0.132	5972
60	218	0.10	1929	60	466	0.149	3036
90	178	0.11	1528	90	533	0.145	3518
120	187	0.12	1508	120	566	0.142	3773
150	200	0.14	1493	150	633	0.152	4084
180	266	0.14	1985	180	833	0.156	5306

Season wise variogram modelling for α-HCH data

In order to analyse seasonal variability, the experimental variogram was modelled using the data set of α-HCH for hydrological summer and winter seasons. The data collected during the period from May to October (2003-2009) and November to April (2003-2009) were categorized as hydrological summer and winter seasons. Analysis of the experimental variogram, again with 30° lag direction intervals, using α-HCH data for the hydrological summer season still shows that the range is highest in the North direction in both Quaternary and Tertiary aquifers, as shown in table 5.12.

Table 5.12: Directional variogram modelling α-HCH concentration in the LTM network in Quaternary and Tertiary aquifers for summer seasons (May to October in 2003–2009).

α-HCH for Quaternary aquifer (May to October in 2003–2009)				α-HCH for Tertiary aquifer (May to October in 2003–2009)			
Model: Gaussian, Variance: 0.70				Model: Gaussian, Variance: 0.70			
Direction	Range	Sill	RV Index	Direction	Range	Sill	RV Index
Omni	491	0.78	661.99	Omni	1166	0.41	2854.69
0	491	0.70	701.43	0	1258	0.47	2875.43
30	387	0.75	532.54	30	1062	0.46	2455.49
60	340	0.77	461.52	60	939	0.38	2392.36
90	354	0.78	477.28	90	888	0.43	2122.12
120	364	0.79	488.59	120	737	0.43	1761.26
150	333	0.76	456.16	150	793	0.42	1934.15
180	390	0.65	577.78	180	882	0.44	2082.89

Similarly, the RV index, corresponding to aquifer homogeneity, is highest in the Northern direction. These results show that preferential groundwater flow and α-HCH concentration movement was in the Northern direction.

The experimental variogram was then modelled using α-HCH data for the hydrological winter season (November to April, 2003-2009). In the directional dependency analysis, the experimental variogram, with 30° lag direction intervals, shows that the range is highest in the direction of 60° from North in the Quaternary aquifer, as shown in table 5.13. However, in the Tertiary aquifer, the range is highest in the direction of 120° from North. Further, the RV index is lower in the Quaternary aquifer than the Tertiary aquifer, indicating high heterogeneity in Quaternary aquifer (table 5.13).

Table 5.13: Directional variogram modelling of α-HCH concentration in the LTM network in Quaternary and Tertiary aquifers for winter seasons (November to April from 2003–2009).

α-HCH for Quaternary aquifer in winter seasons (Nov. to April from 2003–2009)				α-HCH for Tertiary aquifer in winter seasons (Nov. to April from 2003–2009)			
Model: Gaussian, Variance: 0.68				Model: Gaussian, Variance: 1.25			
Direction	Range	Sill	RV Index	Direction	Range	Sill	RV Index
Omni	669	0.73	954.01	Omni	585	1.41	439.85
0	398	0.74	562.54	0	579	1.31	452.34
30	534	0.71	771.12	30	550	1.25	440.00
60	543	0.68	801.48	60	600	1.33	465.12
90	397	0.72	570.20	90	850	1.26	677.29
120	411	0.73	585.47	120	1050	1.22	850.20
150	422	0.74	596.89	150	823	1.25	658.40
180	513	0.73	729.21	180	526	1.32	409.34

Year wise directional variogram modelling for α-HCH data

In order to analyse geometrical anisotropy of the data set and to compare it with the simulated groundwater flow direction based on the hydrogeological model, variogram modelling was carried out for the monitoring data sets of the years 2005 and 2006. The experimental variogram, with 30° lag direction intervals, shows that the range is highest in the Northern direction, as shown in tables 5.14 and 5.15.

Again, the range was highest at 30^{o} from North in the Tertiary aquifer. The RV index varies with different lag directions, showing no distinct pattern or peak (tables 5.14 and 5.15).

Table 5.14: Directional variogram modelling α-HCH concentration in the LTM Network in Quaternary and Tertiary aquifers for 2005.

α-HCH for Quaternary aquifer in 2005				α-HCH for Tertiary aquifer in 2005			
Model: Gaussian, Variance: 0.89				Model: Gaussian, Variance: 1.05			
Direction	Range	Sill	RV Index	Direction	Range	Sill	Index
Omni	850	0.89	955.06	Omni	750	1.33	631.31
0	500	0.93	550.96	0	937	1.30	797.45
30	533	0.92	588.30	30	1125	1.35	937.50
60	758	0.95	826.16	60	933	1.30	794.04
90	856	0.93	939.63	90	750	1.30	638.30
120	800	0.94	874.32	120	750	1.30	638.30
150	533	0.95	580.93	150	562	1.32	474.26
180	500	0.91	555.56	180	687	1.33	577.31

Table 5.15: Directional variogram modelling α-HCH concentration in the LTM Network in Quaternary and Tertiary aquifers for 2006.

α-HCH for Quaternary aquifer in 2006				α-HCH for Tertiary aquifer in 2006			
Model: Gaussian, Variance: 0.59				Model: Gaussian, Variance: 1.05			
Direction	Range	Sill	RV Index	Direction	Range	Sill	RV Index
Omni	375	0.65	605.23	Omni	1333	0.81	1904.29
0	468	0.61	793.22	0	1684	0.72	2405.71
30	437	0.68	740.68	30	1727	0.84	2467.14
60	375	0.67	635.59	60	1333	0.86	1904.29
90	375	0.67	635.59	90	1058	0.84	1511.43
120	375	0.66	635.59	120	1058	0.84	1511.43
150	375	0.66	635.59	150	1055	0.68	1507.14
180	375	0.53	635.59	180	1277	0.69	1824.29

5.4 Hydrogeological modelling and LTM network optimization

A groundwater contaminant scenario in the Bitterfeld/Wolfen site was simulated using groundwater steady state flow and transient transport models. Initial transport and boundary conditions were implemented so as to represent a historical scenario of multi-source groundwater contamination (section 4.5).

The simulated contaminant scenario was observed at 462 reference wells in the Quaternary aquifer and 357 reference wells in the Tertiary aquifer.

5.4.1 3-D groundwater hydrogeological modelling

The hydrogeological model, which simulated a 21-year period from 2005 to 2025, was used to estimate head, mass and flow velocity at different potential unmonitored and monitored locations. The groundwater solute mass is the medium for advective and dispersive transport. Solute transport was used to locate the solute mass that is used for the monitoring network optimization.

Model geometry

An existing 3-D numerical groundwater flow model of the study area, established by Gossel, Stollberg et al. (2009) at the department of hydrogeology and environmental geology of Martin Luther University (MLU), Halle, Germany, was used to define problem.

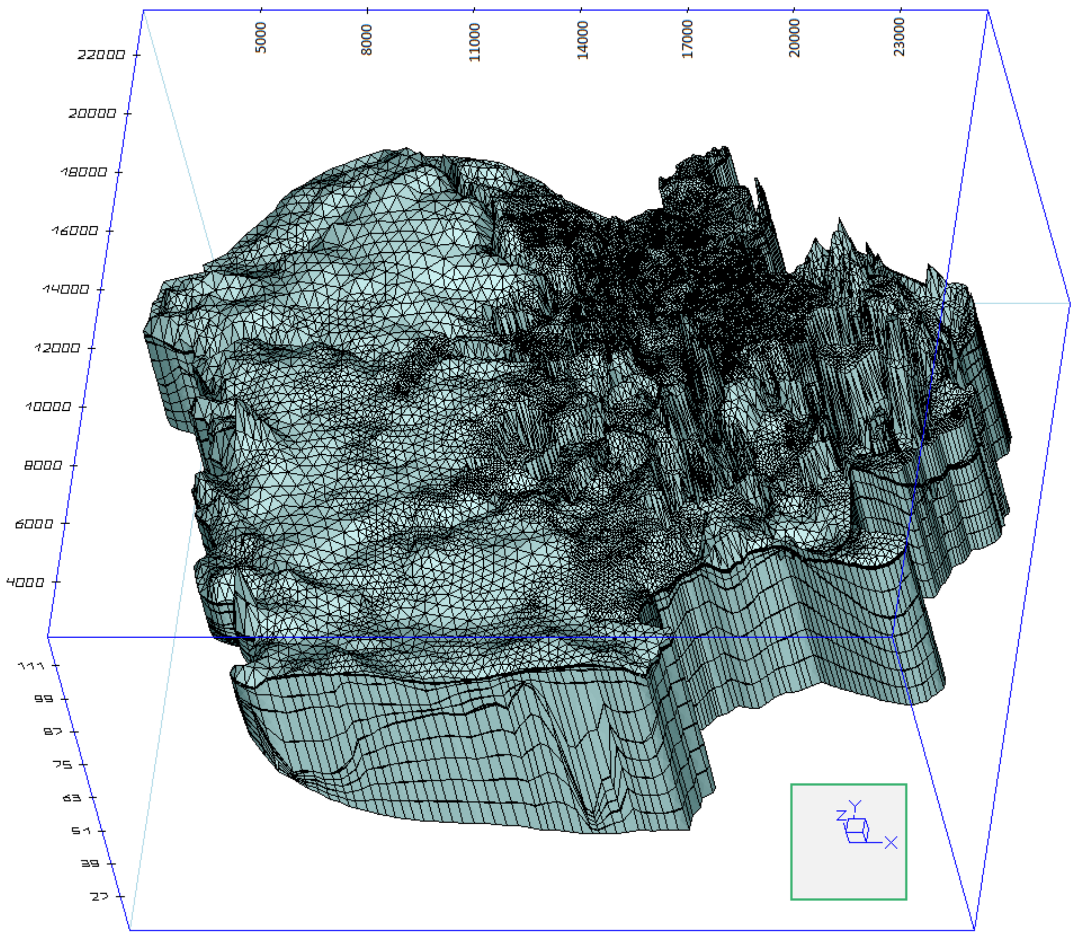

Figure 5.27: The structural FE model showing the mesh density distribution. The mining and dump-sites area have a higher mesh density than outer areas.

It was modified for use with BC transport and the results were exported for groundwater monitoring network optimization. The model domain Ω of 320 km² was subdivided into a number of triangular shaped elements in the horizontal and vertical scale (figure 5.27). The model area had a finite element mesh that consisted of 1475,708 triangle elements connected with 770,450 nodes (in 37 hydrogeological layers) (Stollberg, 2013). Mining and dump-sites have a higher mesh density than outer areas.

Table 5.16: Overview of hydrogeological units and layers of the model with their respective hydraulic conductivities (Gossel *et al.*, 2009).

					Hydrogeological Units	HGU	Numerical Layer	Hydraulic Conductivity (m/s)	
Caenozoic	Quaternary	Holocene			Anthropogenic made ground	1	1/2	$7 \cdot 10^{-4}$	$5 \cdot 10^{-4}$
					Anthropogenic landfill			$1 \cdot 10^{-7}$	$7 \cdot 10^{-4}$
					Meadow loam			$5 \cdot 10^{-6}$	$1 \cdot 10^{-5}$
					River gravel terrace			$3 \cdot 10^{-3}$	
		Pleistocene	Weichselian		Loess or loess loam			$2 \cdot 10^{-7}$	
					Glacial cover sands			$9 \cdot 10^{-4}$	$2 \cdot 10^{-4}$
					Weichselian river gravel (upper part)	2	3/4/5	$3 \cdot 10^{-4}$	$2 \cdot 10^{-3}$
					Periglacial horizon	3	6/7/3	$1 \cdot 10^{-6}$	$2 \cdot 10^{-5}$
					Weichselian river gravel (lower part)	4	9/10/11	$4 \cdot 10^{-4}$	$1 \cdot 10^{-3}$
			Saalian		Fluvial to glacial-fluvial outwash			$3 \cdot 10^{-5}$	$2 \cdot 10^{-3}$
					Sediments			$3 \cdot 10^{-5}$	$2 \cdot 10^{-3}$
					Saalian till complex	5	12/13/14	$5 \cdot 10^{-10}$	$1 \cdot 10^{-8}$
					Saalian Main Terrace	6	15/16/17	$5 \cdot 10^{-4}$	$2 \cdot 10^{-3}$
			Elsterian		Glacial-fluvial out wash sediments			$2 \cdot 10^{-4}$	$1 \cdot 10^{-4}$
					Glacial–limnetic sediments			$1 \cdot 10^{-5}$	
					Elsterian till complex	7	18/19/29	$1 \cdot 10^{-8}$	$8 \cdot 10^{-5}$
		Mio-cene	Bitterfeld Complex	Clay Cover Complex	Bitterfeld clay cover	8	21/22/23	$1 \cdot 10^{-8}$	$8 \cdot 10^{-7}$
					Roitzsch Sands			$8 \cdot 10^{-8}$	$3 \cdot 10^{-3}$
	Tertiary				Bitterfeld clay cover			$1 \cdot 10^{-8}$	$8 \cdot 10^{-7}$
					Bitterfeld seam complex	9	24/25/26	$2 \cdot 10^{-7}$	
		Oligocene		Mica Sand Complex	Bitterfeld sands	10	27/28/29	$1 \cdot 10^{-4}$	
					Bitterfeld horizon	11	30/31/32	$1 \cdot 10^{-10}$	
					Zoeckeritz sands	12	33/34/35	$2 \cdot 10^{-5}$	
					Glauconite sands			$2 \cdot 10^{-5}$	
					Glauconite silts	13	36/37	$1 \cdot 10^{-10}$	
			Rupelian		Rupelian clay				

As described in section 3.1, the vertical structure of the model has 13 individual hydrogeological units. These hydrogeological units are represented by 37 hydrogeological layers in the model, whose respective hydraulic conductivity correspond to hydrogeological units as per Wollmann (2004), Hubert (2005) and Gossel, Stollberg et al. (2009). Based on the nature of the hydrogeological units, a hydraulic conductivity was assigned to each hydrogeological layer in the model, as given in table 5.16.

In order to incorporate model parameters, and initial and boundary conditions for the respective hydrogeological units, each of the hydrogeological units was represented by three numerical layers. However, the first and last units were represented by only two numerical layers.

5.4.2 3-D groundwater flow model

Steady state flow velocity was observed using numerical flow modelling for a time period of 21 years. As per the objective to use the flow model for LTM network optimization, the simulated groundwater flow scenario of Bitterfeld/Wolfen for 25th December, 2025 was visualized. The groundwater flow velocity was visualized using contour lines and particle tracks from the FEFLOW result file (*.dac). The 3-D groundwater flow scenario illustrates a dominant flow with a high gradient in the natural reserves area (figure 5.28).

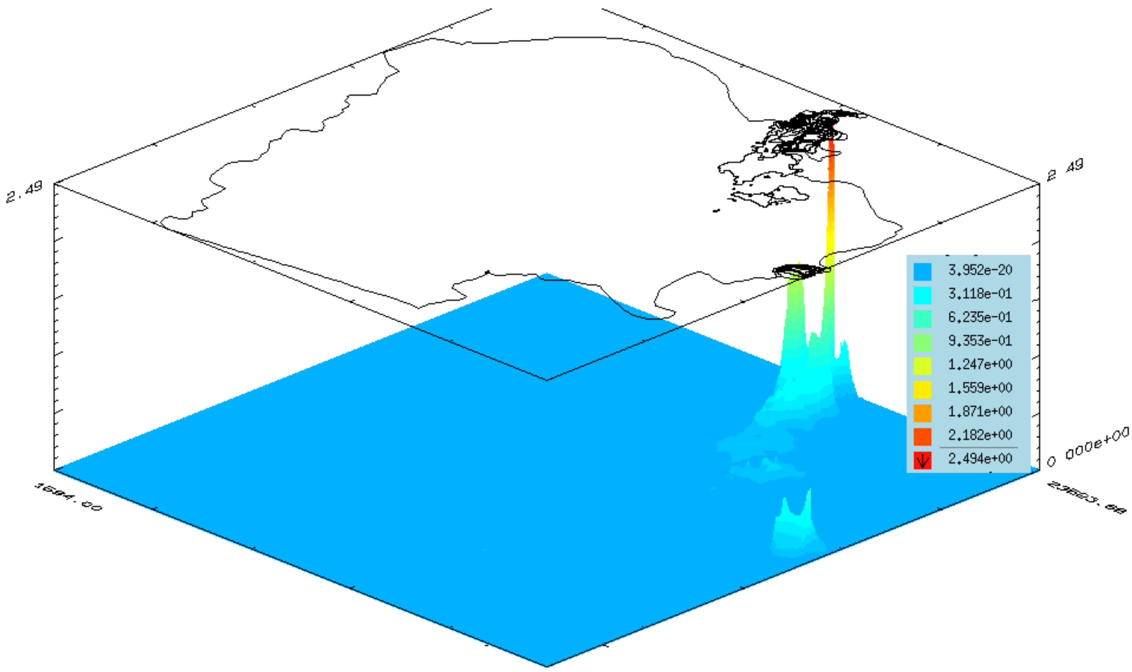

Figure 5.28: 3-D groundwater flow velocity scenario showing the future groundwater flow scenario of 25th December 2025, which has dominant flow with high gradient in the industrial area.

Comparatively high groundwater flow was observed in the historical mining area in the Quaternary aquifer. In the modelled area (320 km^2) in the latter part of the model period, the groundwater flow velocity ranges from 2.49 m/day to 3.95×10^{-20} m/day. However, the monitoring network, which should be optimized using the model result, only covers the mining area, dump site, industrial and urban area of about 100 km^2. In the proposed monitoring network optimization area, the groundwater flow velocity ranges from 2.12×10^{-6} to 5.1×10^{-2} m/day. Furthermore, the extracted set of groundwater velocity results data and accessory information (i.e. name, coordinates, and elevation of the monitoring well, screen depth, stratigraphical geological layer, stratigraphical horizon [Quaternary (Q), Tertiary (T) and Quaternary-Tertiary (Q-T)]) have been used for the LTM network optimization.

5.4.2 3-D groundwater transport model (forward-in-time)

The 3-D groundwater transient transport model was used to simulate transport of a single species, α-HCH, incorporating initial and boundary conditions and the nature of the transport material of the study area, as explained in section 4.5.2. To use the transport model for LTM network optimization, the simulated groundwater mass scenario of Bitterfeld/Wolfen for 25th December 2025 was visualized (Figure 5.29).

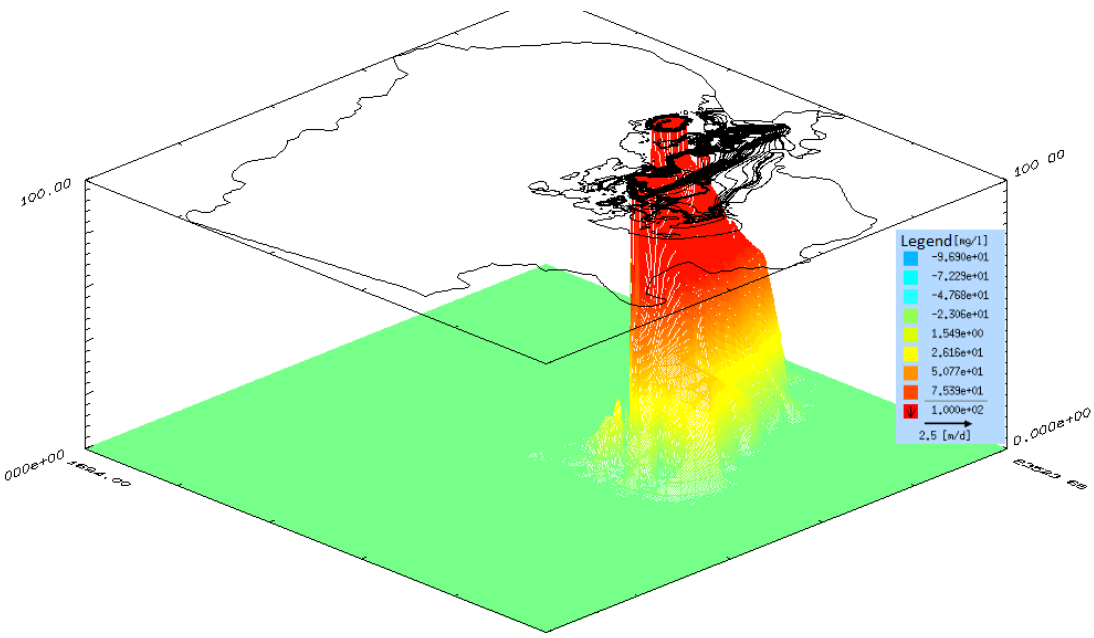

Figure 5.29: The simulated 3-D groundwater mass scenario of 25th December, 2025 showing the future groundwater mass scenario, which has a high concentration of contaminant at the centre of the industrial area in the Quaternary aquifer. The contaminant mass has also spread around and to the Tertiary aquifer.

The groundwater contaminant mass scenario was visualized using contour lines from the FEFLOW result file (*.dac). The solute concentration [mg/l] was recorded in the form of time series data at the reference monitoring wells. These recorded solute concentrations were exported and used as accessory information for the analysis of spatiotemporal change of the ideal contaminant species in the existing LTM network. Specially, the solute concentration [mg/l] changes alone with time at the reference monitoring well were observed. Comparatively, the groundwater mass transport system is very complex at the Bitterfeld/Wolfen megasite. In this transport simulation of the α-HCH concentration, 100 [mg/l] α-HCH concentration was induced in various hydrogeological layers of the model at the multi-source locations as the initial conditions. Even after 21 years of simulation, the α-HCH concentration is still higher at Antonie, Titanteich, Übergabebahnhof, and Fasanen Dump sites. This scenario of high concentration of the contaminant needs to be considered in the optimization of the monitoring network. In order to visualize the location of contaminant mass, advective particle tracking methods were used to track path lines of the course of solute transport in the groundwater (figure 5.30).

5.4.3 LTM network optimization using hydrogeological model

The simulated 3-D groundwater hydrogeological model gives values of the head, mass and flow velocity at 462 reference wells in the Quaternary aquifer and 357 reference wells in the Tertiary aquifer. The model also helps to visualize the scenario of the head, mass (figure 5.29) and flow velocity (figure 5.28) at unmonitored locations, which is also necessary for better optimization of the LTM network. In order to optimize the LTM network for future groundwater scenarios, the head, mass and flow velocity from the date 25th December 2025 was used.

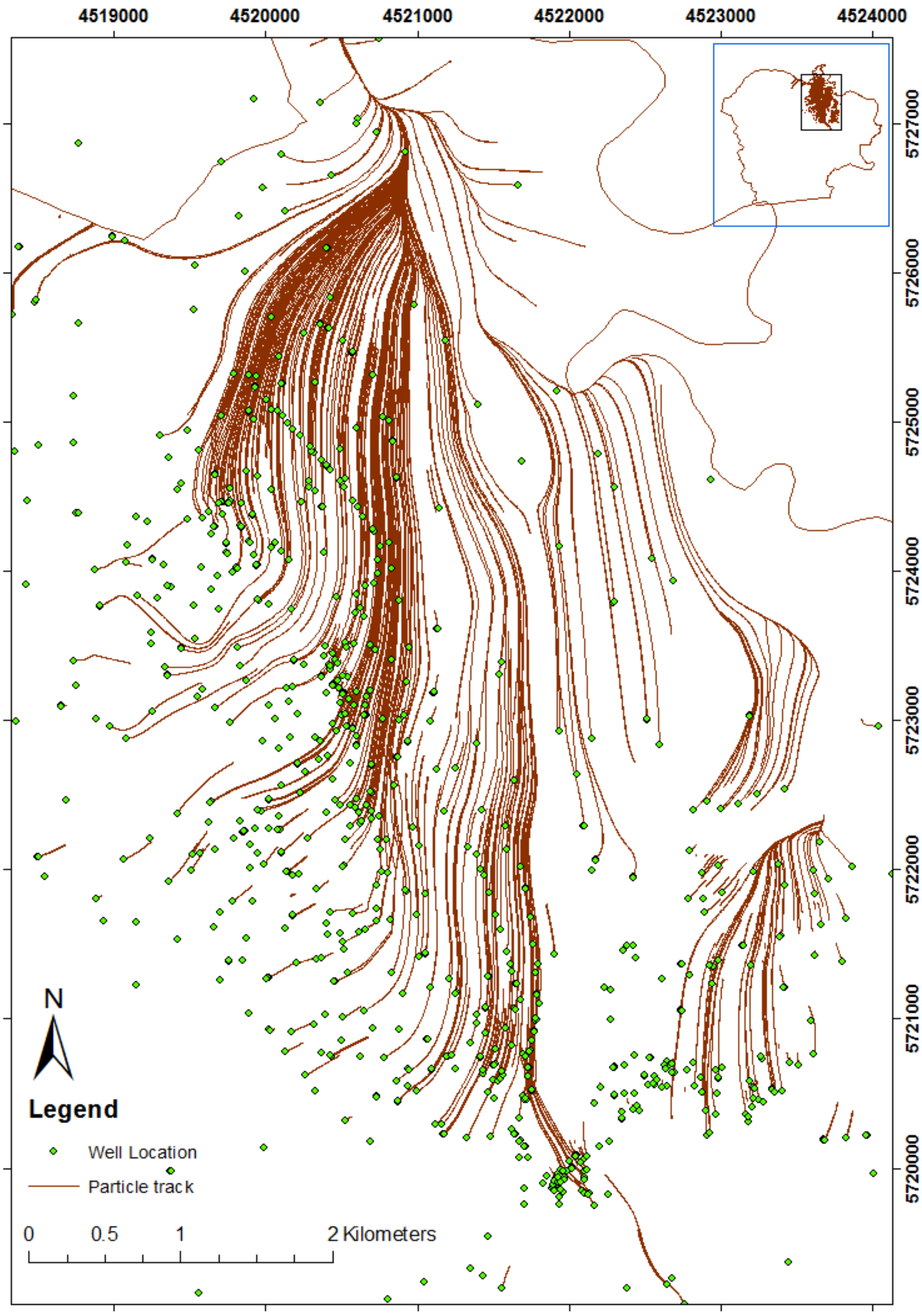

Figure 5.30: Overlaying locations of the monitoring wells on particle track path lines, showing instances with more than one well located on the some particle track path line.

5.4.4 Spatial optimization of the LTM network

Optimization of the LTM network according to the method and model described in section 4.4.6 was carried out for both aquifers separately. In both aquifers, overlying the particle tracks with the locations of existing monitoring wells shows that more than one well was located on some of the contaminant flow path lines (figure 5.30). Hence, according to the first LTM network optimization model statement that “more than one well on the same path line from same aquifer is redundant. If there are more than two wells on the same particle track, the middle one well is selected as essential well.", there is redundancy in the monitoring network.

The optimization result based on the first model mentioned in section 4.4.6 suggests that 30 of the 462 wells in the Quaternary aquifer (6.49%) and 14 of the 357 wells in the Tertiary aquifer (3.92%) were redundant. The monitoring wells tagged as essential or, redundant well in both aquifers are tabulated in appendix 5. Comparing this to the numbers of redundant wells obtained from the clustering approach, i.e. statistical method (section 4.2.4) and geostatistical methods (section 4.3.1), these numbers of redundant wells are very low. These lower numbers of redundant wells were due to the narrow width of the particle track. In order to elucidate more redundant wells in both aquifers, the width of the particle track path line was gradually increased from 0 m to 100 m. This increase in the width of the particle track path line increased the number of redundant wells remarkably in both aquifers, as shown in table 5.17.

As the groundwater scenario does not generally change drastically in nature, the width of the particle track was increased gradually by creating a buffer zone from 0 – 100 m around the particle track using ArcGis. Table 5.17 presents list of the numbers of redundant monitoring wells in each aquifer in optimized the LTM network using first spatial optimization models with the buffer zone increasing from 0 – 100 m around the particle track.

Table 5.17: Numbers of redundant monitoring wells in each aquifer in the optimized LTM network using the first spatial optimization models with the buffer zone increasing from 0 – 100 m around the particle track.

Aquifer	Total no of wells	Number of redundant wells with buffer zone from 0 – 100 m around the particle track.					
		0 m	20 m	40 m	60 m	80 m	100 m
Q	462	30	41	65	89	105	145
T	357	14	35	48	66	72	105

When considering 100 m of buffer zone around the particle track, the LTM network optimization using the first model shows that 145 of the 462 wells in the Quaternary aquifer (31.38%) and 105 of the 357 wells in the Tertiary aquifer (29.41%) were redundant. Figure 5.31 shows the distribution of essential and redundant wells in the existing monitoring network.

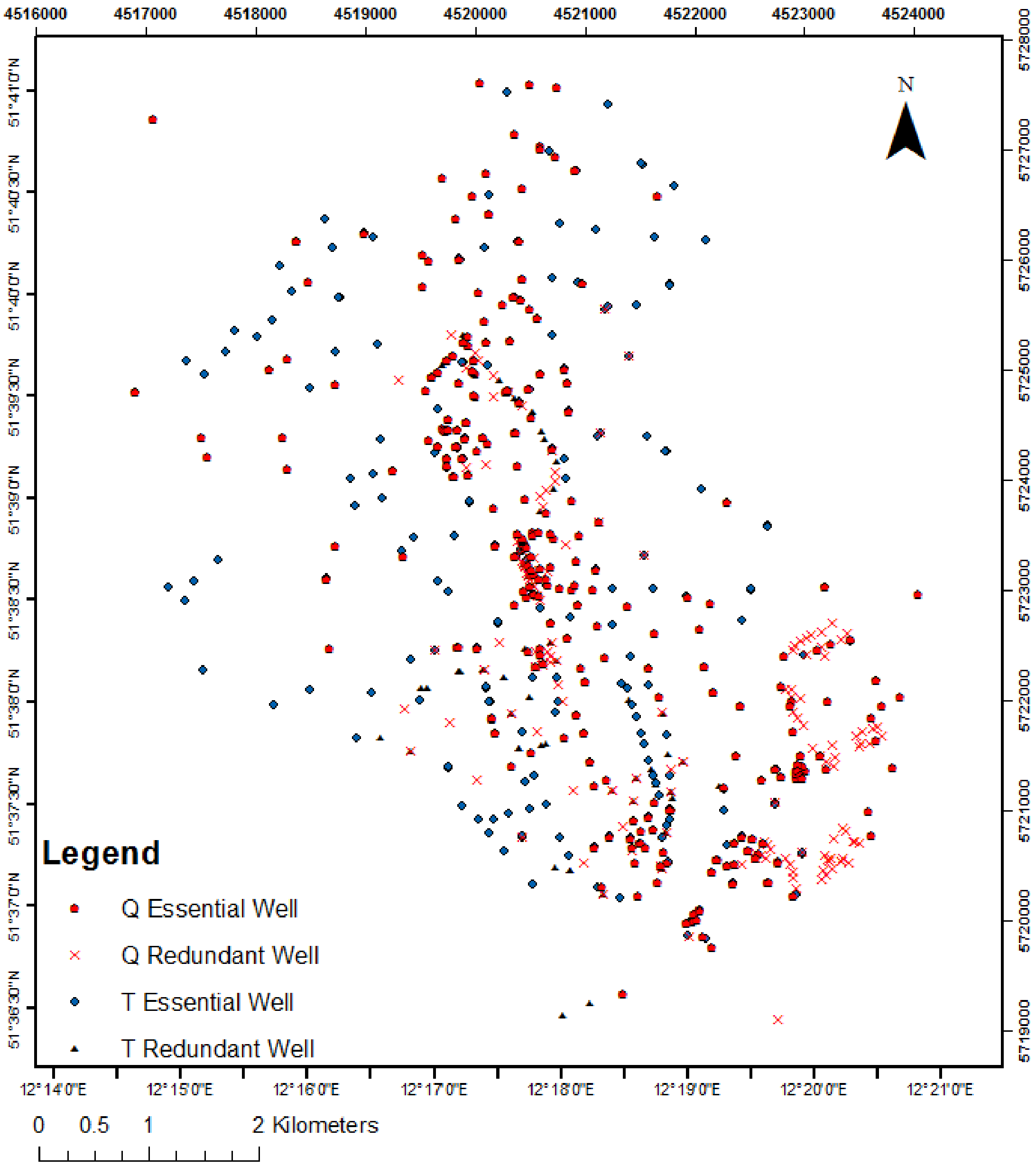

Figure 5.31: Optimized LTM network map showing essential and redundant wells in the Quaternary (Q) and Tertiary (T) aquifers.

Particle tracking and contaminant concentration was used for the monitoring network optimization, whilst head and flow velocity were used as accessory information for comparative analyses of random fluctuations of mass at various reference monitoring wells in the study area. Compared to the first proposed optimization model, the second and third models categorize the wells as essential and redundant with a subjective priority of redundancy.

5.4.5 Temporal optimization of the LTM network

The groundwater monitoring network was temporally optimized using the method described in section 4.4.6. Figure 5.32 shows locations of monitoring wells with each different recommended sampling interval. The simulated flow velocity and recommended sampling interval along with well location for each of the monitoring wells are tabulated in appendix 5.

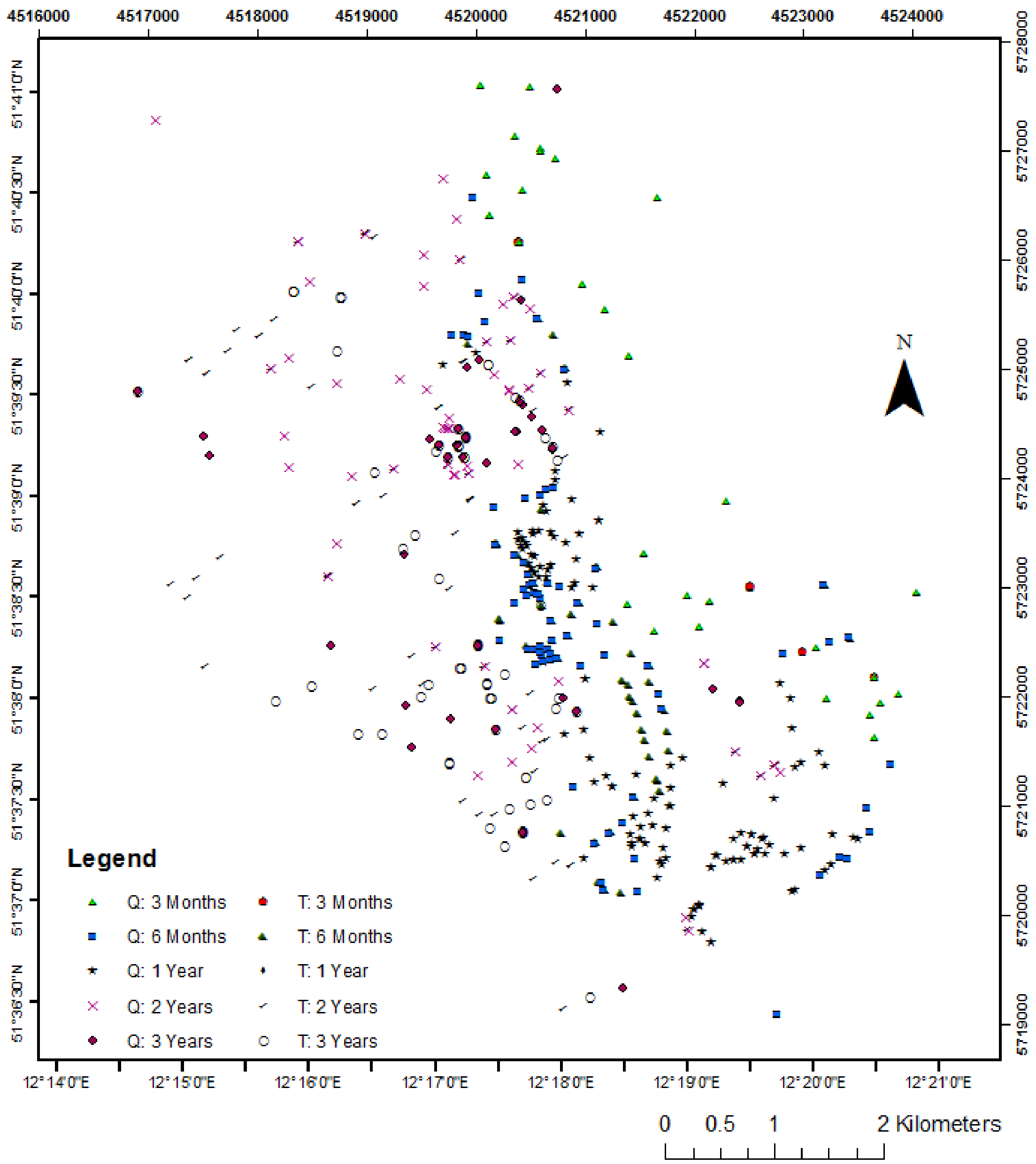

Figure 5.32: Locations of monitoring wells with each different recommended sampling interval in the Quaternary (Q) and Tertiary (T) aquifers.

The temporal optimization shows that the groundwater monitoring wells, i.e. all 819 monitoring wells in the Quaternary and Tertiary aquifers, should be sampled at the intervals given in table 5.18.

Table 5.18: Number of monitoring wells with each recommended sampling interval from both aquifers, i.e. the Quaternary (Q) and Tertiary aquifers (T).

Sampling Interval	3 month	6 month	1 year	2 years	3 years	Total
No of wells	50	155	287	160	167	819
Q	34	86	173	76	93	462
T	16	69	114	84	74	357

It is recommended that the monitoring wells located in the mining and urban areas should be sampled more frequently, whilst the monitoring wells located in south-eastern part of the study area should be sampled less frequently.

5.5 Comparison of results

Although the objectives of all of the proposed methods were the same, the application of these methods over the groundwater contamination data from the Bitterfeld/Wolfen megasite shows different monitoring network optimization recommendations. These three optimization methods have different optimization recommendations because their assumptions vary from each other. Statistical methods and hydrogeological method were used for spatiotemporal optimization of the existing monitoring network, whilst the geostatistical method was used for spatial optimization of the network. Within the applied approaches, the statistical method was not able to generate new monitoring location recommendations. However, the geostatistical method was used to make recommendations for new monitoring well locations in the existing network based on an uncertainties analysis.

5.5.1 Comparison of the statistical and geostatistical methods used

In the statistical approach, the AHC method was used to classify monitoring wells into essential and redundant wells (section 4.2.4), whilst in the geostatistial approach, Kriging—a geostatistical estimator—was used to compute numerical weights for a plume map and the monitoring wells were categorized into essential and redundant wells depending on the influence of removal of the well from the network on the plume map (section 4.3.1). The correlation between the results from these two methods was low (correlation coefficient: 23.45%). Of the 819 wells in both aquifers, only 256 were classified as essential wells using both statistical and geostatistial methods.

Some monitoring wells were tagged as essential using the statistical method but as redundant using geostatistical methods, and vice versa (table 5.19).

The monitoring wells located in the south-eastern part of the research area were found to be redundant according to both statistical and geostatistical methods (figure 5.33).

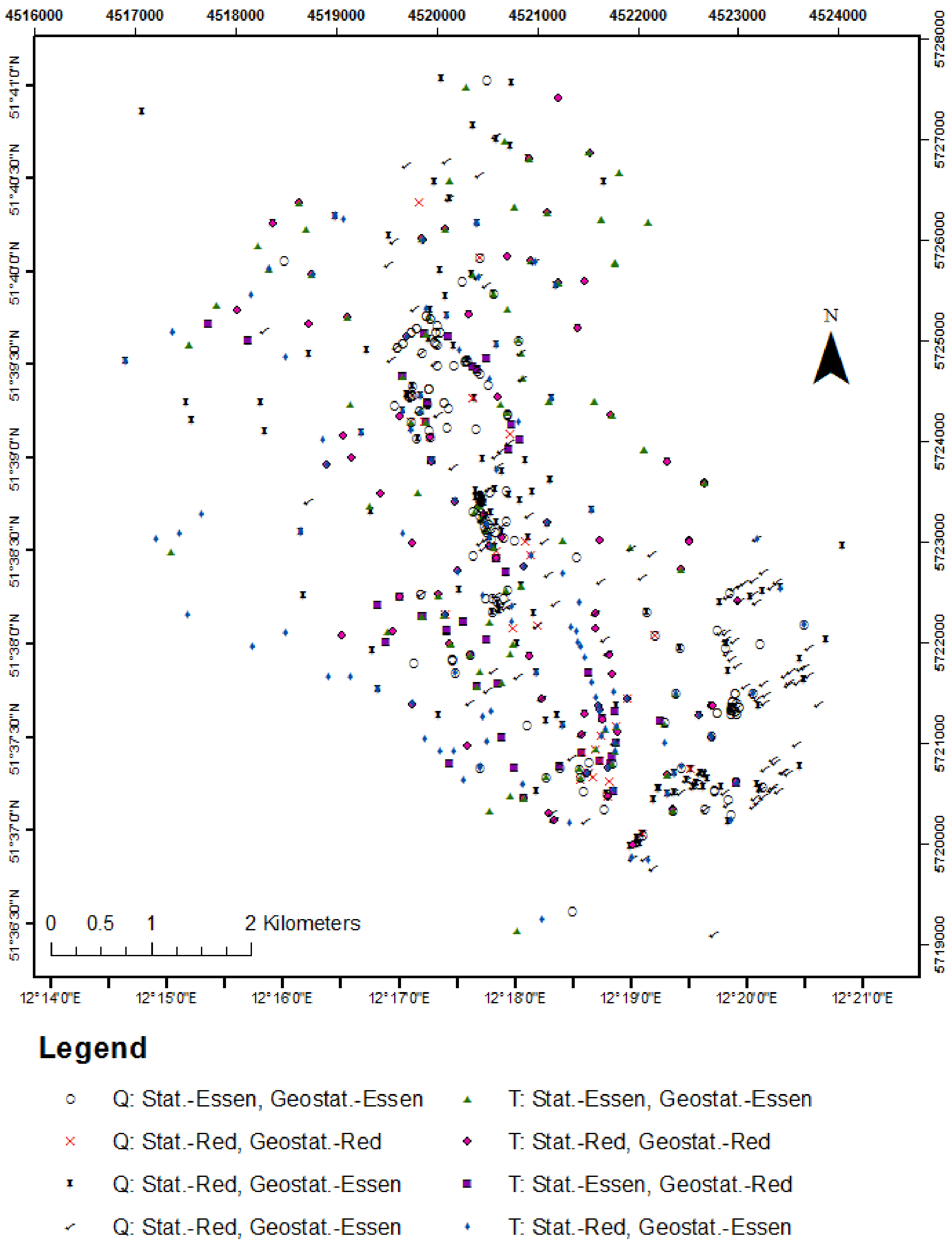

Figure 5.33: Locations of monitoring wells, showing wells categorized as essential or redundant according to both statistical and geostatistical methods. (note: Stat:

Statistical method, Geostat: Geostatistical method, Ess: Essential well, Red: Redundant well).

Table 5.19: Number of monitoring wells categorized as essential and redundant using statistical and geostatistial methods in both aquifers, i.e. Quaternary (Q) and Tertiary (T) aquifers.

Aquifer	Both statistical and geostatistical essential	Statistical essential and geostatistical redundant	Statistical redundant and geostatistical essential	Both statistical and geostatistical redundant
Q	154	30	145	133
T	102	48	115	92
Both	256	78	260	225

In the statistical methods, the optimization results could not give any information about unmonitored locations in the research area, whereas the geostatistial methods could identify locations for new monitoring wells (figure 5.9), which could help to find more information about the monitoring area.

5.5.2 Comparison of the geostatistical and hydrogeologial methods used

As explained in chapter 4, optimizations of the monitoring network using both geostatistial and numerical methods have different assumptions. The geostatistical method was applied to the real groundwater quality data set (section 4.3.1), whilst the hydrogeological methods of spatiotemporal monitoring network optimization were based on the modelled groundwater contaminants scenario. The application of these two methods to different types of data with different origins (real groundwater monitoring data and simulated data from a hydrogeological model) gives different optimization results.

As well as using geostatistical methods for optimizing the monitoring network, these methods were also used to estimate the contaminant spreading direction and aquifer homogeneity. The spatial variability in the flow direction was revealed using experimental variogram modelling, as presented in sections 4.3.4 and 5.3.4. The contaminant spreading direction is different for MCB, α-HCH and SO_4^{2-}. The α-HCH spreading direction, based on the α-HCH data set from 2003 to 2009, was predicted to be northwards. This estimated spreading direction was approximately verified by the contaminant flow direction elucidated from the analysis of particle tracks for α-HCH in the hydrogeological model for Quaternary and Tertiary aquifers.

To be more specific, the year-wise analysis of the groundwater and α-HCH contaminant flow direction based on experimental variogram modelling predicted a prominent flow direction towards the North in 2006 (section 5.3.4). This flow direction result from the experimental variogram modelling was verified by the groundwater and contaminant flow direction observed using the hydrogeological model. The contaminant flow direction was also found to be northwards in the analysis of particle tracks for α-HCH from the hydrogeological model for Quaternary and Tertiary aquifers (figure 5.34).

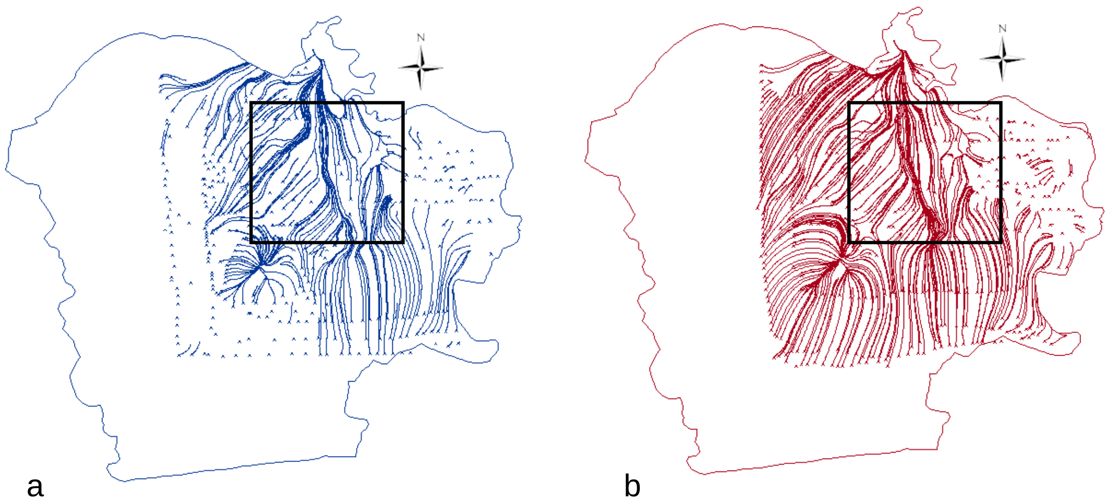

Figure 5.34: Particle tracking showing the α-HCH flow direction in the (a) Quaternary and (b) Tertiary aquifers from the hydrogeological model (model time: 101 days, 12th April 2005).

In figure 5.34, it can be observed that the contaminant flow direction changes slightly but the overall prominent flow direction is towards the north.

5.5.3 Comparison of hydrogeological methods and statistical methods used.

Both hydrogeological and statistical methods were used for spatiotemporal optimization of the monitoring network. The monitoring network was optimized using model based predicted data in the hydrogeological method (section 5.4.3), whilst the monitoring network was optimized using observed real groundwater quality data in the statistical method (section 5.2.3). The spatial optimization of the monitoring network shows less redundancy in the monitoring network when using the hydrogeological method compared to the statistical method. The temporal optimizations using these two methods have different results for each monitoring well in the monitoring network.

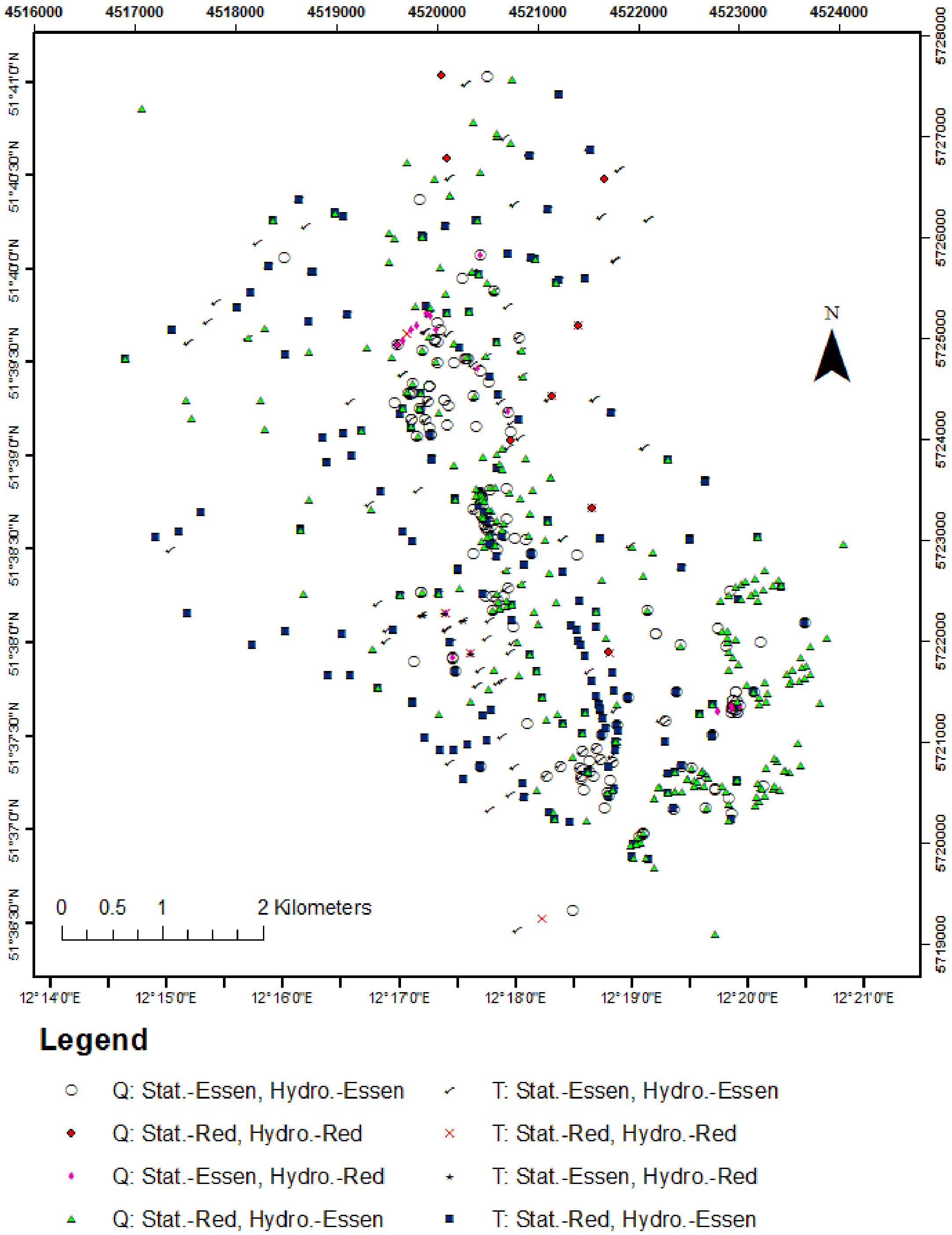

Figure 5.35: Locations of monitoring wells showing wells categorized as essential or redundant using hydrogeological and statistical methods. (note: stat: statistical method, Essen: Essential well, Hydro: Hydrogeologial method, Red: Redundant well).

5.6 Improving groundwater monitoring strategies

5.6.1 Integrating approaches for improving groundwater monitoring

New and improved methods were integrated with existing methods based on the statistical, geostatistical, and hydrogeological methods to make several sets of methods with different optimization objectives.

As an example, figure 5.36 depicts integration of statistical and geostatistical methods only. However, these methods could also be integrated with hydrogeological methods, depending upon the objective. In this example, the statistical and geostatistical methods were integrated to understand, evaluate and optimize groundwater monitoring with the reference to groundwater monitoring of a contaminated site (figure 5.36). As the first element of the groundwater monitoring framework, descriptive and multivariate statistics were used for analysis, classification, modelling and interpretation of the large dataset.

As the second element of the groundwater monitoring framework, the existing LTM network was optimized based on target variables (MCB, α-HCH and SO_4^{2-}) that represent physicochemical properties of groundwater using a geostatistical spatial optimization algorithm. In the geostatistical spatial optimization algorithm itself, the dimension dependency, influence of grid width for interpolation, and influence of multiple contaminants on the LTM network spatial optimization were discovered. However the groundwater flow direction and heterogeneity of aquifers were numerically estimated based on variogram modelling.

As third and fourth elements of the groundwater monitoring framework, the results obtained were analysed and interpreted in the light of other influencing factors, such as legal requirements and land use changes, in order to recommend essential, redundant and new monitoring wells in the existing LTM network.

Another example could be integration of statistical and hydrogeological methods. In this case, for the research area, where a large amount of data is available, the monitoring network could be optimized using statistical methods based on the observed data set. However, in areas where not enough real observed data is available, a hydrogeological model and particle tracking method could be used for the monitoring network optimization.

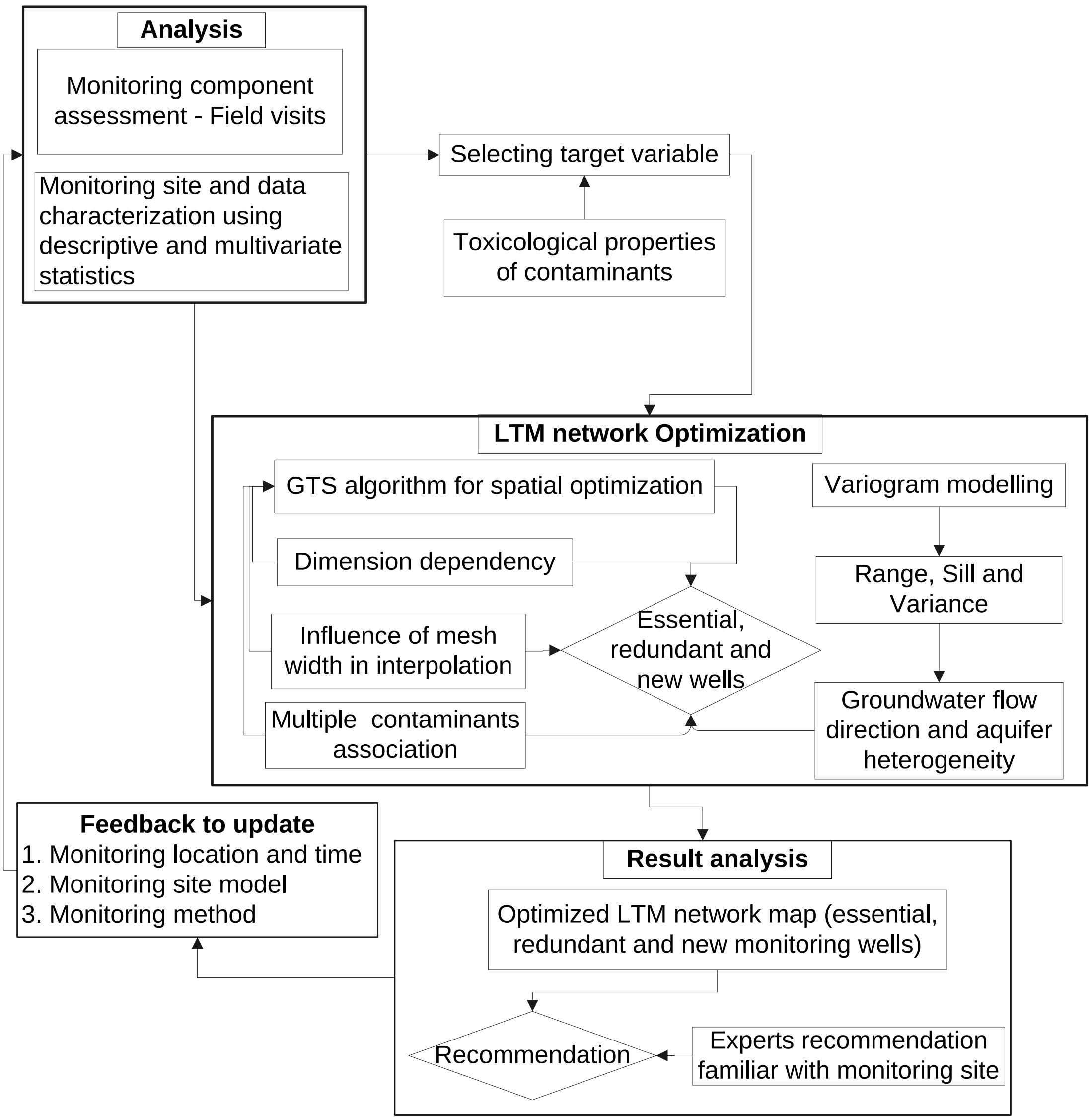

Figure 5.36: Research steps showing the integration of statistical and geostatistical methods for groundwater monitoring.

5.6.2 Uncertainties in the LTM network optimization in Megasites

In this study, new and improved methods, along with existing methods, and observed results were presented for the optimization of a groundwater LTM network, considering a few contaminants such as SO_4^{2-}, α-HCH, MCB, NO_3^-, NH_4^+, Fe^{3+}. In a megasite scenario, several contaminants need to be monitored.

The uncertainties in data and modelling also have an impact on the site characterization process and the optimization results. For this reason, the optimized LTM network should be considered to have some uncertainties involved when choosing the optimal locations of monitoring wells. In addition to groundwater quality data, optimization of monitoring wells also depends on a number of other factors such as aquifer characteristics, terrain conditions, contamination sources and sinks, and availability of resources.

6. Discussion

Previous studies have considered and documented various approaches for optimizing groundwater monitoring networks in order to improve groundwater monitoring strategies (summarized in chapter 3). However, as outlined in the motivation section (chapter 1), there are a number of challenges in the methods for groundwater monitoring network optimization, in addition to any problems with data availability. Although a number of methods are available for network optimization, the majority of methods do not consider hydrology and hydrogeological characteristics of the aquifer, nor factors that influence the optimization methods (Loaiciga *et al.*, 1992a). In this chapter, key results for new and improved approaches based on statistical, geostatistical, and hydrogeological methods for monitoring network optimization are discussed along with possible implications of these methods and comparisons with existing methods. In addition, a range of external factors and their influence on the application of these methods in the tested research area are analysed.

6.1. Statistical methods

Univariate and multivariate statistics were applied to the objective of this study, to formulate possible approaches for spatiotemporal optimization of the groundwater monitoring network. In recent studies, univariate and multivariate statistics have been used for qualitative and quantitative analysis of groundwater data sets (Alexakis, 2011; Obeidat *et al.*, 2012). However, in this study, the application of univariate and multivariate statistics was extended to the spatiotemporal optimization of the LTM network. Univariate statistics of the groundwater monitoring data set of Bitterfeld/Wolfen were quantitatively used to describe each physicochemical parameter individually in terms of central tendency, distribution, and dispersion. The data set of Eh, MCB, SO_4^{2-}, Fe^{3+}, and α-HCH had remarkably high deviations from mean values. The pH values were from 0.79 to 12.75 (table 5.1). This shows that rather than normal pH environments, the monitoring wells had extreme acidic and alkaline environments at different locations, indicating possible extreme environmental habitats (Zenova *et al.*, 2011). Although the recommended maximum contamination limits, MCL, for α-HCH and MCB were very low, high concentrations of α-HCH and MCB were found to be heterogeneously distributed in the mining and dump areas (Wycisk *et al.*, 2003). The concentration of α-HCH had several sharp peaks and was right skewed. The data set of α-HCH has a high kurtosis distribution, which means it has a distinct peak near the mean, declines rather rapidly, and has a heavy tail (Thakur *et al.*, 2011a). This high concentration of chlorinated hydrocarbon arose from a nearby dump site (Brack *et al.*, 2003; Dermietzel and Christoph, 2001). High concentrations of chlorinated hydrocarbon were observed throughout the monitoring period at some locations, including Antonie landfill, Hermine landfill, and Greppin landfill (Stollberg, 2013; Weiß *et al.*, 1998). The percentage of samples with α-HCH above MCL declines from 2003 to 2009 (figure 5.1). This declining trend indicates that remediation program for of α-HCH was being able to reduce the α-HCH concentration in the groundwater (Weiß *et al.*, 2002b; Weiß *et al.*, 2001). However, the MCB has inclining trend for the percentage of samples above MCL during 2003 to 2009 (figure 5.2). This trend of an increasing percentage of samples above MCL indicates that optimization is necessary, even in on-going remediation programs (Lorbeer *et al.*, 2002).

SO_4^{2-}, an inorganic contaminant, was relatively homogeneously distributed in the study area. Meanwhile, Fe^{3+} concentration was found to be very high in the mining and waste dump areas. Industrial metallic waste, residues from ore smelting, and pyrite-containing mining waste were major sources of Fe^{3+} pollution in the study area.

In order to find the homogeneity of variance of the data set, a mean vs. variance test and Levene's test were carried out. In contrast to the Brown–Forsythe test (Brown and Forsythe, 1974), Levene's test uses the mean instead of the median and when the underlying data does not followed a Chi-squared distribution. The mean vs. variance test shows that the groundwater quality data from the monitoring wells located in western part of the study area has distinct abnormalities in its variance. In this analysis, the overall study area was geographically divided into five groups and the mean was compared with the variance for each group. In the overall study area, large parts of the groundwater are contaminated with mining waste and industrial effluents. The monitoring wells located in the western part of the study area had lower contamination from pollution sources. The Levene's test result was significant at $p \leq .0$. The values of p for the physicochemical parameters were from 0.001 to 0.01. This shows a high heterogeneity in the distribution of variance in the study area. Any monitoring network optimization based on a monitoring data set that has a highly heterogeneous distribution of variance would be subject to high uncertainties in the application of the optimization recommendation (Ahmed *et al.*, 2008).

Recent studies have shown that the application of multivariate statistical methods is very useful for classification and interpretation of large data sets obtained from environmental monitoring programs, since these methods allow the reduction of dimensionality of the data and extraction of information (Boyacioglu and Boyacioglu, 2008; Srivastava and Ramanathan, 2008). In this study, spatiotemporal variations of the groundwater quality of ten parameters were evaluated through the PCA and CA techniques. The PCA technique is an effective pattern recognition technique that attempts to explain the variance of a data set of intercorrelated variables with a smaller set of independent variables (Singh *et al.*, 2009). To prevent misclassification due to wide differences in data dimensionality, the data set is also standardized through z-scale transformation. Standardization eliminates the influence of different units of measurement and renders the data dimensionless.

The scree plot (figure 5.4) shows that the first four principal components had eigenvalues greater than one. The eigenvalue gives a measure of the significance of the factor, making the factors with the highest eigenvalues the most significant (Kim and Mueller, 1978). In this analysis, eigenvalues greater than 1.0 were considered significant. On this basis, SO_4^{2-} and Fe^{3+} show major roles in first component. Fe^{3+} concentrations were found to be very high in mining areas and waste dump areas for industrial metallic waste, residues from ore smelting, and pyrite-containing mining waste. The cations could cause clogging problems, due to the formation of sulphide salts of iron, calcium and, to a lesser extent, magnesium. In sulphate reducing conditions, the high sulphate concentration could lead to iron, calcium and magnesium precipitation (Middeldorp *et al.*, 2004). Similarly, Eh and α-HCH were second principal components, and MCB was recognized as a third principal component. Representative variables for groups of groundwater contaminants in the study area were selected for monitoring network optimization based on these PCA results.

Cluster analysis was applied to detect the similarity between different sampling sites as described in section 4.2.2 (figure 4.3). These clusters include monitoring sampling locations that have similar characteristic features and natural background, and are affected by sources of similar type or strength. Several studies have documented the use of cluster analysis (Eisen *et al.*, 1998; Ketchen and Shook, 1996; Lu *et al.*, 2011). However, this method was not used for the monitoring network optimization in this study. This study demonstrates the possibility of applying new clustering techniques to find representative monitoring wells in the study area.

6.1.1 Spatial optimization of the network using the clustering method

Figure 5.6 shows the spatial distribution of monitoring wells in the monitoring network. In the optimization process, two major topics arise as interesting points of discussion. First, in the clustered group of monitoring wells, which well should be considered as an essential well? Second, if a well is assigned as redundant, is that monitoring well really redundant? The answers to these questions depend upon understanding and applicability of these methods. In this study, for the first question, the monitoring wells were clustered into each group based on their increasing linkage distance. The monitoring wells with median linkage distance values were selected as the essential monitoring wells (Thakur *et al.*, 2011a). For second question, whether wells assigned to be redundant really are redundant, the overall data set was divided into several data subgroups and cluster analysis was carried out for each of these subgroups. After this, each of the monitoring wells in the subgroups was tagged as essential or redundant. Based on the percentages that were tagged in the subgroups, the monitoring wells were finally categorized as essential or redundant. In this case, the total number of samples taken during the monitoring period also influences the validity of the results. In this case, a limit on the percentage determines the optimization result in terms of essential and redundant wells. The number of redundant wells increases with decreasing limits of percentage, as shown in figure 5.6. In this study, a 50% cut off limit was used for tagging a well as essential or redundant.

6.1.2 Temporal optimization of the LTM network

For the temporal optimization, the monitoring network was optimized using Sen's method (Gilbert, 1987) as described in section 4.2.5. Sen's method predicts a median slope. The presence of seasonal variability in contaminant concentration time series data can make discerning trends difficult (EPA, 2005). Short term variations caused by water level fluctuations and other seasonal effects contribute to the background noise in conventional trend analyses such as the Mann-Kendall test (Kendall, 1975; Mann, 1945; NJDEP, 2012). The temporal objective of the LTM was addressed by identifying trends in contaminant concentrations by estimating the long-term average ("median") values of concentrations using Sen's method (Gilbert, 1987).

In this method, the values of lower (M1) and upper (M2 + 1) confidence limits were used to define the lower and upper boundary of the median slope. In this study, a two-sided confidence interval of 95% was used to optimize the sampling frequency for α-HCH, MCB and SO_4^{2+} monitoring. If a lower two-sided confidence interval is used the temporal optimization could give rise to high temporal redundancy. In this study, the monitoring network was temporally optimized considering pairs of contaminants and three contaminants together. The temporal optimization sampling intervals were recorded in terms of lower quartile, median quartile, and upper quartile for each monitoring well for each monitoring parameter (tables 5.4-5.8). The temporal optimization of the monitoring network shows that the optimization differs remarkably when considering different combination of pairs and multiple contaminants.

6.2 Geostatistical spatial optimization methods

Geostatistical methods were used for spatial optimization of the LTM network, as explained in section 4.3.1. The monitoring network optimization using geostatistical methods recommends only 292 of the 462 wells in the Quaternary aquifer and only 256 of the 357 wells in the Tertiary aquifer (figure 5.8). In addition to this, the spatial uncertainties analysis, in terms of the kriging variance, also suggests that 22 and 41 new monitoring wells should be installed in the Tertiary and Quaternary aquifers, respectively. These optimization results were wound when considering all three representative contaminants together in the monitoring optimization.

The monitoring network optimization in a flat 2-D analysis differs from a "layered" analysis involving multiple 2-D layers (2.5-D). In other words, a 2-D analysis treats all well locations as if they exist in a flat 2-D plane (regardless of or ignoring potentially different depths of the well screens), which of course is most applicable when there is just a single, fairly uniform and well-connected aquifer (Knotters *et al.*, 1995). By contrast, a 2.5-D analysis assumes that there are multiple aquifers or hydrostratigraphic layers, each of which is optimized separately within the GTS (Cameron and Hunter, 2002). With 2.5-D analysis, each layer is treated as a separate 2-D analysis and so there is no interconnection (hydraulic or otherwise) assumed between the layers (Cameron and Hunter, 2010). Within the R code in the GTS, the separate layers of the 2.5-D analysis are designated using a vertical zone variable. All well locations with a common label (i.e., sampling depth) are treated as a single 2-D layer and optimized separately from the other layers. This also means that any maps within the GTS for 2.5-D analysis are constructed separately for each layer and only use data from that layer (Cameron, 2004). Optimization of the existing monitoring network with MCB and α-HCH data sets gives rise to a recommendation for a large number of essential wells with few redundant wells in both aquifers (figures 5.14 - 5.15). Similarly, with the MCB and α-HCH data sets new sampling locations were recommended in the existing monitoring network in the Quaternary aquifer (figure 5.13). However, when the monitoring network was optimized with data sets of pairs of contaminants that included SO_4^{2-} in 2 and 2.5 dimensional aquifers, the optimization results in less essential wells and high spatial redundancy (figures 5.12, 5.13, 5.16 and 5.17). In this optimization process, new sampling locations were still recommended in the Quaternary aquifer (figures 5.12 and 5.16).

In the overall optimization method, kriging interpolation, which is based upon variogram modelling, was a fundamental step. In variogram modelling, the number of lags and the lag separation distance determines the model. Therefore, the influence of grid width was studied by optimizing the existing monitoring network for different grid widths (1000 m to 1 m). Optimization of existing monitoring network showed a remarkable dependence on grid width, with the recommendation for the number of essential and redundant wells changing with grid width. Moreover, the recommended number of new monitoring wells increases with decreasing grid width (figure 5.9–5.25). This concept of incorporating the role of grid width into the monitoring network optimization has not been documented in previous studies based on geostatistical methods (Chadalavada *et al.*, 2011; Nabi *et al.*, 2011). As such, this study gives the first insight into the importance of grid width in the monitoring network optimization process.

The optimization results, in terms of the numbers of essential, redundant and new wells, were different when considering these three representative contaminants in different pairs or all together (figures 5.10 - 5.17). In the optimization process, once the spatial variogram for each contaminant was estimated, a non-linear modelling program was used to determine the appropriate spatial covariance model. This modelling utilized the Levenberg–Marquardt algorithm (Press *et al.*, 1992; Press *et al.*, 2007). The fitting algorithm was set up to fit either a combination of up to three spherical, exponential and/or Gaussian components or a combination of up to three power model structures (Cameron and Hunter, 2002). As the spatial variogram for each contaminant varies, the combination of two or more contaminants determines the covariance of the contaminants for the kriging interpolation.

The flow directions of the groundwater and contaminants were determined from the geometric anisotropy of the groundwater contaminant concentration data set using the experimental variogram, as described in section 4.3.4. Tables 5.8 – 5.10 show the prominent groundwater and contaminant flow direction that are revealed from the data sets of α-HCH, MCB and SO_4^{2-} concentration. Although the groundwater and contaminants flow northwards, the contaminant spreading directions vary for each contaminant and duration of time. α-HCH flows northwards in the Quaternary aquifer during the period from January 2003 to February 2009, but in the direction 30° from north in the Tertiary aquifer in that period. The deviation in the direction to 30° from north in the Tertiary aquifer shows the influence of historic shift in the groundwater flow direction from northwards to eastwards and then back to northwards. In this case, the flow direction represents the α-HCH contaminant spreading direction, which mainly depends upon the location of the sources.

For the MCB data set from January 2003 to February 2009, the spreading direction was northwards in Quaternary aquifer, but in the direction 60° from North in the Tertiary aquifer (table 5.10). The experimental variogram modelling based on the data set of SO_4^{2-} indicates a flow direction 30° east of the northern direction in both aquifers. The predicted contaminant spreading directions differ slightly for each contaminant, as it represents the flow direction of the particular contaminants and not the general groundwater flow.

The geometric anisotropy of the data set was used to observe seasonal influence over the flow direction. The experimental variogram modelling using the α-HCH data shows north as the preferential flow direction during the hydrological summer season (May to October in 2003-2009) in both aquifers, whilst during hydrological winter season the flow direction was 60° from north in the Quaternary aquifer and 120° from north in the Tertiary aquifer, as shown in table 5.12. This seasonal variation in the flow direction is strongly influenced by the location of the contaminant source, and the seasonal fluctuation in the water level in Mulde river and surrounding water bodies (Thakur *et al.*, 2011b).

The aquifer homogeneity was numerically estimated in term of RV index as described in section 4.3.4. As this index is based on the range, sill and variance, the hydrogeological homogeneity in the aquifer was found to be high in the direction of high range. The yearly analysis of flow direction and aquifer homogeneity shows a preferential flow direction towards the east in Quaternary aquifer during 2005, but in the direction of 30° from north in the Tertiary aquifer. This flow direction scenario completely changed in 2006. The preferential flow direction was northwards in the Quaternary aquifer and 30° from north in the Tertiary aquifer.

6.3 Hydrogeological modelling and LTM network optimization

One of the major challenges in the planning and formulation of strategies for groundwater monitoring is the availability of groundwater quality data from potential sampling locations (Beck, 1987; Harmel *et al.*, 2009). Bashi-Azghadi and Kerachian (2009) attempted to use a hydrogeological model to locate monitoring wells in groundwater systems in order to identify an unknown pollution source using monitoring data. In contrast, in this study, an attempt was made to find contaminant flow path lines in order to analyse the importance of the existence of monitoring wells at the potential monitoring well locations. In this study, a hydrogeological modelling method was used to incorporate unmonitored concentrations at potential monitoring locations for the spatiotemporal optimization of the monitoring network, as described in section 4.4. The spatial optimization of the monitoring network indicates that 30 (6.49%) of the 462 wells in the Quaternary aquifer and 14 (3.92%) of the 357 wells in the Tertiary aquifer were redundant.

The contaminant flow path lines were very narrow 3-D path lines. When overlaying the locations of the existing monitoring wells over the particle track, only a few monitoring wells were located on the path line. However, when the width of the particle track was increased by gradually increasing a buffer zone from 0 – 100 m around the particle track, a higher number of redundant wells resulted (table 5.17). When the buffer zone around the particle track was 100 m wide, the LTM network optimization using the first model showed that 145 (31.38%) of the 462 wells in the Quaternary aquifer and 105 (29.41%) of the 357 wells in the Tertiary aquifer were redundant (figure 5.30). A buffer zone of more than 100 m around the particle track may result in a recommendation for a very high number of redundant monitoring wells. In real world scenario, removal of monitoring wells that are located more than 100 m away from the path line, and thus from the existing wells in network, could increase uncertainties in the monitoring network.

Another issue of interest was the depth of sampling for the essential monitoring wells (Thakur, 2013). In this study, contaminant concentration fluctuations with vertical profile of the monitoring well over the model simulation were analysed. It was recommended that the monitoring well sampling depth should be at the depth where high temporal fluctuations were observed in the visualization of the vertical contaminant profile of the well.

The temporal optimization of the monitoring network was carried out using the method described in section 4.4.6. Table 5.18 presents a number of monitoring wells that have different sampling frequencies in both aquifers. Figure 5.31 depicts the locations of monitoring wells that have different sampling frequencies. This hydrogeological model was based on the simulated groundwater flow velocity. This groundwater flow velocity depends on the initial and boundary conditions of the model and the transport material (Gossel, 2011). In order to obtain more reliable recommendations for the temporal sampling interval, i.e., for better temporal optimization of the essential monitoring wells, the model should be frequently calibrated and validated, because in the real world scenario of the study area, the groundwater flow velocity is influenced by the water level in Mulde river, pumping activities around the mining locations, rain fall and snow melting.

In this spatiotemporal optimization of the monitoring network based on a hydrogeological model, an ideal contaminant concentration of 100 mg/l was used. The comparison of this ideal concentration of 100 mg/l at the contaminant source location and its spreading via various methods in the model environment with the observed contaminant concentrations at various potential monitoring locations helps to make a comparative analysis of possible contaminant scenarios. This comparative analysis strengthens the optimization process of the monitoring network.

6.4 Comparison of results

As per objective of study, the methods and observed results from the spatiotemporal optimization of the monitoring network based on of statistical, geostatistical, and hydrogeological methods were carried out, as described in section 4.5. The statistical approach using the AHC method finds representative wells from the group of wells in each statistically defined cluster. However, this method does not analyse how the removal of these redundant wells affects the monitoring network. The statistical approach based on Sen's method for temporal optimization of sampling frequency in the monitoring network considers uncertainties in the network in terms of upper and lower limit of median slope. Unlike the methods presented by Zhou (1996) and Johnson, Ridley et al. (1996), this method recommends reliable sampling frequencies in terms of lower quartile days, median quartile days and upper quartile days. These statistical methods for optimizing monitoring networks are limited by a number of factors, including the geography, geology and hydrology of the network area (Andricevic and Foufoula-Georgiou, 1991), the scale of the network, budgetary constraints, and potential sources and locations of contaminants in the aquifers.

The issues of hydrogeological layers in the aquifer, the scale of the network, and potential sources and locations of contaminants in the aquifers were incorporated in the geostatistical methods. Kriging weights were used to compute plume maps. Randomly selected wells with lower kriging weights were removed to distinguish those wells as essential or redundant (section 4.3.1). The kriging technique was also used as a tool to select optimum sites for monitoring groundwater levels (Prakash and Singh, 2000).

The geostatistical spatial optimization algorithm, GTS (Cameron and Hunter, 2002), considers the aquifer as a 2 or 2.5 dimensional aquifer. The 2.5-dimension analysis assumes that there are multiple aquifers or hydrostratigraphic layers in the aquifer, which have no hydraulic interconnection. However, geological features like fractured-rock systems (Nativ *et al.*, 1999), which act as sources and sinks of groundwater contaminants, were not considered. Comparatively, the geostatistical spatial optimization algorithm shows convincing optimization results in terms of essential, redundant, and new monitoring well locations.

Factors like the geography, geology, and hydrology of the network area, the scale of the network, and locations of potential sources of contaminants in the aquifers are incorporated in hydrogeological modelling based spatiotemporal optimization methods. Figures 5.6, 5.9, and 5.31 depict the locations of monitoring wells that are tagged as essential or redundant based on statistical, geostatistical, and hydrogeological modelling methods. If a monitoring well is tagged as redundant well in two or more methods, the monitoring well can be recommended as a redundant well.

6.5 Improving groundwater monitoring strategies

As described in the section 4.1, in order to improve monitoring network strategies, each component of the monitoring framework needs to be improved. The step-wise incorporation of components of the monitoring framework was not well documented in previous studies (Chen *et al.*, 2012; Hudak, 1998; Hudak, 2006). Van Geer, Bierkens et al. (2006) provided insight into technical aspects of groundwater monitoring frameworks. Indeed, as presented in this study, step-wise component analysis helps to trace out the importance of different components and possible factors that influence the LTM network optimization. In this component analysis, the monitoring network optimization was high priority because of several other management factors like monitoring cost and infrastructures. New and improved methods were therefore applied along with existing methods on the data set from the test research area, in order to find ways of optimizing the monitoring network. Along with the component analysis, improvement objectives for the monitoring strategies had to be specified. Depending upon the scenario of the groundwater and monitoring status, the improvement objectives could include enhancement in understanding of monitoring network, legal requirements, or socio-economic aspect of monitoring (Thakur *et al.*, 2011c). For a specified objective of the spatiotemporal optimization of the monitoring network, representative variables must be selected. In order to select representative variables, a good understanding of groundwater contaminants is required. It is also possible that unknown heavy metal pollutants were not noticed at the contaminated site, alongside the monitored organic pollutants. Representative contaminants can be selected for network optimization in the study area once there is a good understanding of the contaminants and the specified objective. The monitoring strategy is based on groundwater monitoring effort (like location and frequency of sampling), reduction of uncertainties, socioeconomic needs, legal requirements etc. Periodic evaluation of the monitoring network in terms of monitoring efforts (like location and frequency of sampling) will continue to reduce uncertainties and help to achieve the goals of the monitoring strategies.

7. Conclusions and recommendation

In this thesis, new methods and improvements to existing methods based on statistical, geostatistical, and hydrogeological approaches for optimising monitoring networks have been investigated and tested using the case study of Bitterfeld/Wolfen. The conclusions, recommendations and limitations of the research, along with suggestions for future work, are presented in this chapter.

7.1 Conclusions

It has been demonstrated that the existing monitoring network could be optimized using the presented statistical, geostatistical, and hydrogeological methods without losing essential information from the monitoring network. As improvements to groundwater monitoring strategies are the key for groundwater resource management, the efforts presented to optimize and evaluate the monitoring network will enhance the performance of the water management system. The methods presented hare are useful for both inadequate networks with insufficient wells and dense monitoring networks with too many wells. In developing countries, inadequacy of financial resources is the reason for insufficiently dense monitoring networks. In such conditions, the presented methods can be used to find redundancy in the existing monitoring network and to identify suitable locations for new monitoring wells. Similarly, in developed countries, the methods presented can be applied to reduce the density of monitoring wells without losing valuable information from the monitoring area.

Univariate and multivariate statistics, as demonstrated for identifying redundant monitoring wells in the existing monitoring network, can be applied when the monitoring network has a dense distribution of wells. The analysis also presents a way to find whether a well tagged as redundant well is really redundant. Similarly, iterative thinning using Sen’s method was successfully applied for the temporal optimization of the monitoring wells. The use of these methods reduces the number of samples needed, which could make the monitoring program more cost effective.

At the same time, the application of a geostatistical method, which is based on the kriging interpolation weight, shows more realistic optimization results in terms of recommended essential, redundant, and new monitoring wells. Meanwhile, several influencing factors such as grid width, number of contaminants considered, and contaminant spreading direction were analysed. This analysis revealed that such factors need to be considered in the monitoring optimization process. Both the statistical and geostatistical approaches applied are flexible, so that the users can set the level of the confidence limit. These methods could be applied to a field based real groundwater quality data set.

In cases when there is inadequate data from the monitoring area, the hydrogeological methods can be used. In this case study of Bitterfeld/Wolfen, the application of a hydrogeological model for optimization of the monitoring network was demonstrated. The application of a hydrogeological model opens the possibility of optimizing networks with insufficient real measured data on which to base the optimization. This study presents a method for incorporating unmonitored concentrations at different potential monitoring locations in the modelled area. When using a hydrogeological model to optimize a monitoring network, the calibration and validation of the model strengthen the reliability of the optimization results.

In addition to presenting the different optimization approaches, this study also presents a comparative analysis of these new and improved approaches. The comparative analysis of spatial optimization methods shows that statistical methods are more efficient when optimizing an existing monitoring network with high well density. However, the presented geostatistical methods could be used both in situations of high and low monitoring well density. If the density of monitoring wells is too low, this optimization method recommends new monitoring well locations. The optimization results based on the use of statistical and geostatistical method cannot be directly compared with the results of hydrogeological modelling based optimizations, as the assumptions and source of the data set are different. Optimization of a monitoring network using hydrogeological model is more useful when there is an existing hydrogeological model.

The temporal optimization based on simulated groundwater flow velocity shows convincing results for recommending sampling frequencies at potential sampling locations. This approach can be used for prognostic optimization of the monitoring network. Another benefit of the use of a hydrogeological model is that the groundwater contaminants and optimization result can be interactively visualized. Because it is a 3-D model visualization, the contaminant scenario can be visualized at various sampling depths and times.

As discussed in chapter 5 and 6, these methods have strengths and weakness. The strengths of these methods can be integrated on the basis of the optimization objectives of the groundwater monitoring strategies. For example, in a monitoring network where there is a low density of monitoring wells, statistical and geostatistical methods can be integrated. The statistical method in terms of univariate and multivariate statistics can be used for analysis of contaminates distribution, component analysis, etc. Geostatistical methods can be used for the spatial optimization of the monitoring network. Temporal optimization of the monitoring network can be carried out using statistical methods. In this way, according to the objectives of the groundwater monitoring strategies, these methods can be integrated in order to optimize the monitoring network in best possible manner.

Despite the strengths of the presented methods, it must be noted that the list of spatiotemporally redundant wells proposed for removal were proposed strictly on the basis of the statistical, geostatistical, and hydrogeological methods. Therefore, before such a recommendation is implemented, the specific well locations would need to be checked by considering other major contaminants, and to be examined by hydrogeologists and experts familiar with the site and by appropriate regulators to ensure that other valuable information not considered in this study is not lost. Other than a change in cost estimates, the optimization algorithm would not be damaged or altered if someone decided, for reasons besides those considered in this study, that one or more wells tagged as redundant should be kept on the monitoring list and not be removed. Furthermore, the proposed new monitoring wells can still be installed in order to improve the understanding of the LTM network.

7.2 Recommendations

Although these methods have different assumptions, they were all applied for the spatiotemporal optimization of the monitoring network. It is expected that these new methods, along with improved existing methods, can be integrated to consider the objectives of groundwater monitoring programs.

The application of univariate and multivariate statistical methods is recommended for the spatial optimization of existing monitoring networks with a high well density. The statistical method based on Sen's method can be used for temporal optimization of networks with both high and low spatial density of monitoring wells.

The application of geostatistical methods can be recommended for both low and high density monitoring networks in aquifers considered as both 2 and 2.5 dimensional. As done in this study, factors that influence monitoring network optimization methods should always be considered for both statistical and geostatistical methods. Possible anisotropy in the groundwater quality data can be observed with experimental variogram modelling to estimate preferential contaminant spreading direction. Variogram modelling can be also useful to estimating aquifer hydrogeological heterogeneity numerically.

As demonstrated in the case study of Bitterfeld/Wolfen, the use of a hydrogeological model gives a convincing prognostic spatiotemporal optimization result. The use of a hydrogeological model based method is only recommended when a reliable calibrated and validated hydrogeological model is available for the study area.

7.3 Limitations of the research

The new methods and improved existing methods based on statistical, geostatistical, and hydrogeological methods were tested in the mega contaminated site scenario of Bitterfeld/Wolfen for optimization of an existing groundwater monitoring network. Because of the unique groundwater quality and hydrogeology of the tested study area, the obtained result may not be directly applied to the other monitoring areas.

Optimization of the monitoring network using univariate and multivariate statistics assumes the monitoring network to be in a 2-D aquifer plain. In this method, the hydrogeology of the aquifer in the monitoring area is not considered.

The study of anisotropy in the groundwater quality data gives encouraging results for the analysis of potential contaminant flow directions. The aquifer heterogeneity can also be numerically estimated using RV Indices based on the experimental variogram modelling. Variogram modelling requires good expertise and understanding of the range, sill and nugget effect. Both statistical and geostatistical methods do not consider water balancing nor the influence of climate change on the monitoring network optimization.

Optimization of the monitoring network using a hydrogeological model requires a reliable hydrogeological model. Use of a calibrated and validated hydrogeological model is still only recommended for the prognostic optimization of the monitoring network.

7.4 Suggestions for further work

In this study, a hydrogeological model was used for the prognostic optimization of a monitoring network. In this case, the simulated particle track and flow velocity from the model were used as an input data set for optimizing the monitoring network. In the model simulation, only one representative contaminant was considered. An idealistic α-HCH concentration of 100 mg/l was induced to various hydrogeological layers of the model at multi-source locations as the initial condition. The simulated particle track, flow velocity, and mass would be more realistic if real concentrations of contaminants could have been induced to the different hydrogeological layers at their real source locations as the initial condition. In a mega-contaminated area, several contaminants, along with their respective diffusion, decay, and reaction rate need to be considered. The application of a good calibrated and validated hydrogeological model for monitoring network optimization is recommended for further research work.

In this study, monitoring network optimization using statistical and geostatistical methods was carried out considering the aquifer as 2 and 2.5 dimensional, respectively. Extending geostatistical modelling to the 3-D case for contaminant concentration interpolation and its application to monitoring network optimization is a potential research need.

With increasing demand for web access to new applications, web GIS needs to be incorporated into the hydrogeological modelling and real time monitoring network optimization along with an interactive user interface for contributing real time data input from the contaminated area.

Bibliography

Ahmed, S., A. N. Kumar, Sreedevi, and J. Perrin (2008): Optimizing Groundwater Monitoring Network In Highly Heterogeneous Aquifers Using Geostatistics: Technique Development With A Few Case Studies, in *The 3rd International Conference on Water Resources and Arid Environments (2008) and the 1st Arab Water Forum*, edited, Arab Water Forum.

Alexakis, D. (2011): Assessment of water quality in the Messolonghi–Etoliko and Neochorio region (West Greece) using hydrochemical and statistical analysis methods, *Environmental Monitoring and Assessment*, *182*(1-4), 397-413.

Anderson, M. P., and J. A. Cherry (1979): Using models to simulate the movement of contaminants through groundwater flow systems, *Critical Reviews in Environmental Science and Technology*, *9*(2), 97-156.

Andricevic, R., and E. Foufoula-Georgiou (1991): A Transfer Function Approach to Sampling Network Design for Groundwater Contamination, *Water resources research*, *27*(10), 2759-2769.

Arnell, N. W. (1999): Climate change and global water resources, *Global Environmental Change*, *9, Supplement 1*(0), S31-S49.

Asefa, T., M. Kemblowski, G. Urroz, and M. McKee (2005): Support vector machines (SVMs) for monitoring network design, *Ground Water*, *43*(3), 413-422.

Ashraf, A., and Z. Ahmad (2008): Regional groundwater flow modelling of Upper Chaj Doab of Indus Basin, Pakistan using finite element model (Feflow) and geoinformatics, *Geophysical Journal International*, *173*(1), 17-24.

Aziz, J. J., M. Ling, H. S. Rifai, C. J. Newell, and J. R. Gonzales (2003): MAROS: A Decision Support System for Optimizing Monitoring Plans, *Ground Water*, *41*(3), 355-367.

Babbar-Sebens, M., and B. Minsker (2010): A Case-Based Micro Interactive Genetic Algorithm (CBMIGA) for interactive learning and search: Methodology and application to groundwater monitoring design, *Environmental Modelling & Software*, *25*(10), 1176-1187.

Bashi-Azghadi, S. N., and R. Kerachian (2009): Locating monitoring wells in groundwater systems using embedded optimization and simulation models, *Science of The Total Environment*, *408*(10), 2189-2198.

Beck, M. B. (1987): Water quality modeling: a review of the analysis of uncertainty, *Water Resources Research*, *23*(8), 1393-1442.

Ben-Jemaa, F., M. A. Marino, and H. A. Loaiciga (1994): Multivariate Geostatistical Design of Ground-Water Monitoring Networks, *Journal of Water Resources Planning and Management*, *120*(4), 505-522.

BGR (2011): Groundwater resources in Germany, edited, Federal Institute for Geosciences and Natural Resources (BGR).

Boyacioglu, H., and H. Boyacioglu (2008): Water pollution sources assessment by multivariate statistical methods in the Tahtali Basin, Turkey, *Environmental Geology*, *54*(2), 275-282.

Brack, W., T. Kind, S. Schrader, M. Möder, and G. Schüürmann (2003): Polychlorinated naphthalenes in sediments from the industrial region of Bitterfeld, *Environmental Pollution*, *121*(1), 81-85.

Brauner, J. (2006): Nonparametric Estimation of Slope: Sen’s Method in Environmental Pollution, edited.

Broers, H. P. (2002): Strategies for regional groundwater quality monitoring, 231 pp, Universiteit Utrecht, Utrecht, the Netherlands.
Brown, M. B., and A. B. Forsythe (1974): Robust Tests for Equality of Variances, *Journal of the American Statistical Association*(69), 364–367.
Cameron, K. (2004): Better Optimization of Long-Term Monitoring Networks, *Bioremediation Journal*, *8*(3), 89 - 107.
Cameron, K., and P. Hunter (2002): Using spatial models and kriging techniques to optimize long-term ground-water monitoring networks: a case study, *Environmetrics*, *13*(5-6), 629-656.
Cameron, K., and P. Hunter (2010): Optimization of LTM Networks Using GTS: Statistical Approaches to Spatial and Temporal Redundancy*Rep.*, 1-16 pp, Air Force Center for Environmental Excellence (AFCEE).
Cameron, K., and Philip M. Hunter (2010): Geostatistical Temporal-Spatial (GTS) 1.0.0, MacStat Consulting, Ltd., Colorado, USA.
Chadalavada, S., and B. Datta (2008): Dynamic Optimal Monitoring Network Design for Transient Transport of Pollutants in Groundwater Aquifers, *Water Resources Management*, *22*(6), 651-670.
Chadalavada, S., B. Datta, and R. Naidu (2011): Uncertainty based optimal monitoring network design for a chlorinated hydrocarbon contaminated site, *Environmental Monitoring and Assessment*, *173*(1-4), 929-940.
Chemie AG, B.-W. (1983): *Bitterfelder Chronik : 100 Jahre Chemiestandort Bitterfeld-Wolfen*, 200 pp.
Chen, C.-S. (1987): Analytical solutions for radial dispersion with cauchy boundary at injection well, *Water Resources Research*, *23*(7), 1217-1224.
Chen, Y., L. Smith, and R. Beckie (2012): Modeling of strategies for performance monitoring of groundwater contamination at sites underlain by fractured bedrock, *Journal of Contaminant Hydrology*, *134–135*(0), 37-53.
Cheng, A. H. D., and D. T. Cheng (2005): Heritage and early history of the boundary element method, *Engineering Analysis with Boundary Elements*, *29*(3), 268-302.
Cieniawski, S. E., J. W. Eheart, and S. Ranjithan (1995): Using Genetic Algorithms to Solve a Multiobjective Groundwater Monitoring Problem, *Water Resources Research*, *31*(2), 399-409.
Clement, T., W. R. Wise, and F. J. Molz (1994): A physically based, two-dimensional, finite-difference algorithm for modeling variably saturated flow, *Journal of Hydrology*, *161*(1), 71-90.
Darcy, H. (1856): Les fontaines publiques de la ville de Dijon, *Dalmont, Paris*, *70*.
Datta, B., D. Chakrabarty, and A. Dhar (2009): Optimal Dynamic Monitoring Network Design and Identification of Unknown Groundwater Pollution Sources, *Water Resources Management*, *23*(10), 2031-2049.
Day, W. H. E., and H. Edelsbrunner (1984): Efficient algorithms for agglomerative hierarchical clustering methods, *Journal of Classification*, *1*(1), 7-24.
Dermietzel, J., and G. Christoph (2001): The Impact of a Lignite Seam on Contaminated Groundwater in the Aquifer System of the Bitterfeld Region, *Water, Air, and Soil Pollution*, *125*(1), 157-170.
Dhar, A., and B. Datta (2009): Global Optimal Design of Ground Water Monitoring Network Using Embedded Kriging, *Ground Water*, *47*(6), 806-815.
Diersch, H.-J. G. (1998): Treatment of free surfaces in 2D and 3D groundwater modeling, *Math. Géologie*, *2*, 17-43.

Diersch, H.-J. G. (2008): Streamline Computations Available in FEFLOW *Rep.*, DHI-WASY GmbH, Berlin.
Diersch, H. (2009): WASY Software FEFLOW 5.4 User's Manual, *DHI-WASY, Berlin*.
Eisen, M. B., P. T. Spellman, P. O. Brown, and D. Botstein (1998): Cluster analysis and display of genome-wide expression patterns, *Proceedings of the National Academy of Sciences*, *95*(25), 14863-14868.
Eissmann, L. (1994): Leitfaden der Geologie des Präquartärs im Saale-Elbe-Gebiet., in *Das Quartär Mitteldeutschlands – Ein Leitfaden und Exkursionsführer mit einer Übersicht über das Präquartär des Saale-Elbe-Gebietes*, edited by L. Eissmann and T. Litt, Altenbg. Nat. wiss. Forsch., Mauritianum 7, Altenburg, 11-46.
Eissmann, L. (2002): Tertiary geology of the Saale-Elbe Region. Quaternary Science Reviews 21, 1245-1274
Eissmann, L., and A. Müller (1978): Lithofazieskarten Quartär, 1:50000, Blatt 2465 Bitterfeld. 7 Karten; Zentrales edited, Geologisches Institut, Berlin.
Eissmann, L., H. Heidecke, G. Krumbiegel, J. Rascher, P. Tropp, S. Wansa, and R. Wimmer (2008): Zur Geologie, Bergbaugeschichte, Bergbausanierung und Entwicklung der Bergbaufolge-landschaft, Geo- und Biotope im und am Außenrand des Bitterfelder Braunkohlenreviers, Exkursionsführer und Veröffentlichungen der Deutschen *Gesellschaft für Geowissenschaften, II. Bitterfelder Bernsteinkolloqium, Heft 236*, 144-161.
El Harrouni, K., D. Ouazar, G. A. Walters, and A. H. D. Cheng (1996): Groundwater optimization and parameter estimation by genetic algorithm and dual reciprocity boundary element method, *Engineering Analysis with Boundary Elements*, *18*(4), 287-296.
Elango, L., F. Stagnitti, D. Gnanasundar, N. Rajmohan, S. Salzman, M.LeBlanc, and J. Hill (2004): A Review of Recent Solute Transport Models and a Case Study, in *Environmental Sciences and Environmental Computing. Vol. II*, edited by P. Zannetti, The EnviroComp Institute, Fremont, CA 94539, USA.
EPA (2005): Roadmap to long-term monitoring optimization*Rep.*, U.S. Environmental Protection Agency (EPA)/National Service Center for Environmental Publications.
EPA (2012): National Primary Drinking Water Regulations, edited, United States Environmenal Protection Agency, USA.
Erechtchoukova, M. G., S. Y. Chen, and P. A. Khaiter (2009): Application of Optimization Algorithms for the Improvement of Water Quality Monitoring Systems, in *Information Technologies in Environmental Engineering*, edited, pp. 176-188.
EU (2006): DIRECTIVE 2006/118/EC OF THE EUROPEAN PARLIAMENT AND OF THE COUNCIL of 12 December 2006 on the protection of groundwater against pollution and deterioration, *Official Journal of the European Union*, *372*, 19-31.
European Commission, E. D. (2011): WATER edited, Environment Directorate-General of the European Commission.
Everett, L. G. (1984): Groundwater monitoring: Guidelines and methodology for developing and implementing a ground-water quality monitoring program.
Gilbert, R. O. (1987): *Statistical methods for environmental pollution monitoring*, Wiley.

Gossel, W. (2011): *Interfaces in coupling of hydrogeological modeling systems*, 87 pp., Shaker Verlag, Aachen, Germany.
Gossel, W., R. Stollberg, and P. Wycisk (2009): Regionales Langzeitmodell zur Simulation von Grundwasserströmung und Stofftransport im Gebiet der Unteren Mulde/Fuhne, *Grundwasser*, *14*(1), 47-60.
Gremmen, N. J. M., M. J. S. M. Reijnen, J. Wiertz, and G. van Wirdum (1990): A model to predict and assess the effects of groundwater withdrawal on the vegetation in the pleistocene areas of the Netherlands, *Journal of Environmental Management*, *31*(2), 143-155.
Harmel, R., D. Smith, K. King, and R. Slade (2009): Estimating storm discharge and water quality data uncertainty: A software tool for monitoring and modeling applications, *Environmental Modelling & Software*, *24*(7), 832-842.
Heidrich, S., H. Weiß, and A. Kaschl (2004a): Attenuation reactions in a multiple contaminated aquifer in Bitterfeld (Germany), *Environmental Pollution*, *129*(2), 277-288.
Heidrich, S., M. Schirmer, H. Weiss, P. Wycisk, J. Grossmann, and A. Kaschl (2004b): Regionally contaminated aquifers - toxicological relevance and remediation options (Bitterfeld case study), *Toxicology*, *205*(3), 143-155.
Herrera, G. S., and G. F. Pinder (2005): Space-time optimization of groundwater quality sampling networks, *Water Resources Research*, *41*(12), W12407.
Hubert, T. (2005): Vergleichende 3D-Modellierung eines geologischen Strukturmodells am Beispiel einer industrie- und bergbaugeprägten Region – Bitterfeld, Martin Luther University Halle-Wittenberg
Hubert, T. (2011): Methodische Ansätze zur geologischen 3D-Modellierung oberflächennaher Schichtenfolgen und ihre Auswirkung auf die numerische Grundwassermodellierung Martin Luther Univesity, Halle.
Hudak, P. F. (1998): Groundwater Monitoring Strategies for Variable Versus Constant Contaminant Loading Functions, *Environmental Monitoring and Assessment*, *50*(3), 271-288.
Hudak, P. F. (2006): Groundwater monitoring strategies for variable contaminant migration boundaries, *Hydrological Sciences Journal*, *51*(3), 524 - 530.
Hunt, R. J., M. P. Anderson, and V. A. Kelson (1998): Improving a Complex Finite-Difference Ground Water Flow Model Through the Use of an Analytic Element Screening Model, *Ground Water*, *36*(6), 1011-1017.
Johnson, N., C. Revenga, and J. Echeverria (2001): Managing water for people and nature, *Science*, *292*(5519), 1071.
Johnson, R., and D. Wichern (2002): Applied Multivariate Statistical Analysis., edited, London: Prentice-Hall.
Johnson, V. M., M. N. Ridley, R. C. Tuckfield, and R. A. Anderson (1996): Reducing the sampling frequency of groundwater monitoring wells, *Journal Name: Environmental Science and Technology; Journal Volume: 30; Journal Issue: 1; Other Information: PBD: Jan 1996*, Medium: X; Size: pp. 355-358.
Kaiser, H. (1958): The varimax criterion for analytic rotation in factor analysis, *Psychometrika*, *23*(3), 187-200.
Kendall, M. (1975): Rank Correlation Methods: Charles Griffin, *London, UK*.
Kendall, M. G., and A. Stuart (1976): *The Advanced Theory of Statistics: Design and analysis, and time-series*, Macmillan Pub Co.
Ketchen, D. J., and C. L. Shook (1996): The application of cluster analysis in strategic management research: an analysis and critique, *Strategic management journal*, *17*(6), 441-458.

Khan, S., H. F. Chen, and T. Rana (2008): Optimizing Ground Water Observation Networks in Irrigation Areas Using Principal Component Analysis, *Ground Water Monitoring & Remediation*, *28*(3), 93-100.
Kim, J.-O., and C. W. Mueller (1978): *Introduction to factor analysis: What it is and how to do it*, SAGE Publications, Incorporated.
Knödel, K., G. Lange, and H. J. Voigt (2007): *Environmental geology: handbook of field methods and case studies*, Springer Verlag.
Knoth, W. (1995): Sachsen-Anhalt, in *Das Quartär Deutschlands*, edited by L. Benda, pp. 148-170, Borntraeger, Berlin.
Knotters, M., D. Brus, and J. Oude Voshaar (1995): A comparison of kriging, co-kriging and kriging combined with regression for spatial interpolation of horizon depth with censored observations, *Geoderma*, *67*(3), 227-246.
Kollat, J. B., and P. M. Reed (2006): Comparing state-of-the-art evolutionary multi-objective algorithms for long-term groundwater monitoring design, *Advances in Water Resources*, *29*(6), 792-807.
Kollat, J. B., and P. M. Reed (2007a): A computational scaling analysis of multiobjective evolutionary algorithms in long-term groundwater monitoring applications, *Advances in Water Resources*, *30*(3), 408-419.
Kollat, J. B., and P. Reed (2007b): A framework for Visually Interactive Decision-making and Design using Evolutionary Multi-objective Optimization (VIDEO), *Environmental Modelling & Software*, *22*(12), 1691-1704.
Lauterbach, D., and L. Luckner (1999): Grundlagen und Konzepte des Grundwasser-Monitorings aus Sicht des Dresdner Grundwasserforschungszentrums. – In: Fachtagung Grundwasser-Monitoring, paper presented at des DGFZ e.V., Heft 17, Dresden.
Levene, H. (1960): Robust tests for equality of variances1, *Contributions to probability and statistics: Essays in honor of Harold Hotelling*, *2*, 278.
Li, Y., and A. B. Chan Hilton (2007): Optimal groundwater monitoring design using an ant colony optimization paradigm, *Environmental Modelling & Software*, *22*(1), 110-116.
Loaiciga, H., R. Charbeneau, L. Everett, G. Fogg, B. Hobbs, and S. Rouhani (1992a): Review of Ground-Water Quality Monitoring Network Design, *Journal of Hydraulic Engineering*, *118*(1), 11-37.
Loaiciga, H. A., L. A. F. C. A. B. W. G. G. M.A. Celia, and G. F. Pinder (1988): Groundwater Monitoring Network Design, in *Developments in Water Science*, edited, pp. 371-376, Elsevier.
Loaiciga, H. A., R. J. Charbeneau, L. G. Everett, G. E. Fogg, B. F. Hobbs, and S. Rouhani (1992b): Review of Ground-Water Quality Monitoring Network Design, *Journal of Hydraulic Engineering*, *118*(1), 11-37.
Lorbeer, H., S. Starke, M. Gozan, A. Tiehm, and P. Werner (2002): Bioremediation of Chlorobenzene-Contaminated Groundwater on Granular Activated Carbon Barriers, *Water, Air, & Soil Pollution: Focus*, *2*(3), 183-193.
Lu, W.-Z., H.-D. He, and L.-y. Dong (2011): Performance assessment of air quality monitoring networks using principal component analysis and cluster analysis, *Building and Environment*, *46*(3), 577-583.
MacKenzie, M. C., R. N. Palmer, and S. P. Millard (1987): Analysis of Statistical Monitoring Network Design, *Journal of Water Resources Planning and Management*, *113*(5), 599-615.
Mann, H. B. (1945): Nonparametric tests against trend, *Econometrica: Journal of the Econometric Society*, 245-259.

Mardia, K. V. (1970): Measures of multivariate skewness and kurtosis with applications, *Biometrika*, *57*(3), 519-530.
Masoumi, F., and R. Kerachian (2010): Optimal redesign of groundwater quality monitoring networks: a case study, *Environmental Monitoring and Assessment*, *161*(1), 247-257.
McCluskey, A., and A. G. Lalkhen (2007): Statistics II: Central tendency and spread of data, *Continuing Education in Anaesthesia, Critical Care & Pain*, *7*(4), 127-130.
Meyer, P. D., and E. D. Brill (1988): A method for locating wells in a groundwater monitoring network under conditions of uncertainty, *Water Resources Research*, *24*(8), 1277-1282.
Meyer, P. D., A. J. Valocchi, and J. W. Eheart (1994): Monitoring network design to provide initial detection of groundwater contamination, *Water Resour. Res.*, *30*(9), 2647-2659.
Middeldorp, P. J. M., M. H. A. v. Eekert, J. J. M. Staps, H. H. M. Rijnaarts, R. Hetterschijt, H. Rovers, and E. P. C. Visser-Westerweele (2004): Bitterfeld: Bioremediation of regional contaminated aquifers *Rep.*
Morey, L. C., R. K. Blashfield, and H. A. Skinner (1983): A Comparison of Cluster Analysis Techniques Withing a Sequential Validation Framework, *Multivariate Behavioral Research*, *18*(3), 309-329.
Nabi, A., A. Gallardo, and S. Ahmed (2011): Optimization of a Groundwater Monitoring Network for a Sustainable Development of the Maheshwaram Catchment, India, *Sustainability*, *3*(2), 396-409.
Nativ, R., E. M. Adar, and A. Becker (1999): Designing a Monitoring Network for Contaminated Ground Water in Fractured Chalk, *Ground Water*, *37*(1), 38-47.
NJDEP (2012): Monitored Natural Attenuation Technical Guidance *Rep.*, New Jersey Department of Environmental Protection (NJDEP), New Jersey, USA.
Nunes, L. M., M. C. Cunha, and L. Ribeiro (2004a): Groundwater Monitoring Network Optimization with Redundancy Reduction, *Journal of Water Resources Planning and Management*, *130*(1), 33-43.
Nunes, L. M., M. C. Cunha, and L. Ribeiro (2004b): Optimal Space-time Coverage and Exploration Costs in Groundwater Monitoring Networks, *Environmental Monitoring and Assessment*, *93*(1), 103-124.
Obeidat, M. M., M. Awawdeh, and F. Abu Al-Rub (2012): Multivariate statistical analysis and environmental isotopes of Amman/Wadi Sir (B2/A7) groundwater, Yarmouk River Basin, Jordan, *Hydrological Processes*.
Paschke, A., B. Vrana, P. Popp, and G. Schüürmann (2006): Comparative application of solid-phase microextraction fibre assemblies and semi-permeable membrane devices as passive air samplers for semi-volatile chlorinated organic compounds. A case study on the landfill "Grube Antonie" in Bitterfeld, Germany, *Environmental Pollution*, *144*(2), 414-422.
Petelet-Giraud, E., P. Négrel, L. Gourcy, C. Schmidt, and M. Schirmer (2007): Geochemical and isotopic constraints on groundwater-surface water interactions in a highly anthropized site. The Wolfen/Bitterfeld megasite (Mulde subcatchment, Germany), *Environmental Pollution*, *148*(3), 707-717.
Poeter, E. P., and M. C. Hill (1997): Inverse Models: A Necessary Next Step in Ground-Water Modeling, *Ground Water*, *35*(2), 250-260.
Polemio, M., V. Dragone, and P. Limoni (2009): Monitoring and methods to analyse the groundwater quality degradation risk in coastal karstic aquifers (Apulia, Southern Italy), *Environmental Geology*, *58*(2), 299-312.

Popp, P., L. Brüggemann, P. Keil, U. Thuß, and H. Weiß (2000): Chlorobenzenes and hexachlorocyclohexanes (HCHs) in the atmosphere of Bitterfeld and Leipzig (Germany), *Chemosphere*, *41*(6), 849-855.
Prakash, M., and V. Singh (2000): Network design for groundwater monitoring–a case study, *Environmental Geology*, *39*(6), 628-632.
Prakash, O., and B. Datta (2012): Sequential optimal monitoring network design and iterative spatial estimation of pollutant concentration for identification of unknown groundwater pollution source locations, *Environmental Monitoring and Assessment*, 1-16.
Press, W. H., B. P. Flannery, S. A. Teukolsky, and W. T. Vetterling (1992): *Numerical Recipes in FORTRAN 77: Volume 1, Volume 1 of Fortran Numerical Recipes: The Art of Scientific Computing*, Cambridge University Press.
Press, W. H., S. A. Teukolsky, W. T. Vetterling, and B. P. Flannery (2007): *Numerical recipes 3rd edition: The art of scientific computing*, Cambridge University Press.
Prickett, T. (1975): Modelling techniques for groundwater evaluation, *Advances in hydroscience*, *10*, 1-143.
Reed, P., B. Minsker, and A. J. Valocchi (2000): Cost-Effective Long-Term Groundwater Monitoring Design Using a Genetic Algorithm and Global Mass Interpolation, *Water Resources Research*, *36*(12), 3731-3741.
Reed, P., B. S. Minsker, and D. E. Goldberg (2001): A multiobjective approach to cost effective long-term groundwater monitoring using an elitist nondominated sorted genetic algorithm with historical data, *Journal of Hydroinformatics*, *3*(2), 71-89.
Repetto, R., and T. Holmes (1983): The Role of Population in Resource Depletion in Developing Countries, *Population and Development Review*, *9*(4), 609-632.
Ruske, R., J. Hübner, O. Böhme, and P. Falke (1997): Ergebnisse der geologisch-hydrogeologisch-geotechnischen Standorterkundung, in *Sanierungsforschung in regional kontaminierten Aquiferen (SAFIRA) UFZ-Bericht 27/97*, edited by H. Weiss, G. Teutsch and B. Daus, pp. 14-17, Leipzig.
Sen, P. K. (1968): Estimates of the Regression Coefficient Based on Kendall's Tau, *Journal of the American statistical association*, *63*(324), 1379-1389.
Simeonov, V., J. Stratis, C. Samara, G. Zachariadis, D. Voutsa, A. Anthemidis, M. Sofoniou, and T. Kouimtzis (2003): Assessment of the surface water quality in Northern Greece, *Water Research*, *37*(17), 4119-4124.
Simpson, M., and T. Clement (2003): Comparison of finite difference and finite element solutions to the variably saturated flow equation, *Journal of Hydrology*, *270*(1), 49-64.
Singh, A., B. S. Minsker, and A. J. Valocchi (2008): An interactive multi-objective optimization framework for groundwater inverse modeling, *Advances in Water Resources*, *31*(10), 1269-1283.
Singh, S. K., C. K. Singh, K. S. Kumar, R. Gupta, and S. Mukherjee (2009): Spatial-temporal monitoring of groundwater using multivariate statistical techniques in Bareilly District of Uttar Pradesh, India, *Journal of Hydrology and Hydromechanics*, *57*(1), 45-54.
Singh, V., and D. Woolhiser (2002): Mathematical Modeling of Watershed Hydrology, *Journal of Hydrologic Engineering*, *7*(4), 270-292.
Software, G. (2011): Surfer 11, edited, Golden Software.

Srebotnjak, T., G. Carr, A. de Sherbinin, and C. Rickwood (2011): A global Water Quality Index and hot-deck imputation of missing data, *Ecological Indicators*, *17*, 108–119.
Srivastava, S., and A. L. Ramanathan (2008): Geochemical assessment of groundwater quality in vicinity of Bhalswa landfill, Delhi, India, using graphical and multivariate statistical methods, *Environmental Geology, 53*(7), 1509-1528.
Standke, G. (2004): Geologische Kartierung im Bernsteintagebau Goitsche und regionale stratigraphische Korrelation der tertiären Sedimente, in *Bitterfelder Bernstein: Lagerstätte, Rohstoff, Folgenutzung. Exkurs.f. u. Veröfftl. 224*, edited by R. Wimmer, U. Holz and J. Rascher, pp. 18-22, GGW, Berlin.
Stollberg, R. (2013): Groundwater contaminant source zone identification at an industrial and abandoned mining site : a forensic backward-in-time modelling approach, 183 pp, Martin Luther University, Halle (Saale), Germany.
Stollberg, R., W. Gossel, P. Wycisk, and H. Weiß (2009): Source and pathway identification of groundwater contaminants using a backward modeling technique, paper presented at 2nd International FEFLOW User Conference, Potsdam, Germany, 14-18 September, 2009.
Storck, P., J. W. Eheart, and A. J. Valocchi (1997): A Method for the Optimal Location of Monitoring Wells for Detection of Groundwater Contamination in Three-Dimensional Heterogenous Aquifers, *Water Resources Research*, *33*(9), 2081-2088.
Tabachnick, B. G., L. S. Fidell, and S. J. Osterlind (2001): Using multivariate statistics.
Tan, P.-N., M. Steinbach, and V. Kumar (2005): Cluster analysis: basic concepts and algorithms, in *Introduction to data mining*, edited, pp. 487-586, Pearson Education, USA.
Tang, Y., P. M. Reed, and J. B. Kollat (2007): Parallelization strategies for rapid and robust evolutionary multiobjective optimization in water resources applications, *Advances in Water Resources*, *30*(3), 335-353.
Thakur, J. K. (2013): New approaches for groundwater monitoring network optimization – statistical, geostatistical and hydrogeologial models, paper presented at International Humboldt Kolleg on Management of Water, Energy and Bio-resources in Changing Climate Regime: Emerging Issues and Environmental Challenges, Jawaharlal Nehru University, New Delhi, India.
Thakur, J. K., W. Gossel, H. Weiß, and P. Wycisk (2011a): Long-Term Groundwater Monitoring Optimization: Improving Performance and Reducing Costs Associated for a 3d Regionalization of Groundwater Contamination – A case study of Bitterfeld/Wolfen, East Germany, paper presented at Sustainable Water Resource Management and Treatment Technology, NEERI, Nagpur, India.
Thakur, J. K., W. Gossel, H. Weiß, and P. Wycisk (2011b): Optimizing long term groundwater monitoring network in a complex contaminated site, paper presented at HIGRADE Conference, Helmholtz Centre for Environmental Research (UFZ), Leipzig, Germany, 26, March, 2012.
Thakur, J. K., W. Gossel, H. Weiß, and P. Wycisk (2011c): Improving groundwater monitoring strategies based on groundwater monitoring network optimization, in *TASK – The Centre of Competence for Soil, Groundwater and Site Revitalisation*, edited, Liepzig, Germany.

Thakur, J. K., W. Gossel, H. Weiß, and P. Wycisk (2012): Optimizing long-term groundwater monitoring network using geostatistical methods, in *IAHS Red book: Models – Repositories of Knowledge* edited, pp. 133-138, IAHS.
Thomsen, R., V. Søndergaard, and K. Sørensen (2004): Hydrogeological mapping as a basis for establishing site-specific groundwater protection zones in Denmark, *Hydrogeology Journal*, *12*(5), 550-562.
Trefry, M. G., and C. Muffels (2007): FEFLOW: A Finite-Element Ground Water Flow and Transport Modeling Tool, *Ground Water*, *45*(5), 525-528.
Tripathi, V. S. (1991): A model for simulating transport of reactive multispecies components: model development and demonstration, *Water Resources Research*, *27*(12), 3075-3094.
van Geer, F. C., M. F. P. Bierkens, and H. P. Broers (2006): Groundwater Monitoring Strategies, in *Encyclopedia of Hydrological Sciences*, edited, John Wiley & Sons, Ltd.
Van Genuchten, M. T. (1978): Simulation models and their application to landfill disposal siting: A review of current technology, paper presented at Proceedings Fourth Annual Hazardous Waste Management Symposium," Land Disposal of Hazardous Wastes", Southwest Research Institute and USEPA, San Antonio, Texas.
Wang, H. F., and M. P. Anderson (1995): *Introduction to groundwater modeling: Finite difference and finite element methods*, Academic Press.
Wang, X. Y., X. D. Cui, H. Y. Ma, and Z. P. Tao (2012): The Optimization of Groundwater Dynamic Monitoring Network–An Example of the North Ordos Basin, *Advanced Materials Research*, *518*, 4057-4061.
Wansa, S., and R. Wimmer (1990): Geologie des Jungpleistozäns der Becken von Gröbern und Grabschütz, *Altenburger Naturwissenschaftliche Forschungen Heft 5, Altenburg*, 49-91.
Ward Jr, J. H. (1963): Hierarchical grouping to optimize an objective function, *Journal of the American Statistical Association*, 236-244.
Weiß, H., M. Schirmer, G. Teutsch, and P. Merkel (2002a): Sanierungsforschung in regional kontaminierten Aquiferen (SAFIRA) – 2. Projektüberblick und Pilotanlage, *Grundwasser*, *7*(3), 135-139.
Weiß, H., M. Schirmer, G. Teutsch, and P. Merkel (2002b): Sanierungsforschung in regional kontaminierten Aquiferen (SAFIRA)–2. Projektüberblick und Pilotanlage, *Grundwasser*, *7*(3), 135-139.
Weiß, H., B. Daus, P. Fritz, F.-D. Kopinke, P. Popp, and L. Wuensche (1998): In situ groundwater remediation research in the Bitterfeld region in eastern Germany (SAFIRA), *IAHS Publication(International Association of Hydrological Sciences)*(250), 443-450.
Weiß, H., G. Teutsch, P. Fritz, B. Daus, A. Dahmke, P. Grathwohl, R. Trabitzsch, B. Feist, R. Ruske, and O. Böhme (2001): Sanierungsforschung in regional kontaminierten Aquiferen (SAFIRA)–1. Information zum Forschungsschwerpunkt am Standort bitterfeld, *Grundwasser*, *6*(3), 113-122.
WHO (2011): Guidelines for drinking-water quality, fourth edition*Rep.*
Wold, S., K. Esbensen, and P. Geladi (1987): Principal component analysis, *Chemometrics and Intelligent Laboratory Systems*, *2*(1–3), 37-52.
Wollmann, A. (2004): Geologische Bearbeitung einer ehemaligen Bergbau- und Industriefolgelandschaft Bitterfeld/Wolfen, Martin-Luther-Universität Halle-Wittenberg, Halle (Saale), Germany.

Wollmann:, A. (2008): *Geologisches 3D-Rauminformationssystem*, 204 pp., Verlag Dr. Muller.

Wu, J., C. Zheng, C. C. Chien, and L. Zheng (2006): A comparative study of Monte Carlo simple genetic algorithm and noisy genetic algorithm for cost-effective sampling network design under uncertainty, *Advances in Water Resources*, *29*(6), 899-911.

Wycisk, P., C. Neumann, and W. Gossel (2005): Flooding Induced Effects from the Mining Lake Goitzsche on Groundwater and Land-use in the Bitterfeld Area, *Acta hydrochimica et hydrobiologica*, *33*(5), 507-518.

Wycisk, P., T. Hubert, W. Gossel, and C. Neumann (2009): High-resolution 3D spatial modelling of complex geological structures for an environmental risk assessment of abundant mining and industrial megasites, *Computers & Geosciences*, *35*(1), 165-182.

Wycisk, P., H. Weiss, A. Kaschl, S. Heidrich, and K. Sommerwerk (2003): Groundwater pollution and remediation options for multi-source contaminated aquifers (Bitterfeld/Wolfen, Germany), *Toxicology Letters*, *140-141*, 343-351.

Yeh, G.-T. (1981): On the computation of Darcian velocity and mass balance in the finite element modeling of groundwater flow, *Water Resources Research*, *17*(5), 1529-1534.

Zenova, G. M., N. A. Manucharova, and D. G. Zvyagintsev (2011): Extremophilic and extremotolerant actinomycetes in different soil types, *Eurasian Soil Sc.*, *44*(4), 417-436.

Zhang, Y., G. F. Pinder, and G. S. Herrera (2005): Least cost design of groundwater quality monitoring networks, *Water Resources Research*, *41*(8), W08412.

Zhou, Y. (1996): Sampling frequency for monitoring the actual state of groundwater systems, *Journal of Hydrology*, *180*(1–4), 301-318.

Appendix

Appendix 1: Formula

Central tendency

The central tendency of a distribution locates the "centre" of a distribution of values of a variable. The central tendency is estimated in term of mean, median, and mode. The most common, mean of the variables, was estimated by arithmetic average:

$$\bar{x} = \frac{1}{n}\sum_{i=1}^{n} x_i \qquad \text{Appendix Eqn. 1}$$

where, $\bar{x}$ is mean and n is number of x_i data points.

Distribution

The distribution is a summary of the frequency or ranges of values for a variable. One of the most common ways to describe a single variable is with a frequency distribution in table or, in a graph (histogram or bar chart). The distribution of variables was analyzed by skewness and Kurtosis analysis.

Skewness

The skewness (g_1) is a measure of the asymmetry of a distribution and is given by:

$$g_1 = \frac{1}{n}\sum_{i=1}^{n}\left(\frac{x_i - \bar{x}}{\sigma}\right)^3 \qquad \text{Appendix Eqn. 2}$$

where, n is number of data points, $\bar{x}$ is mean, σ is the standard deviation. The skewness for a normal distribution is zero. Negative values for the skewness indicate that data are skewed to left. It means that the left tail is long relative to the right tail. Positive values for the skewness indicate that data are skewed to right. It means that the right tail is relatively longer than the left tail (Mardia, 1970).

Kurtosis

Kurtosis is measure of "peakedness" of the probability distribution of a real-valued random variable which is given by

$$g_2 = \left[\frac{1}{n}\sum_{i=1}^{n}\left(\frac{x_i - \bar{x}}{\sigma}\right)^4\right] - 3 \qquad \text{Appendix Eqn. 3}$$

where, n is number of data points, $\bar{x}$ is mean, δ is the standard deviation. A distribution with a high peak ($g_2 > 0$) is called leptokurtic, a flat-topped curve is called ($g_2 < 0$) platykurtic, and the normal distribution ($g_2 = 0$) is known as mesokurtic.

Dispersion

Dispersion is the spread of values around the central tendency. It is commonly measured in terms of range and standard deviation. The range is the highest value minus the lowest value. The standard deviation (σ) is a more accurate and detailed estimate of dispersion which is given by

$$\sigma = \sqrt{\frac{1}{n}\sum_{i=1}^{n}(x_i - \bar{x})^2} \quad \text{Appendix Eqn. 4}$$

where, $\bar{x}$ is mean and n is number of x_i data points.

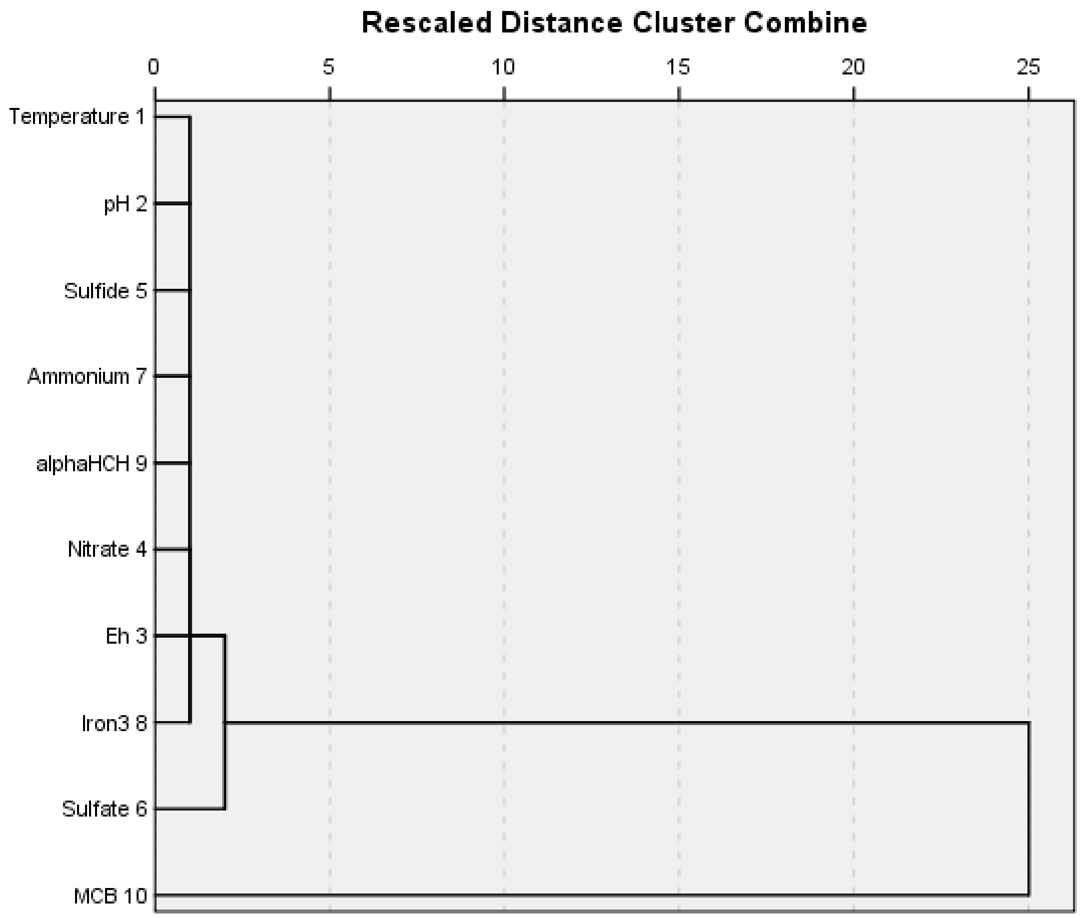

Appendix 2: Dendrogram using agglomerative hierarchical cluster (AHC) of monitoring parameters showing distance among the parameters.

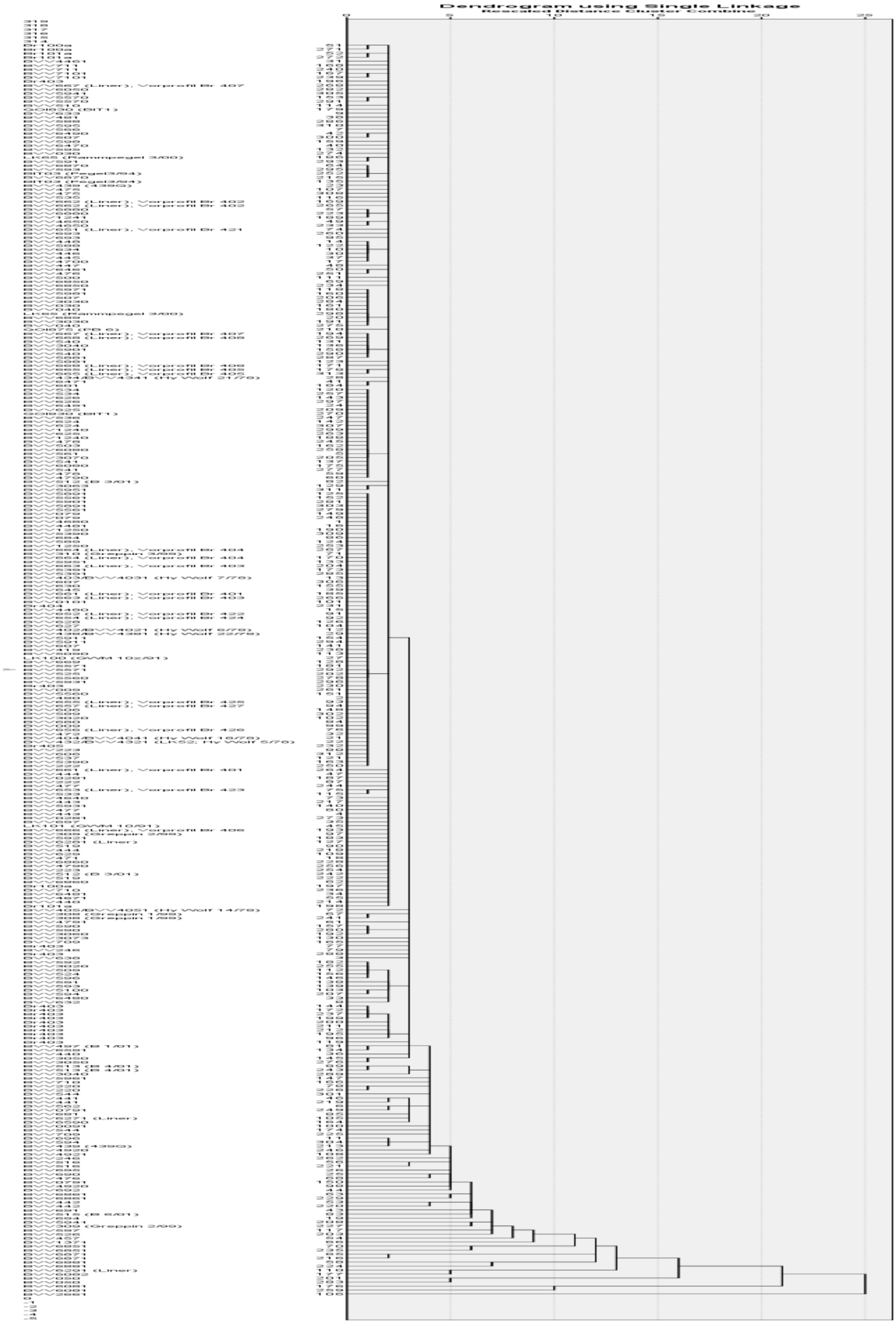

Appendix 3: Dendrogram using agglomerative hierarchical cluster (AHC) of well locations showing distance between clusters.

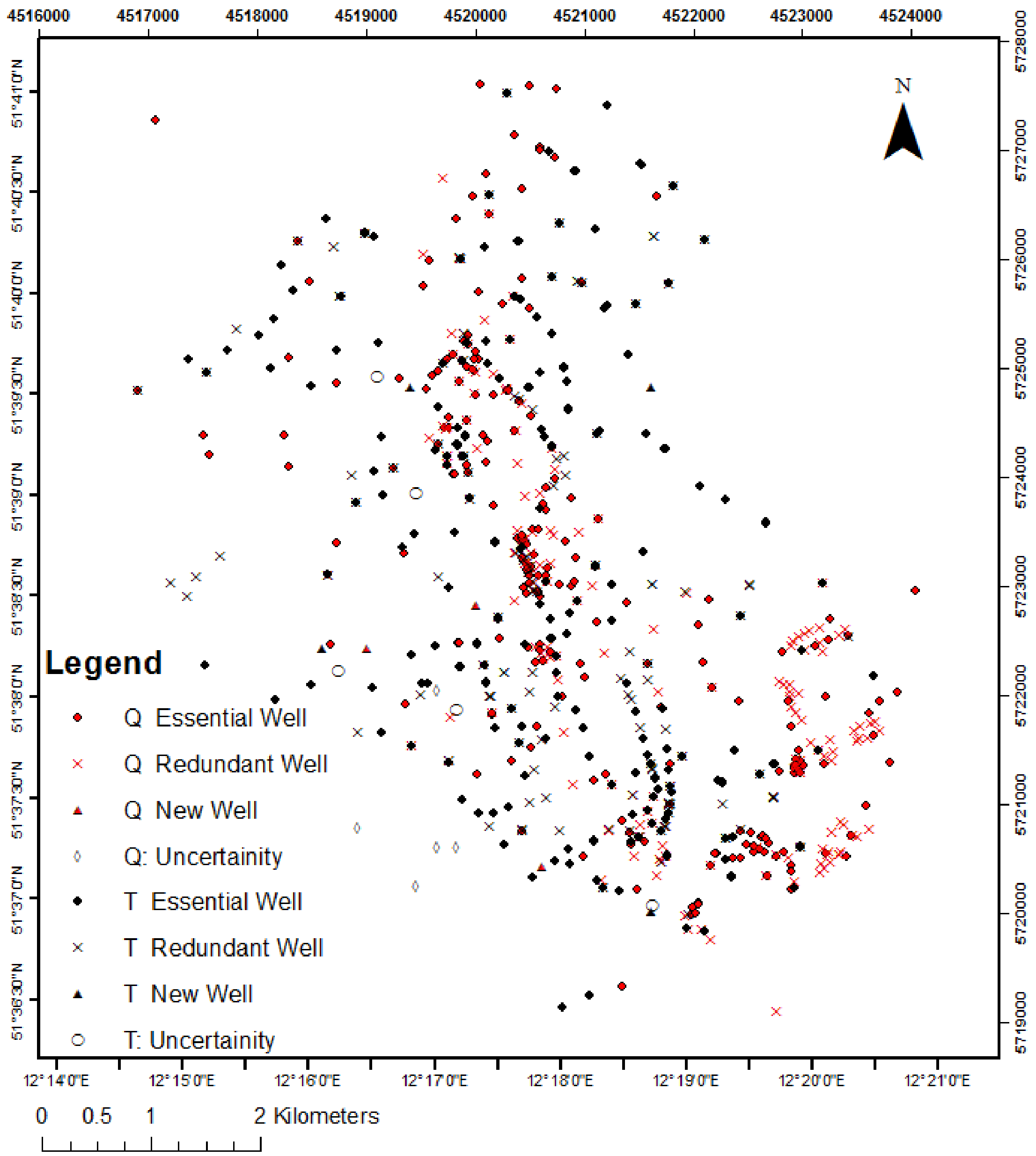

Appendix 4: Optimized LTM network map showing essential, redundant, and proposed new wells alone with location of uncertainties in the Quaternary and Tertiary aquifers.

Appendix 5: Optimized LTM network map showing essential and redundant wells in the monitoring network (note: Stat. Spatial Opt.: statistical spatial optimization, Geostat. Spatial: geostatistical optimization, Hydrogeo Spatial: hydrogeological spatial optimization, Stat. Temp.: statistical temporal optimization, Hydrogeological Temp. Opt.: hydrogeological temporal optimization, Essen.: essential well, Red.: redundant well).

	Monitoring groundwater wells details					Stat. Spatial Opt.		Geostat. Spatial		Hydrogeo Spatial	Stat. Temp.		Hydrogeological Temp. Opt.	
S. No.	Loc. ID / Well Name	Easting	Northing	Sample elevation	Vertical zone	% of redundancy	Essen / Red	Essen / Red	Critical Index	Essen / Red	Baseline frequency (per year)	Baseline interval (days)	Flow velocity	Monitoring Time
1	AUS03	4520570	5721703	74.35	Q	25%	Red	No	0	Essen	4Q (1)	363	7.15E-05	2 year
2	bb021	4522432	5720499.1	74.26	Q	0	Essen	No	0	Essen	1Q (4)	28	1.13E-03	1 year
3	bb023	4522563	5720556.2	73.27	Q	100%	Red	Yes	0.5	Essen	1Q (4)	29	1.12E-03	1 year
4	bb024	4522651	5720551.3	73.53	Q	0	Essen	Yes	0.5	Essen	1Q (4)	28	8.52E-04	1 year
5	bb025	4522644	5720709.6	74.27	Q	0	Essen	No	0	Essen	1Q (4)	29	9.18E-04	1 year
6	bb027	4522696	5720635.8	73.32	Q	0	Essen	Yes	0.5	Essen	1Q (4)	28	9.55E-04	1 year
7	bb028	4522830	5720548.3	1.00	0%	100%	Red	Yes	0.5	Essen	1Q (4)	29	6.10E-04	1 year
8	bb030	4522931	5720285.6	73.14	Q	0	Essen	Yes	1	Essen	NA (NA)	NA	6.10E-04	1 year
9	bb031	4523210	5720407.6	72.78	Q	100%	Red	No	0	Essen	NA (NA)	NA	4.78E-03	1 year
10	bb032	4523165	5720361.6	73.11	Q	0	Essen	No	0	Essen	NA (NA)	NA	7.68E-03	6 month
11	bb033	4523343	5720534.4	71.07	Q	0	Essen	No	0	Essen	NA (NA)	NA	7.17E-03	6 month
12	bb034	4523345	5720521.4	71.36	Q	0	Essen	No	0	Essen	NA (NA)	NA	7.17E-03	6 month
13	bb036	4523404	5720516.3	71.55	Q	0	Essen	No	0	Essen	NA (NA)	NA	7.17E-03	6 month
14	bb041	4523512	5720685.7	73.49	Q	0	Essen	No	0	Essen	NA (NA)	NA	4.05E-03	1 year
15	bb043	4523460	5720703.7	72.89	Q	100%	Red	No	0	Essen	NA (NA)	NA	1.46E-03	1 year
16	bb044	4523448	5720707.6	72.89	Q	0	Essen	No	0	Essen	NA (NA)	NA	1.46E-03	1 year
17	bb045	4523272	5720728.3	73.26	Q	0	Essen	No	0	Essen	NA (NA)	NA	8.37E-04	1 year
18	bb046	4523360	5720550.6	73.26	Q	0	Essen	No	0	Essen	NA (NA)	NA	8.37E-04	1 year
19	bb047	4523254	5720455.8	70.70	Q	100%	Red	No	0	Essen	NA (NA)	NA	4.78E-03	1 year

20	bb048	4523271	5721386	70.70	Q	0	Essen	No	0	Essen	NA (NA)	NA	4.78E-03	1 year
21	bb049	4523209	5721438	70.70	Q	0	Essen	No	0	Essen	NA (NA)	NA	4.78E-03	1 year
22	bb050	4523148	5721489	70.70	Q	0	Essen	No	0	Essen	NA (NA)	NA	4.78E-03	1 year
23	bb051	4523084	5721557	70.70	Q	0	Essen	No	0	Essen	NA (NA)	NA	4.78E-03	1 year
24	bb053	4523262	5721589	70.70	Q	0	Essen	No	0	Essen	NA (NA)	NA	4.78E-03	1 year
25	bb055	4523290	5721477	70.70	Q	0	Essen	No	0	Essen	NA (NA)	NA	4.78E-03	1 year
26	bb058	4523483	5721664	70.70	Q	0	Essen	No	0	Essen	NA (NA)	NA	4.78E-03	1 year
27	bb059	4523522	5721595	70.70	Q	0	Essen	No	0	Essen	NA (NA)	NA	4.78E-03	1 year
28	bb060	4523626	5721734	70.70	Q	0	Essen	No	0	Essen	NA (NA)	NA	4.78E-03	1 year
29	bb083	4522840	5722096	70.70	Q	0	Essen	No	0	Essen	NA (NA)	NA	4.78E-03	1 year
30	bb084	4522889	5722019	70.70	Q	0	Essen	No	0	Essen	NA (NA)	NA	4.78E-03	1 year
31	bb085	4522977	5722008	70.70	Q	0	Essen	No	0	Essen	NA (NA)	NA	4.78E-03	1 year
32	bb086	4522902	5721886	70.70	Q	0	Essen	No	0	Essen	NA (NA)	NA	4.78E-03	1 year
33	bb087	4522950	5721833	70.70	Q	0	Essen	No	0	Essen	NA (NA)	NA	4.78E-03	1 year
34	bb091	4522994	5721760	70.70	Q	0	Essen	No	0	Essen	NA (NA)	NA	4.78E-03	1 year
35	bb092	4522918	5722495	70.70	Q	0	Essen	Yes	1	Essen	NA (NA)	NA	4.78E-03	1 year
36	bb093	4523025	5722413	70.70	Q	0	Essen	No	0	Essen	NA (NA)	NA	4.78E-03	1 year
37	bb094	4523165	5722477	70.70	Q	0	Essen	No	0	Essen	NA (NA)	NA	4.78E-03	1 year
38	bb095	4523197	5722399	70.70	Q	0	Essen	No	0	Essen	NA (NA)	NA	4.78E-03	1 year
39	bb096	4523336	5722543	70.70	Q	0	Essen	No	0	Essen	NA (NA)	NA	4.78E-03	1 year
40	bb097	4523165	5722620	70.70	Q	0	Essen	No	0	Essen	NA (NA)	NA	4.78E-03	1 year
41	bb098	4523401	5722595	70.70	Q	0	Essen	No	0	Essen	NA (NA)	NA	4.78E-03	1 year
42	bb099	4523021	5722557	70.70	Q	0	Essen	No	0	Essen	NA (NA)	NA	4.78E-03	1 year
43	bb100	4523066	5722582	70.70	Q	0	Essen	No	0	Essen	NA (NA)	NA	4.78E-03	1 year
44	bb101	4523386	5720806.8	70.70	Q	0	Essen	No	0	Essen	NA (NA)	NA	4.78E-03	1 year
45	bb102	4523192	5720578	69.41	Q	0	Essen	Yes	1	Essen	NA (NA)	NA	4.78E-03	1 year
46	bb104	4523221	5720538.5	72.15	Q	0	Essen	Yes	0.5	Essen	1Q (4)	28	4.78E-03	1 year
47	bb1041	4523240	5720561.8	72.15	Q	0	Essen	Yes	1	Essen	NA (NA)	NA	4.78E-03	1 year

48	bb105	4523229	5720530.3	70.18	Q	100%	Red	No	0	Essen	NA (NA)	NA	4.78E-03	1 year
49	bb106	4523174	5720451.2	70.18	Q	0	Essen	No	0	Essen	NA (NA)	NA	4.78E-03	1 year
50	bb107	4522909	5722455	70.18	Q	0	Essen	No	0	Essen	NA (NA)	NA	4.78E-03	1 year
51	bb108	4522965	5722526	70.18	Q	0	Essen	No	0	Essen	NA (NA)	NA	4.78E-03	1 year
52	bb110	4523264	5722696	70.18	Q	0	Essen	No	0	Essen	NA (NA)	NA	4.78E-03	1 year
53	bb111	4522892	5722088	70.18	Q	0	Essen	No	0	Essen	NA (NA)	NA	4.78E-03	1 year
54	bb113	4523675	5721756	70.18	Q	0	Essen	No	0	Essen	NA (NA)	NA	4.78E-03	1 year
55	bb114	4523536	5721714	70.18	Q	0	Essen	No	0	Essen	NA (NA)	NA	4.78E-03	1 year
56	bb115	4523712	5721665	70.18	Q	0	Essen	No	0	Essen	NA (NA)	NA	4.78E-03	1 year
57	bb116	4523603	5721592	70.18	Q	0	Essen	No	0	Essen	NA (NA)	NA	4.78E-03	1 year
58	bb117	4523512	5721569	70.18	Q	0	Essen	No	0	Essen	NA (NA)	NA	4.78E-03	1 year
59	bb303	4522564	5720612.8	74.10	Q	100%	Red	No	0	Essen	1Q (4)	40690	4.78E-03	1 year
60	bb304	4522613	5720575.7	74.10	Q	0	Essen	Yes	0.5	Essen	1Q (4)	28	4.78E-03	1 year
61	bb305	4522664	5720684.4	67.21	Q	0	Essen	Yes	0.5	Essen	1Q (4)	28	4.78E-03	1 year
62	bb306	4522880	5720502.8	69.42	Q	0	Essen	No	0	Essen	1Q (4)	28	4.78E-03	1 year
63	bb307	4522904	5720424.9	69.42	Q	0	Essen	Yes	0.5	Essen	1Q (4)	36	4.78E-03	1 year
64	bb308	4522901	5720383.3	70.61	Q	100%	Red	No	0	Essen	1Q (4)	35	4.78E-03	1 year
65	bb312	4523358	5720827.6	69.87	Q	0	Essen	No	0	Essen	NA (NA)	NA	4.78E-03	1 year
66	BIT03	4521962	5719838	74.20	Q	100%	Red	No	0	Essen	2Q (2)	136.5	5.07E-04	2 year
67	Br01	4520602	5723843	59.40	Q	0	Essen	No	0.3333	Essen	1Q (4)	7	1.18E-02	6 month
68	Br02	4520657	5723898	58.80	Q	11%	Red	No	0	Essen	1Q (4)	7	8.80E-03	6 month
69	Br03	4520714	5723920	58.90	T	100%	Red	No	0.3333	Essen	1Q (4)	7	7.77E-03	6 month
70	Br05	4520737	5724074	67.10	Q	100%	Red	No	0.3333	Essen	1Q (4)	7	2.09E-03	1 year
71	Br06	4520752	5724164	64.80	T	100%	Red	No	0.3333	Essen	1Q (4)	7	4.36E-05	3 year
72	Br07	4520713	5724265	68.80	Q	0	Essen	Yes	0.6667	Essen	1Q (4)	7	3.75E-05	3 year
73	Br08	4520642	5724364	64.60	T	13%	Red	Yes	0.6667	Essen	1Q (4)	7	4.88E-05	3 year
74	Br100a	4520658	5721597	61.40	T	29%	Red	Yes	1	Essen	2Q (2)	216.5	5.94E-05	2 year
75	Br101a	4520612	5721583	62.50	T	31%	Red	No	0.3333	Essen	2Q (2)	216.5	5.94E-05	2 year

76	Br11	4520426	5724679	65.00	Q	100%	Red	Yes	0.6667	Essen	1Q (4)	7	4.30E-05	3 year
77	Br12	4520367	5724748	64.60	T	100%	Red	No	0.3333	Essen	1Q (4)	7	4.30E-05	3 year
78	Br14	4520224	5724909	64.80	T	100%	Red	Yes	0.5	Essen	1Q (4)	7	6.56E-04	1 year
79	Br1Greppin	4520418	5723376.7	70.01	Q	75%	Red	Yes	0.6667	Essen	1Q (4)	7	2.09E-03	1 year
80	Br201	4520428	5723355	68.25	Q	55%	Red	No	0.3333	Essen	1Q (4)	7	2.09E-03	1 year
81	Br202	4520426	5723357	59.25	T	40%	Red	Yes	0.6667	Essen	1Q (4)	7	2.09E-03	1 year
82	Br203	4520442	5723237	70.20	Q	11%	Red	Yes	0.6667	Essen	2Q (2)	206.5	6.66E-03	6 month
83	Br204	4520441	5723234	58.70	T	11%	Red	Yes	0.5	Essen	2Q (2)	206.5	6.66E-03	6 month
84	Br205	4520490	5723119	70.40	Q	22%	Red	Yes	1	Essen	2Q (2)	206.5	6.69E-03	6 month
85	Br206	4520492	5723116	58.90	T	30%	Red	Yes	0.5	Essen	2Q (2)	206.5	6.69E-03	6 month
86	Br207	4520524	5723044	70.70	Q	11%	Red	Yes	0.6667	Essen	2Q (2)	206.5	6.44E-03	6 month
87	Br208	4520527	5723043	59.20	T	44%	Red	Yes	0.5	Essen	2Q (2)	206.5	6.44E-03	6 month
88	Br209	4520576	5722942	70.10	Q	10%	Red	Yes	0.6667	Essen	2Q (2)	217	8.08E-03	6 month
89	Br210	4520575	5722946	58.60	T	11%	Red	Yes	0.5	Essen	2Q (2)	217	8.08E-03	6 month
90	Br211	4520515	5723179	67.31	Q	50%	Red	Yes	0.5	Essen	1Q (4)	7	1.62E-03	1 year
91	Br221	4520432	5723260.1	67.31	Q	0	Essen	Yes	0.5	Essen	1Q (4)	83	1.62E-03	1 year
92	Br222	4520453	5723219.5	67.31	Q	0	Essen	No	0	Essen	1Q (4)	86.5	1.62E-03	1 year
93	Br223	4520464	5723199.2	67.31	Q	0	Essen	No	0	Essen	1Q (4)	83	1.62E-03	1 year
94	Br224	4520473	5723154.1	67.31	Q	0	Essen	Yes	0.5	Essen	1Q (4)	88.5		6 month
95	Br225	4520498	5723100.9	67.31	Q	0	Essen	Yes	0.5	Essen	1Q (4)	90		6 month
96	Br226	4520535	5723022.8	67.31	Q	0	Essen	Yes	0.5	Essen	1Q (4)	92.5		6 month
97	Br26	4520621	5723750	58.80	Q	100%	Red	No	0.3333	Essen	1Q (4)	7	0.0015073	1 year
98	Br27	4520593	5723717	58.00	T	0	Essen	Yes	0.6667	Essen	1Q (4)	7	0.0090737	6 month
99	Br40	4519790	5725320.8	68.83	Q	33%	Red	No	0.3333	Essen	1Q (4)	7	0.0076858	6 month
100	Br401	4521621	5721319	67.76	T	0	Essen	No	0	Essen	1Q (4)	7	0.0033438	1 year
101	Br402	4521649	5721231.4	62.21	T	17%	Red	No	0	Essen	1Q (4)	7	0.0054046	6 month
102	Br403	4521677	5721125.5	62.29	T	88%	Red	Yes	0.5	Essen	1Q (4)	7	0.005057	1 year
103	Br404	4521645	5721060.6	60.51	T	57%	Red	Yes	0.5	Essen	1Q (4)	7	0.005057	1 year

104	Br405	4521781	5720999.8	60.55	T	43%	Red	Yes	0.5	Essen	1Q (4)	7	0.0040546	1 year
105	Br406	4521710	5720746.6	61.07	T	17%	Red	Yes	0.6667	Essen	1Q (4)	7	0.0037662	1 year
106	Br407	4521698	5720480.2	69.18	Q	33%	Red	Yes	0.6667	Essen	1Q (4)	7	0.0028582	1 year
107	Br41	4519891	5725315	66.28	T	50%	Red	Yes	0.6667	Essen	1Q (4)	7	0.008438	6 month
108	Br42	4519927	5725231.8	64.62	T	100%	Red	Yes	0.6667	Essen	1Q (4)	7	0.0037776	1 year
109	Br43	4520001	5725148.4	66.39	Q	100%	Red	Yes	0.6667	Essen	1Q (4)	7	4.138E-05	3 year
110	Br44	4520037	5725080	65.34	Q	0	Essen	Yes	0.5	Essen	1Q (4)	7	0.0002368	2 year
111	Br45	4520176	5724953.1	67.38	Q	100%	Red	Yes	0.6667	Essen	1Q (4)	7	0.0002047	2 year
112	Br47	4520314	5724797	63.26	Q	100%	Red	Yes	0.6667	Essen	1Q (4)	7	0.0001082	2 year
113	Br48	4520522	5724622	65.34	T	100%	Red	Yes	0.6667	Essen	1Q (4)	7	0.0087427	6 month
114	Br49	4520610	5724433.8	59.62	T	100%	Red	No	0.3333	Essen	1Q (4)	7	0.0053301	6 month
115	Br50	4520737	5723987.8	63.59	Q	100%	Red	No	0.3333	Essen	1Q (4)	7	0.0084179	6 month
116	Br501	4520662	5722431	73.35	Q	100%	Red	Yes	0.6667	Essen	2Q (2)	216	0.0040679	1 year
117	Br502	4520697	5722341	73.86	Q	100%	Red	No	0.3333	Essen	2Q (2)	216.5	0.0067934	6 month
118	Br503	4520695	5722390	73.39	Q	100%	Red	No	0.3333	Essen	2Q (2)	216.5	0.0091949	6 month
119	Br504	4520624	5722310	73.60	Q	100%	Red	Yes	0.6667	Essen	2Q (2)	216.5	0.0381629	6 month
120	Br505	4520616	5722384	73.82	Q	100%	Red	Yes	0.6667	Essen	2Q (2)	216.5	0.0055461	6 month
121	Br506	4520561	5722434	73.72	Q	0	Essen	Yes	0.6667	Essen	2Q (2)	216.5	0.004362	1 year
122	BRI08	4522759	5719087	72.04	Q	0	Essen	No	0.3333	Essen	NA (NA)	NA	0.004362	1 year
123	BSZB3	4520902	5721170	74.77	Q	0	Essen	Yes	0.5	Essen	4Q (1)	400	0.004362	1 year
124	BVV009	4521474	5721282	70.47	Q	62%	Red	Yes	0.5	Essen	2Q (2)	138	0.0033438	1 year
125	BVV0091	4521473	5721285.5	58.32	T	33%	Red	No	0.3333	Essen	5Q (0.8)	415	0.0033438	1 year
126	BVV0092	4521469	5721283.1	39.19	T	100%	Red	No	0.3333	Essen	8Q (0.5)	747	0.0022937	1 year
127	BVV0101	4521618	5721366.9	56.43	T	71%	Red	No	0.3333	Essen	2Q (2)	139	0.0057831	6 month
128	BVV0102	4521618	5721364.3	38.62	T	67%	Red	Yes	0.5	Essen	NA (NA)	NA	0.0057831	6 month
129	BVV011	4521795	5721368.1	68.94	Q	100%	Red	Yes	0.5	Essen	NA (NA)	NA	0.0042815	1 year
130	BVV0281	4521447	5721070.9	61.69	Q	50%	Red	No	0.3333	Essen	3Q (1.3333)	244	0.0052692	6 month

131	BVV0282	4521451	5721072.7	36.25	T	0	Essen	No	0.3333	Essen	8Q (0.5)	744	0.0045934	1 year
132	BVV030	4521802	5721103	69.11	T	42%	Red	No	0	Essen	2Q (2)	146	0.0040283	1 year
133	BVV040	4521347	5720840.1	66.72	Q	50%	Red	No	0	Essen	2Q (2)	141	0.0045135	1 year
134	BVV050	4521430	5720630	66.20	Q	8%	Red	No	0.3333	Essen	2Q (2)	150	0.0045135	1 year
135	BVV053	4520999	5720512	71.13	Q	25%	Red	Yes	0.6667	Essen	4Q (1)	337	0.0045135	1 year
136	BVV079	4521258	5721179.5	70.94	Q	64%	Red	Yes	0.6667	Essen	1Q (4)	129.5	4.326E-05	3 year
137	BVV0791	4521249	5721169.3	58.35	Q	15%	Red	Yes	0.5	Essen	3Q (1.3333)	250	0.0005541	1 year
138	BVV0792	4521252	5721169.5	43.36	T	0	Essen	Yes	0.5	Essen	NA (NA)	NA	5.669E-05	2 year
139	BVV088	4521044	5719234.4	49.93	T	0	Essen	Yes	0.5	Essen	NA (NA)	NA	5.669E-05	2 year
140	BVV092	4522232	5721212.1	55.79	T	0	Essen	No	0	Essen	4Q (1)	338	5.669E-05	2 year
141	BVV100	4520806	5719121.1	66.06	T	0	Essen	Yes	0.5	Essen	2Q (2)	189	5.726E-05	2 year
142	BVV1121	4520406	5721561	51.06	T	50%	Red	No	0	Essen	4Q (1)	360	5.726E-05	2 year
143	BVV1122	4520406	5721561	37.06	T	0	Essen	Yes	0.6667	Essen	8Q (0.5)	720	5.726E-05	2 year
144	BVV118	4520337	5721867	74.10	Q	0	Essen	Yes	1	1st red	NA (NA)	NA	6.075E-05	2 year
145	BVV1181	4520337	5721867	54.89	T	0	Essen	Yes	0.5	2nd red	4Q (1)	343	6.075E-05	2 year
146	BVV1182	4520337	5721867	39.91	T	0	Essen	No	0	1st red	8Q (0.5)	747	6.075E-05	2 year
147	BVV119	4520091	5722270	75.31	Q	0	Essen	No	0.3333	2nd red	2Q (2)	170	5.385E-05	2 year
148	BVV1191	4520091	5722270	62.81	T	0	Essen	Yes	0.6667	3rd red	2Q (2)	185	4.344E-05	3 year
149	BVV1192	4520091	5722270	36.81	T	0	Essen	No	0.3333	1st red	2Q (2)	186		3 year
150	BVV1193	4520077	5722264.7	36.81	T	0	Essen	Yes	0.5	2nd red	NA (NA)	NA	4.328E-05	3 year
151	BVV121	4520274	5722208.3	70.40	T	0	Essen	No	0.3333	3rd red	4Q (1)	396	4.328E-05	3 year
152	BVV1212	4520274	5722208.3	36.40	T	0	Essen	No	0.3333	Essen	NA (NA)	NA	4.328E-05	3 year
153	BVV1221	4519865	5722259.2	48.85	T	0	Essen	No	0.3333	1st red	NA (NA)	NA	0.0081196	6 month
154	BVV1222	4519855	5722252.4	67.81	T	0	Essen	Yes	0.6667	2nd red	NA (NA)	NA	0.0081196	6 month
155	BVV1223	4519859	5722255.4	37.59	T	0	Essen	No	0	Essen	8Q (0.5)	737	0.0073402	6 month
156	BVV1230	4521168	5720229.3	70.30	Q	40%	Red	No	0.3333	Essen	5Q (0.8)	415	0.0027715	1 year
157	BVV1231	4521173	5720227	54.26	T	40%	Red	No	0.3333	Essen	5Q (0.8)	414	0.0027715	1 year

158	BVV1232	4521177	5720224	35.03	T	100%	Red	No	0	Essen	8Q (0.5)	761	0.0027715	1 year
159	BVV1240	4521747	5720790	68.12	Q	31%	Red	Yes	0.6667	Essen	2Q (2)	216	0.0042815	1 year
160	BVV1241	4521745	5720785.9	52.90	T	36%	Red	Yes	0.6667	Essen	3Q (1.3333)	305.5	0.0042815	1 year
161	BVV1242	4521742	5720781.8	34.30	T	0	Essen	No	0.3333	Essen	8Q (0.5)	756	0.0042815	1 year
162	BVV1250	4521788	5721160	69.80	Q	0	Essen	No	0	Essen	2Q (2)	210	6.91E-05	2 year
163	BVV1251	4521787	5721164	51.79	T	17%	Red	Yes	0.5	Essen	4Q (1)	391.5	5.595E-05	2 year
164	BVV1252	4521790	5721155.3	34.88	T	0	Essen	Yes	0.5	Essen	8Q (0.5)	743	5.595E-05	2 year
165	BVV1281	4520730	5720469.7	58.10	T	0	Essen	Yes	0.6667	Essen	4Q (1)	384	0.0006914	1 year
166	BVV1290	4520868	5720443	76.10	T	100%	Red	No	0.3333	Essen	4Q (1)	333	4.963E-05	3 year
167	BVV1291	4520871	5720444	59.10	T	33%	Red	No	0.3333	Essen	4Q (1)	387	0.0003437	2 year
168	BVV1292	4520875	5720445	34.74	T	0	Essen	Yes	0.6667	Essen	8Q (0.5)	734	6.921E-05	2 year
169	BVV132	4520806	5721981	65.43	Q	33%	Red	Yes	1	Essen	4Q (1)	363	4.192E-05	3 year
170	BVV136	4520757	5722135.4	67.60	Q	20%	Red	No	0.3333	Essen	4Q (1)	350	0.0019959	1 year
171	BVV1371	4520505	5722018.9	55.68	T	29%	Red	No	0	Essen	4Q (1)	357	0.0070627	6 month
172	BVV144	4520100	5724131.4	68.66	Q	100%	Red	Yes	0.5	Essen	NA (NA)	NA	0.0064138	6 month
173	BVV220	4520388	5723431	71.59	Q	8%	Red	Yes	0.5	Essen	2Q (2)	140	0.0020872	1 year
174	BVV222	4521764	5721496	65.30	T	62%	Red	Yes	0.5	Essen	2Q (2)	215	0.0056576	6 month
175	BVV223	4521413	5721998	65.80	T	86%	Red	Yes	0.6667	Essen	2Q (2)	225	0.0077022	6 month
176	BVV2241	4520423	5723338.9	63.40	T	100%	Red	No	0.3333	Essen	1Q (4)	29	0.0077022	6 month
177	BVV232	4520223	5722517.3	72.19	Q	0	Essen	Yes	1	Essen	NA (NA)	NA	0.0120969	6 month
178	BVV240	4520749	5722357	69.70	Q	0	Essen	No	0.3333	Essen	4Q (1)	364	4.577E-05	3 year
179	BVV2401	4520750	5722354.4	59.70	T	0	Essen	Yes	0.5	Essen	3Q (1.3333)	279.5	5.671E-05	2 year
180	BVV246	4520596	5722898	64.79	Q	0	Essen	No	0	Essen	3Q (1.3333)	230.5	0.0070245	6 month
181	BVV248	4519566	5722112	75.40	T	0	Essen	No	0	Essen	2Q (2)	184	0.0137278	6 month
182	BVV254	4519514	5722099.4	52.10	T	0	Essen	Yes	0.5	Essen	2Q (2)	179.5	0.0104524	6 month
183	BVV264	4520554	5722294.9	66.10	Q	25%	Red	Yes	0.6667	Essen	NA (NA)	NA	0.0104524	6 month
184	BVV265	4520460	5722467	66.10	T	25%	Red	Yes	1	Essen	NA (NA)	NA	4.902E-05	3 year

185	BVV266	4520701	5722514.8	68.00	Q	0	Essen	Yes	0.5	Essen	4Q (1)	359	1.781E-05	3 year
186	BVV2661	4520693	5722519	55.40	T	17%	Red	Yes	1	Essen	3Q (1.3333)	287	4.701E-05	3 year
187	BVV267	4519779	5721789	77.30	Q	0	Essen	Yes	0.5	Essen	NA (NA)	NA	2.332E-05	3 year
188	BVV283	4519144	5721646.8	61.44	T	0	Essen	Yes	0.5	Essen	8Q (0.5)	747	2.332E-05	3 year
189	BVV284	4519362	5721917.6	76.50	Q	0	Essen	Yes	0.5	Essen	3Q (1.3333)	252	0.0021579	1 year
190	BVV285	4519417	5721528	75.66	Q	0	Essen	Yes	0.5	Essen	3Q (1.3333)	253	0.0021579	1 year
191	BVV2851	4519417	5721528	63.80	T	0	Essen	Yes	0.5	Essen	NA (NA)	NA	0.0089538	6 month
192	BVV301	4519710	5725039	65.82	T	0	Essen	No	0	1st red	NA (NA)	NA	0.0089538	6 month
193	BVV3011	4519710	5725039	49.85	T	0	Essen	Yes	1	2nd red	NA (NA)	NA	0.0006308	1 year
194	BVV3020	4521715	5721880	67.95	Q	69%	Red	No	0	1st red	2Q (2)	223	0.0006308	1 year
195	BVV3022	4521717	5721870	34.40	T	50%	Red	No	0	2nd red	9Q (0.4444)	777	0.0006308	1 year
196	BVV3030	4521905	5721435	68.05	Q	31%	Red	No	0.3333	Essen	2Q (2)	218	0.0028582	1 year
197	BVV3031	4521902	5721434	55.20	T	0	Essen	No	0	Essen	4Q (1)	371	0.0028582	1 year
198	BVV3032	4521900	5721433	35.50	T	25%	Red	Yes	0.5	Essen	9Q (0.4444)	771	0.0014649	1 year
199	BVV3040	4521708	5720458	62.30	Q	19%	Red	No	0.3333	Essen	2Q (2)	215	0.0014649	1 year
200	BVV3042	4521710	5720465	34.10	T	75%	Red	No	0.3333	Essen	NA (NA)	NA	0.0014649	1 year
201	BVV3050	4522352	5720322	70.05	T	43%	Red	Yes	0.5	Essen	1Q (4)	90	0.0005774	1 year
202	BVV3051	4522350	5720326	47.20	T	44%	Red	Yes	1	Essen	4Q (1)	333	0.0005774	1 year
203	BVV3052	4522348	5720331	31.20	T	40%	Red	No	0	Essen	8Q (0.5)	749	0.0005774	1 year
204	BVV3060	4522737	5721060.4	68.30	Q	40%	Red	Yes	0.5	Essen	3Q (1.3333)	242	0.0005774	1 year
205	BVV3061	4522739	5721056.5	49.70	T	25%	Red	Yes	0.5	Essen	NA (NA)	NA	0.0006367	1 year
206	BVV3062	4522741	5721052.9	33.20	T	40%	Red	Yes	0.5	Essen	8Q (0.5)	756	0.0006367	1 year
207	BVV3063	4522743	5721050.4	49.71	T	43%	Red	No	0	Essen	3Q (1.3333)	289.5	0.0006367	1 year
208	BVV3070	4522989	5720605	61.25	Q	64%	Red	Yes	0.5	Essen	3Q (1.3333)	277.5	0.0006367	1 year
209	BVV3071	4522987	5720601	50.00	T	25%	Red	Yes	0.5	Essen	NA (NA)	NA	0.0016002	1 year
210	BVV3072	4522984	5720597	31.90	T	0	Essen	No	0.3333	Essen	8Q (0.5)	757	0.001475	1 year

211	BVV3073	4522990	5720605.3	45.53	T	29%	Red	No	0	Essen	3Q (1.3333)	276.5	0.0012421	1 year
212	BVV308	4520543	5723289.9	63.18	Q	33%	Red	Yes	0.5	Essen	2Q (2)	212	0.0020181	1 year
213	BVV309	4520661	5723158.9	56.60	Q	100%	Red	No	0	Essen	2Q (2)	210	0.0020181	1 year
214	BVV310	4520828	5723404.5	63.66	Q	100%	Red	Yes	0.5	Essen	3Q (1.3333)	293.5	0.0001912	2 year
215	BVV311	4521131	5723614.8	67.45	Q	0	Essen	Yes	0.5	Essen	4Q (1)	374	4.196E-05	3 year
216	BVV317	4520177	5724749.5	67.45	Q	0	Essen	Yes	1	Essen	NA (NA)	NA	7.284E-05	2 year
217	BVV331	4519305	5724906	72.08	Q	25%	Red	Yes	1	Essen	5Q (0.8)	434	1.195E-05	3 year
218	BVV350	4519925	5725018	71.47	Q	0	Essen	Yes	1	Essen	NA (NA)	NA	6.802E-05	2 year
219	BVV362	4519922	5724107	65.30	Q	100%	Red	Yes	0.5	Essen	NA (NA)	NA	6.406E-05	2 year
220	BVV371	4519642	5724251.4	33.78	T	0	Essen	No	0	Essen	2Q (2)	179	6.406E-05	2 year
221	BVV376	4519812	5723492	55.85	T	0	Essen	Yes	0.5	Essen	2Q (2)	178.5	6.406E-05	2 year
222	BVV3800	4519643	5722453.6	77.65	Q	0	Essen	Yes	1	Essen	NA (NA)	NA	0.0002923	2 year
223	BVV3801	4519637	5722452.5	52.65	T	0	Essen	No	0	Essen	8Q (0.5)	742	4.598E-05	3 year
224	BVV3802	4519631	5722451	44.55	T	50%	Red	No	0	Essen	NA (NA)	NA	4.598E-05	3 year
225	BVV3810	4520017	5721274.1	73.68	Q	0	Essen	Yes	0.6667	Essen	NA (NA)	NA	4.175E-05	3 year
226	BVV3821	4520457	5721250.4	57.53	T	75%	Red	Yes	0.6667	Essen	4Q (1)	390	4.175E-05	3 year
227	BVV3822	4520453	5721248.9	40.53	T	0	Essen	Yes	0.6667	Essen	8Q (0.5)	763	4.175E-05	3 year
228	BVV3830	4520429	5720752.3	75.19	Q	0	Essen	Yes	0.5	Essen	4Q (1)	378	0.0159995	6 month
229	BVV3831	4520430	5720748.3	59.42	T	0	Essen	Yes	0.5	Essen	NA (NA)	NA	0.0159995	6 month
230	BVV3832	4520428	5720755.8	38.63	T	0	Essen	Yes	1	Essen	8Q (0.5)	756	0.0159995	6 month
231	BVV3840	4520212	5722700.2	67.62	T	80%	Red	Yes	0.5	Essen	4Q (1)	386	4.836E-05	3 year
232	BVV3841	4520210	5722707.1	57.62	T	33%	Red	No	0	Essen	NA (NA)	NA	0.1991753	3 month
233	BVV3842	4520208	5722713.7	46.52	T	25%	Red	No	0	Essen	6Q (0.6667)	574.5	0.1991753	3 month
234	BVV385	4520024	5722464.4	48.22	T	0	Essen	Yes	1	Essen	5Q (0.8)	487	0.2355488	3 month
235	BVV402	4521187	5725549	66.80	Q	0	Essen	Yes	0.5	Essen	3Q (1.3333)	266	0.2355488	3 month
236	BVV4021	4521187	5725549	51.30	T	0	Essen	Yes	0.5	Essen	4Q (1)	367	0.0023971	1 year
237	BVV403	4521402	5725119	64.90	Q	0	Essen	Yes	0.5	1st red	3Q (1.3333)	286	0.0023971	1 year

238	BVV4031	4521402	5725119	51.80	T	0	Essen	No	0	2nd red	4Q (1)	379.5	0.0808632	3 month
239	BVV404	4521142	5724426	68.30	Q	0	Essen	Yes	0.5	1st red	3Q (1.3333)	302	0.0808632	3 month
240	BVV4041	4521142	5724426	59.20	T	0	Essen	Yes	0.5	2nd red	4Q (1)	365	0.2939127	3 month
241	BVV405	4521537	5723309	67.60	Q	100%	Red	Yes	0.5	1st red	2Q (2)	221	0.4171282	3 month
242	BVV4051	4521537	5723309	61.40	T	0	Essen	Yes	0.5	2nd red	4Q (1)	380.5	0.0001472	2 year
243	BVV406	4520106	5726791	65.30	Q	0	Essen	No	0.3333	1st red	5Q (0.8)	428	0.2686783	3 month
244	BVV419	4520047	5727609.4	66.66	Q	100%	Red	Yes	0.6667	2nd red	NA (NA)	NA	0.2686783	3 month
245	BVV429	4520810	5724188.9	45.95	T	67%	Red	Yes	0.5	Essen	NA (NA)	NA	0.4439258	3 month
246	BVV432	4520982	5725782	64.80	Q	100%	Red	No	0	Essen	3Q (1.3333)	287	0.4439258	3 month
247	BVV4321	4520982	5725782	54.60	T	0	Essen	Yes	0.5	Essen	4Q (1)	363	4.483E-05	3 year
248	BVV434	4521668	5726587	64.40	Q	0	Essen	Yes	0.5	1st red	2Q (2)	142	4.483E-05	3 year
249	BVV4381	4520918	5726808	61.70	Q	0	Essen	Yes	0.5	2nd red	5Q (0.8)	449	4.715E-05	3 year
250	BVV439	4520706	5724281	68.60	Q	8%	Red	Yes	0.6667	Essen	1Q (4)	125	4.295E-05	3 year
251	BVV4391	4520705	5724283	44.41	T	33%	Red	Yes	0.5	Essen	NA (NA)	NA	4.295E-05	3 year
252	BVV440	4520519	5724565	68.60	Q	29%	Red	Yes	0.6667	Essen	3Q (1.3333)	271	4.84E-05	3 year
253	BVV441	4520401	5724706	68.05	Q	42%	Red	Yes	0.5	Essen	1Q (4)	123	4.84E-05	3 year
254	BVV4411	4520400	5724708	40.95	T	33%	Red	No	0	Essen	NA (NA)	NA	0.0120915	6 month
255	BVV442	4520111	5725040	67.94	T	8%	Red	No	0	Essen	3Q (1.3333)	294	0.0135958	6 month
256	BVV4421	4520110	5725041	40.20	T	0	Essen	No	0.3333	Essen	NA (NA)	NA	0.0002634	2 year
257	BVV443	4519938	5725304	68.49	Q	36%	Red	Yes	0.5	Essen	3Q (1.3333)	271	5.759E-05	2 year
258	BVV444	4520088	5725440	68.46	Q	29%	Red	Yes	0.6667	Essen	3Q (1.3333)	271	5.759E-05	2 year
259	BVV445	4520254	5725592	68.53	Q	30%	Red	Yes	0.6667	Essen	3Q (1.3333)	294	4.99E-05	3 year
260	BVV446	4520356	5725659	68.59	Q	60%	Red	Yes	0.6667	Essen	3Q (1.3333)	285.5	6.077E-05	2 year
261	BVV4461	4520357	5725655	48.04	T	29%	Red	Yes	0.5	Essen	3Q (1.3333)	300.5	0.0197633	6 month
262	BVV447	4520412	5725631	68.46	Q	33%	Red	No	0	Essen	2Q (2)	217	0.0197633	6 month
263	BVV4471	4520414	5725630	42.46	T	25%	Red	Yes	0.5	Essen	8Q (0.5)	755	0.0197633	6 month

264	BVV448	4520563	5725462	68.17	Q	22%	Red	Yes	0.5	Essen	1Q (4)	114	0.0001607	2 year
265	BVV4480	4520575	5725467	63.24	Q	67%	Red	Yes	0.5	Essen	3Q (1.3333)	310.5	0.0001235	2 year
266	BVV4481	4520573	5725469.8	43.04	T	50%	Red	Yes	0.5	Essen	4Q (1)	395	0.0001235	2 year
267	BVV4540	4519560	5724811	57.71	Q	50%	Red	No	0	Essen	5Q (0.8)	433	0.0001235	2 year
268	BVV4560	4519664	5724651.1	57.88	T	33%	Red	No	0	Essen	4Q (1)	371	9.078E-05	2 year
269	BVV4561	4519662	5724649.1	37.88	T	25%	Red	Yes	0.5	Essen	9Q (0.4444)	791	1.633E-05	3 year
270	BVV4562	4519664	5724648.3	35.77	T	0	Essen	No	0.3333	Essen	NA (NA)	NA	3.514E-05	3 year
271	BVV457	4519762	5724551.2	63.03	Q	11%	Red	Yes	0.5	Essen	3Q (1.3333)	298.5	3.514E-05	3 year
272	BVV458	4519581	5724352.4	62.95	Q	14%	Red	Yes	0.6667	Essen	3Q (1.3333)	279.5	3.514E-05	3 year
273	BVV4590	4519914	5724376.3	63.91	Q	0	Essen	Yes	0.5	Essen	NA (NA)	NA	4.586E-05	3 year
274	BVV4591	4519917	5724372.5	49.91	T	29%	Red	No	0	Essen	3Q (1.3333)	276.5	4.586E-05	3 year
275	BVV4592	4519911	5724380	39.91	T	50%	Red	No	0	Essen	4Q (1)	384.5	4.586E-05	3 year
276	BVV4600	4519886	5724198	65.74	Q	17%	Red	No	0.3333	Essen	3Q (1.3333)	279.5	6.779E-05	2 year
277	BVV4601	4519893	5724194	60.74	T	17%	Red	Yes	0.5	Essen	3Q (1.3333)	280.5	6.779E-05	2 year
278	BVV4602	4519894	5724189	40.77	T	20%	Red	No	0.3333	Essen	4Q (1)	362	6.779E-05	2 year
279	BVV4610	4519939	5724035	67.69	Q	17%	Red	Yes	0.5	Essen	3Q (1.3333)	282.5	6.814E-05	2 year
280	BVV4611	4519942	5724039	65.74	Q	20%	Red	No	0	Essen	5Q (0.8)	456	6.814E-05	2 year
281	BVV4612	4519938	5724042	40.86	T	40%	Red	No	0	Essen	4Q (1)	388	6.814E-05	2 year
282	BVV4620	4519955	5723801	64.26	T	0	Essen	No	0	Essen	4Q (1)	368.5	0.0323072	6 month
283	BVV4621	4519951	5723805	42.31	T	25%	Red	No	0	Essen	9Q (0.4444)	775	0.0323072	6 month
284	BVV4622	4519947	5723810	33.20	T	33%	Red	Yes	0.5	Essen	NA (NA)	NA	0.0323072	6 month
285	BVV4640	4521107	5723182.2	65.86	Q	25%	Red	Yes	0.5	Essen	3Q (1.3333)	287	0.0062422	6 month
286	BVV4641	4521107	5723185.3	60.72	T	60%	Red	Yes	0.5	Essen	4Q (1)	365	0.0062422	6 month
287	BVV4642	4521109	5723189.2	49.57	T	67%	Red	No	0	Essen	8Q (0.5)	763	0.0157127	6 month
288	BVV4650	4520664	5723033.6	66.56	Q	46%	Red	Yes	0.5	Essen	2Q (2)	179	0.0157127	6 month
289	BVV4652	4520652	5723035.6	36.43	T	67%	Red	No	0	Essen	8Q (0.5)	738	0.0157127	6 month

290	BVV4660	4520182	5723397.9	68.30	Q	17%	Red	Yes	0.5	Essen	4Q (1)	392	0.0004426	2 year
291	BVV4661	4520184	5723400.8	55.28	T	33%	Red	No	0	Essen	4Q (1)	396	0.0002784	2 year
292	BVV4662	4520187	5723404.1	35.30	T	50%	Red	Yes	0.5	Essen	8Q (0.5)	756	0.0002672	2 year
293	BVV4671	4519890	5725069	53.84	T	25%	Red	Yes	0.5	Essen	3Q (1.3333)	303	0.0002672	2 year
294	BVV4672	4519886	5725073.6	36.84	T	0	Essen	No	0	Essen	8Q (0.5)	752	0.0002672	2 year
295	BVV4680	4519860	5726006.2	63.92	Q	67%	Red	Yes	0.6667	Essen	3Q (1.3333)	281	0.2571562	3 month
296	BVV4681	4519864	5726006.1	51.66	T	33%	Red	Yes	0.5	Essen	3Q (1.3333)	279	0.0090602	6 month
297	BVV4682	4519867	5726006.1	29.59	T	25%	Red	No	0	Essen	8Q (0.5)	749	0.1261757	3 month
298	BVV4700	4520437	5726653.8	65.40	Q	56%	Red	No	0	Essen	3Q (1.3333)	308.5	0.1261757	3 month
299	BVV471	4520041	5725698.6	67.80	Q	33%	Red	Yes	0.5	Essen	3Q (1.3333)	297.5	0.1261757	3 month
300	BVV472	4520407	5726166.7	66.19	Q	89%	Red	Yes	0.5	Essen	3Q (1.3333)	304.5	0.0144387	6 month
301	BVV4721	4520410	5726168.8	43.89	T	71%	Red	Yes	0.5	Essen	3Q (1.3333)	294.5	0.2744587	3 month
302	BVV4722	4520397	5726165.4	33.91	T	40%	Red	Yes	0.5	Essen	5Q (0.8)	453.5	0.0134557	6 month
303	BVV473	4519981	5726573.8	64.25	Q	0	Essen	Yes	0.6667	Essen	4Q (1)	392	0.0107154	6 month
304	BVV474	4520731	5726942.9	67.02	Q	50%	Red	Yes	1	Essen	4Q (1)	391	0.0105917	6 month
305	BVV475	4520362	5722860.1	71.89	Q	31%	Red	Yes	0.6667	Essen	2Q (2)	221	0.0064363	6 month
306	BVV476	4520469	5722923.7	73.22	Q	55%	Red	No	0.3333	Essen	1Q (4)	124	0.0080751	6 month
307	BVV477	4520444	5722979.5	68.28	Q	17%	Red	No	0.3333	Essen	2Q (2)	209	0.0080751	6 month
308	BVV478	4520501	5723031.4	71.54	Q	42%	Red	No	0.3333	Essen	1Q (4)	122.5	0.0080751	6 month
309	BVV4790	4520537	5722957.6	71.41	Q	36%	Red	No	0.3333	Essen	1Q (4)	125.5	0.0002002	2 year
310	BVV4791	4520534	5722963.1	54.85	T	0	Essen	No	0	Essen	3Q (1.3333)	305.5	0.0002002	2 year
311	BVV4792	4520536	5722960.4	41.93	T	50%	Red	Yes	0.6667	Essen	8Q (0.5)	747	0.0428505	6 month
312	BVV480	4519533	5726049	65.70	Q	56%	Red	Yes	1	Essen	3Q (1.3333)	295	0.0428505	6 month
313	BVV4801	4519580	5725988.8	67.95	Q	0	Essen	No	0	Essen	2Q (2)	153	8.883E-06	3 year
314	BVV481	4520429	5725831.1	67.95	Q	27%	Red	No	0	Essen	3Q (1.3333)	295.5	0.0117625	6 month
315	BVV4811	4520432	5725831.7	67.95	Q	0	Essen	Yes	0.5	Essen	2Q (2)	159	0.0117625	6 month

316	BVV4920	4520596	5722835.8	66475.00	T	23%	Red	No	0	Essen	2Q (2)	209	0.0020872	1 year
317	BVV4921	4520598	5722831.2	58.40	T	22%	Red	No	0	Essen	3Q (1.3333)	307.5	0.0633846	3 month
318	BVV4922	4520600	5722827.2	44275.00	T	50%	Red	No	0.3333	Essen	8Q (0.5)	745	0.0038441	1 year
319	BVV497	4520424	5723364	57.79	T	100%	Red	Yes	0.6667	Essen	2Q (2)	135	0.0005605	1 year
320	BVV500	4523003	5722405.8	69.30	T	22%	Red	No	0	Essen	3Q (1.3333)	294.5	3.832E-05	3 year
321	BVV503	4522882	5721978	70.70	Q	56%	Red	Yes	0.5	Essen	3Q (1.3333)	282	3.832E-05	3 year
322	BVV507	4521986	5719978.9	72.27	Q	63%	Red	Yes	0.5	Essen	1Q (4)	129.5	0.0004323	2 year
323	BVV509	4522424	5721945.4	66.15	Q	22%	Red	Yes	0.5	Essen	3Q (1.3333)	296	0.0004323	2 year
324	BVV5090	4522425	5721947.6	70.40	Q	33%	Red	Yes	0.5	Essen	3Q (1.3333)	296	0.001844	1 year
325	BVV510	4522097	5722294.4	65.45	Q	22%	Red	Yes	0.6667	Essen	3Q (1.3333)	276.5	0.0016222	1 year
326	BVV5100	4522099	5722293.1	72.30	Q	11%	Red	Yes	0.5	Essen	3Q (1.3333)	279	0.0018395	1 year
327	BVV511	4520473	5723268	47.65	T	17%	Red	No	0	Essen	8Q (0.5)	758	0.0076203	6 month
328	BVV512	4520546	5723140	64.60	Q	21%	Red	Yes	0.5	Essen	2Q (2)	211	0.0018359	1 year
329	BVV513	4520654	5723100	58.39	Q	7%	Red	Yes	0.5	Essen	2Q (2)	211	0.0176828	6 month
330	BVV514	4520769	5723013	54.10	Q	0	Essen	Yes	0.5	Essen	4Q (1)	372	0.0002047	2 year
331	BVV515	4520880	5723001	68.43	Q	100%	Red	No	0.3333	Essen	2Q (2)	211	0.1120937	3 month
332	BVV516	4520464	5723825	69.81	Q	31%	Red	Yes	0.5	Essen	1Q (4)	134	0.1120937	3 month
333	BVV519	4520304	5724804	69.87	Q	21%	Red	Yes	0.5	Essen	3Q (1.3333)	267	0.0298194	6 month
334	BVV520	4523659	5722181.1	66.40	Q	25%	Red	Yes	0.5	Essen	4Q (1)	372	0.0298194	6 month
335	BVV5201	4523656	5722179.5	54.15	T	100%	Red	Yes	0.5	Essen	NA (NA)	NA	0.0369818	6 month
336	BVV521	4523427	5722540	67.20	Q	50%	Red	Yes	0.5	Essen	4Q (1)	371	0.0369818	6 month
337	BVV5211	4523426	5722536.6	55.20	T	0	Essen	Yes	0.5	Essen	NA (NA)	NA	0.0021246	1 year
338	BVV522	4523192	5723032	66.20	Q	50%	Red	No	0.3333	Essen	4Q (1)	378.5	0.0021246	1 year
339	BVV5221	4523193	5723029.3	54.20	T	67%	Red	Yes	0.6667	Essen	4Q (1)	375.5	0.0021246	1 year
340	BVV523	4523145	5721493.2	69075.00	Q	0	Essen	Yes	0.5	Essen	4Q (1)	346	0.0004604	2 year
341	BVV5231	4523146	5721492.1	63075.00	T	60%	Red	Yes	0.5	Essen	4Q (1)	346	0.0004604	2 year

342	BVV5232	4523148	5721490.8	36.05	T	50%	Red	Yes	0.5	Essen	8Q (0.5)	728	0.0004604	2 year
343	BVV524	4522739	5721362.9	67.75	Q	44%	Red	Yes	0.5	Essen	3Q (1.3333)	279	0.0003634	2 year
344	BVV5241	4522742	5721365.6	59.85	T	50%	Red	No	0	Essen	4Q (1)	348	0.0003634	2 year
345	BVV5242	4522746	5721368	38.80	T	75%	Red	No	0	Essen	8Q (0.5)	750	0.0003634	2 year
346	BVV525	4522387	5721491.1	68.30	Q	50%	Red	Yes	0.5	Essen	3Q (1.3333)	305	0.0007034	1 year
347	BVV5251	4522384	5721490.4	54.25	T	0	Essen	Yes	0.5	Essen	3Q (1.3333)	310.5	0.0007034	1 year
348	BVV5252	4522381	5721489.6	38875.00	T	50%	Red	Yes	1	Essen	8Q (0.5)	756	0.0007034	1 year
349	BVV526	4522298	5720676.2	67.60	T	45%	Red	No	0	Essen	3Q (1.3333)	294.5	0.0354492	6 month
350	BVV5261	4522297	5720675	59.50	T	33%	Red	Yes	0.6667	Essen	4Q (1)	351	0.0095335	6 month
351	BVV5262	4522296	5720673.5	39.05	T	38%	Red	Yes	0.5	Essen	8Q (0.5)	727	0.0095335	6 month
352	BVV533	4521422	5722394.5	58.50	T	33%	Red	Yes	0.6667	Essen	3Q (1.3333)	268.5	0.0089641	6 month
353	BVV534	4521580	5722288.5	68.18	Q	62%	Red	No	0.3333	Essen	2Q (2)	224	0.0080453	6 month
354	BVV5341	4521584	5722289.5	57.60	T	50%	Red	No	0.3333	Essen	3Q (1.3333)	280	0.0075227	6 month
355	BVV535	4521587	5722134.5	58.23	T	29%	Red	No	0	Essen	3Q (1.3333)	281.5	0.0049908	1 year
356	BVV536	4521678	5722020	68.04	Q	79%	Red	No	0	Essen	2Q (2)	222	0.0040546	1 year
357	BVV537	4521743	5721683.6	59.27	T	60%	Red	No	0.3333	Essen	3Q (1.3333)	277	0.0040546	1 year
358	BVV538	4521783	5721311.2	40.26	T	0	Essen	No	0	Essen	NA (NA)	NA	0.0040546	1 year
359	BVV5390	4521784	5720990.7	72.07	Q	82%	Red	Yes	0.6667	Essen	1Q (4)	126	0.0026234	1 year
360	BVV5391	4521782	5720993.8	69.00	Q	73%	Red	No	0.3333	Essen	1Q (4)	127.5	0.0063147	6 month
361	BVV5392	4521785	5720997.8	41.07	T	67%	Red	No	0.3333	Essen	NA (NA)	NA	0.0085934	6 month
362	BVV540	4521672	5720333	66.08	Q	40%	Red	Yes	0.6667	Essen	3Q (1.3333)	232	0.0020177	1 year
363	BVV541	4521487	5720209.5	61.30	Q	40%	Red	No	0.3333	Essen	2Q (2)	224	0.0081051	6 month
364	BVV542	4521328	5720203.5	53.11	T	60%	Red	Yes	0.5	Essen	NA (NA)	NA	0.0007244	1 year
365	BVV544	4521729	5720614	68.78	Q	21%	Red	No	0.3333	Essen	2Q (2)	222	0.0007244	1 year
366	BVV555	4521251	5722682	55.42	T	71%	Red	Yes	0.5	Essen	4Q (1)	364	0.0006864	1 year
367	BVV5560	4522049	5720088.1	73.10	Q	55%	Red	No	0	Essen	1Q (4)	129	0.0006864	1 year

368	BVV5561	4522048	5720087	68.85	Q	58%	Red	Yes	0.5	Essen	1Q (4)	129	0.0004473	2 year
369	BVV5570	4522004	5720047.3	73.25	Q	33%	Red	Yes	0.5	Essen	1Q (4)	127	0.000305	2 year
370	BVV5571	4522003	5720046.6	68.30	Q	83%	Red	Yes	0.5	Essen	1Q (4)	127	0.000305	2 year
371	BVV559	4517065	5727280.9	71.33	Q	67%	Red	Yes	0.5	Essen	3Q (1.3333)	279.5	0.000305	2 year
372	BVV561	4518375	5726172	68.83	Q	30%	Red	Yes	0.5	Essen	2Q (2)	162	2.129E-06	3 year
373	BVV5611	4518367	5726172.3	52.92	Q	50%	Red	Yes	0.5	Essen	3Q (1.3333)	280	2.129E-06	3 year
374	BVV5612	4518370	5726171.9	30.89	T	20%	Red	No	0	Essen	8Q (0.5)	721	2.129E-06	3 year
375	BVV562	4518327	5725722.3	73.29	T	40%	Red	Yes	0.5	Essen	2Q (2)	176	2.178E-05	3 year
376	BVV5621	4518328	5725719.8	53.29	T	17%	Red	Yes	0.5	Essen	4Q (1)	393	2.178E-05	3 year
377	BVV5622	4518330	5725722.2	34.49	T	40%	Red	Yes	0.5	Essen	5Q (0.8)	459	8.204E-05	2 year
378	BVV5631	4518763	5725665.2	50.20	T	71%	Red	No	0	Essen	3Q (1.3333)	256	0.0002382	2 year
379	BVV5632	4518767	5725662.2	40.30	T	40%	Red	Yes	0.5	Essen	5Q (0.8)	451	0.0002382	2 year
380	BVV564	4518988	5726241	66.89	Q	20%	Red	Yes	0.5	Essen	6Q (0.6667)	556.5	0.0004208	2 year
381	BVV5641	4518990	5726245.2	53.38	T	71%	Red	Yes	0.5	Essen	4Q (1)	393	0.0002903	2 year
382	BVV5642	4518989	5726243.2	30.86	T	40%	Red	Yes	0.5	Essen	8Q (0.5)	713	0.7607547	3 month
383	BVV565	4519703	5726744.6	64.45	Q	40%	Red	No	0	Essen	6Q (0.6667)	556.5	0.7607547	3 month
384	BVV566	4519824	5726381	68.78	Q	30%	Red	No	0	Essen	2Q (2)	162	0.3913913	3 month
385	BVV567	4520603	5727030.2	67.35	Q	33%	Red	No	0	Essen	4Q (1)	391	0.001664	1 year
386	BVV5671	4520595	5727003.1	58.64	Q	100%	Red	Yes	0.5	Essen	4Q (1)	391	0.0006152	1 year
387	BVV568	4520502	5727594.8	66.70	Q	0	Essen	Yes	0.5	Essen	4Q (1)	360	0.0006152	1 year
388	BVV571	4520439	5723451.3	72.98	Q	67%	Red	Yes	1	Essen	NA (NA)	NA	0.0005907	1 year
389	BVV588	4522168	5720429.6	72.19	Q	46%	Red	Yes	0.6667	Essen	2Q (2)	224	0.0005907	1 year
390	BVV5881	4522167	5720431.2	67645.00	Q	54%	Red	Yes	0.5	Essen	3Q (1.3333)	231	0.0007871	1 year
391	BVV589	4522210	5720539.4	72685.00	Q	69%	Red	Yes	0.5	Essen	2Q (2)	225	0.0007871	1 year
392	BVV5891	4522209	5720538.8	68.65	Q	92%	Red	Yes	0.5	Essen	2Q (2)	225	0.0009225	1 year
393	BVV590	4522301	5720484.8	73.37	Q	36%	Red	Yes	1	Essen	1Q (4)	131.5	0.0009225	1 year

394	BVV5901	4522299	5720490.8	67.46	T	85%	Red	Yes	0.5	Essen	2Q (2)	225	0.0007414	1 year
395	BVV591	4522363	5720497.7	72.58	Q	45%	Red	No	0	Essen	1Q (4)	90	0.0007414	1 year
396	BVV5911	4522365	5720496	67.49	Q	55%	Red	Yes	1	Essen	1Q (4)	90	0.0009936	1 year
397	BVV592	4522367	5720690.2	72.47	Q	42%	Red	Yes	0.5	Essen	3Q (1.3333)	286	0.0009936	1 year
398	BVV5921	4522370	5720692.4	67.49	T	67%	Red	Yes	0.5	Essen	3Q (1.3333)	286	0.000782	1 year
399	BVV593	4522496	5720617.8	73.86	Q	36%	Red	No	0	Essen	1Q (4)	91	0.000782	1 year
400	BVV5931	4522497	5720619.4	66.92	Q	64%	Red	Yes	0.6667	Essen	1Q (4)	89	0.0008416	1 year
401	BVV594	4522434	5720753.5	73.50	Q	42%	Red	Yes	0.5	Essen	3Q (1.3333)	245	0.0008416	1 year
402	BVV5941	4522435	5720754.8	67.48	T	58%	Red	Yes	0.5	Essen	3Q (1.3333)	245	0.0005796	1 year
403	BVV595	4522536	5720738.6	73.43	Q	9%	Red	No	0	Essen	1Q (4)	88	0.0005796	1 year
404	BVV5951	4522535	5720737.3	67.63	Q	73%	Red	Yes	0.5	Essen	1Q (4)	88	4.324E-05	3 year
405	BVV596	4522273	5721194.4	71.67	Q	0	Essen	Yes	0.5	Essen	3Q (1.3333)	280	4.324E-05	3 year
406	BVV5961	4522275	5721192.7	66.68	T	11%	Red	Yes	0.5	Essen	3Q (1.3333)	280	0.0005	2 year
407	BVV597	4522176	5722063.7	71.22	Q	11%	Red	No	0	Essen	3Q (1.3333)	270.5	0.0005	2 year
408	BVV5971	4522178	5722062.5	66.76	Q	56%	Red	Yes	0.5	Essen	3Q (1.3333)	270.5	0.0005	2 year
409	BVV598	4522617	5721264.9	73.45	Q	44%	Red	Yes	0.5	Essen	3Q (1.3333)	283	0.001434	1 year
410	BVV5981	4522615	5721265.9	68.42	T	44%	Red	No	0	Essen	3Q (1.3333)	283	0.0019198	1 year
411	BVV5982	4522613	5721267.2	51.39	T	60%	Red	Yes	0.5	Essen	3Q (1.3333)	271	0.0023293	1 year
412	BVV599	4522985	5721391.9	70.74	Q	67%	Red	No	0.3333	Essen	1Q (4)	94	0.0008285	1 year
413	BVV600	4523203	5721359.5	67.24	Q	100%	Red	Yes	0.5	Essen	4Q (1)	349	0.0008285	1 year
414	BVV601	4522899	5721711.8	68.00	Q	22%	Red	Yes	0.5	Essen	3Q (1.3333)	274.5	0.0008285	1 year
415	BVV6050	4521756	5720515.4	67.40	Q	17%	Red	Yes	1	Essen	2Q (2)	213	0.0010536	1 year
416	BVV6051	4521757	5720518.2	52.94	T	0	Essen	No	0	Essen	4Q (1)	384	0.0011196	1 year
417	BVV6052	4521758	5720520.8	34.98	T	0	Essen	Yes	0.6667	Essen	8Q (0.5)	747	0.004281	1 year
418	BVV606	4522585	5720592.1	66.84	Q	38%	Red	Yes	0.5	Essen	2Q (2)	217	0.004281	1 year

419	BVV607	4522556	5720560.7	66.23	Q	77%	Red	No	0	Essen	2Q (2)	224	0.004281	1 year
420	BVV6080	4521503	5720689.6	67.90	Q	38%	Red	No	0.3333	Essen	3Q (1.3333)	229	0.004281	1 year
421	BVV6081	4521512	5720693	61.87	Q	0	Essen	No	0.3333	Essen	1Q (4)	133	0.0006334	1 year
422	BVV6082	4521508	5720692	52.20	T	22%	Red	No	0.3333	Essen	3Q (1.3333)	308.5	0.0019343	1 year
423	BVV6083	4521505	5720690.4	37.47	T	75%	Red	Yes	0.6667	Essen	8Q (0.5)	736	0.0019343	1 year
424	BVV624	4522020	5719997.4	64.70	Q	82%	Red	Yes	0.5	Essen	1Q (4)	130	4.686E-05	3 year
425	BVV625	4522082	5719843.2	63.93	Q	73%	Red	No	0.3333	Essen	1Q (4)	133.5	4.686E-05	3 year
426	BVV626	4522164	5719748	64.94	Q	62%	Red	No	0	Essen	3Q (1.3333)	228	0.0028031	1 year
427	BVV627	4520926	5721853.5	64.10	Q	67%	Red	Yes	0.5	Essen	3Q (1.3333)	274.5	0.0028031	1 year
428	BVV6271	4520925	5721857.3	59.60	T	17%	Red	No	0	Essen	3Q (1.3333)	274.5	0.0047597	1 year
429	BVV628	4520991	5721692.6	65.50	Q	83%	Red	Yes	0.5	Essen	3Q (1.3333)	271.5	0.0047597	1 year
430	BVV6281	4520995	5721693.8	58.50	T	33%	Red	Yes	0.5	Essen	3Q (1.3333)	271.5	0.0043757	1 year
431	BVV629	4521053	5721432.3	64.70	Q	20%	Red	No	0	Essen	4Q (1)	389	5.171E-05	2 year
432	BVV6291	4521051	5721436.9	59.70	T	67%	Red	No	0	Essen	4Q (1)	389	7.671E-05	2 year
433	BVV630	4521089	5721209.6	60.90	Q	33%	Red	Yes	0.5	Essen	3Q (1.3333)	272	6.647E-05	2 year
434	BVV632	4517806	5725358.6	75.99	T	57%	Red	Yes	0.5	Essen	2Q (2)	176	2.964E-05	3 year
435	BVV633	4518160	5725455.1	75.83	T	71%	Red	Yes	0.5	Essen	3Q (1.3333)	290	0.0137278	6 month
436	BVV634	4518734	5724859.2	75.66	Q	43%	Red	Yes	0.5	Essen	3Q (1.3333)	290.5	0.0087427	6 month
437	BVV638	4521354	5719324.4	77.00	Q	29%	Red	Yes	0.5	Essen	4Q (1)	371	0.0091949	6 month
438	BVV640	4520490	5722434.1	73.06	Q	50%	Red	Yes	0.5	Essen	4Q (1)	377.5	0.0070245	6 month
439	BVV641	4520599	5722469	72.87	Q	0	Essen	No	0	Essen	NA (NA)	NA	0.0067934	6 month
440	BVV642	4520591	5722411.6	72.87	Q	0	Essen	Yes	0.5	Essen	NA (NA)	NA	6.059E-05	2 year
441	BVV643	4520556	5722294.6	73.00	Q	0	Essen	Yes	0.6667	Essen	NA (NA)	NA	0.0195495	6 month
442	BVV644	4520629	5722326.8	72.77	Q	50%	Red	No	0.3333	Essen	NA (NA)	NA	0.0060626	6 month
443	BVV645	4520505	5725545.8	63.40	Q	57%	Red	No	0	Essen	3Q (1.3333)	296	0.0060626	6 month

444	BVV6461	4520710	5725317.9	46.06	T	43%	Red	Yes	0.5	Essen	3Q (1.3333)	296.5	0.0048071	1 year
445	BVV6470	4520816	5725004.8	62.46	Q	43%	Red	Yes	0.5	Essen	3Q (1.3333)	307	0.0048071	1 year
446	BVV6471	4520815	5725009.6	50.93	T	43%	Red	Yes	0.5	Essen	3Q (1.3333)	291	0.0001373	2 year
447	BVV6480	4520839	5724876.1	63.25	Q	29%	Red	No	0.3333	Essen	3Q (1.3333)	286.5	0.0001373	2 year
448	BVV6481	4520839	5724872	53.74	T	29%	Red	Yes	0.5	Essen	3Q (1.3333)	274	0.0062695	6 month
449	BVV6490	4520861	5724623.7	65.06	Q	43%	Red	No	0	Essen	3Q (1.3333)	286	0.0062063	6 month
450	BVV6491	4520861	5724627.9	50.08	T	14%	Red	Yes	0.5	Essen	3Q (1.3333)	261	0.0060958	6 month
451	BVV651	4521333	5722153.7	61.91	T	0	Essen	Yes	0.5	Essen	3Q (1.3333)	275	0.0055585	6 month
452	BVV652	4521395	5722102.1	61.83	T	0	Essen	Yes	0.5	Essen	2Q (2)	223	0.0057955	6 month
453	BVV653	4521437	5721959.4	62.96	T	0	Essen	Yes	1	Essen	2Q (2)	195	0.0064832	6 month
454	BVV654	4521473	5721841.3	63.29	T	0	Essen	Yes	0.5	Essen	3Q (1.3333)	279	0.0054576	6 month
455	BVV655	4521516	5721695.3	63.45	T	100%	Red	No	0	Essen	3Q (1.3333)	278	0.0149697	6 month
456	BVV656	4521546	5721593.3	62.45	T	22%	Red	Yes	0.5	Essen	3Q (1.3333)	278	4.877E-05	3 year
457	BVV657	4521590	5721446.2	63.94	T	100%	Red	Yes	0.5	Essen	3Q (1.3333)	281.5	4.877E-05	3 year
458	BVV658	4520167	5723745.1	66.17	Q	33%	Red	No	0	Essen	5Q (0.8)	419	4.836E-05	3 year
459	BVV6590	4520180	5721689.6	75.14	Q	80%	Red	Yes	0.5	Essen	4Q (1)	377.5	4.836E-05	3 year
460	BVV6591	4520180	5721694.8	66.05	T	50%	Red	Yes	0.5	Essen	2Q (2)	212	0.0033438	1 year
461	BVV6600	4520023	5722467.8	73.85	Q	50%	Red	Yes	0.5	Essen	2Q (2)	168	0.0054046	6 month
462	BVV6601	4520023	5722470.7	66.68	T	88%	Red	No	0	Essen	2Q (2)	168	0.0052059	6 month
463	BVV661	4521622	5721315.8	66.91	T	0	Essen	Yes	0.5	Essen	1Q (4)	133.5	0.005057	1 year
464	BVV662	4521655	5721235.4	66.22	T	0	Essen	No	0	Essen	1Q (4)	132.5	0.0040546	1 year
465	BVV663	4521680	5721126.2	65.99	T	100%	Red	Yes	0.5	Essen	2Q (2)	145	0.0037662	1 year
466	BVV664	4521643	5721065.6	67.91	Q	100%	Red	No	0.3333	Essen	1Q (4)	132.5	0.0028582	1 year
467	BVV665	4521780	5721004.8	65.30	T	0	Essen	Yes	0.6667	Essen	2Q (2)	214	0.0053208	6 month
468	BVV666	4521715	5720749.4	66.04	T	0	Essen	No	0	Essen	2Q (2)	142	0.0041653	1 year

469	BVV667	4521697	5720485.3	65.75	Q	100%	Red	Yes	0.6667	Essen	1Q (4)	133	0.0080751	6 month
470	BVV668	4521465	5720508.7	67.37	Q	100%	Red	Yes	0.6667	Essen	3Q (1.3333)	228	0.0021583	1 year
471	BVV669	4521206	5721269.9	64.68	Q	60%	Red	Yes	0.5	Essen	2Q (2)	140	0.0071203	6 month
472	BVV678	4520577	5722949.7	71215.00	Q	0	Essen	Yes	0.6667	Essen	5Q (0.8)	410	0.0510505	3 month
473	BVV680	4520833	5724019	50.20	T	43%	Red	No	0.3333	Essen	2Q (2)	221	5.396E-05	2 year
474	BVV681	4520371	5723294.4	62.47	T	29%	Red	Yes	0.6667	Essen	3Q (1.3333)	304.5	5.396E-05	2 year
475	BVV684	4521392	5722845.1	67.34	Q	43%	Red	Yes	0.5	Essen	3Q (1.3333)	287	6.188E-05	2 year
476	BVV6850	4520108	5725253.1	65.90	Q	43%	Red	Yes	0.5	Essen	3Q (1.3333)	272	6.128E-05	2 year
477	BVV6851	4520106	5725255.4	47.87	T	14%	Red	Yes	0.5	Essen	2Q (2)	220.5	5.369E-05	2 year
478	BVV6860	4520326	5725265.9	66.55	Q	43%	Red	Yes	1	Essen	3Q (1.3333)	272	5.369E-05	2 year
479	BVV6861	4520328	5725263.6	48.53	T	50%	Red	No	0	Essen	3Q (1.3333)	277.5	5.417E-05	2 year
480	BVV6870	4520602	5724956.6	69.04	Q	29%	Red	Yes	1	Essen	3Q (1.3333)	272	5.417E-05	2 year
481	BVV6871	4520600	5724958.7	49.05	T	29%	Red	Yes	0.5	Essen	3Q (1.3333)	272	4.148E-05	3 year
482	BVV6880	4520492	5724822.4	65.46	Q	14%	Red	Yes	0.5	Essen	3Q (1.3333)	286	4.148E-05	3 year
483	BVV6881	4520494	5724820.2	49.61	T	29%	Red	No	0.3333	Essen	3Q (1.3333)	286	7.754E-05	2 year
484	BVV689	4520369	5724427.9	70.16	Q	40%	Red	No	0.3333	Essen	3Q (1.3333)	298	7.754E-05	2 year
485	BVV690	4520372	5724430.1	65.55	Q	40%	Red	Yes	0.6667	Essen	3Q (1.3333)	291.5	0.0071203	6 month
486	BVV691	4519713	5724459.6	71.78	Q	50%	Red	Yes	0.6667	Essen	3Q (1.3333)	294.5	0.0001424	2 year
487	BVV692	4519705	5724467.3	66.86	Q	33%	Red	Yes	0.5	Essen	3Q (1.3333)	300.5	5.687E-05	2 year
488	BVV693	4520366	5723302.6	72.02	Q	38%	Red	Yes	0.6667	Essen	2Q (2)	217	5.982E-05	2 year
489	BVV694	4520386	5724128.8	67.11	Q	60%	Red	Yes	0.5	Essen	3Q (1.3333)	301.5	8.253E-05	2 year
490	BVV695	4517723	5725168.6	75.85	T	20%	Red	No	0	Essen	3Q (1.3333)	299	0.0001196	2 year
491	BVV697	4519806	5724027.6	71.59	Q	60%	Red	Yes	0.5	Essen	3Q (1.3333)	293.5	7.358E-05	2 year
492	BVV6971	4519810	5724020.9	60.60	Q	25%	Red	Yes	0.5	Essen	3Q (1.3333)	294	0.0016883	1 year

493	BVV705	4520338	5721398.1	74.48	Q	0	Essen	No	0	Essen	NA (NA)	NA	0.0016222	1 year
494	BVV707	4520508	5721511.8	69.44	Q	100%	Red	No	0	Essen	4Q (1)	335	0.0016222	1 year
495	BVV709	4520482	5723215	67.90	Q	33%	Red	Yes	0.5	Essen	2Q (2)	225	0.0016181	1 year
496	BVV710	4520510	5723180	64725.00	Q	0	Essen	Yes	0.5	Essen	2Q (2)	190.5	0.011689	6 month
497	BVV7101	4520507	5723178	57825.00	T	33%	Red	Yes	0.6667	Essen	2Q (2)	182	0.011689	6 month
498	BVV711	4520584	5723101	62.70	Q	50%	Red	Yes	0.5	Essen	2Q (2)	223	0.0134648	6 month
499	BVV712	4520696	5722695.8	61.30	Q	50%	Red	Yes	0.5	Essen	3Q (1.3333)	293.5	0.0134648	6 month
500	BVV7121	4520695	5722700.5	57.40	T	0	Essen	No	0	Essen	3Q (1.3333)	293.5	0.0137006	6 month
501	BVV713	4520867	5722753	64.00	T	0	Essen	Yes	0.5	Essen	2Q (2)	216	0.0137006	6 month
502	BVV7131	4520872	5722754.3	57.00	T	25%	Red	No	0	Essen	3Q (1.3333)	278.5	0.0137006	6 month
503	BVV714	4520937	5722856	67.30	Q	25%	Red	No	0.3333	Essen	3Q (1.3333)	286	0.0117615	6 month
504	BVV7141	4520937	5722858.9	62.30	T	50%	Red	Yes	1	Essen	3Q (1.3333)	286	0.0117615	6 month
505	BVV7142	4520936	5722861.6	54.30	T	50%	Red	Yes	0.5	Essen	3Q (1.3333)	286	0.0077397	6 month
506	BVV7151	4520846	5722565	60.70	Q	25%	Red	Yes	0.5	Essen	3Q (1.3333)	281	0.0037715	1 year
507	BVV7152	4520847	5722560.2	55.70	T	0	Essen	Yes	0.5	Essen	3Q (1.3333)	281	0.0013721	1 year
508	BVV716	4520968	5722281.5	52.80	Q	75%	Red	Yes	0.5	Essen	4Q (1)	367.5	0.0089309	6 month
509	BVV717	4520743	5722199.6	58.80	T	25%	Red	Yes	0.6667	Essen	2Q (2)	225	0.0093022	6 month
510	BVV718	4520822	5721659.1	60.30	Q	50%	Red	No	0.3333	Essen	3Q (1.3333)	276	0.0038072	1 year
511	BVV719	4521124	5722667.1	66.20	Q	25%	Red	No	0	Essen	3Q (1.3333)	286.5	0.0038072	1 year
512	BVV720	4521180	5722385.9	66.60	Q	25%	Red	No	0	Essen	3Q (1.3333)	283	4.963E-05	3 year
513	BVV721	4521012	5722162.2	61.30	Q	25%	Red	No	0	Essen	3Q (1.3333)	278.5	4.734E-05	3 year
514	BVV7211	4521014	5722162.1	53.30	Q	25%	Red	No	0	Essen	3Q (1.3333)	278.5	7.065E-05	2 year
515	BVV722	4520761	5721983.7	55.40	T	50%	Red	Yes	0.5	Essen	4Q (1)	366.5	7.065E-05	2 year
516	BVV723	4520728	5721891.2	59.60	T	25%	Red	Yes	0.5	Essen	4Q (1)	364	0.0030813	1 year
517	BVV724	4519746	5724118.6	71.60	Q	100%	Red	Yes	0.5	Essen	3Q (1.3333)	298.5	0.0078698	6 month

518	BVV7241	4519748	5724116.7	63.60	T	50%	Red	Yes	0.5	Essen	3Q (1.3333)	299	6.801E-05	2 year
519	BVV725	4520860	5720583.5	57.70	T	0	Essen	Yes	0.6667	Essen	6Q (0.6667)	552	0.0054572	6 month
520	BVV726	4520777	5720740.7	57.70	T	0	Essen	No	0.3333	Essen	4Q (1)	388	5.554E-05	2 year
521	BVV729	4520427	5721712.7	57.60	T	50%	Red	Yes	0.5	Essen	5Q (0.8)	434.5	4.517E-05	3 year
522	BVV730	4521120	5720294.2	53.80	T	50%	Red	No	0.3333	Essen	6Q (0.6667)	548	4.524E-05	3 year
523	BVV731	4520523	5720317.7	53.70	T	50%	Red	Yes	0.5	Essen	5Q (0.8)	472	4.988E-05	3 year
524	BVV732	4520263	5720622.5	57.50	T	100%	Red	Yes	0.6667	Essen	6Q (0.6667)	540	0.0004208	2 year
525	BVV733	4520129	5720782.2	54.10	T	50%	Red	No	0.3333	Essen	5Q (0.8)	434.5	5.598E-05	2 year
526	BVV734	4520646	5721048.1	54.70	T	50%	Red	No	0.3333	Essen	4Q (1)	321	3.105E-05	3 year
527	BVV735	4519887	5721038.9	61.00	T	50%	Red	Yes	0.5	Essen	5Q (0.8)	444	4.396E-05	3 year
528	BVV736	4520545	5721309.5	57.00	T	0	Essen	Yes	0.5	Essen	NA (NA)	NA	5.439E-05	2 year
529	BVV737	4518928	5721656.4	58.00	T	50%	Red	Yes	1	Essen	5Q (0.8)	450	5.355E-05	2 year
530	BVV738	4519505	5721997.3	58.80	T	50%	Red	No	0	Essen	6Q (0.6667)	513	6.501E-05	2 year
531	BVV740	4519061	5722068.4	58.20	T	0	Essen	No	0	Essen	5Q (0.8)	450	4.804E-05	3 year
532	BVV742	4519416	5722370.7	59.20	T	100%	Red	No	0	Essen	6Q (0.6667)	511	4.947E-05	3 year
533	BVV743	4519763	5722982	58.00	T	100%	Red	No	0	Essen	5Q (0.8)	457.5	8.604E-05	2 year
534	BVV744	4519666	5723085.8	53.60	T	50%	Red	Yes	1	Essen	5Q (0.8)	457.5	0.0012966	1 year
535	BVV745	4519336	5723358	55.70	T	50%	Red	Yes	0.5	Essen	5Q (0.8)	449	0.0097233	6 month
536	BVV746	4519152	5723837.9	51.30	T	50%	Red	No	0	Essen	5Q (0.8)	449	0.000873	1 year
537	BVV747	4519144	5724368	51.60	T	50%	Red	Yes	0.5	Essen	5Q (0.8)	456	3.812E-05	3 year
538	BVV748	4521160	5720288.2	74.70	Q	50%	Red	No	0.3333	Essen	6Q (0.6667)	548	3.812E-05	3 year
539	BVV749	4520527	5722196.3	65.00	T	100%	Red	Yes	0.5	Essen	5Q (0.8)	437	3.812E-05	3 year
540	BVV750	4519831	5724305.9	71.86	Q	0	Essen	Yes	0.5	Essen	5Q (0.8)	421	3.812E-05	3 year
541	BVV7501	4519835	5724301.2	68.56	Q	50%	Red	No	0	Essen	5Q (0.8)	421	3.324E-05	3 year
542	BVV7502	4519843	5724291.9	53.22	T	0	Essen	Yes	0.5	Essen	5Q (0.8)	427	3.324E-05	3 year
543	BVV7503	4519839	5724296.5	40.15	T	0	Essen	Yes	0.5	Essen	5Q (0.8)	427	3.811E-05	3 year

544	BVV751	4519662	5724296.1	45.53	Q	0	Essen	Yes	0.5	Essen	5Q (0.8)	426	4.063E-05	3 year
545	BVV7511	4519657	5724300.1	37.54	T	0	Essen	Yes	0.5	Essen	5Q (0.8)	426	4.134E-05	3 year
546	BVV752	4519840	5724453.9	69.54	Q	0	Essen	Yes	1	Essen	5Q (0.8)	427	4.134E-05	3 year
547	BVV7522	4519838	5724456.1	39.58	T	50%	Red	Yes	1	Essen	5Q (0.8)	433	4.134E-05	3 year
548	BVV753	4519743	5724186.7	68.00	Q	0	Essen	No	0	Essen	5Q (0.8)	426.5	0.0001722	2 year
549	BVV7531	4519741	5724189.6	47.98	Q	0	Essen	Yes	0.5	Essen	5Q (0.8)	426.5	4.272E-05	3 year
550	BVV7532	4519740	5724192.6	39.93	T	50%	Red	Yes	0.5	Essen	5Q (0.8)	434	3.81E-05	3 year
551	BVV754	4520028	5720917.2	58.10	T	100%	Red	Yes	0.6667	Essen	3Q (1.3333)	238	8.417E-05	2 year
552	BVV755	4520314	5720960.4	57.20	T	0	Essen	No	0	Essen	3Q (1.3333)	287	0.0015359	1 year
553	BVV756	4520505	5721008.1	57.80	T	50%	Red	Yes	0.5	Essen	3Q (1.3333)	286.5	0.0017219	1 year
554	BVV757	4520165	5720910.9	55.30	T	50%	Red	Yes	0.5	Essen	3Q (1.3333)	243	0.0016002	1 year
555	BVV758	4520521	5723521	71.30	Q	50%	Red	No	0.3333	Essen	2Q (2)	180	0.0014785	1 year
556	BVV759	4520456	5723406.3	72.95	Q	100%	Red	Yes	0.6667	Essen	2Q (2)	181	0.0018359	1 year
557	BVV760	4520512	5723299	72.40	Q	50%	Red	No	0	Essen	2Q (2)	180	0.0018556	1 year
558	BVV761	4520595	5723189.8	72.60	Q	0	Essen	Yes	0.5	Essen	2Q (2)	180	0.0011585	1 year
559	BVV762	4520908	5723038.3	71.50	Q	100%	Red	Yes	0.5	Essen	2Q (2)	140	0.0012264	1 year
560	BVV763	4521082	5722993.7	71.40	Q	50%	Red	No	0	Essen	2Q (2)	180	0.0012679	1 year
561	BVV764	4520722	5723470.7	71.00	Q	50%	Red	Yes	0.5	Essen	2Q (2)	180	0.0009228	1 year
562	BVV765	4520925	5723253.4	71.40	Q	0	Essen	No	0	Essen	2Q (2)	180	0.0020181	1 year
563	BVV766	4520947	5723487.4	71.40	Q	0	Essen	Yes	0.5	Essen	2Q (2)	180	0.0020181	1 year
564	BVV767	4520878	5723806	71.50	Q	100%	Red	Yes	1	Essen	2Q (2)	181	0.0020181	1 year
565	BVV768	4521133	5723613.6	70.90	Q	0	Essen	Yes	0.5	Essen	2Q (2)	180	0.0020181	1 year
566	BVV771	4520440	5723443.4	70.90	Q	0	Essen	No	0	Essen	1Q (4)	48	0.0020181	1 year
567	BVV772	4520447	5723424.6	70.90	Q	0	Essen	Yes	1	Essen	1Q (4)	48	0.0020181	1 year
568	BVV773	4520452	5723415.2	70.90	Q	0	Essen	Yes	1	Essen	1Q (4)	48	0.0020181	1 year
569	BVV774	4520450	5723390.8	70.90	Q	0	Essen	No	0	Essen	1Q (4)	48	0.0020181	1 year
570	BVV775	4520444	5723403	70.90	Q	0	Essen	Yes	1	Essen	1Q (4)	48	0.0020181	1 year

571	BVV776	4520440	5723413.5	70.90	Q	0	Essen	Yes	1	Essen	1Q (4)	49	0.0020181	1 year
572	BVV777	4520430	5723435	70.90	Q	0	Essen	Yes	1	Essen	1Q (4)	44	0.0045993	1 year
573	BVV778	4520426	5723452.1	70.90	Q	0	Essen	Yes	1	Essen	1Q (4)	49	0.0045993	1 year
574	BVV779	4520426	5723460.1	70.90	Q	0	Essen	Yes	1	Essen	3Q (1.3333)	282.5	0.0040437	1 year
575	BVV7800	4521580	5720932.1	62.80	Q	0	Essen	No	0	Essen	NA (NA)	NA	0.0040437	1 year
576	BVV7801	4521583	5720933	57.80	T	0	Essen	Yes	0.5	Essen	NA (NA)	NA	0.0038975	1 year
577	BVV7810	4521622	5720821	64.10	Q	0	Essen	No	0	Essen	NA (NA)	NA	0.0038975	1 year
578	BVV7811	4521623	5720817.3	57.10	T	0	Essen	No	0.3333	Essen	NA (NA)	NA	0.0050897	1 year
579	BVV7820	4521772	5720916.7	63.70	T	0	Essen	Yes	1	Essen	NA (NA)	NA	0.0050897	1 year
580	BVV7821	4521772	5720913.8	53.70	T	0	Essen	Yes	0.6667	Essen	NA (NA)	NA	0.0050231	1 year
581	BVV7830	4521447	5720899.6	58.60	Q	0	Essen	No	0.3333	Essen	NA (NA)	NA	0.0050231	1 year
582	BVV7831	4521449	5720900.4	53.40	T	0	Essen	No	0	Essen	NA (NA)	NA	0.0045934	1 year
583	BVV7840	4521417	5720739.5	63.40	Q	0	Essen	Yes	0.5	Essen	NA (NA)	NA	0.0045934	1 year
584	BVV7841	4521416	5720743.9	54.40	T	0	Essen	Yes	0.6667	Essen	NA (NA)	NA	0.0037047	1 year
585	BVV7850	4521436	5720656.4	65.60	Q	0	Essen	Yes	0.6667	Essen	NA (NA)	NA	0.004281	1 year
586	BVV7851	4521437	5720653.1	53.60	T	0	Essen	Yes	0.6667	Essen	NA (NA)	NA	0.0038496	1 year
587	BVV786	4521756	5720853.8	67.90	T	0	Essen	No	0	Essen	NA (NA)	NA	4.359E-05	3 year
588	BVV787	4521514	5720796.4	60.80	Q	0	Essen	Yes	0.6667	Essen	NA (NA)	NA	4.359E-05	3 year
589	BVV788	4521559	5720644.8	60.10	Q	0	Essen	No	0.3333	Essen	NA (NA)	NA	4.359E-05	3 year
590	BVV7960	4520143	5721986.3	68.20	T	0	Essen	Yes	0.6667	Essen	NA (NA)	NA	4.444E-05	3 year
591	BVV7961	4520139	5721985.4	57.20	T	0	Essen	Yes	0.6667	Essen	NA (NA)	NA	4.444E-05	3 year
592	BVV7962	4520135	5721984.3	48.30	T	0	Essen	No	0.3333	Essen	NA (NA)	NA	4.444E-05	3 year
593	BVV7981	4520103	5722112.5	56.00	T	0	Essen	No	0	Essen	NA (NA)	NA	4.444E-05	3 year
594	BVV7982	4520106	5722116.1	43.00	T	0	Essen	No	0	Essen	NA (NA)	NA	4.444E-05	3 year
595	BVV801	4521251	5723014.9	43.00	T	0	Essen	Yes	0.5	Essen	2Q (2)	149	4.444E-05	3 year
596	BVV8011	4521254	5723015.5	43.00	T	0	Essen	Yes	0.5	Essen	2Q (2)	149	4.444E-05	3 year
597	BVV802	4521633	5723007.4	43.00	T	0	Essen	No	0	Essen	2Q (2)	152	4.444E-05	3 year

598	BVV8021	4521632	5723009.3	43.00	T	0	Essen	No	0	Essen	2Q (2)	152	4.444E-05	3 year
599	BVV803	4521923	5722937.2	43.00	T	0	Essen	Yes	1	Essen	2Q (2)	141	4.444E-05	3 year
600	BVV804	4522431	5722719.8	43.00	T	0	Essen	Yes	0.5	Essen	NA (NA)	NA	4.444E-05	3 year
601	BVV8041	4522432	5722724.3	43.00	T	0	Essen	No	0	Essen	NA (NA)	NA	4.444E-05	3 year
602	BVV805	4521122	5724399.2	43.00	T	0	Essen	Yes	0.5	Essen	2Q (2)	151	4.444E-05	3 year
603	BVV8051	4521120	5724397	43.00	T	0	Essen	Yes	0.5	Essen	2Q (2)	151	4.444E-05	3 year
604	BVV806	4521565	5724400.9	43.00	T	0	Essen	Yes	0.5	Essen	NA (NA)	NA	4.444E-05	3 year
605	BVV8061	4521566	5724403.6	43.00	T	0	Essen	Yes	0.5	Essen	NA (NA)	NA	4.444E-05	3 year
606	BVV807	4521744	5724256.9	43.00	T	0	Essen	Yes	0.5	Essen	NA (NA)	NA	4.444E-05	3 year
607	BVV8071	4521740	5724254.1	43.00	T	0	Essen	No	0	Essen	NA (NA)	NA	4.444E-05	3 year
608	BVV808	4522061	5723918.4	43.00	T	0	Essen	Yes	0.5	Essen	NA (NA)	NA	4.444E-05	3 year
609	BVV8081	4522059	5723921.4	43.00	T	0	Essen	Yes	0.5	Essen	NA (NA)	NA	4.444E-05	3 year
610	BVV809	4522295	5723795.7	43.00	T	0	Essen	No	0	Essen	NA (NA)	NA	4.444E-05	3 year
611	BVV8091	4522296	5723799.5	43.00	T	0	Essen	No	0	Essen	NA (NA)	NA	4.444E-05	3 year
612	BVV810	4522676	5723584.4	43.00	T	0	Essen	No	0	Essen	NA (NA)	NA	4.444E-05	3 year
613	BVV8101	4522676	5723581.9	43.00	T	0	Essen	Yes	0.5	Essen	NA (NA)	NA	4.444E-05	3 year
614	BVV8102	4522676	5723579.4	43.00	T	0	Essen	No	0	Essen	NA (NA)	NA	4.444E-05	3 year
615	BVV811	4520707	5725838.2	43.00	T	0	Essen	No	0	Essen	2Q (2)	146	4.444E-05	3 year
616	BVV8111	4520704	5725838.2	43.00	T	0	Essen	No	0	Essen	NA (NA)	NA	4.444E-05	3 year
617	BVV812	4520941	5725794.4	43.00	T	0	Essen	No	0	Essen	2Q (2)	153	4.444E-05	3 year
618	BVV8121	4520945	5725792.2	43.00	T	0	Essen	Yes	0.5	Essen	NA (NA)	NA	4.444E-05	3 year
619	BVV813	4521215	5725573.8	43.00	T	0	Essen	No	0	Essen	NA (NA)	NA	4.444E-05	3 year
620	BVV8131	4521213	5725576	43.00	T	0	Essen	Yes	1	Essen	NA (NA)	NA	4.444E-05	3 year
621	BVV8132	4521211	5725577.8	43.00	T	0	Essen	Yes	0.5	Essen	NA (NA)	NA	4.444E-05	3 year
622	BVV814	4521469	5725587.3	43.00	T	0	Essen	No	0	Essen	2Q (2)	153	4.444E-05	3 year
623	BVV8141	4521473	5725589.1	43.00	T	0	Essen	No	0	Essen	NA (NA)	NA	4.444E-05	3 year
624	BVV815	4521779	5725779.9	43.00	T	0	Essen	Yes	0.5	Essen	NA (NA)	NA	4.444E-05	3 year
625	BVV8151	4521777	5725776.6	43.00	T	0	Essen	Yes	0.5	Essen	NA (NA)	NA	4.444E-05	3 year

626	BVV816	4519855	5726011.4	43.00	T	0	Essen	Yes	0.5	Essen	2Q (2)	152	4.444E-05	3 year
627	BVV8161	4519857	5726013.7	43.00	T	0	Essen	No	0	Essen	2Q (2)	152	4.444E-05	3 year
628	BVV817	4520087	5726116.1	43.00	T	0	Essen	No	0	Essen	2Q (2)	146	4.444E-05	3 year
629	BVV8172	4520092	5726117.6	43.00	T	0	Essen	Yes	0.5	Essen	2Q (2)	146	4.444E-05	3 year
630	BVV819	4520768	5726338.2	43.00	T	0	Essen	Yes	1	Essen	NA (NA)	NA	4.444E-05	3 year
631	BVV8191	4520771	5726336.3	43.00	T	0	Essen	Yes	1	Essen	NA (NA)	NA	4.444E-05	3 year
632	BVV820	4521100	5726277.9	43.00	T	0	Essen	Yes	0.5	Essen	NA (NA)	NA	4.444E-05	3 year
633	BVV8201	4521099	5726280.7	43.00	T	0	Essen	No	0	Essen	NA (NA)	NA	4.444E-05	3 year
634	BVV821	4521646	5726211.2	43.00	T	0	Essen	Yes	0.5	Essen	NA (NA)	NA	4.444E-05	3 year
635	BVV8211	4521643	5726210.6	43.00	T	0	Essen	Yes	0.5	Essen	NA (NA)	NA	4.444E-05	3 year
636	BVV822	4522105	5726175.7	43.00	T	0	Essen	Yes	0.5	Essen	NA (NA)	NA	4.444E-05	3 year
637	BVV8221	4522102	5726177.1	43.00	T	0	Essen	Yes	0.5	Essen	NA (NA)	NA	4.444E-05	3 year
638	BVV824	4520136	5726597.5	43.00	T	0	Essen	Yes	0.5	Essen	2Q (2)	148	4.444E-05	3 year
639	BVV8241	4520136	5726594.9	43.00	T	0	Essen	Yes	0.5	Essen	2Q (2)	148	4.444E-05	3 year
640	BVV825	4520681	5726988.7	43.00	T	0	Essen	Yes	0.5	Essen	NA (NA)	NA	4.444E-05	3 year
641	BVV826	4520920	5726820.4	43.00	T	0	Essen	Yes	0.5	Essen	NA (NA)	NA	4.444E-05	3 year
642	BVV8261	4520922	5726816.8	43.00	T	0	Essen	No	0	Essen	NA (NA)	NA	4.444E-05	3 year
643	BVV827	4521526	5726873.5	43.00	T	0	Essen	No	0	Essen	NA (NA)	NA	4.444E-05	3 year
644	BVV8271	4521523	5726876.6	43.00	T	0	Essen	Yes	0.5	Essen	NA (NA)	NA	4.444E-05	3 year
645	BVV828	4521821	5726674.8	43.00	T	0	Essen	Yes	0.5	Essen	NA (NA)	NA	4.444E-05	3 year
646	BVV8281	4521820	5726678.4	43.00	T	0	Essen	Yes	0.5	Essen	NA (NA)	NA	4.444E-05	3 year
647	BVV830	4520289	5727525.6	43.00	T	0	Essen	Yes	0.5	Essen	2Q (2)	146	4.444E-05	3 year
648	BVV8301	4520293	5727523.9	43.00	T	0	Essen	Yes	0.5	Essen	2Q (2)	146	4.444E-05	3 year
649	BVV831	4521215	5727415.7	43.00	T	0	Essen	No	0	Essen	NA (NA)	NA	4.444E-05	3 year
650	BVV8311	4521215	5727418.5	43.00	T	0	Essen	No	0	Essen	NA (NA)	NA	4.444E-05	3 year
651	BVV836	4518635	5726372.7	43.00	T	0	Essen	No	0	Essen	NA (NA)	NA	4.444E-05	3 year
652	BVV8361	4518636	5726376	43.00	T	0	Essen	Yes	0.5	Essen	NA (NA)	NA	4.444E-05	3 year
653	BVV837	4518707	5726120.7	43.00	T	0	Essen	Yes	0.5	Essen	2Q (2)	154	4.444E-05	3 year

654	BVV838	4518219	5725954.5	43.00	T	0	Essen	Yes	0.5	Essen	NA (NA)	NA	4.444E-05	3 year
655	BVV839	4518763	5725661.7	43.00	T	0	Essen	Yes	0.5	Essen	NA (NA)	NA	0.0060121	6 month
656	BVV840	4519110	5725230	43.00	T	0	Essen	Yes	0.5	Essen	NA (NA)	NA	0.0060121	6 month
657	BVV8401	4519110	5725233	43.00	T	0	Essen	No	0	Essen	NA (NA)	NA	0.0058524	6 month
658	BVV8420	4521093	5720657.6	66.60	Q	0	Essen	Yes	0.5	Essen	NA (NA)	NA	0.0058524	6 month
659	BVV8421	4521092	5720660.7	57.70	T	100%	Red	Yes	0.5	Essen	NA (NA)	NA	0.0013501	1 year
660	BVV8430	4521227	5720754	66.40	Q	100%	Red	Yes	0.5	Essen	NA (NA)	NA	0.0017219	1 year
661	BVV8431	4521230	5720754.5	53.40	T	0	Essen	No	0	Essen	NA (NA)	NA	0.0017623	1 year
662	BVV851	4520692	5723199.3	72.86	Q	100%	Red	Yes	1	Essen	NA (NA)	NA	0.001453	1 year
663	BVV852	4520477	5723379.4	72.76	Q	100%	Red	Yes	1	Essen	NA (NA)	NA	0.001453	1 year
664	BVV853	4520393	5723499.8	72.90	Q	100%	Red	Yes	0.5	Essen	NA (NA)	NA	0.0012643	1 year
665	BVV854	4520534	5723488	72.72	Q	100%	Red	Yes	1	Essen	NA (NA)	NA	0.0017723	1 year
666	BVV855	4520585	5723514.8	72.63	Q	0	Essen	Yes	1	Essen	NA (NA)	NA	0.0017723	1 year
667	BVV856	4520687	5723509	72.64	Q	100%	Red	Yes	1	Essen	NA (NA)	NA	0.0017723	1 year
668	BVV857	4520646	5723693.5	71.93	Q	100%	Red	Yes	1	Essen	NA (NA)	NA	0.0017723	1 year
669	BVV8590	4519723	5724449.3	71.93	Q	0	Essen	Yes	0.5	Essen	NA (NA)	NA	0.0017723	1 year
670	BVV8591	4519728	5724444.7	71.93	Q	0	Essen	Yes	0.5	Essen	NA (NA)	NA	0.0017723	1 year
671	BVV860	4520014	5724257.5	71.93	Q	0	Essen	No	0	Essen	NA (NA)	NA	0.0017723	1 year
672	BVV861	4519764	5724548.3	71.93	Q	0	Essen	Yes	0.5	Essen	NA (NA)	NA	0.0017723	1 year
673	BVV862	4520112	5724332.6	71.93	Q	0	Essen	Yes	0.5	Essen	NA (NA)	NA	0.0017723	1 year
674	BVV8630	4520069	5724391.2	71.93	Q	0	Essen	Yes	0.5	Essen	NA (NA)	NA	0.0017723	1 year
675	BVV8631	4520072	5724390.9	71.93	Q	0	Essen	Yes	1	Essen	NA (NA)	NA	0.0017723	1 year
676	BVV8640	4519919	5724526.1	71.93	Q	0	Essen	Yes	0.5	Essen	NA (NA)	NA	0.0118134	6 month
677	BVV8641	4519920	5724524.2	71.93	Q	0	Essen	Yes	1	Essen	NA (NA)	NA	0.0118134	6 month
678	BVV8642	4519922	5724522.2	71.93	Q	0	Essen	Yes	0.5	Essen	NA (NA)	NA	0.0118134	6 month
679	BVV8643	4519923	5724520.3	71.93	Q	0	Essen	Yes	0.5	Essen	NA (NA)	NA	0.0118134	6 month
680	BVV8650	4520005	5724761.2	71.93	Q	0	Essen	Yes	0.5	Essen	NA (NA)	NA	0.0118134	6 month
681	BVV8651	4519996	5724771.4	71.93	Q	0	Essen	No	0	Essen	NA (NA)	NA	0.0118134	6 month

682	BVV8660	4519857	5724875.7	71.93	Q	0	Essen	Yes	0.5	Essen	NA (NA)	NA	0.0118134	6 month
683	BVV8661	4519856	5724883	71.93	Q	0	Essen	No	0	Essen	NA (NA)	NA	0.0118134	6 month
684	BVV8680	4520283	5724794.3	71.93	Q	0	Essen	Yes	0.5	Essen	NA (NA)	NA	0.0118134	6 month
685	BVV8681	4520288	5724798.4	71.93	Q	0	Essen	Yes	0.5	Essen	NA (NA)	NA	0.0118134	6 month
686	BVV8682	4520295	5724804.9	71.93	Q	0	Essen	No	0	Essen	NA (NA)	NA	0.0118134	6 month
687	BVV8690	4520002	5724965.4	71.93	Q	0	Essen	Yes	0.5	Essen	NA (NA)	NA	0.0118134	6 month
688	BVV8691	4519977	5724993.2	71.93	Q	0	Essen	Yes	0.5	Essen	NA (NA)	NA	0.0118134	6 month
689	BVV8692	4519997	5724970.4	71.93	Q	0	Essen	Yes	0.5	Essen	NA (NA)	NA	0.0118134	6 month
690	BVV8693	4519983	5724986.8	71.93	Q	0	Essen	Yes	0.5	Essen	NA (NA)	NA	0.0118134	6 month
691	BVV881	4519842	5722477.4	71.93	Q	0	Essen	Yes	0.5	Essen	NA (NA)	NA	0.0118134	6 month
692	BVV8811	4519847	5722478	71.93	Q	0	Essen	Yes	0.5	Essen	NA (NA)	NA	0.0118134	6 month
693	BVV8812	4519851	5722478.7	71.93	Q	0	Essen	No	0	Essen	NA (NA)	NA	0.0707235	3 month
694	BVV883	4520160	5721828.7	71.93	Q	0	Essen	Yes	0.5	Essen	NA (NA)	NA	0.0825761	3 month
695	BVV8831	4520161	5721821.8	71.93	Q	0	Essen	Yes	0.5	Essen	NA (NA)	NA	0.0555261	3 month
696	BVV8832	4520161	5721825.2	71.93	Q	0	Essen	Yes	0.5	Essen	NA (NA)	NA	0.0552013	3 month
697	GOI1010	4521938	5722927.4	66.10	Q	50%	Red	No	0.3333	Essen	4Q (1)	360	0.0006334	1 year
698	GOI1011	4522149	5722879.4	69.20	Q	50%	Red	No	0.3333	Essen	4Q (1)	360	0.0005072	2 year
699	GOI1013	4522050	5722641	70.90	Q	0	Essen	No	0.3333	Essen	4Q (1)	367	0.0005605	1 year
700	GOI1016	4521643	5722599.3	70.90	Q	0	Essen	No	0	Essen	NA (NA)	NA	0.0441299	6 month
701	GOI1040	4522100	5719830	50.28	T	0	Essen	Yes	0.5	Essen	3Q (1.3333)	309	0.0549457	3 month
702	GOI1041	4521945	5719855.7	49.14	T	0	Essen	Yes	1	Essen	NA (NA)	NA	0.0026408	1 year
703	GOI1042	4521958	5719974.2	50.14	T	0	Essen	No	0	Essen	NA (NA)	NA	0.0026408	1 year
704	GOI1090	4523242	5722507.1	72.24	Q	0	Essen	Yes	0.5	Essen	4Q (1)	323	0.1168649	3 month
705	GOI1091	4523116	5722442.8	72.33	Q	0	Essen	Yes	0.5	Essen	4Q (1)	323	0.0955241	3 month
706	GOI1092	4522799	5722124.3	73.85	Q	0	Essen	Yes	0.5	Essen	4Q (1)	323	0.0841413	3 month
707	GOI1094	4522872	5721941.7	71.96	Q	0	Essen	Yes	1	Essen	1Q (4)	84	0.0623146	3 month
708	GOI1096	4523874	5722020.4	71.96	Q	0	Essen	Yes	0.5	Essen	3Q (1.3333)	313	0.0623146	3 month

709	GOI1097	4523713	5721937.7	72.25	Q	0	Essen	No	0	Essen	3Q (1.3333)	313	0.0623146	3 month
710	GOI1098	4523620	5721838.1	73.60	Q	0	Essen	Yes	0.5	Essen	3Q (1.3333)	314	0.0623146	3 month
711	GOI1099	4523663	5721631.2	71.92	Q	0	Essen	Yes	0.5	Essen	3Q (1.3333)	309	0.0027296	1 year
712	GOI1101	4522763	5720521.6	71.92	Q	0	Essen	Yes	1	Essen	1Q (4)	86.5	0.0027296	1 year
713	GOI1102	4522765	5720517.1	71.92	Q	0	Essen	Yes	1	Essen	1Q (4)	84.5	0.0027296	1 year
714	GOI1103	4522675	5720332.2	71.92	Q	0	Essen	Yes	1	Essen	1Q (4)	92.5	0.0027296	1 year
715	GOI1104	4522678	5720333.6	71.92	Q	0	Essen	No	0	Essen	1Q (4)	92	0.0223837	6 month
716	GOI1105	4522632	5720696.1	71.92	Q	0	Essen	No	0	Essen	1Q (4)	86	0.0085492	6 month
717	GOI1108	4522358	5720325.8	71.92	Q	0	Essen	Yes	1	Essen	1Q (4)	84	0.0076047	6 month
718	GOI830	4522909	5720215.1	70.10	Q	100%	Red	Yes	0.6667	Essen	2Q (2)	218	0.0861748	3 month
719	GOI864	4523805	5721380.2	67.10	Q	0	Essen	No	0	Essen	4Q (1)	329	0.0369188	6 month
720	GOI865	4523594	5720981.9	70.20	Q	50%	Red	No	0.3333	Essen	4Q (1)	323	0.1208818	3 month
721	GOI866	4523617	5720759.9	68.90	Q	0	Essen	Yes	0.5	Essen	4Q (1)	330	0.0006629	1 year
722	GOI869	4522298	5723797.8	72.10	Q	67%	Red	Yes	0.5	Essen	4Q (1)	368	0.0009799	1 year
723	GOI870	4522818	5722398.3	64.80	Q	67%	Red	Yes	0.5	Essen	4Q (1)	378	0.1505581	3 month
724	GOI871	4523221	5721983.2	64.60	Q	33%	Red	Yes	0.5	Essen	4Q (1)	375	0.0045319	1 year
725	GOI875	4522273	5720992.6	68.10	T	100%	Red	Yes	1	Essen	3Q (1.3333)	271.5	0.0045319	1 year
726	GOI876	4522629	5720690.4	66.20	Q	100%	Red	Yes	1	Essen	1Q (4)	88	0.0045319	1 year
727	GOI878	4524040	5722961.7	68.10	Q	0	Essen	Yes	0.6667	Essen	2Q (2)	223	0.0045319	1 year
728	GOI898	4522928	5720231	31.20	T	60%	Red	Yes	0.5	Essen	NA (NA)	NA	0.0045319	1 year
729	KRB26-1	4519988	5725084.2	73.10	Q	0	Essen	Yes	1	1st red	NA (NA)	NA	0.0045319	1 year
730	KRB26-2	4519988	5725084.2	73.10	Q	0	Essen	Yes	1	2nd red	NA (NA)	NA	0.0045319	1 year
731	KRB30-1	4519935	5725220.3	73.10	Q	0	Essen	Yes	1	1st red	NA (NA)	NA	0.0045319	1 year
732	KRB30-2	4519935	5725220.3	73.10	Q	0	Essen	Yes	1	2nd red	NA (NA)	NA	0.0045319	1 year
733	KRB31-1	4519891	5725254.3	73.10	Q	0	Essen	Yes	1	1st red	NA (NA)	NA	0.0001774	2 year
734	KRB31-2	4519891	5725254.3	73.10	Q	0	Essen	Yes	1	2nd red	NA (NA)	NA	0.0001774	2 year
735	KRB33-1	4519801	5725126.9	73.10	Q	0	Essen	Yes	1	1st red	NA (NA)	NA	0.0001774	2 year

736	KRB33-2	4519801	5725126.9	73.10	Q	0	Essen	Yes	1	2nd red	NA (NA)	NA	0.0001774	2 year
737	KRB35-1	4519743	5725080.1	73.10	Q	0	Essen	Yes	1	1st red	NA (NA)	NA	0.0001774	2 year
738	KRB35-2	4519743	5725080.1	73.10	Q	0	Essen	Yes	1	2nd red	NA (NA)	NA	0.0001774	2 year
739	KRB37-1	4519668	5724979.4	73.10	Q	0	Essen	Yes	1	1st red	NA (NA)	NA	0.0001774	2 year
740	KRB37-2	4519668	5724979.4	73.10	Q	0	Essen	Yes	1	2nd red	NA (NA)	NA	0.0001774	2 year
741	KRB39-1	4519612	5724927.3	73.10	Q	0	Essen	Yes	1	Essen	NA (NA)	NA	0.122707	3 month
742	KRB39-2	4519612	5724927.3	73.10	Q	0	Essen	No	0	1st red	NA (NA)	NA	0.122707	3 month
743	KRB39-3	4519612	5724927.3	73.10	Q	0	Essen	Yes	1	2nd red	NA (NA)	NA	3.715E-05	3 year
744	LK09	4518479	5725799	56.40	Q	67%	Red	Yes	0.5	Essen	4Q (1)	369	3.715E-05	3 year
745	LK100	4520128	5726415	63.33	Q	56%	Red	Yes	0.5	Essen	3Q (1.3333)	307.5	0.0956853	3 month
746	LK101	4520128	5726412	40.63	Q	0	Essen	No	0	Essen	3Q (1.3333)	307	0.0956853	3 month
747	LK171	4519753	5721385	66.80	T	25%	Red	No	0	Essen	5Q (0.8)	463	1.1360337	3 month
748	LK172	4519753	5721387	50.80	T	50%	Red	Yes	0.5	Essen	8Q (0.5)	719	4.267E-05	3 year
749	LK181	4522513	5723003	63.00	T	20%	Red	No	0	Essen	4Q (1)	353	0.0007244	1 year
750	LK182	4522516	5723007	42.10	T	75%	Red	No	0.3333	Essen	8Q (0.5)	744	0.0007244	1 year
751	LK30	4520360	5727141	54.00	Q	0	Essen	Yes	0.5	Essen	4Q (1)	358	0.0004667	2 year
752	LK31	4520749	5727565.8	38.20	Q	100%	Red	Yes	0.5	Essen	4Q (1)	353.5	0.0004667	2 year
753	LK65	4522046	5720074	75.53	Q	100%	Red	Yes	0.5	Essen	1Q (4)	127	0.0004667	2 year
754	RT01	4522931	5721328.7	72.30	Q	0	Essen	Yes	0.5	1st red	1Q (4)	92	0.0010122	1 year
755	RT011	4522931	5721328.7	72.30	Q	0	Essen	Yes	0.5	2nd red	1Q (4)	92	0.0010122	1 year
756	RT02	4522796	5721289.4	72.30	Q	0	Essen	Yes	0.5	1st red	1Q (4)	98.5	0.0010122	1 year
757	RT021	4522796	5721289.4	67.50	Q	0	Essen	Yes	0.5	2nd red	1Q (4)	98.5	0.0010122	1 year
758	RT07	4522930	5721354.6	72.20	Q	33%	Red	Yes	0.5	1st red	1Q (4)	97	0.0010122	1 year
759	RT071	4522930	5721354.6	67.20	Q	0	Essen	Yes	0.5	2nd red	2Q (2)	141	0.0010122	1 year
760	RT14	4522931	5721279	73.60	Q	0	Essen	Yes	0.5	Essen	1Q (4)	98	0.0010122	1 year
761	RT15	4523009	5721352.3	73.60	Q	0	Essen	Yes	0.5	Essen	1Q (4)	94.5	0.0010122	1 year
762	RT151	4523008	5721353.6	73.60	Q	0	Essen	Yes	0.5	Essen	1Q (4)	94.5	0.0010122	1 year

763	RT16	4522944	5721323.4	73.60	Q	0	Essen	Yes	0.5	Essen	1Q (4)	99	0.0010122	1 year
764	RT161	4522943	5721322.7	73.60	Q	0	Essen	Yes	0.5	Essen	1Q (4)	97.5	0.0010122	1 year
765	RT18	4522929	5721326.7	73.60	Q	0	Essen	Yes	0.5	Essen	1Q (4)	94	0.0004931	2 year
766	RT19	4522986	5721392.4	73.60	Q	0	Essen	Yes	1	Essen	1Q (4)	96.5	0.0004931	2 year
767	RT20	4522948	5721405.1	73.60	Q	0	Essen	Yes	1	Essen	1Q (4)	96	0.0004931	2 year
768	RT201	4522946	5721404.9	73.60	Q	0	Essen	Yes	0.5	Essen	1Q (4)	96	0.0004931	2 year
769	RT21	4522948	5721355.2	73.60	Q	0	Essen	Yes	0.5	Essen	2Q (2)	144	0.0004931	2 year
770	RT211	4522948	5721354.1	73.60	Q	0	Essen	Yes	0.5	Essen	2Q (2)	143.5	0.0004931	2 year
771	RT22	4522969	5721313.4	73.60	Q	0	Essen	Yes	0.5	Essen	1Q (4)	96	0.0004931	2 year
772	RT221	4522968	5721314.9	73.60	Q	0	Essen	Yes	0.5	Essen	1Q (4)	97	0.0004931	2 year
773	RT24	4522969	5721485	73.60	Q	0	Essen	Yes	0.5	Essen	1Q (4)	93	0.0004931	2 year
774	RT241	4522970	5721486.2	73.60	Q	0	Essen	Yes	0.5	Essen	1Q (4)	96	7.449E-05	2 year
775	RT25	4522986	5721287.8	73.60	Q	0	Essen	Yes	0.5	Essen	1Q (4)	98	7.449E-05	2 year
776	RT251	4522986	5721286.7	73.60	Q	0	Essen	Yes	0.5	Essen	1Q (4)	97	7.449E-05	2 year
777	SAF23	4521930	5719958.7	60.57	Q	0	Essen	Yes	0.6667	Essen	3Q (1.3333)	267	1.095E-05	3 year
778	SAFW040	4519750	5724457.5	71.98	Q	0	Essen	Yes	0.6667	Essen	11Q (0.3636)	994	7.558E-05	2 year
779	SAFW041	4519753	5724454.8	66.58	Q	33%	Red	No	0.3333	Essen	11Q (0.3636)	994	6.361E-05	2 year
780	SAFW042	4519756	5724452.1	66.51	Q	33%	Red	Yes	0.5	Essen	11Q (0.3636)	994	5.177E-05	2 year
781	WVV004	4516903	5724800	75.20	Q	0	Essen	Yes	0.5	Essen	4Q (1)	393	5.177E-05	2 year
782	WVV005	4518289	5725092	75.00	Q	0	Essen	No	0	Essen	4Q (1)	399	8.96E-05	2 year
783	WVV009	4518290	5724100	75.00	Q	0	Essen	Yes	1	Essen	NA (NA)	NA	5.42E-05	2 year
784	WVV011	4517367	5725084	40.57	T	0	Essen	Yes	0.5	Essen	8Q (0.5)	721	5.542E-05	2 year
785	WVV012	4517378	5725084	58.30	T	0	Essen	Yes	0.5	Essen	4Q (1)	377	1.432E-05	3 year
786	WVV015	4518502	5724843	74.30	T	0	Essen	Yes	0.5	Essen	4Q (1)	333	5.697E-05	2 year
787	WVV016	4518021	5725305.6	34.40	T	0	Essen	No	0	Essen	NA (NA)	NA	5.697E-05	2 year
788	WVV017	4518015	5725309.8	72.00	T	0	Essen	No	0	Essen	4Q (1)	380	5.737E-05	2 year
789	WVV023	4517503	5724383	81.50	Q	0	Essen	Yes	0.5	Essen	4Q (1)	399	5.737E-05	2 year

790	WVV031	4517532	5724962	35.50	T	0	Essen	Yes	0.5	Essen	8Q (0.5)	707	7.261E-05	2 year
791	WVV032	4517532	5724957	72.50	T	0	Essen	Yes	0.5	Essen	4Q (1)	399	4.917E-05	3 year
792	WVV034	4518124	5725004	51.00	T	0	Essen	No	0	Essen	NA (NA)	NA	6.089E-05	2 year
793	WVV035	4518128	5725006	75.50	Q	0	Essen	Yes	0.5	Essen	4Q (1)	399	8.15E-05	2 year
794	WVV045	4518251	5724387	78.20	Q	0	Essen	Yes	0.5	Essen	4Q (1)	325.5	8.674E-05	2 year
795	WVV048	4517564	5724212	80.60	Q	0	Essen	Yes	0.5	Essen	3Q (1.3333)	264	8.674E-05	2 year
796	WVV059	4517436	5723075.9	71.05	T	0	Essen	Yes	0.5	Essen	2Q (2)	177.5	3.079E-05	3 year
797	WVV063	4518872	5724012	37.27	T	0	Essen	Yes	1	Essen	3Q (1.3333)	264	0.0001406	2 year
798	WVV064	4518904	5723765	39.79	T	0	Essen	Yes	0.5	Essen	2Q (2)	174	0.000169	2 year
799	WVV065	4518902	5723766	63.60	T	0	Essen	No	0	Essen	3Q (1.3333)	251	2.74E-05	3 year
800	WVV074	4519077	5724060	62.90	T	0	Essen	No	0	Essen	2Q (2)	171	1.204E-05	3 year
801	WVV086	4519072	5726213	64.52	T	0	Essen	Yes	0.5	Essen	NA (NA)	NA	5.042E-05	3 year
802	WVV090	4519522	5725755	67.50	Q	0	Essen	No	0	Essen	4Q (1)	327.5	3.113E-05	3 year
803	WVV093	4518729	5725173	47.30	T	0	Essen	No	0	Essen	NA (NA)	NA	5.854E-05	2 year
804	WVV095	4516900	5724795	40.20	T	0	Essen	Yes	0.5	Essen	8Q (0.5)	737	0.0001435	2 year
805	WVV107	4518679	5722464	74.01	Q	0	Essen	Yes	1	Essen	2Q (2)	182.5	4.933E-05	3 year
806	WVV109	4518172	5721955	65.70	T	0	Essen	Yes	0.5	Essen	4Q (1)	373	0.0001314	2 year
807	WVV110	4517660	5723276	69.74	T	0	Essen	Yes	0.5	Essen	2Q (2)	177.5	4.847E-05	3 year
808	WVV113	4517525	5722270	71.44	T	0	Essen	Yes	0.5	Essen	2Q (2)	178.5	5.919E-05	2 year
809	WVV115	4518498	5722088	47.37	T	0	Essen	Yes	0.5	Essen	NA (NA)	NA	5.919E-05	2 year
810	WVV117	4518732	5723401	76.70	Q	0	Essen	No	0	Essen	NA (NA)	NA	5.919E-05	2 year
811	WVV119	4519353	5723304	66.60	Q	0	Essen	Yes	1	Essen	2Q (2)	178	6.824E-05	2 year
812	WVV121	4518645	5723101.3	40.70	T	0	Essen	Yes	0.5	Essen	2Q (2)	188	6.363E-05	2 year
813	WVV122	4518647	5723096	58.26	T	0	Essen	Yes	0.5	Essen	2Q (2)	178	7.381E-05	2 year
814	WVV123	4518647	5723098	74.39	Q	0	Essen	Yes	0.5	Essen	3Q (1.3333)	253	7.381E-05	2 year
815	WVV130	4517207	5723022	72.10	T	0	Essen	Yes	0.5	Essen	2Q (2)	178	4.983E-05	3 year
816	WVV132	4517362	5722908.9	70.67	T	0	Essen	Yes	0.5	Essen	2Q (2)	175	0.0127573	6 month

817	WVV141	4519254	5724079	63.90	T	0	Essen	Yes	0.5	Essen	2Q (2)	180	0.0049298	1 year
818	WVV142	4519255	5724078	74.40	Q	0	Essen	Yes	0.6667	Essen	2Q (2)	189	0.0017723	1 year
819	WVV159	4519442	5723483	61.40	T	0	Essen	No	0	Essen	2Q (2)	178.5	4.734E-05	3 year

Appendix 6: Optimized LTM network map showing proposed new wells in the monitoring network.

S. No.	Vertical Zone	Easting	Northing	Search Radius	Wells Within Radius	Quartile Score	CV Score
1	Q	4520191	5722823	122.1841	0	0.803124	0.633092
2	Q	4521106	5720411	122.1841	0	0.850934	0.523122
3	Q	4521189	5720577	122.1841	0	0.92324	0.507604
4	Q	4521272	5724154	122.1841	0	0.80821	0.45507
5	Q	4519609	5724154	122.1841	0	0.761159	0.443165
6	Q	4520274	5722989	122.1841	0	0.845547	0.442933
7	Q	4520025	5721991	122.1841	0	0.76492	0.431951
8	Q	4519692	5723904	122.1841	0	0.793493	0.391903
9	Q	4520191	5722157	122.1841	0	0.783527	0.377828
10	Q	4521106	5724154	122.1841	0	0.810607	0.377769
11	Q	4518860	5722490	122.1841	0	0.754244	0.370161
12	Q	4520607	5720660	122.1841	0	0.782721	0.368283
13	Q	4519941	5723904	122.1841	0	0.880507	0.364098
14	Q	4519692	5722324	122.1841	0	0.75831	0.358853
15	Q	4521189	5720910	122.1841	0	0.837771	0.35586
16	Q	4520440	5723987	122.1841	0	0.848634	0.352246
17	Q	4519110	5722074	122.1841	0	0.750867	0.345998
18	Q	4519442	5724237	122.1841	0	0.77569	0.337163
19	Q	4519359	5722074	122.1841	0	0.752282	0.330295
20	Q	4519775	5722157	122.1841	0	0.757107	0.319928
21	Q	4520524	5722573	122.1841	0	0.806483	0.317308
22	Q	4520524	5724237	122.1841	0	0.905614	0.315125
23	Q	4519609	5721991	122.1841	0	0.754953	0.309586
24	Q	4520191	5719496	122.1841	0	0.754032	0.307234
25	Q	4521189	5723821	122.1841	0	0.752949	0.305779
26	Q	4520856	5724486	122.1841	0	0.906078	0.298808
27	Q	4521023	5723821	122.1841	0	0.764603	0.297586
28	Q	4518943	5722074	122.1841	0	0.757918	0.296145
29	Q	4520440	5720910	122.1841	0	0.756154	0.289599
30	Q	4520856	5724320	122.1841	0	0.908526	0.287822
31	Q	4519692	5721575	122.1841	0	0.757304	0.278925
32	Q	4520607	5720910	122.1841	0	0.761071	0.278903
33	Q	4520940	5719995	122.1841	0	0.758549	0.274987
34	Q	4521938	5723904	122.1841	0	0.789928	0.271871
35	Q	4520940	5721991	122.1841	0	0.782334	0.269878
36	Q	4519692	5719912	122.1841	0	0.755445	0.269235
37	Q	4519941	5725485	122.1841	0	0.805619	0.264667
38	Q	4521938	5724154	122.1841	0	0.785505	0.260522
39	Q	4521355	5723655	122.1841	0	0.757736	0.259083
40	Q	4520191	5724237	122.1841	0	0.788237	0.2569
41	Q	4521272	5722157	122.1841	0	0.752611	0.252006
42	T	4517030	5724570	122.1841	0	0.809698	0.540122
43	T	4521688	5724570	122.1841	0	0.756628	0.418749
44	T	4519609	5724071	122.1841	0	0.883371	0.41582
45	T	4519026	5722407	122.1841	0	0.838667	0.411503
46	T	4520108	5721825	122.1841	0	0.813091	0.392853

47	T	4519442	5724154	122.1841	0	0.794405	0.392373
48	T	4518694	5722157	122.1841	0	0.754882	0.375125
49	T	4519359	5723904	122.1841	0	0.794746	0.344547
50	T	4521189	5720411	122.1841	0	0.774637	0.333716
51	T	4521355	5720993	122.1841	0	0.758751	0.330235
52	T	4519193	5723156	122.1841	0	0.811722	0.329186
53	T	4518527	5722823	122.1841	0	0.772686	0.326238
54	T	4518694	5722906	122.1841	0	0.785228	0.32372
55	T	4521355	5720328	122.1841	0	0.762951	0.32175
56	T	4518860	5723072	122.1841	0	0.794967	0.319172
57	T	4519193	5724653	122.1841	0	0.757859	0.315272
58	T	4519359	5724486	122.1841	0	0.794016	0.314325
59	T	4519858	5722407	122.1841	0	0.839568	0.31036
60	T	4519858	5722074	122.1841	0	0.810248	0.303512
61	T	4522354	5724154	122.1841	0	0.756755	0.296272
62	T	4521688	5719912	122.1841	0	0.757053	0.291449
63	T	4518527	5723156	122.1841	0	0.763716	0.268963

Appendix 7: Temporal optimization of individual monitoring wells showing sampling interval in the various aquifer.

S. No.	COC	Vertical Zone	Well Name	Fraction Thinned	Base Interval (Days)	Optimal Interval (Days)	Optimal Interval (per year)
1	MCB	Q	BIT03	0.28	137	190	2Q (2)
2	MCB	Q	BVV009	0.41	234	393	4Q (1)
3	MCB	Q	BVV0281	0.28	244	339	4Q (1)
4	MCB	Q	BVV040	0.34	141	215	2Q (2)
5	MCB	Q	BVV050	0.31	150	218	2Q (2)
6	MCB	Q	BVV079	0.56	130	296	3Q (1.33)
7	MCB	Q	BVV0791	0.34	250	381	4Q (1)
8	MCB	Q	BVV119	0.78	243	1109	12Q (0.33)
9	MCB	Q	BVV1240	0.44	216	384	4Q (1)
10	MCB	Q	BVV1250	0.41	210	354	4Q (1)
11	MCB	Q	BVV220	0.47	140	264	3Q (1.33)
12	MCB	Q	BVV246	0.22	231	295	3Q (1.33)
13	MCB	Q	BVV266	0.56	359	821	9Q (0.44)
14	MCB	Q	BVV3020	0.41	223	376	4Q (1)
15	MCB	Q	BVV3030	0.44	218	388	4Q (1)
16	MCB	Q	BVV3040	0.50	178	356	4Q (1)
17	MCB	Q	BVV3060	0.50	309	617	7Q (0.59)
18	MCB	Q	BVV3070	0.69	232	742	8Q (0.5)
19	MCB	Q	BVV308	0.22	279	356	4Q (1)
20	MCB	Q	BVV309	0.41	210	354	4Q (1)
21	MCB	Q	BVV402	0.47	266	501	6Q (0.67)
22	MCB	Q	BVV405	0.63	379	1009	11Q (0.36)
23	MCB	Q	BVV439	0.44	125	222	2Q (2)
24	MCB	Q	BVV440	0.44	271	482	5Q (0.8)
25	MCB	Q	BVV441	0.56	123	281	3Q (1.33)
26	MCB	Q	BVV443	0.44	271	482	5Q (0.8)
27	MCB	Q	BVV444	0.53	271	578	6Q (0.67)

28	MCB	Q	BVV445	0.59	317	780	9Q (0.44)
29	MCB	Q	BVV446	0.59	494	1216	14Q (0.24)
30	MCB	Q	BVV447	0.47	160	301	3Q (1.33)
31	MCB	Q	BVV448	0.66	114	332	4Q (1)
32	MCB	Q	BVV457	0.47	299	562	6Q (0.67)
33	MCB	Q	BVV458	0.25	280	373	4Q (1)
34	MCB	Q	BVV4640	0.22	363	465	5Q (0.8)
35	MCB	Q	BVV4650	0.44	179	318	4Q (1)
36	MCB	Q	BVV4660	0.63	392	1045	12Q (0.33)
37	MCB	Q	BVV4680	0.47	281	529	6Q (0.67)
38	MCB	Q	BVV471	0.44	298	529	6Q (0.67)
39	MCB	Q	BVV472	0.28	279	388	4Q (1)
40	MCB	Q	BVV475	0.41	221	372	4Q (1)
41	MCB	Q	BVV476	0.47	124	233	3Q (1.33)
42	MCB	Q	BVV477	0.50	209	418	5Q (0.8)
43	MCB	Q	BVV478	0.78	123	560	6Q (0.67)
44	MCB	Q	BVV4790	0.41	126	211	2Q (2)
45	MCB	Q	BVV481	0.75	398	1592	18Q (0.22)
46	MCB	Q	BVV503	0.72	282	1003	11Q (0.36)
47	MCB	Q	BVV507	0.56	130	296	3Q (1.33)
48	MCB	Q	BVV509	0.50	375	750	8Q (0.5)
49	MCB	Q	BVV5090	0.31	375	545	6Q (0.67)
50	MCB	Q	BVV510	0.66	217	631	7Q (0.52)
51	MCB	Q	BVV5100	0.50	217	434	5Q (0.8)
52	MCB	Q	BVV513	0.25	211	281	3Q (1.33)
53	MCB	Q	BVV515	0.22	211	270	3Q (1.33)
54	MCB	Q	BVV516	0.78	270	1234	14Q (0.28)
55	MCB	Q	BVV519	0.81	267	1424	16Q (0.25)
56	MCB	Q	BVV524	0.53	279	595	7Q (0.57)
57	MCB	Q	BVV525	0.72	316	1124	12Q (0.33)
58	MCB	Q	BVV534	0.38	179	286	3Q (1.33)
59	MCB	Q	BVV536	0.25	222	296	3Q (1.33)
60	MCB	Q	BVV5390	0.34	126	192	2Q (2)
61	MCB	Q	BVV5391	0.34	128	194	2Q (2)
62	MCB	Q	BVV540	0.44	232	412	5Q (0.8)
63	MCB	Q	BVV541	0.84	224	1434	16Q (0.25)
64	MCB	Q	BVV544	0.53	222	474	5Q (0.8)
65	MCB	Q	BVV5560	0.44	129	229	3Q (1.33)
66	MCB	Q	BVV5561	0.31	129	188	2Q (2)
67	MCB	Q	BVV5570	0.19	127	156	2Q (2)
68	MCB	Q	BVV5571	0.34	127	194	2Q (2)
69	MCB	Q	BVV566	0.66	161	468	5Q (0.8)
70	MCB	Q	BVV568	0.72	360	1280	14Q (0.28)
71	MCB	Q	BVV588	0.25	141	188	2Q (2)
72	MCB	Q	BVV5881	0.50	231	462	5Q (0.8)
73	MCB	Q	BVV589	0.44	225	400	4Q (1)
74	MCB	Q	BVV5891	0.44	225	400	4Q (1)
75	MCB	Q	BVV590	0.41	132	221	2Q (2)
76	MCB	Q	BVV591	0.63	90	240	3Q (1.33)
77	MCB	Q	BVV5911	0.75	90	360	4Q (1)
78	MCB	Q	BVV592	0.31	286	416	5Q (0.8)
79	MCB	Q	BVV593	0.59	94	230	3Q (1.33)

80	MCB	Q	BVV5931	0.38	89	142	2Q (2)
81	MCB	Q	BVV594	0.34	245	373	4Q (1)
82	MCB	Q	BVV595	0.53	88	188	2Q (2)
83	MCB	Q	BVV5951	0.47	88	166	2Q (2)
84	MCB	Q	BVV596	0.50	280	560	6Q (0.67)
85	MCB	Q	BVV597	0.28	213	296	3Q (1.33)
86	MCB	Q	BVV5971	0.44	393	698	8Q (0.5)
87	MCB	Q	BVV598	0.66	228	663	7Q (0.57)
88	MCB	Q	BVV599	0.59	100	246	3Q (1.33)
89	MCB	Q	BVV6050	0.66	213	620	7Q (0.57)
90	MCB	Q	BVV606	0.53	217	463	5Q (0.8)
91	MCB	Q	BVV607	0.81	224	1195	13Q (0.30)
92	MCB	Q	BVV6080	0.28	229	319	4Q (1)
93	MCB	Q	BVV6081	0.50	133	266	3Q (1.33)
94	MCB	Q	BVV624	0.38	130	208	2Q (2)
95	MCB	Q	BVV625	0.19	134	164	2Q (2)
96	MCB	Q	BVV626	0.47	142	267	3Q (1.33)
97	MCB	Q	BVV634	0.66	291	845	9Q (0.44)
98	MCB	Q	BVV645	0.50	296	592	7Q (0.57)
99	MCB	Q	BVV6470	0.72	307	1092	12Q (0.33)
100	MCB	Q	BVV6480	0.28	287	399	4Q (1)
101	MCB	Q	BVV6490	0.47	286	538	6Q (0.66)
102	MCB	Q	BVV6600	0.16	179	212	2Q (2)
103	MCB	Q	BVV664	0.63	133	353	4Q (1)
104	MCB	Q	BVV667	0.41	133	224	2Q (2)
105	MCB	Q	BVV668	0.66	228	663	7Q (0.57)
106	MCB	Q	BVV6860	0.47	272	512	6Q (0.66)
107	MCB	Q	BVV6870	0.56	272	622	7Q (0.57)
108	MCB	Q	BVV6880	0.53	286	610	7Q (0.57)
109	MCB	Q	BVV693	0.25	217	289	3Q (1.33)
110	MCB	Q	Br01	0.81	7	37	1Q (4)
111	MCB	Q	Br02	0.81	7	37	1Q (4)
112	MCB	Q	Br05	0.81	7	37	1Q (4)
113	MCB	Q	Br07	0.66	7	20	1Q (4)
114	MCB	Q	Br11	0.69	7	22	1Q (4)
115	MCB	Q	Br1Greppin	0.81	7	37	1Q (4)
116	MCB	Q	Br201	0.63	7	19	1Q (4)
117	MCB	Q	Br209	0.38	217	347	4Q (1)
118	MCB	Q	Br211	0.94	7	112	1Q (4)
119	MCB	Q	Br26	0.72	7	25	1Q (4)
120	MCB	Q	Br40	0.84	7	45	1Q (4)
121	MCB	Q	Br407	0.88	7	56	1Q (4)
122	MCB	Q	Br43	0.78	7	32	1Q (4)
123	MCB	Q	Br44	0.75	7	28	1Q (4)
124	MCB	Q	Br45	0.75	7	28	1Q (4)
125	MCB	Q	Br47	0.84	7	45	1Q (4)
126	MCB	Q	Br50	0.78	7	32	1Q (4)
127	MCB	Q	Br502	0.47	217	408	5Q (0.8)
128	MCB	Q	Br503	0.22	217	277	3Q (1.33)
129	MCB	Q	Br504	0.50	217	433	5Q (0.8)
130	MCB	Q	Br505	0.59	217	533	6Q (0.67)
131	MCB	Q	Br506	0.41	217	365	4Q (1)

132	MCB	Q	GOI1094	0.38	84	134	1Q (4)
133	MCB	Q	GOI1101	0.66	87	252	3Q (1.33)
134	MCB	Q	GOI1102	0.59	85	208	2Q (2)
135	MCB	Q	GOI1104	0.59	92	226	3Q (1.33)
136	MCB	Q	GOI1105	0.63	86	229	3Q (1.33)
137	MCB	Q	GOI1108	0.63	84	224	2Q (2)
138	MCB	Q	GOI830	0.31	182	265	3Q (1.33)
139	MCB	Q	GOI876	0.78	88	402	4Q (1)
140	MCB	Q	LK100	0.28	308	428	5Q (0.8)
141	MCB	Q	RT01	0.69	92	294	3Q (1.33)
142	MCB	Q	RT011	0.69	92	294	3Q (1.33)
143	MCB	Q	WVV107	0.81	239	1275	14Q (0.28)
144	MCB	Q	WVV119	0.78	181	825	9Q (0.44)
145	MCB	Q	WVV142	0.69	365	1168	13Q (0.30)
146	MCB	Q	bb021	0.53	28	60	1Q (4)
147	MCB	Q	bb023	0.19	28	34	1Q (4)
148	MCB	Q	bb024	0.63	28	75	1Q (4)
149	MCB	Q	bb027	0.72	28	100	1Q (4)
150	MCB	Q	bb028	0.44	29	52	1Q (4)
151	MCB	Q	bb303	0.16	28	33	1Q (4)
152	MCB	Q	bb304	0.59	28	69	1Q (4)
153	MCB	Q	bb305	0.63	28	75	1Q (4)
154	MCB	Q	bb306	0.63	28	75	1Q (4)
155	MCB	Q	bb307	0.44	36	64	1Q (4)
156	MCB	Q	bb308	0.81	35	187	2Q (2)
157	HCH	Q	BVV050	0.56	150	343	4Q (1)
158	HCH	Q	BVV119	0.47	170	320	4Q (1)
159	HCH	Q	BVV3040	0.88	178	1424	16Q (0.25)
160	HCH	Q	BVV439	0.47	125	235	3Q (1.33)
161	HCH	Q	BVV440	0.31	212	308	3Q (1.33)
162	HCH	Q	BVV444	0.47	203	382	4Q (1)
163	HCH	Q	BVV445	0.47	139	262	3Q (1.33)
164	HCH	Q	BVV446	0.56	274	626	7Q (0.57)
165	HCH	Q	BVV4680	0.59	252	620	7Q (0.57)
166	HCH	Q	BVV475	0.47	175	328	4Q (1)
167	HCH	Q	BVV476	0.56	124	283	3Q (1.33)
168	HCH	Q	BVV477	0.47	172	323	4Q (1)
169	HCH	Q	BVV478	0.31	123	178	2Q (2)
170	HCH	Q	BVV515	0.53	211	450	5Q (0.8)
171	HCH	Q	BVV5390	0.31	126	183	2Q (2)
172	HCH	Q	BVV5391	0.47	128	240	3Q (1.33)
173	HCH	Q	BVV544	0.47	444	836	9Q (0.44)
174	HCH	Q	BVV6050	0.44	180	320	4Q (1)
175	HCH	Q	BVV6080	0.38	182	290	3Q (1.33)
176	HCH	Q	BVV6081	0.66	133	387	4Q (1)
177	HCH	Q	BVV667	0.53	133	284	3Q (1.33)
178	HCH	Q	BVV693	0.56	182	416	5Q (0.8)
179	HCH	Q	Br01	0.31	229	332	4Q (1)
180	HCH	Q	Br02	0.31	228	331	4Q (1)
181	HCH	Q	Br05	0.66	225	653	7Q (0.57)
182	HCH	Q	Br07	0.31	225	327	4Q (1)
183	HCH	Q	Br26	0.41	224	377	4Q (1)

184	HCH	Q	Br50	0.47	225	423	5Q (0.8)
185	So4	Q	BIT03	0.63	137	364	4Q (1)
186	So4	Q	BVV009	0.50	138	276	3Q (1.33)
187	So4	Q	BVV0281	0.56	244	558	6Q (0.67)
188	So4	Q	BVV040	0.63	133	353	4Q (1)
189	So4	Q	BVV050	0.38	150	240	3Q (1.33)
190	So4	Q	BVV079	0.44	130	230	3Q (1.33)
191	So4	Q	BVV0791	0.47	126	237	3Q (1.33)
192	So4	Q	BVV119	0.78	186	848	9Q (0.44)
193	So4	Q	BVV1240	0.53	216	461	5Q (0.8)
194	So4	Q	BVV1250	0.50	179	358	4Q (1)
195	So4	Q	BVV220	0.47	140	264	3Q (1.33)
196	So4	Q	BVV246	0.81	231	1229	14Q (0.28)
197	So4	Q	BVV3020	0.38	223	357	4Q (1)
198	So4	Q	BVV3030	0.59	218	537	6Q (0.67)
199	So4	Q	BVV3040	0.44	215	382	4Q (1)
200	So4	Q	BVV3060	0.66	283	822	9Q (0.44)
201	So4	Q	BVV3070	0.50	278	555	6Q (0.67)
202	So4	Q	BVV308	0.25	212	283	3Q (1.33)
203	So4	Q	BVV309	0.63	210	560	6Q (0.67)
204	So4	Q	BVV310	0.81	294	1565	17Q (0.23)
205	So4	Q	BVV402	0.81	266	1419	16Q (0.25)
206	So4	Q	BVV403	0.69	286	915	10Q (0.4)
207	So4	Q	BVV404	0.59	302	743	8Q (0.5)
208	So4	Q	BVV405	0.72	221	786	9Q (0.444)
209	So4	Q	BVV432	0.47	287	540	6Q (0.667)
210	So4	Q	BVV439	0.56	125	286	3Q (1.33)
211	So4	Q	BVV440	0.44	271	482	5Q (0.8)
212	So4	Q	BVV441	0.41	123	207	2Q (2)
213	So4	Q	BVV443	0.56	271	619	7Q (0.57)
214	So4	Q	BVV444	0.59	203	500	6Q (0.67)
215	So4	Q	BVV445	0.72	271	964	11Q (0.36)
216	So4	Q	BVV446	0.63	274	731	8Q (0.5)
217	So4	Q	BVV447	0.59	217	534	6Q (0.66)
218	So4	Q	BVV448	0.53	114	243	3Q (1.33)
219	So4	Q	BVV457	0.69	299	955	11Q (0.36)
220	So4	Q	BVV4640	0.81	287	1531	17Q (0.23)
221	So4	Q	BVV4650	0.66	179	521	6Q (0.667)
222	So4	Q	BVV4680	0.78	281	1285	14Q (0.28)
223	So4	Q	BVV4700	0.78	309	1410	16Q (0.25)
224	So4	Q	BVV471	0.69	253	810	9Q (0.44)
225	So4	Q	BVV472	0.78	305	1392	15Q (0.27)
226	So4	Q	BVV475	0.44	221	393	4Q (1)
227	So4	Q	BVV476	0.38	124	198	2Q (2)
228	So4	Q	BVV477	0.59	209	514	6Q (0.67)
229	So4	Q	BVV478	0.38	123	196	2Q (2)
230	So4	Q	BVV4790	0.56	126	287	3Q (1.33)
231	So4	Q	BVV480	0.59	295	726	8Q (0.5)
232	So4	Q	BVV481	0.63	296	788	9Q (0.44)
233	So4	Q	BVV503	0.63	282	752	8Q (0.5)
234	So4	Q	BVV507	0.41	130	218	2Q (2)
235	So4	Q	BVV509	0.59	296	729	8Q (0.5)

236	So4	Q	BVV5090	0.81	296	1579	18Q (0.22)
237	So4	Q	BVV510	0.84	277	1770	20Q (0.2)
238	So4	Q	BVV5100	0.84	279	1786	20Q (0.2)
239	So4	Q	BVV512	0.50	211	422	5Q (0.8)
240	So4	Q	BVV513	0.41	182	307	3Q (1.33)
241	So4	Q	BVV515	0.44	211	375	4Q (1)
242	So4	Q	BVV516	0.44	134	238	3Q (1.33)
243	So4	Q	BVV519	0.44	267	475	5Q (0.8)
244	So4	Q	BVV524	0.59	279	687	8Q (0.5)
245	So4	Q	BVV525	0.34	378	576	6Q (0.67)
246	So4	Q	BVV534	0.78	224	1024	11Q (0.36)
247	So4	Q	BVV536	0.50	222	444	5Q (0.8)
248	So4	Q	BVV5390	0.38	126	202	2Q (2)
249	So4	Q	BVV5391	0.41	128	215	2Q (2)
250	So4	Q	BVV540	0.44	232	412	5Q (0.8)
251	So4	Q	BVV541	0.66	178	518	6Q (0.67)
252	So4	Q	BVV544	0.75	222	888	10Q (0.4)
253	So4	Q	BVV5560	0.25	129	172	2Q (2)
254	So4	Q	BVV5561	0.47	129	243	3Q (1.33)
255	So4	Q	BVV5570	0.25	127	169	2Q (2)
256	So4	Q	BVV5571	0.44	127	226	3Q (1.33)
257	So4	Q	BVV561	0.84	291	1862	21Q (0.19)
258	So4	Q	BVV566	0.59	291	715	8Q (0.5)
259	So4	Q	BVV588	0.50	224	448	5Q (0.8)
260	So4	Q	BVV5881	0.41	231	389	4Q (1)
261	So4	Q	BVV589	0.56	225	514	6Q (0.67)
262	So4	Q	BVV5891	0.53	225	480	5Q (0.8)
263	So4	Q	BVV590	0.28	132	183	2Q (2)
264	So4	Q	BVV591	0.81	140	747	8Q (0.5)
265	So4	Q	BVV5911	0.44	130	230	3Q (1.33)
266	So4	Q	BVV592	0.38	229	366	4Q (1)
267	So4	Q	BVV593	0.47	134	252	3Q (1.33)
268	So4	Q	BVV5931	0.63	130	345	4Q (1)
269	So4	Q	BVV594	0.16	245	290	3Q (1.33)
270	So4	Q	BVV595	0.66	129	375	4Q (1)
271	So4	Q	BVV5951	0.31	129	188	2Q (2)
272	So4	Q	BVV596	0.84	280	1792	20Q (0.2)
273	So4	Q	BVV597	0.50	271	541	6Q (0.67)
274	So4	Q	BVV5971	0.50	271	541	6Q (0.67)
275	So4	Q	BVV598	0.72	283	1006	11Q (0.36)
276	So4	Q	BVV599	0.31	231	336	4Q (1)
277	So4	Q	BVV601	0.50	275	549	6Q (0.67)
278	So4	Q	BVV6050	0.34	213	325	4Q (1)
279	So4	Q	BVV606	0.63	217	579	6Q (0.67)
280	So4	Q	BVV607	0.34	224	341	4Q (1)
281	So4	Q	BVV6080	0.50	229	458	5Q (0.8)
282	So4	Q	BVV6081	0.44	133	236	3Q (1.33)
283	So4	Q	BVV624	0.75	130	520	6Q (0.67)
284	So4	Q	BVV625	0.66	134	388	4Q (1)
285	So4	Q	BVV626	0.56	228	521	6Q (0.67)
286	So4	Q	BVV6600	0.44	185	328	4Q (1)
287	So4	Q	BVV664	0.47	133	249	3Q (1.33)

288	So4	Q	BVV667	0.38	133	213	2Q (2)
289	So4	Q	BVV668	0.28	228	317	4Q (1)
290	So4	Q	BVV684	0.53	287	612	7Q (0.57)
291	So4	Q	BVV693	0.47	217	408	5Q (0.8)
292	So4	Q	Br01	0.59	222	545	6Q (0.67)
293	So4	Q	Br02	0.47	217	408	5Q (0.8)
294	So4	Q	Br05	0.53	218	464	5Q (0.8)
295	So4	Q	Br07	0.66	218	633	7Q (0.57)
296	So4	Q	Br11	0.63	218	580	6Q (0.67)
297	So4	Q	Br201	0.84	217	1386	15Q (0.27)
298	So4	Q	Br203	0.56	207	472	5Q (0.8)
299	So4	Q	Br205	0.16	207	245	3Q (1.33)
300	So4	Q	Br207	0.66	207	601	7Q (0.57)
301	So4	Q	Br209	0.63	217	579	6Q (0.67)
302	So4	Q	Br26	0.81	224	1195	13Q (0.30)
303	So4	Q	Br40	0.75	217	868	10Q (0.4)
304	So4	Q	Br407	0.56	217	495	5Q (0.8)
305	So4	Q	Br43	0.81	218	1160	13Q (0.31)
306	So4	Q	Br44	0.72	218	773	9Q (0.44)
307	So4	Q	Br45	0.59	218	535	6Q (0.67)
308	So4	Q	Br47	0.16	217	257	3Q (1.33)
309	So4	Q	Br50	0.72	218	773	9Q (0.44)
310	So4	Q	Br502	0.63	217	577	6Q (0.67)
311	So4	Q	Br503	0.63	217	577	6Q (0.67)
312	So4	Q	Br504	0.66	217	630	7Q (0.57)
313	So4	Q	Br505	0.59	217	533	6Q (0.67)
314	So4	Q	Br506	0.59	217	533	6Q (0.67)
315	So4	Q	GOI830	0.47	218	410	5Q (0.8)
316	So4	Q	LK100	0.53	308	656	7Q (0.57)
317	So4	Q	LK101	0.84	307	1965	22Q (0.18)
318	So4	Q	WVV107	0.63	190	507	6Q (0.66)
319	So4	Q	WVV119	0.81	184	981	11Q (0.36)
320	So4	Q	WVV142	0.72	189	672	7Q (0.57)
321	MCB	T	BVV030	0.75	146	584	6Q (0.66)
322	MCB	T	BVV092	0.75	338	1352	15Q (0.26)
323	MCB	T	BVV100	0.81	273	1456	16Q (0.25)
324	MCB	T	BVV1191	0.53	185	395	4Q (1)
325	MCB	T	BVV1192	0.72	183	651	7Q (0.57)
326	MCB	T	BVV1241	0.50	217	434	5Q (0.8)
327	MCB	T	BVV222	0.34	215	328	4Q (1)
328	MCB	T	BVV223	0.44	225	400	4Q (1)
329	MCB	T	BVV2241	0.75	29	116	1Q (4)
330	MCB	T	BVV248	0.75	363	1452	16Q (0.25)
331	MCB	T	BVV254	0.75	307	1228	14Q (0.28)
332	MCB	T	BVV3050	0.47	90	169	2Q (2)
333	MCB	T	BVV3063	0.41	290	488	5Q (0.8)
334	MCB	T	BVV3073	0.56	277	632	7Q (0.57)
335	MCB	T	BVV371	0.63	190	507	6Q (0.67)
336	MCB	T	BVV376	0.81	187	997	11Q (0.36)
337	MCB	T	BVV442	0.44	294	523	6Q (0.67)
338	MCB	T	BVV4461	0.63	301	801	9Q (0.44)
339	MCB	T	BVV4671	0.66	303	881	10Q (0.4)

340	MCB	T	BVV4721	0.34	295	449	5Q (0.8)
341	MCB	T	BVV4791	0.56	306	698	8Q (0.5)
342	MCB	T	BVV4920	0.38	209	334	4Q (1)
343	MCB	T	BVV4921	0.81	308	1640	18Q (0.22)
344	MCB	T	BVV500	0.19	383	471	5Q (0.8)
345	MCB	T	BVV526	0.59	295	725	8Q (0.5)
346	MCB	T	BVV533	0.31	379	551	6Q (0.67)
347	MCB	T	BVV535	0.66	389	1130	13Q (0.30)
348	MCB	T	BVV537	0.69	277	886	10Q (0.4)
349	MCB	T	BVV562	0.56	176	402	4Q (1)
350	MCB	T	BVV5631	0.34	256	390	4Q (1)
351	MCB	T	BVV5901	0.53	225	480	5Q (0.8)
352	MCB	T	BVV5921	0.56	286	654	7Q (0.57)
353	MCB	T	BVV5941	0.38	245	392	4Q (1)
354	MCB	T	BVV5961	0.63	280	747	8Q (0.5)
355	MCB	T	BVV5981	0.72	228	811	9Q (0.44)
356	MCB	T	BVV6082	0.78	309	1410	16Q (0.25)
357	MCB	T	BVV6271	0.50	275	549	6Q (0.67)
358	MCB	T	BVV6461	0.69	297	949	11Q (0.36)
359	MCB	T	BVV6471	0.16	220	260	3Q (1.33)
360	MCB	T	BVV6491	0.75	261	1044	12Q (0.33)
361	MCB	T	BVV651	0.31	275	400	4Q (1)
362	MCB	T	BVV652	0.31	223	324	4Q (1)
363	MCB	T	BVV653	0.22	195	250	3Q (1.33)
364	MCB	T	BVV654	0.28	279	388	4Q (1)
365	MCB	T	BVV655	0.25	278	371	4Q (1)
366	MCB	T	BVV656	0.28	278	387	4Q (1)
367	MCB	T	BVV657	0.44	282	500	6Q (0.67)
368	MCB	T	BVV661	0.53	134	285	3Q (1.33)
369	MCB	T	BVV662	0.44	133	236	3Q (1.33)
370	MCB	T	BVV663	0.50	145	290	3Q (1.33)
371	MCB	T	BVV665	0.28	214	298	3Q (1.33)
372	MCB	T	BVV666	0.53	142	303	3Q (1.33)
373	MCB	T	BVV681	0.44	305	541	6Q (0.67)
374	MCB	T	BVV6871	0.31	272	396	4Q (1)
375	MCB	T	BVV6881	0.50	286	572	6Q (0.67)
376	MCB	T	Br03	0.75	7	28	1Q (4)
377	MCB	T	Br06	0.66	7	20	1Q (4)
378	MCB	T	Br08	0.78	7	32	1Q (4)
379	MCB	T	Br101a	0.41	216	364	4Q (1)
380	MCB	T	Br12	0.72	7	25	1Q (4)
381	MCB	T	Br14	0.78	7	32	1Q (4)
382	MCB	T	Br202	0.66	7	20	1Q (4)
383	MCB	T	Br210	0.28	217	302	3Q (1.33)
384	MCB	T	Br27	0.81	7	37	1Q (4)
385	MCB	T	Br401	0.88	7	56	1Q (4)
386	MCB	T	Br402	0.81	7	37	1Q (4)
387	MCB	T	Br403	0.44	7	12	1Q (4)
388	MCB	T	Br404	0.88	7	56	1Q (4)
389	MCB	T	Br405	0.84	7	45	1Q (4)
390	MCB	T	Br406	0.88	7	56	1Q (4)
391	MCB	T	Br41	0.84	7	45	1Q (4)

392	MCB	T	Br42	0.78	7	32	1Q (4)
393	MCB	T	Br48	0.81	7	37	1Q (4)
394	MCB	T	Br49	0.75	7	28	1Q (4)
395	MCB	T	GOI875	0.34	272	414	5Q (0.8)
396	MCB	T	WVV059	0.81	190	1013	11Q (0.36)
397	MCB	T	WVV064	0.81	182	968	11Q (0.36)
398	MCB	T	WVV074	0.81	274	1461	16Q (0.25)
399	MCB	T	WVV110	0.84	190	1216	14Q (0.28)
400	MCB	T	WVV113	0.75	187	748	8Q (0.5)
401	MCB	T	WVV121	0.72	364	1292	14Q (0.24)
402	MCB	T	WVV122	0.78	179	818	9Q (0.44)
403	MCB	T	WVV130	0.34	273	416	5Q (0.8)
404	MCB	T	WVV132	0.84	182	1165	13Q (0.30)
405	MCB	T	WVV141	0.69	270	864	10Q (0.4)
406	MCB	T	WVV159	0.81	273	1456	16Q (0.25)
407	HCH	T	BVV1192	0.72	189	672	7Q (0.57)
408	HCH	T	BVV1241	0.56	378	864	10Q (0.4)
409	HCH	T	BVV6082	0.41	368	620	7Q (0.57)
410	HCH	T	BVV666	0.38	142	227	3Q (1.33)
411	HCH	T	Br03	0.63	225	599	7Q (0.57)
412	HCH	T	Br06	0.41	225	378	4Q (1)
413	HCH	T	Br08	0.38	225	359	4Q (1)
414	HCH	T	Br27	0.44	224	398	4Q (1)
415	HCH	T	Br48	0.34	225	342	4Q (1)
416	So4	T	BVV030	0.34	146	222	2Q (2)
417	So4	T	BVV092	0.69	338	1082	12Q (0.33)
418	So4	T	BVV100	0.59	189	465	5Q (0.8)
419	So4	T	BVV1191	0.69	185	592	7Q (0.57)
420	So4	T	BVV1192	0.56	189	432	5Q (0.8)
421	So4	T	BVV1241	0.53	306	652	7Q (0.57)
422	So4	T	BVV222	0.34	178	271	3Q (1.33)
423	So4	T	BVV223	0.41	178	300	3Q (1.33)
424	So4	T	BVV248	0.72	184	654	7Q(0.57)
425	So4	T	BVV254	0.75	184	736	8Q (0.5)
426	So4	T	BVV3050	0.81	132	704	8Q (0.5)
427	So4	T	BVV3063	0.78	290	1323	15Q(0.26)
428	So4	T	BVV3073	0.78	277	1264	14Q (0.28)
429	So4	T	BVV371	0.75	185	740	8Q (0.5)
430	So4	T	BVV376	0.81	183	976	11Q(0.36)
431	So4	T	BVV442	0.69	294	941	10Q (0.4)
432	So4	T	BVV4591	0.31	277	402	4Q (1)
433	So4	T	BVV4671	0.66	303	881	10Q (0.4)
434	So4	T	BVV4721	0.75	393	1572	17Q (0.23)
435	So4	T	BVV4791	0.56	306	698	8Q (0.5)
436	So4	T	BVV4920	0.50	209	418	5Q (0.8)
437	So4	T	BVV4921	0.44	308	547	6Q (0.67)
438	So4	T	BVV500	0.56	295	673	7Q (0.57)
439	So4	T	BVV526	0.56	295	673	7Q (0.57)
440	So4	T	BVV533	0.63	269	716	8Q (0.5)
441	So4	T	BVV535	0.81	282	1501	17Q (0.23)
442	So4	T	BVV537	0.66	277	806	9Q (0.44)
443	So4	T	BVV555	0.72	364	1294	14Q (0.28)
444	So4	T	BVV562	0.88	298	2384	26Q (0.15)

445	So4	T	BVV5631	0.78	380	1737	19Q (0.21)
446	So4	T	BVV5641	0.69	393	1258	14Q (0.28)
447	So4	T	BVV5901	0.69	225	720	8Q (0.5)
448	So4	T	BVV5921	0.72	286	1017	11Q (0.36)
449	So4	T	BVV5941	0.78	245	1120	12Q (0.33)
450	So4	T	BVV5961	0.66	280	815	9Q (0.44)
451	So4	T	BVV5981	0.72	283	1006	11Q (0.36)
452	So4	T	BVV6082	0.50	309	617	7Q (0.57)
453	So4	T	BVV633	0.38	290	464	5Q (0.8)
454	So4	T	BVV651	0.41	221	372	4Q (1)
455	So4	T	BVV652	0.47	223	420	5Q (0.8)
456	So4	T	BVV653	0.69	195	624	7Q (0.57)
457	So4	T	BVV654	0.50	229	458	5Q (0.8)
458	So4	T	BVV655	0.63	223	595	7Q (0.57)
459	So4	T	BVV656	0.72	223	793	9Q (0.44)
460	So4	T	BVV657	0.72	223	793	9Q (0.44)
461	So4	T	BVV6601	0.59	185	454	5Q (0.8)
462	So4	T	BVV661	0.41	134	225	2Q (2)
463	So4	T	BVV662	0.44	133	236	3Q (1.33)
464	So4	T	BVV663	0.56	145	331	4Q (1)
465	So4	T	BVV665	0.38	214	342	4Q (1)
466	So4	T	BVV666	0.44	142	252	3Q (1.33)
467	So4	T	BVV680	0.53	304	647	7Q (0.57)
468	So4	T	BVV681	0.69	305	974	11Q (0.36)
469	So4	T	Br03	0.41	218	366	4Q (1)
470	So4	T	Br06	0.50	218	435	5Q (0.8)
471	So4	T	Br08	0.50	218	435	5Q (0.8)
472	So4	T	Br100a	0.78	217	990	11Q (0.36)
473	So4	T	Br101a	0.63	217	577	6Q (0.67)
474	So4	T	Br12	0.47	217	408	5Q (0.8)
475	So4	T	Br14	0.47	218	409	5Q (0.8)
476	So4	T	Br202	0.72	216	768	9Q (0.44)
477	So4	T	Br204	0.44	207	367	4Q (1)
478	So4	T	Br206	0.81	207	1101	12Q (0.33)
479	So4	T	Br210	0.59	217	534	6Q (0.67)
480	So4	T	Br27	0.75	217	868	10Q (0.4)
481	So4	T	Br401	0.50	217	433	5Q (0.8)
482	So4	T	Br402	0.59	217	533	6Q (0.67)
483	So4	T	Br403	0.66	14	41	1Q (4)
484	So4	T	Br404	0.78	196	896	10Q (0.4)
485	So4	T	Br405	0.63	216	576	6Q (0.67)
486	So4	T	Br406	0.72	217	770	9Q (0.44)
487	So4	T	Br41	0.59	217	534	6Q (0.67)
488	So4	T	Br42	0.59	218	535	6Q (0.67)
489	So4	T	Br48	0.56	218	497	6Q (0.67)
490	So4	T	Br49	0.59	218	535	6Q (0.67)
491	So4	T	GOI875	0.47	272	511	6Q (0.67)
492	So4	T	WVV059	0.56	187	427	5Q (0.8)
493	So4	T	WVV064	0.84	184	1178	13Q (0.30)
494	So4	T	WVV074	0.75	189	756	8Q (0.5)
495	So4	T	WVV110	0.69	187	598	7Q (0.57)
496	So4	T	WVV113	0.63	187	499	6Q (0.67)
497	So4	T	WVV121	0.69	189	605	7Q (0.57)

498	So4	T	WVV122	0.56	188	430	5Q (0.8)
499	So4	T	WVV130	0.56	183	418	5Q (0.8)
500	So4	T	WVV132	0.38	184	294	3Q (1.33)
501	So4	T	WVV141	0.56	189	432	5Q (0.8)
502	So4	T	WVV159	0.56	187	427	5Q (0.8)

Declaration of Authorship

I, Jay Krishna Thakur, hereby declare that this thesis and the work presented in it are entirely my own. The methods presented have been designed by me based on new and existing research understanding, as acknowledged. The presented results of my research were generated by me and have not been submitted, either in part or whole, for a degree at this or any other University. Any use of the works of any other author, in any form, is properly acknowledged at their point of use.

Personal Information

Name	Jay Krishna Thakur
Date of birth	03.02.1983
Place of birth	Janakpur, Nepal
Nationality	Nepalese
Gender	Male
Corresponding address	702, Richard-Paulick-Straße 13, 06124 Halle (Saale), Germany
Permanent address	C/o Ashok Kumar Thakur, Badhari bazar, VDC: Bengadabur -6, Dist.: Dhanusha, Zone: Nepal
E-mail	jay@thakur.co, pdjkth@gmail.com

Education

Since 15.03.2010	PhD candidate at Department of Hydrogeology and Environmental Geology, Institute for Geosciences and Geography, Martin Luther University, Halle (Saale), Germany with HIGRADE scholarships from Helmoltz Centre for Environmental Research - UFZ, Leipzig, Germany
15.09.2008 – 05.03.2010	MSc in Geo-information Science and Earth Observation for Water Resources and Environmental Management from Faculty of International Institute for Geo-Information Science and Earth Observation (ITC), Universiteit Twente, Enschede, The Netherlands
07.06.2006 – 30.05.2008	MSc in Environmental Sciences from School of Environmental Sciences, Jawaharlal Nehru University, New Delhi, India
15.01.2007 – 15.06.2008	Diploma in Industrial Safety (distance mode) from Annamalai University, India
15.06.2004 – 30.05.2006	B.Ed. in Administration and Supervision from Tribhuvan University (TU), Kathmandu, Nepal
02.08.2001 – 15.05.2004	B.Sc in Environmental Sciences, Zoology, Chemistry, Research Methodology, Earth Hazards from Tri-chandra Campus, Tribhuvan University (TU), Kathmandu, Nepal
05.07.1999 – 30.06.2001	I.Sc. from RJRRSD College, BIEC, India
– 13.12.1998	School Leaving Certificate (SLC), 10 years of education, from Sri Sarbajanic Madhyamic Vidhyalaya, VDC: Bengadabur -6, Dist.: Dhanusha, Zone: Nepal

Jay Krishna Thakur